

Figure 6.1 Modelled peak ebb flows during spring tide at Whangarei Harbour entrance.

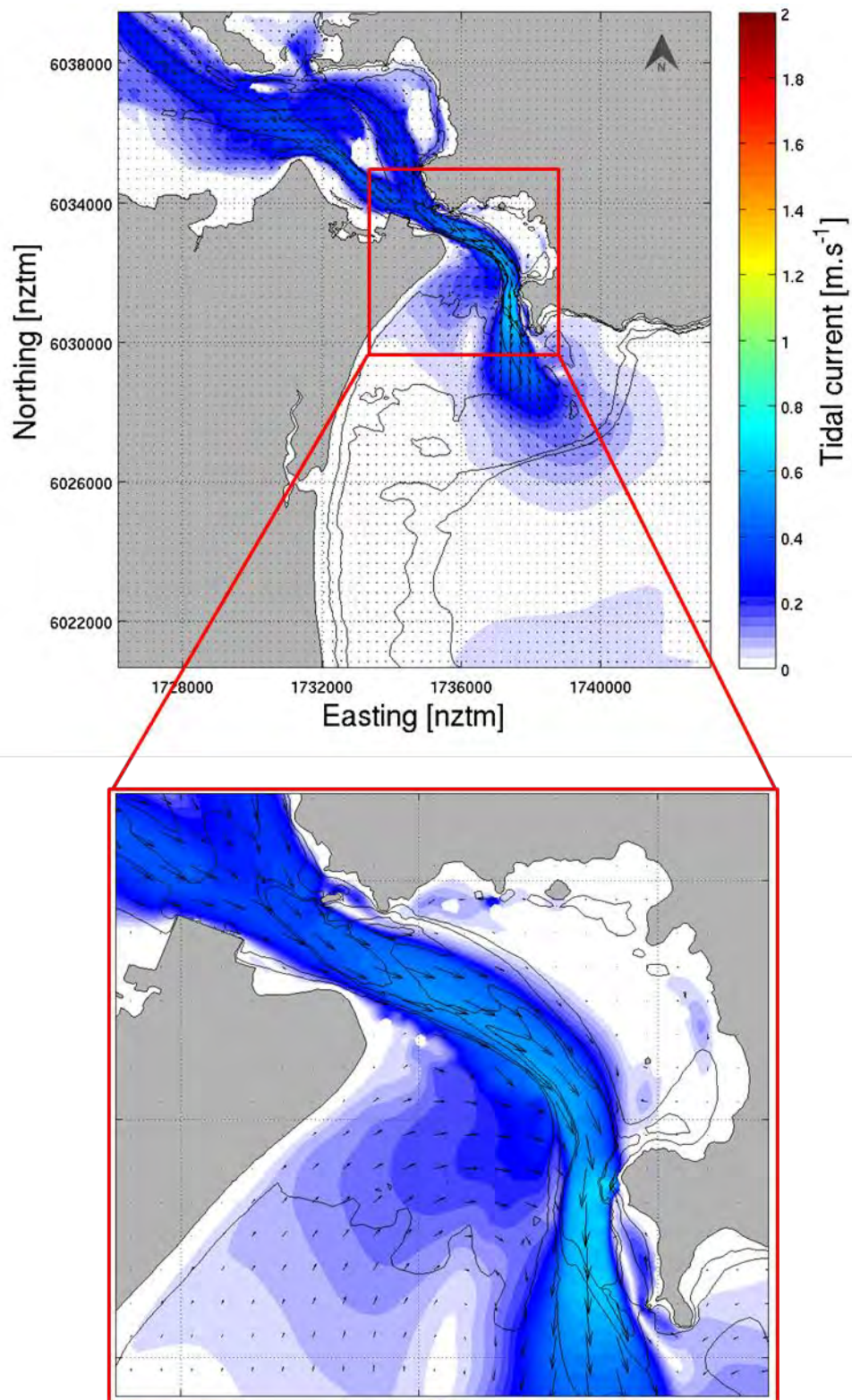


Figure 6.2 Modelled peak ebb flows during neap tide at Whangarei Harbour entrance.

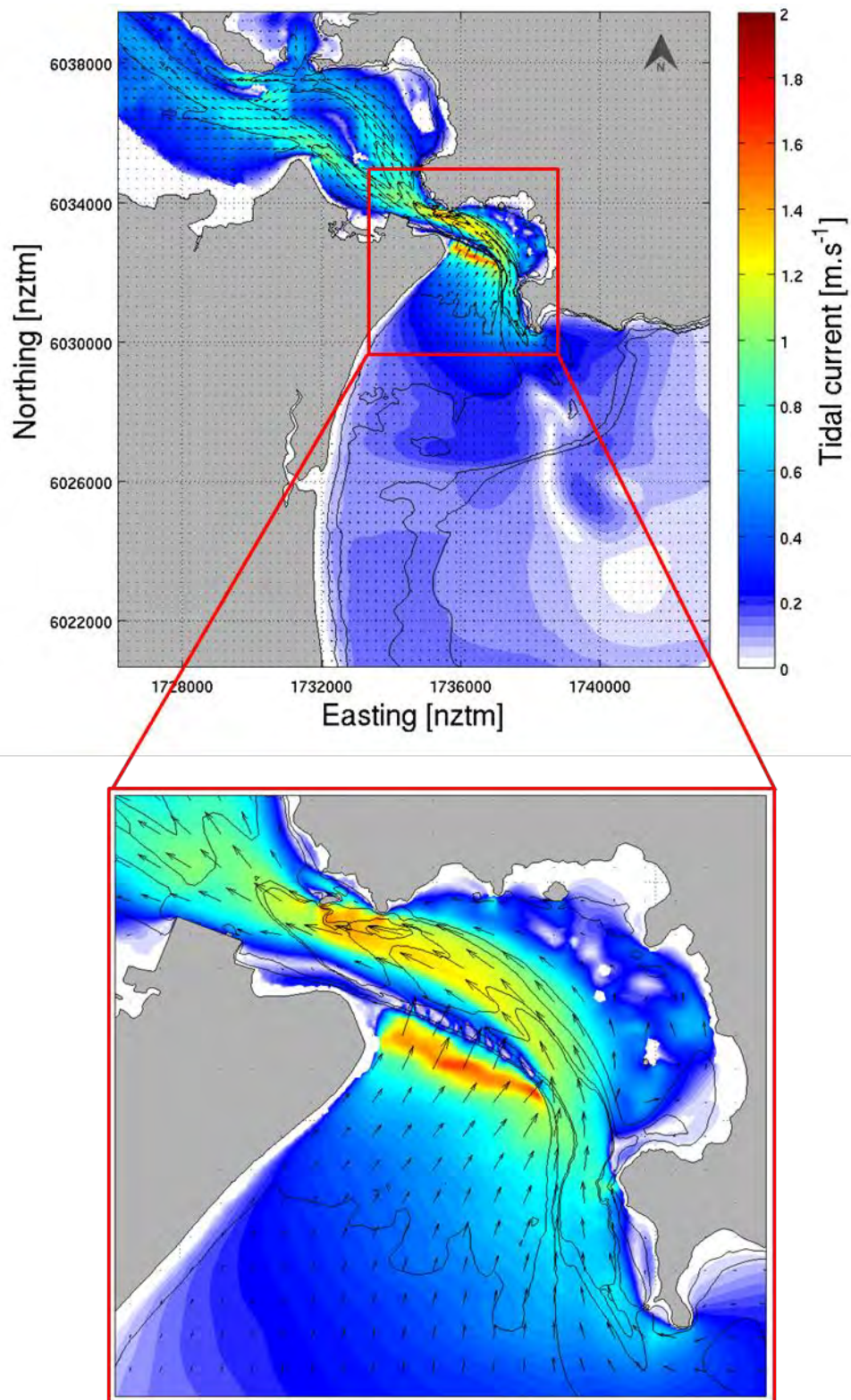


Figure 6.3 Modelled peak flood flows during spring tide at Whangarei Harbour entrance.

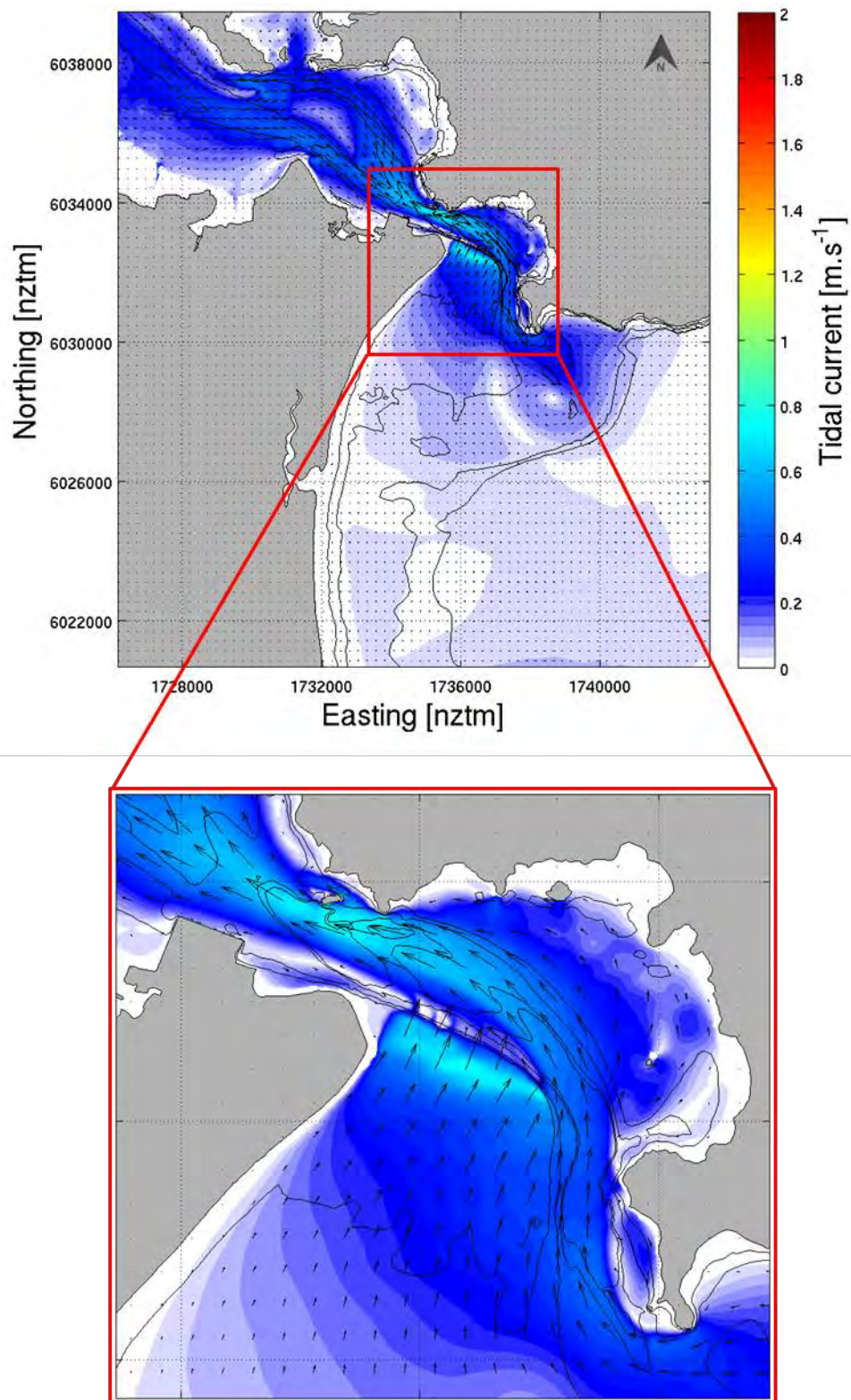


Figure 6.4 Modelled peak flood flows during neap tide at Whangarei Harbour entrance.

## 6.2. Effects of channel deepening on tidal hydrodynamics

The hydrodynamic model was re-run with bathymetry including the deepened channel and all other configurations remaining the same. Comparisons of depth-averaged velocities during the spring tide peak ebb flows are shown in Figure 6.5. These results indicate that the deepening causes a reduction in peak speed of up to  $0.10 \text{ m.s}^{-1}$  at some locations within the main channel, and a maximum acceleration of the flows of  $0.10 \text{ m.s}^{-1}$  in some areas adjacent to the channel. Note that within the areas of highest flow, this represents a very small change, but there are other areas where the localised changes are proportionally much greater, and the effect of those changes requires careful interpretation. For example, near Marsden Point the dredging of the southern flank of the channel is predicted to locally decrease the ebb current flows from  $0.16 \text{ m.s}^{-1}$  to  $0.06 \text{ m.s}^{-1}$ . In response to this new dynamic, the current speed nearby in the marginal channel between Marsden Bank and Mair Bank is expected to increase by  $0.10 \text{ m.s}^{-1}$  (i.e. some 10-15%). Removing the lobe in the central channel to the north of Mair Bank results in a decrease of the maximum ebb current speed from  $0.5$  to  $0.35 \text{ m.s}^{-1}$  (a decrease of  $0.15 \text{ m.s}^{-1}$ ) along the northern flank of the inlet channel between Motukaroro Island and High Island (Figure 1.2). Conversely, there is a predicted strengthening of the ebb tidal flows from  $0.05 \text{ m.s}^{-1}$  to  $0.09 \text{ m.s}^{-1}$  over Little Munroe Bay and McGregor's Bay located to the west of High Island. These two areas are usually characterised by weak tidal dynamics associated with peak ebb and flood velocities ranging from  $0.03 - 0.05 \text{ m.s}^{-1}$ .

The changes in the flood tidal flow fields illustrated in Figure 6.6 clearly show the effect of the complex morphology on the hydrodynamics. For example, the deeper channel and subtle changes to the water level generates spatial variations in the flood tidal flows over Mair Bank. This causes a succession of flow accelerations and decelerations up to  $0.20 \text{ m.s}^{-1}$  (approx. 10 - 20% change). Adjacent to the RNZ jetties, lower flows (by  $0.10 \text{ m.s}^{-1}$ ) occur near the shore, while nearby in deeper water the flows increase by up to  $0.08 \text{ m.s}^{-1}$ . These changes are small compared to the strong tidal flows through the channel

The subtle realignment of the channel by removal of the „toe“ of the ebb tide shoal near Mair Bank has a localised influence on the flows for both the ebb and flood tidal stages. The maximum absolute changes along Section B (Figure 6.7, Figure 6.8 and Figure 6.9) reach  $0.05 \text{ m.s}^{-1}$  on the ebb tidal stage. This is a relatively small change compared to the existing peak ebb and flood current speeds ranging between  $1.2$  and  $1.4 \text{ m.s}^{-1}$  (less than 5%). In contrast, the deepening of the main channel body from Busby Head to the distal margin of the delta is predicted to affect a relatively large area, with some indication of a mild reorientation of the ebb tidal jet. This is predicted to lead to regions with an increase and decrease of up to  $0.015 \text{ m.s}^{-1}$  of the ebb-tidal flow velocities (Figure 6.8, upper plots), which is of the order of a 20% change. The flood flows on the delta margin are slightly reoriented by the dredged channel and exhibit areas of flow acceleration and deceleration (Figure 6.9, upper plots).

Another useful comparison to make is the changes to the bed shear stress imparted by the tidal flows. Bed shear stress is a direct measure of the energy that can be transferred from the flowing water to the seabed, and is a useful analogy for potential sediment transport. Comparisons of bed shear stress at peak ebb and flood stages are presented in Figure 6.10, and these results provide an alternative examination of the potential effects, by accounting for the absolute water depth and the direct effects on the seabed. The channel deepening is not predicted to fundamentally modify the bed shear stress fields over the harbour entrance.

Nevertheless, it may induce local adjustments with a relative low degree of significance for the overall system. The deepening is predicted to reduce the peak bed shear stress in the main channel by up to 20% in the area adjacent to Marsden Point and cause localised increases and decreases up to 30% at the delta entrance during the flood tidal stage. However, these results need to be considered in the context of the absolute magnitudes and how they relate to sediment transport. Accordingly, the percentage of time the bed shear stress exceeds the critical threshold for entrainment of 200  $\mu\text{m}$  sand is provided in Figure 6.11 and Figure 6.12, while the difference of these percentages of exceedance for both the ebb and the flood stages are provided in Figure 6.13.

The channel deepening is expected to decrease the ebb and flood tide values by up to 10% within the channel near Busby Head. Conversely, the percentage of time the bed shear stress exceeds the critical threshold for entrainment of 200  $\mu\text{m}$  sand is predicted to increase by approximately 10% over the eastern margin of the channel close to Busby Head at flood tides (Figure 6.13). This area currently features a slight bathymetric indentation, and it may be an area of active (and asymmetric) sediment transport. Conversely, the percentage of time the bed shear stress exceeds the critical threshold for entrainment of 200  $\mu\text{m}$  sand is predicted to decrease by 5 – 10% over the western margin of the channel. This typically means that the sand drift potential induced by tidal currents over the western margin is expected to be lower than over the eastern margin.

However, this is also a function of the actual sediment properties of the seabed in this area which will be evaluated in the following section.

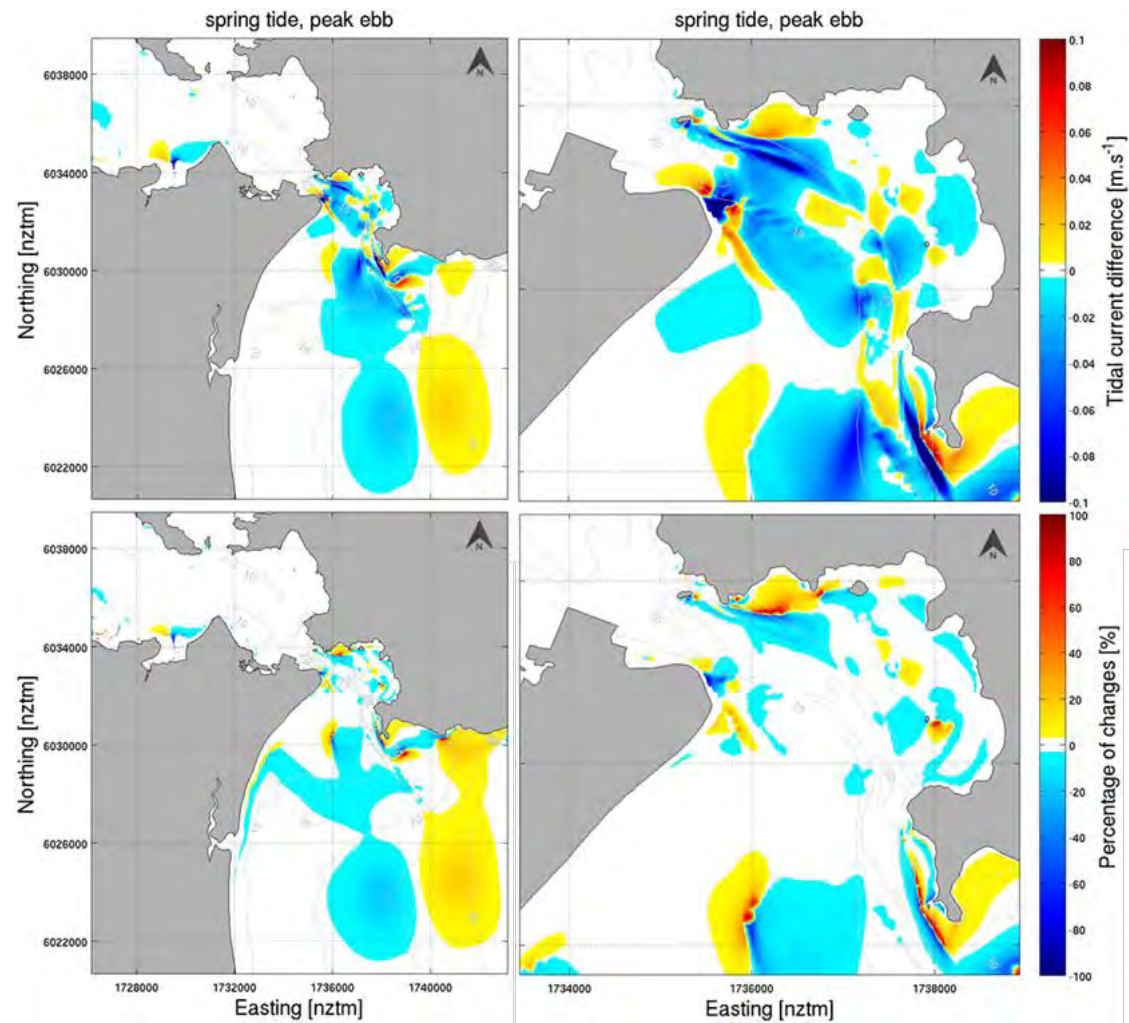


Figure 6.5 Absolute (top) and relative (bottom) difference in tidal flows post-deepening during the peak spring ebb flows. Plots on the right show a zoomed in view of the entrance region. Positive values indicate a predicted increase in flow (red scale), while the negative values indicate a decrease (blue scale).

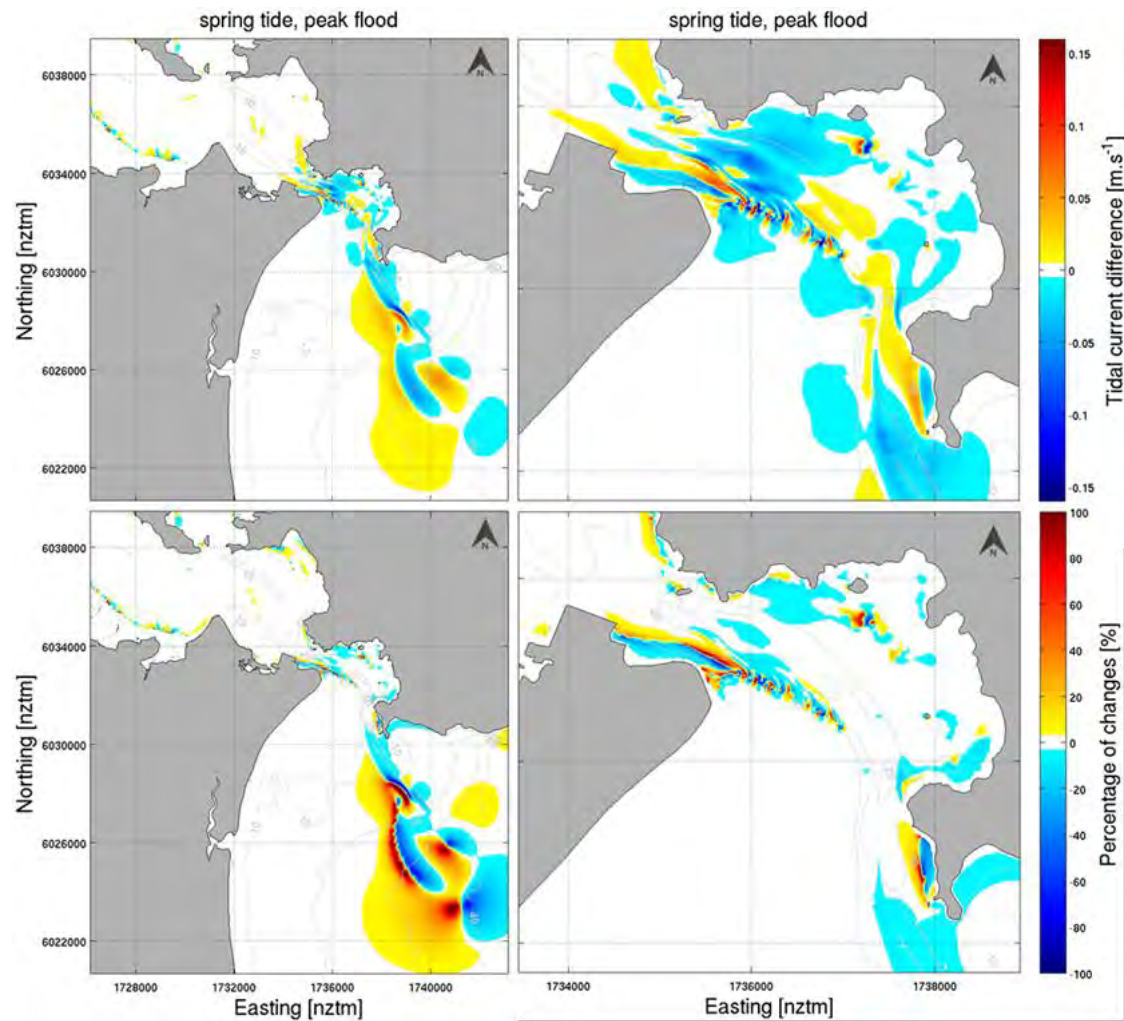


Figure 6.6 Absolute (top) and relative (bottom) difference in tidal flows post-deepening during the peak spring flood flows. Plots on the right show a zoomed in view of the entrance region. Positive values indicate a predicted increase in flow (red scale), while the negative values indicate a decrease (blue scale).

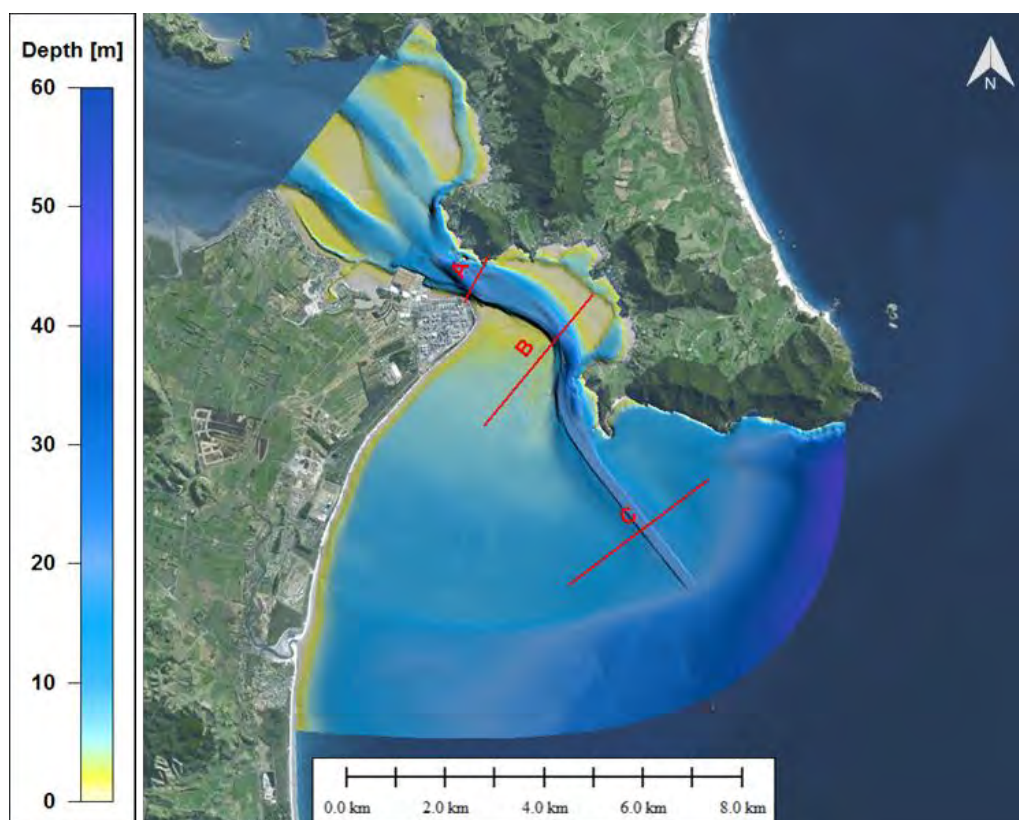


Figure 6.7 Location of the cross-sections used to evaluate the tidal flow differences following channel deepening.

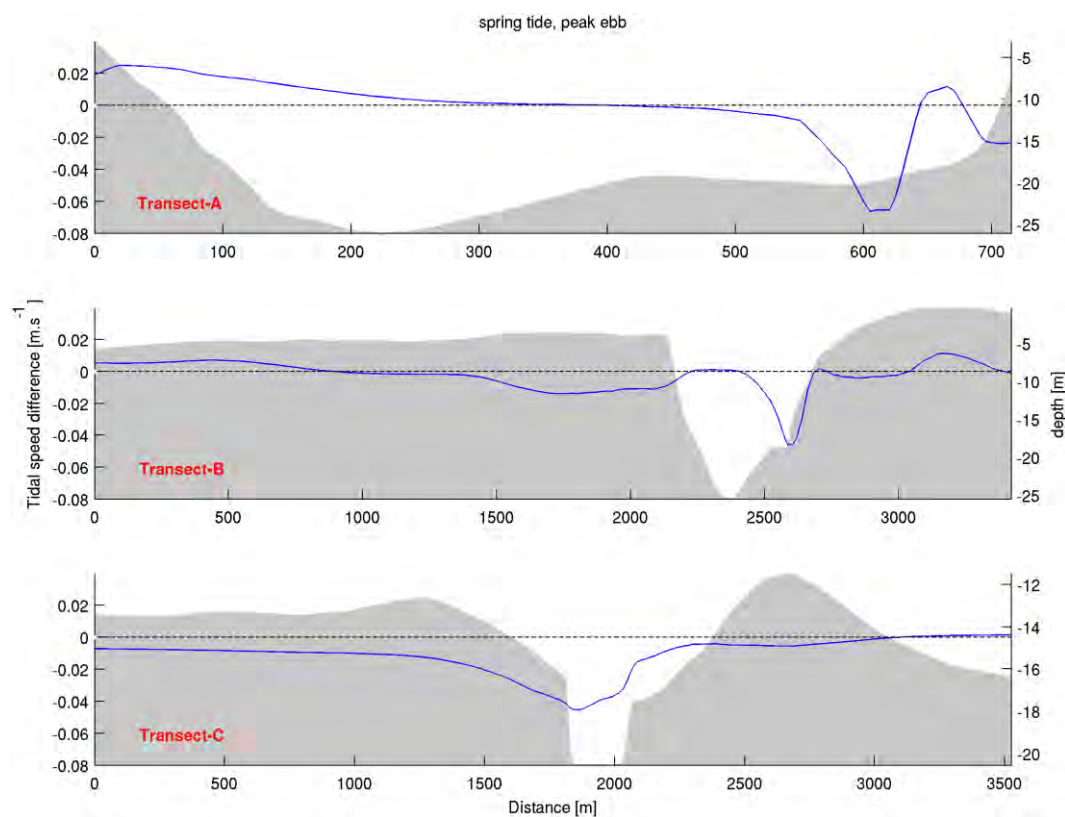


Figure 6.8 Ebb tidal flow differences during spring tide along sections A, B and C shown in Figure 6.7. The dotted line indicates the  $0\text{-m}\cdot\text{s}^{-1}$  velocity threshold.

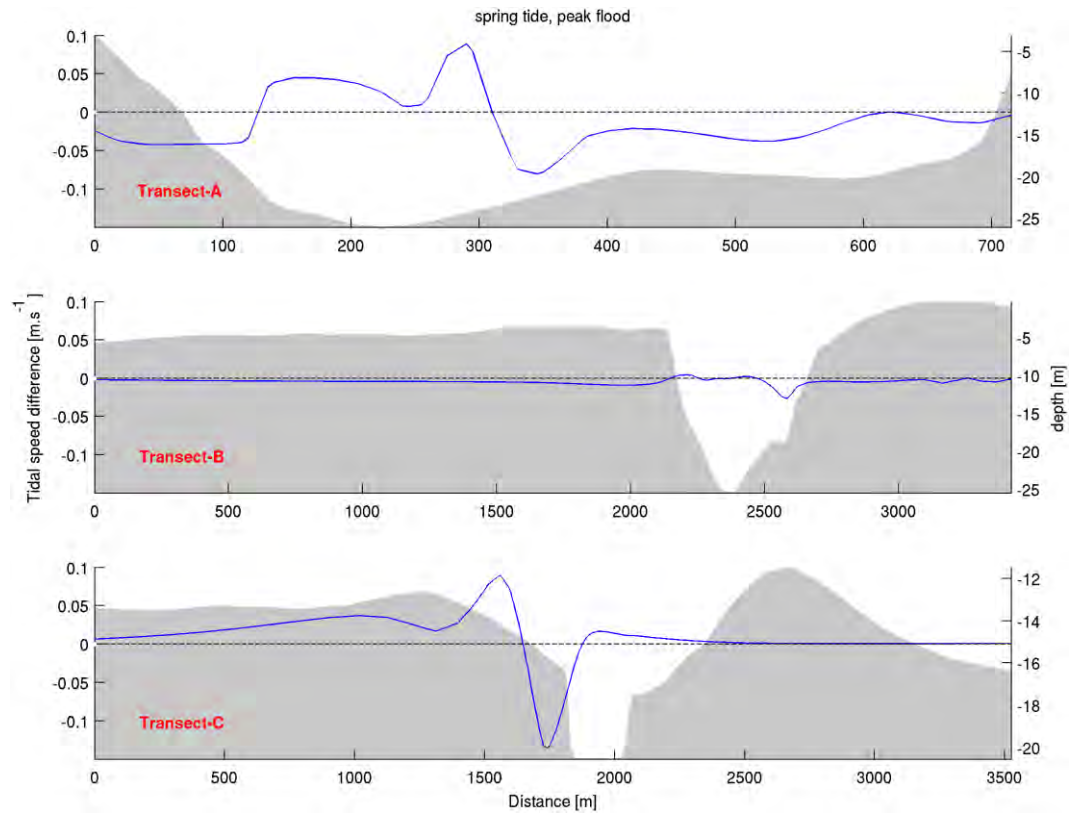


Figure 6.9 Flood tidal flow differences during spring tide along transects A, B and C shown in Figure 6.7. The dotted line indicates the  $0\text{-m.s}^{-1}$  velocity threshold.

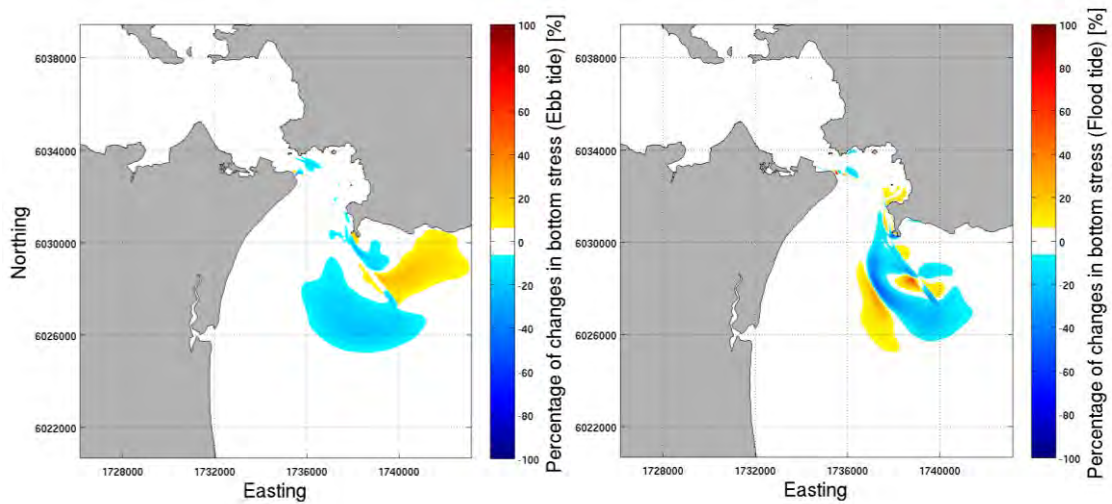


Figure 6.10 Percentage of change in the bed shear stress fields during peak spring ebb (left) and flood stages (right) between the existing and the deepened channel bathymetry.

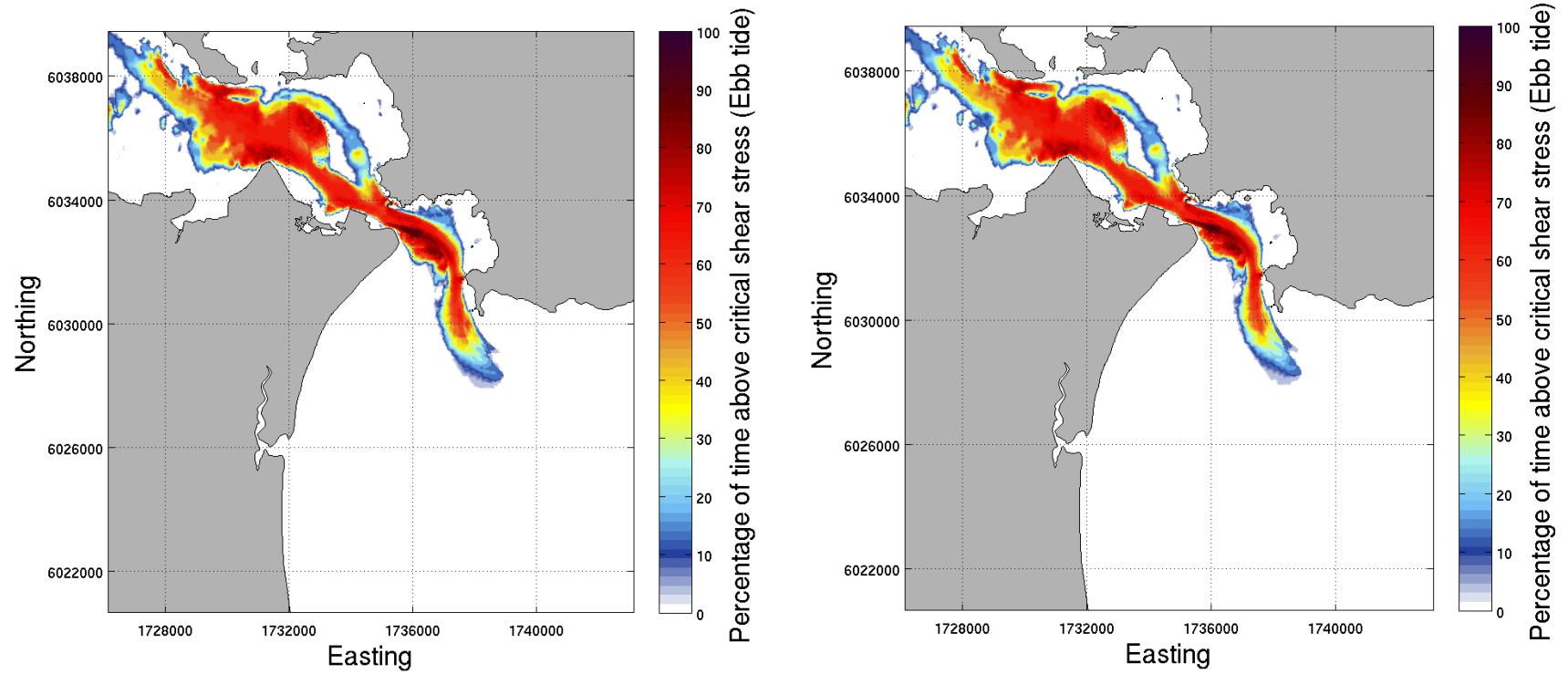


Figure 6.11 Percentage of time the bed shear stress exceeds the critical shear stress threshold for 200 µm sand at ebb tide. Calculated from a 28-day simulation of the existing harbour (left) and the deepened channel (right).

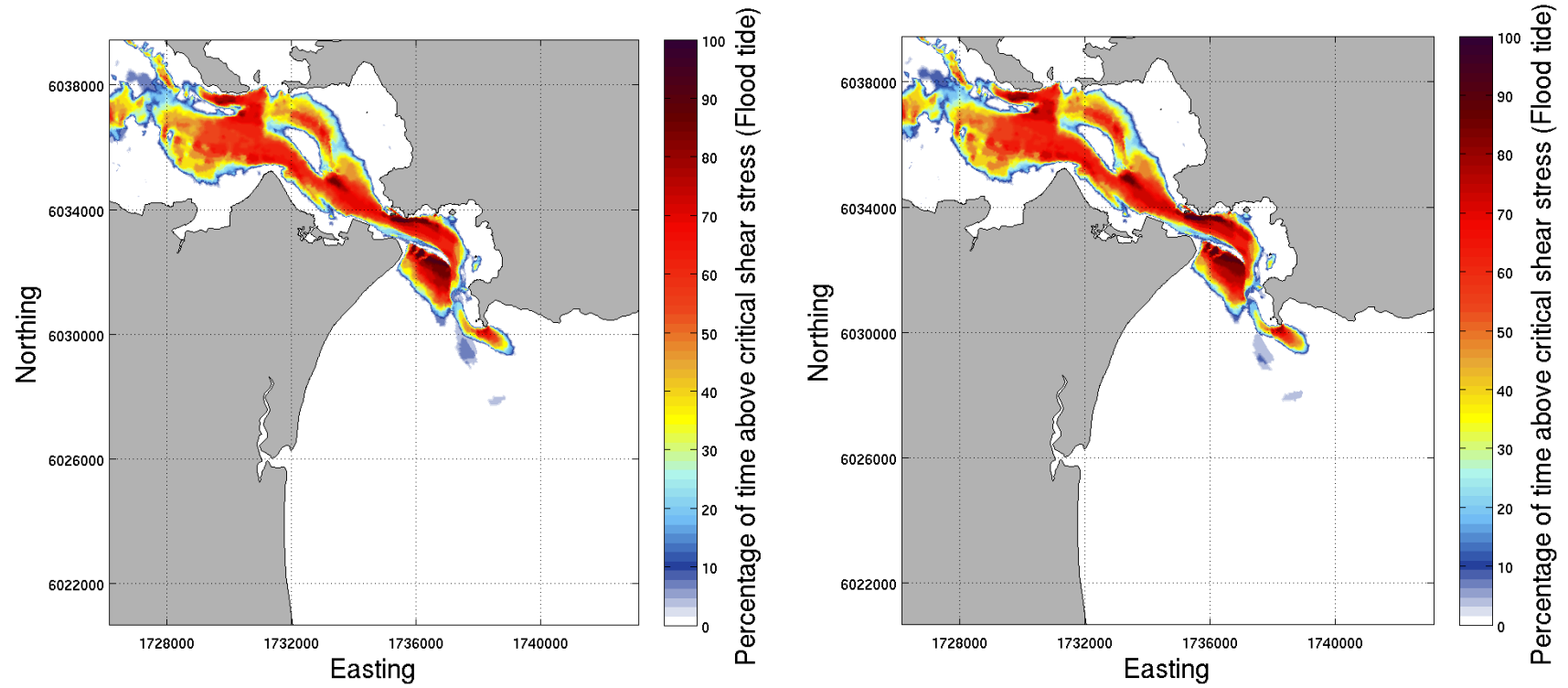


Figure 6.12 Percentage of time the bed shear stress exceeds the critical shear stress threshold for 200 µm sand at flood tide. Calculated from a 28-day simulation of the existing harbour (left) and the deepened channel (right).

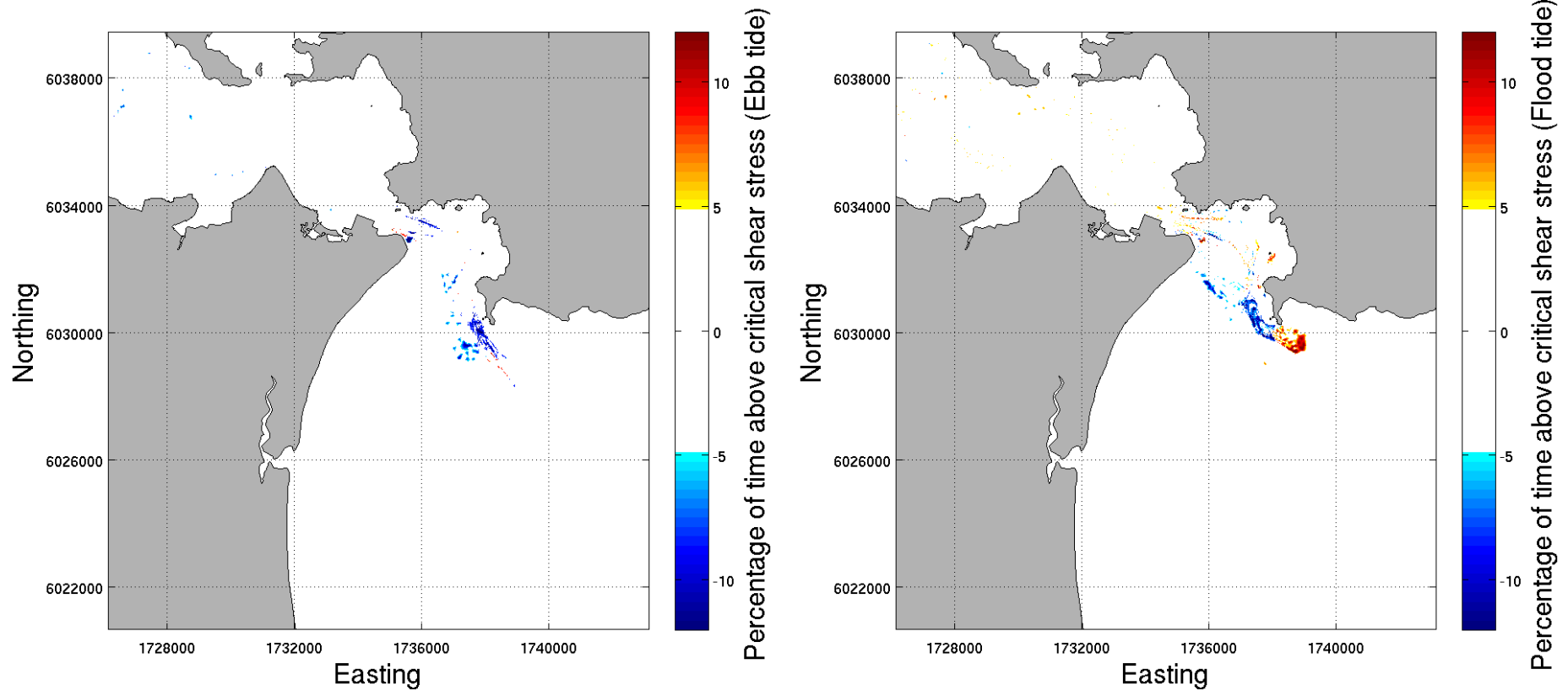


Figure 6.13 Difference of percentage of time the bed shear stress exceeds the critical shear stress threshold for 200 µm sand at ebb (left) and flood (right) tidal stages, calculated from a 28-day simulation of the existing harbour and the deepened channel. Noise in the difference fields was cleaned using an arbitrary minimum threshold of 5% to highlight the areas of significant changes.

### 6.3. Summary of effects on the nearshore tidal hydrodynamics

The predicted effects of the channel deepening on the hydrodynamics are:

- Reduction of the peak tidal speed by up to  $0.10 \text{ m.s}^{-1}$  in the dredged channel, and acceleration up to  $0.10 \text{ m.s}^{-1}$  in some adjacent areas.
- Increase of the tidal current speed by  $0.10 \text{ m.s}^{-1}$  (i.e. about 10-15%) inside the marginal channel between Marsden Bank and Mair Bank.
- Removal of the lobe in the central channel between Marsden Bank and Mair Bank results in a localised decrease of tidal flow velocities of up to  $0.15 \text{ m.s}^{-1}$  (from  $0.5$  to  $0.35 \text{ m.s}^{-1}$ ), while the current speed is expected to increase from  $0.05$  to  $0.09 \text{ m.s}^{-1}$  (maximum increase of  $0.04 \text{ m.s}^{-1}$ ) along the northern flank of the inlet channel between Motukaroro Island and High Island, an area characterised by a very low hydrodynamic regime.
- The subtle realignment of the channel by removal of the „toe“ on some of the bends induce a slight acceleration of the tidal flows over the dredged areas and a deceleration over the adjacent areas for both the ebb and the flood tidal stages. These changes do not exceed 5% of the existing tidal regime.
- The deepening of the channel from Busby Head to the distal margin of the delta is predicted to lead to regions with increases and decreases of the mean ebb-tidal flow velocities of up to  $0.02 \text{ m.s}^{-1}$ . Both ebb and flood flows on the delta margin are slightly reoriented by the dredged channel and exhibit areas of flow acceleration and deceleration.
- Deepening the channel is not expected to fundamentally modify the bed shear stress fields over the harbour entrance but may locally induce some adjustments. A reduction of the peak bed shear stress of up to 20% at ebb and flood stages in the area adjacent to Marsden Point is expected. The dredging may also cause localised peak bed shear increases and decreases up to 30% at the delta entrance during the flood tidal stage. Such changes in the bed shear stress fields are susceptible to generate some subtle adjustments of the local morphodynamics without causing an overall transformation of the sediment transport dynamics between the harbour and the open-ocean region.
- The percentage of time the bed shear stress exceeds the critical level for entrainment of  $200 \mu\text{m}$  sand is expected to decrease up to 10% in the channel due to increasing water. Conversely, this time is predicted to increase by approximately 12% along the eastern margin of the channel to the southeast of Busby Head. Along the western margin of the channel, this time is susceptible to decrease by 5 – 10%. More broadly, changes in the tidal dynamics due to the channel deepening may modify locally the potential of sand mobility inside and on either side of the channel. However, these anticipated adjustments should remain of relative low importance compared to the effect of the waves on the morphodynamics outside the harbour entrance.
- Based on the assumption of a uniform seabed composition of 200 micron sand, the asymmetry for entrainment between ebb and flood tide just east

of Busby Head may change, with the flood stage showing a 10% increase in time above the critical shear stress for 200  $\mu\text{m}$  sand. Such changes may slightly increase the sand mobility induced by tidal currents near Busby Head. However, these adjustments in the sediment transport are predicted to be of relative low importance compared to the effect of waves.

- While the hydrodynamics of the internal harbour are not expected to be affected by the deepening, a very slight adjustment of the timing of the tidal phase may occur. This will likely require a period of measurement at the defined tidal stations to derive the new tidal constituents for Northport and Whangarei Port.

## 7. SEDIMENT TRANSPORT

A process-based numerical model was implemented to simulate the morphodynamics that are driven by the main hydrodynamic tidal and wave forces at the harbour entrance. The key processes controlling the morphodynamics of the coastal region are identified and effects of the channel deepening on sediment dynamics examined in this section. This involved different approaches to determine changes in the potential sediment fluxes, sedimentology and governing morphology of the system.

### 7.1. Conceptual modelling – tide only transport scenarios

Model results related to the peak flood and ebb flows for the existing environment are provided in Figure 7.1, and corresponding bed shear stress and net transport flux fields are presented in Figure 7.2 to Figure 7.6. The harbour entrance is characterised by strong tidal flows that regularly mobilise the fine and medium sands. The eastern edge and the southern areas of Mair Bank are particularly exposed to strong tidal flows during flood tide, with cross-bank velocities of up to  $1.3 \text{ m.s}^{-1}$  over the shallows. Within the channel, tidal flows reach  $1.4 \text{ m.s}^{-1}$  in the deeper areas. During ebb tides, the flows on the eastern edge of Mair Bank are also high, albeit to a lesser extent. Notably, the medium to high current velocities (up to  $0.8 \text{ m.s}^{-1}$ ) over the northern area of Mair Bank results in heterogeneous bed shear stress fields that may favour local erosion and accretion. Diagrams showing the range of average current speeds at which sediment particles of different sizes are eroded and transported are shown in Figure 7.3 and Figure 7.4.

The resulting mean net transport fluxes (up to  $2 \cdot 10^{-4} \text{ m}^3 \cdot \text{s}^{-1} \cdot \text{m}^{-1}$ ) over one tidal cycle highlight the high potential for the tidal component to mobilise sediments around Mair Bank and within the main channel. Note, however, that these potential sediment transport results consider a grain size of  $200 \mu\text{m}$  (fine to medium sand) and do not take the biological component (biomass of pipi, shell hash, etc.) into account.

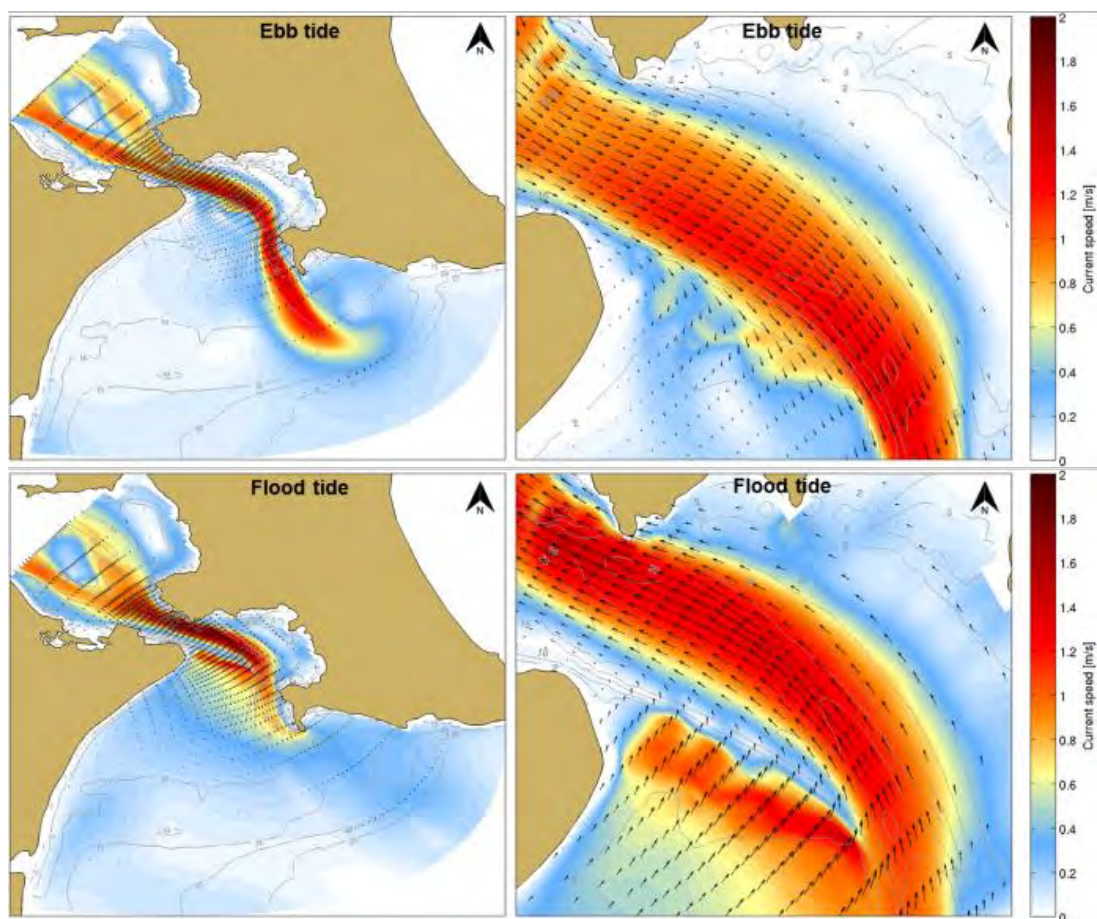


Figure 7.1 Modelled current speed fields over the whole domain (left) and over Mair Bank (right) for the tide-only scenario during spring ebb (top) and flood (bottom) tides.

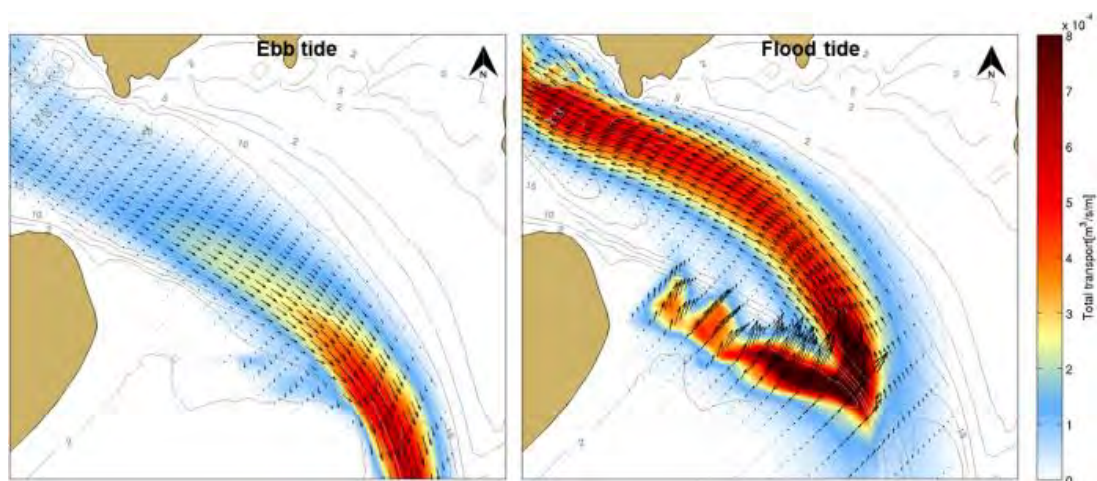


Figure 7.2 Modelled net transport fluxes over Mair Bank for the tide-only scenario during ebb (left) and flood (right) tides.

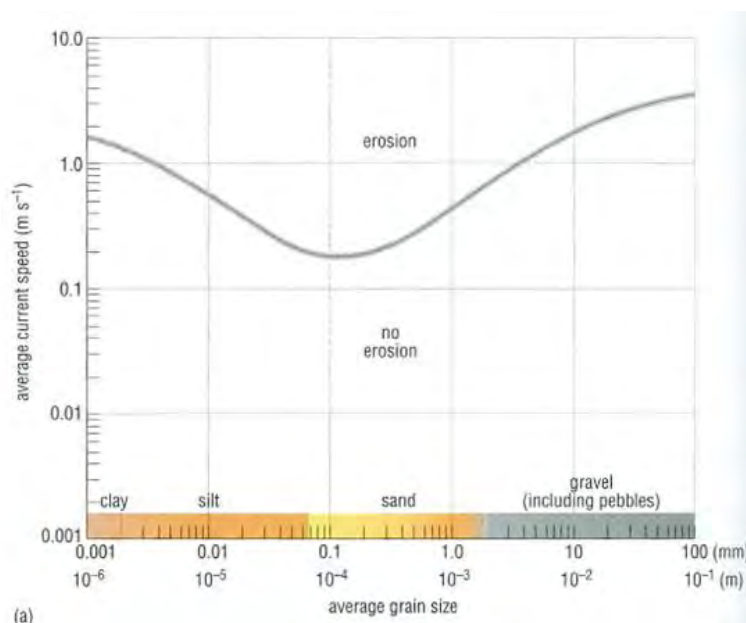


Figure 7.3 Diagram showing the range of average current speeds at which sediment particles of different sizes are eroded, i.e. set in motion. The curve for sediments finer than about 0.1 mm is for relatively uncompact silts and muds (from Wright et al. (1999)).

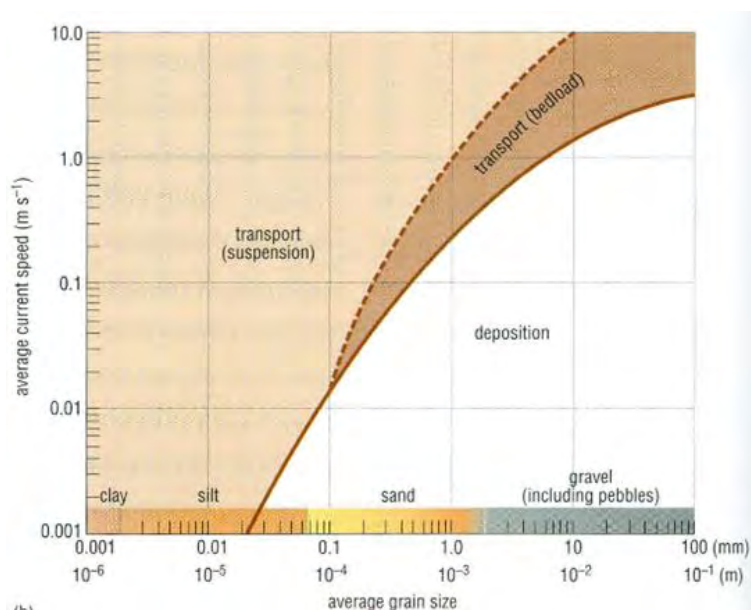


Figure 7.4 Diagram showing the range of average current speeds at which sediment particles of different sizes are transported, in suspension or as bedload, and below which they are deposited. The broken line indicates the transition between bedload and suspension transport (from Wright et al. (1999)).

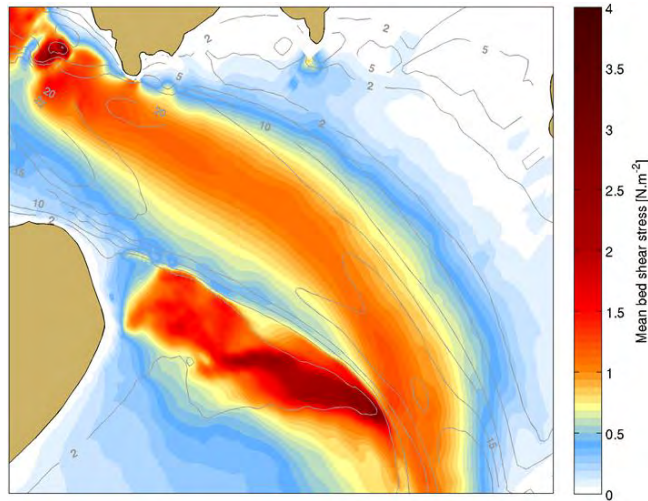


Figure 7.5 Modelled mean bed shear stress calculated over one tidal cycle for the tide-only scenario.

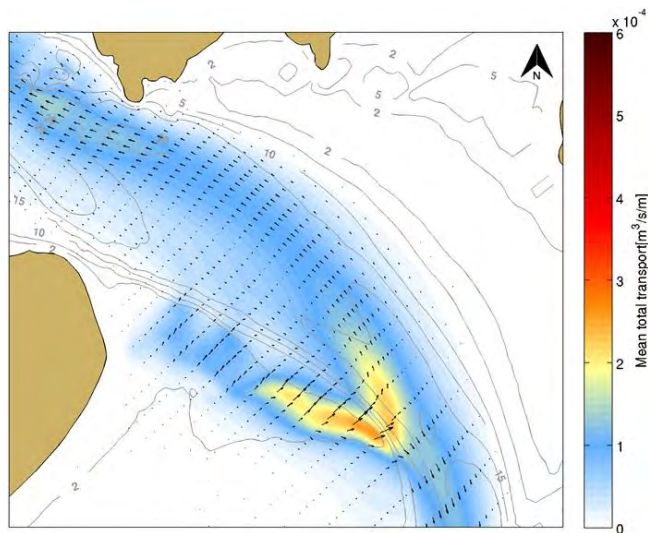


Figure 7.6 Modelled net transport fluxes calculated over one tidal cycle for the tide-only scenario.

## 7.2. Conceptual modelling – wave and tide scenarios

### 7.2.1. Existing environment

A set of 16 representative wave and tidal scenarios detailed in MSL Report 0297-01 (MSL, 2016) were run to assess the net transport fluxes through the Whangarei Harbour entrance under a range of sea conditions. The significant wave height fields corresponding to the different scenarios for the existing environment at Whangarei Harbour and the surroundings are illustrated in Figure 7.7 and Figure 7.8 while the resultant mean net transport fluxes are shown in Figure 7.9 and Figure 7.10. Using the mean net transport fluxes to investigate the existing coastal environment brings particular advantages to the study as it quantifies the potential response of the seabed to the wave and tidal forcing excluding the effect of the morphological changes during the simulation.

Whangarei Harbour entrance exhibits strong gradients in wave energy due to the coastal shape and the relative complex bathymetry. Busby Head reduces the exposure of the channel entrance and Mair Bank to the incident waves from the

dominant easterly octant (Figure 7.7) and the shoreline orientation shelters the entrance from northerly storm wave events to a large extent (Figure 7.8). In spite of the degree of shelter afforded by the topography, adding wave forcing to the sediment modelling process increases the net transport fluxes over Mair Bank and along the edge of the channel (see Figure 7.9 and Figure 7.10). Strong northward residual net transport fluxes are observed over the southern margin of Mair Bank and along Ruakaka Beach. The south-western flank of Mair Bank displayed the strongest and most localised net transport fluxes due to wave refraction. High energy wave events show a high erosive potential for sandy material over these areas with mean net transport fluxes of up to  $1.10^{-3} \text{ m}^3 \cdot \text{s}^{-1} \cdot \text{m}^{-1}$ .

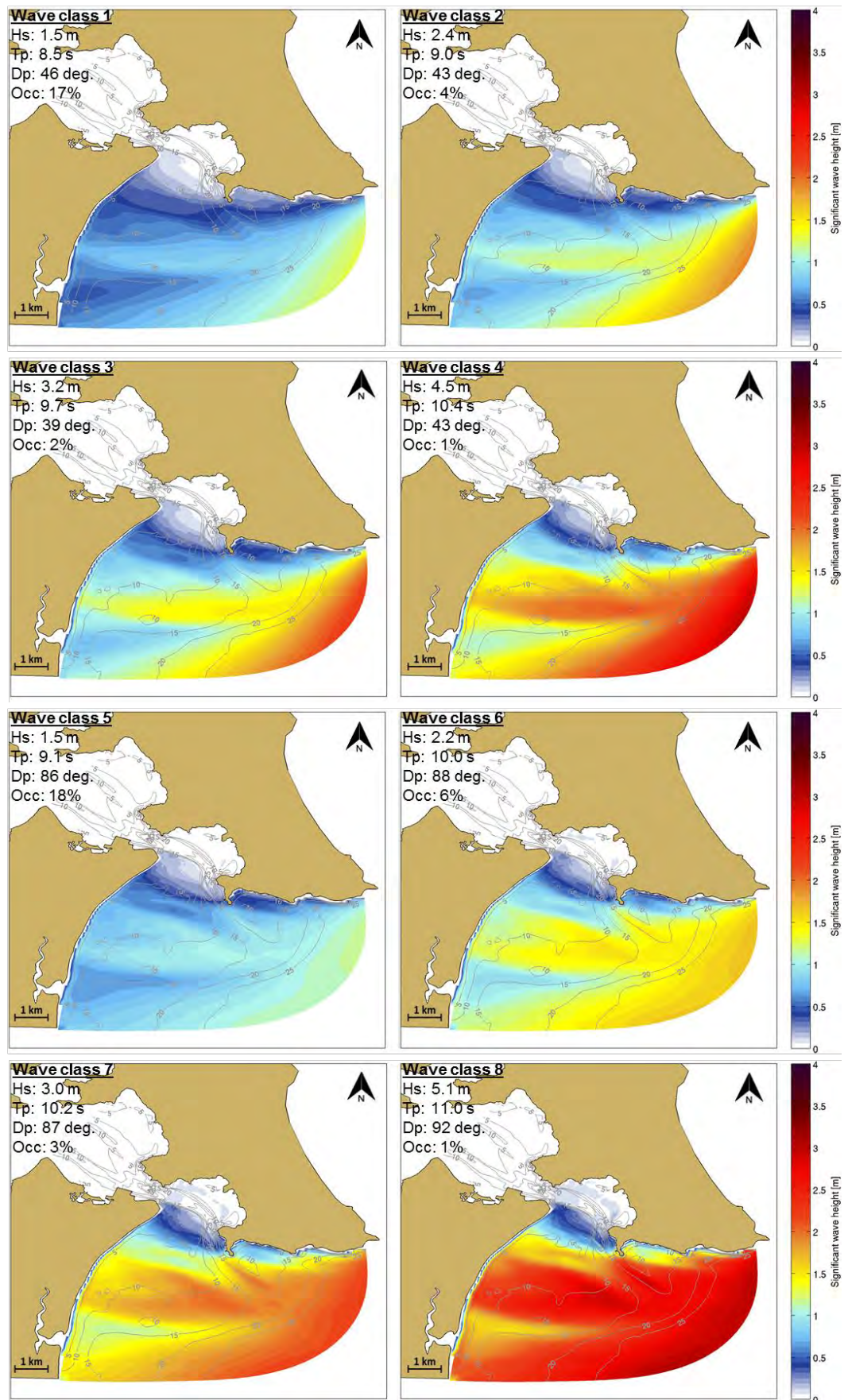


Figure 7.7 Wave height fields for Classes 1 to 8. Black arrows indicate the peak direction.

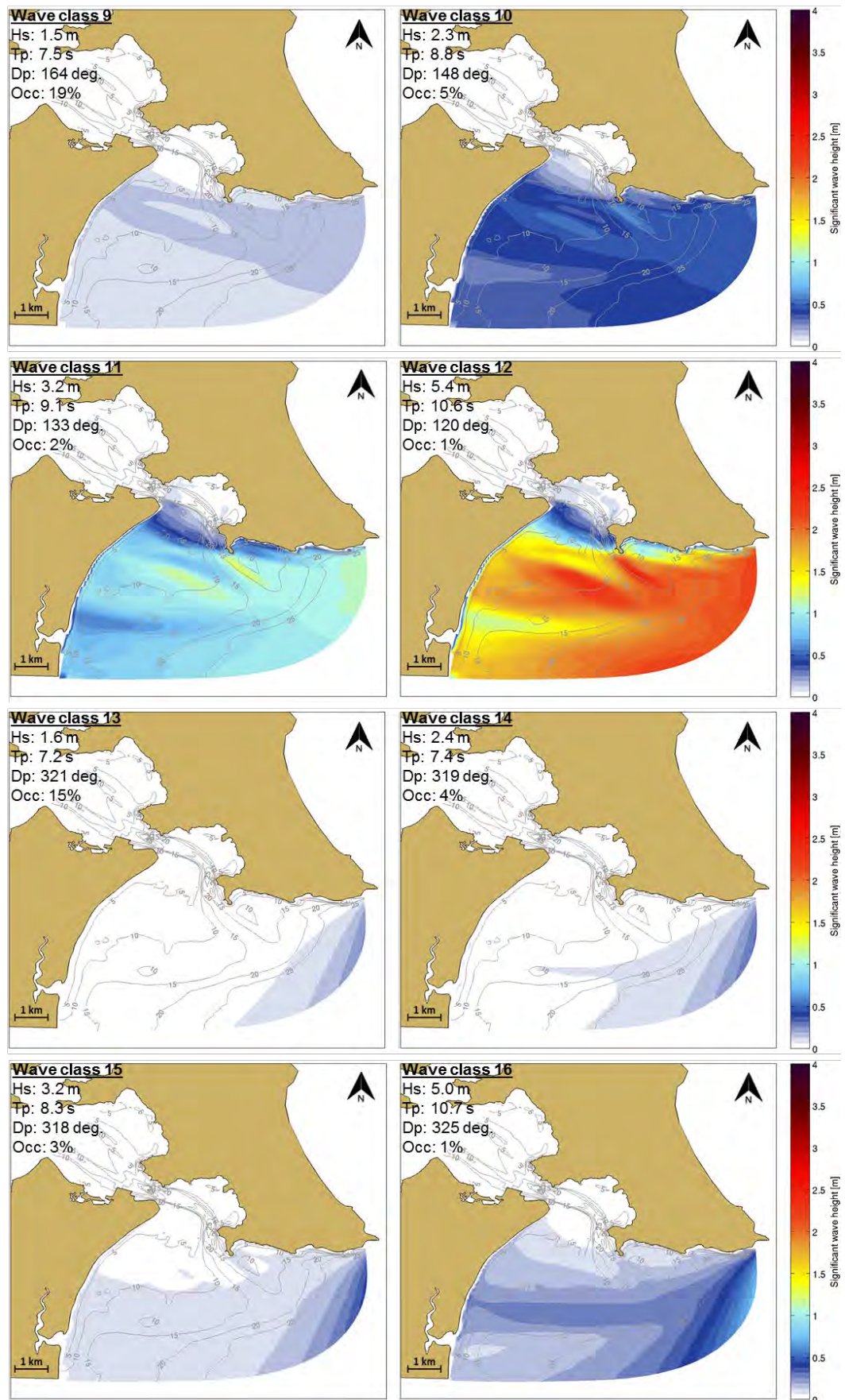


Figure 7.8 Wave height fields for Classes 9 to 16. Black arrows indicate the peak direction.

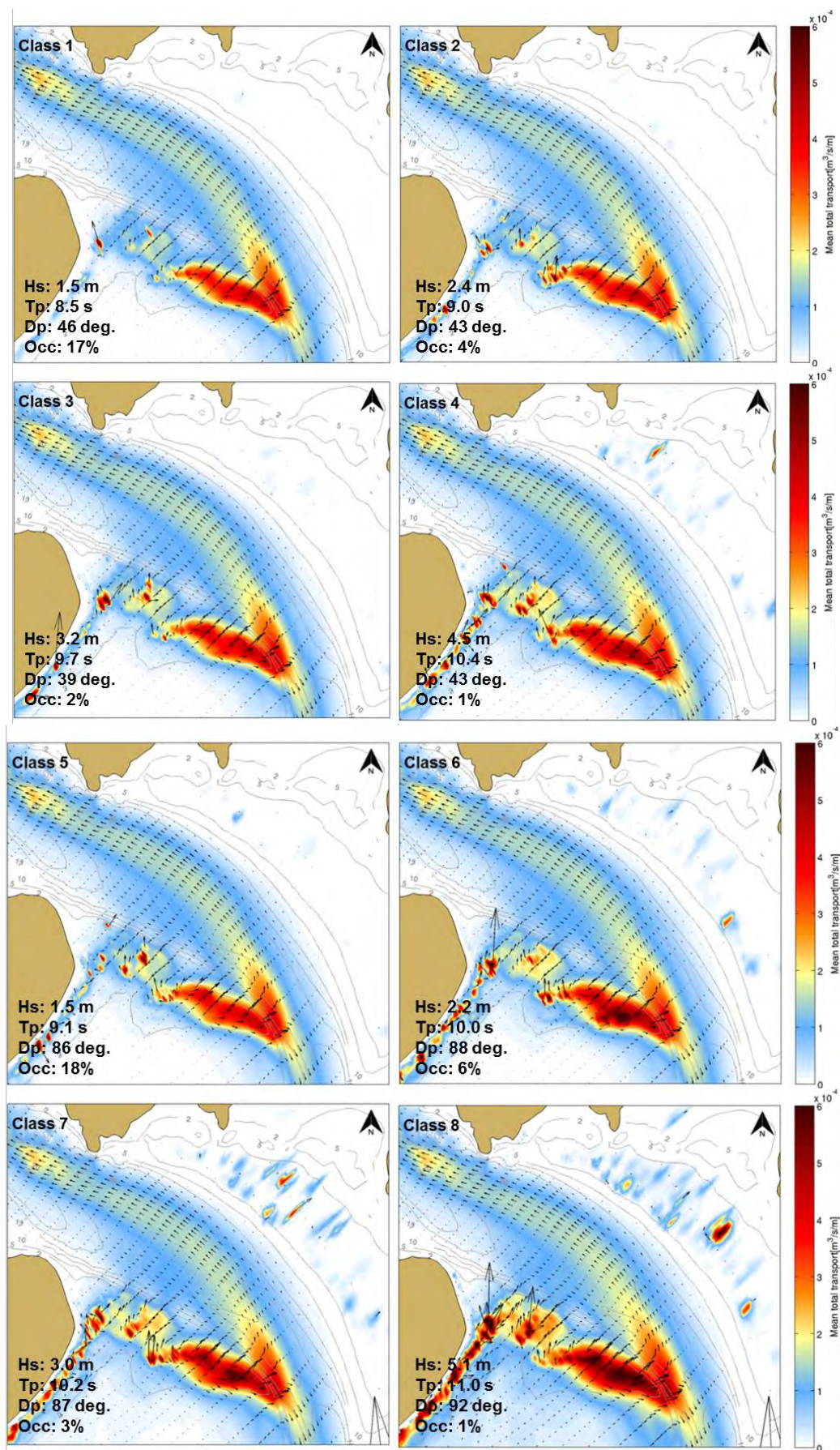


Figure 7.9 Mean net transport fluxes calculated over one tidal cycle for Classes 1 to 8.

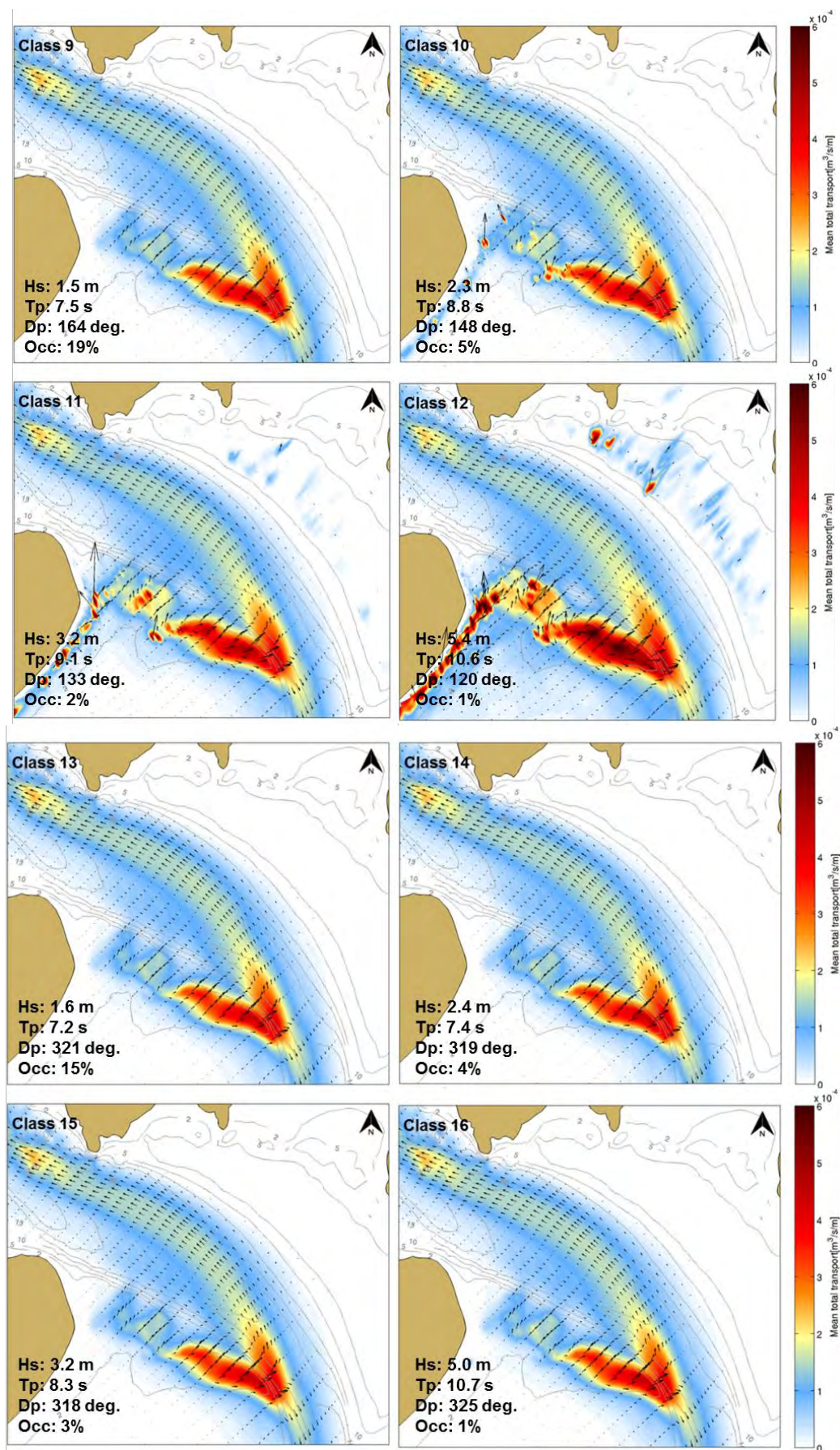


Figure 7.10 Mean net transport fluxes calculated over one tidal cycle for Classes 9 to 16.

### **7.2.2. Predicted changes to the sediment flux due to channel deepening**

The simulations presented in Section 7.2.1 were undertaken again with the deepened channel and the two outputs were compared (Figure 7.11 to Figure 7.14). Mean net transport fluxes induced by a range of wave and tide conditions were investigated and compared to those obtained for the existing environment.

For wave classes 1, 5, 9 and 13, which represent a total of 70% of occurrence, a notable increase of up to 20% of the potential sediment flux is predicted locally along the inner flank of the channel east of Mair Bank. Over Mair Bank changes in the potential net transport fields are predicted to occur along the eastern edge of the sand bank. The increased transport pattern for wave classes 13 to 15 (i.e. low energy conditions) suggests that the effect is dominated by the tidal flows. Note, however, that changes in the wave forcing may occasionally modify somewhat the sediment transport over this particular area during extreme wave events, as illustrated for wave classes 3, 4 and 12.

All other patterns over Mair Bank, Calliope Bank and along Ruakaka Beach can be explained by the effects of the changes to the wave climate resulting from the deepened channel. The residual sediment transport is predicted to strongly increase or decrease over very shallow areas due to high-frequency wave-current interactions, represented by dark red colour and long arrows in Figure 7.11 to Figure 7.14. The high-amplitude changes highlighted in the present section are predicted to be constricted to discrete zones, without causing any overall pronounced effect of the channel deepening on the medium-term or long-term coastal morphodynamics.

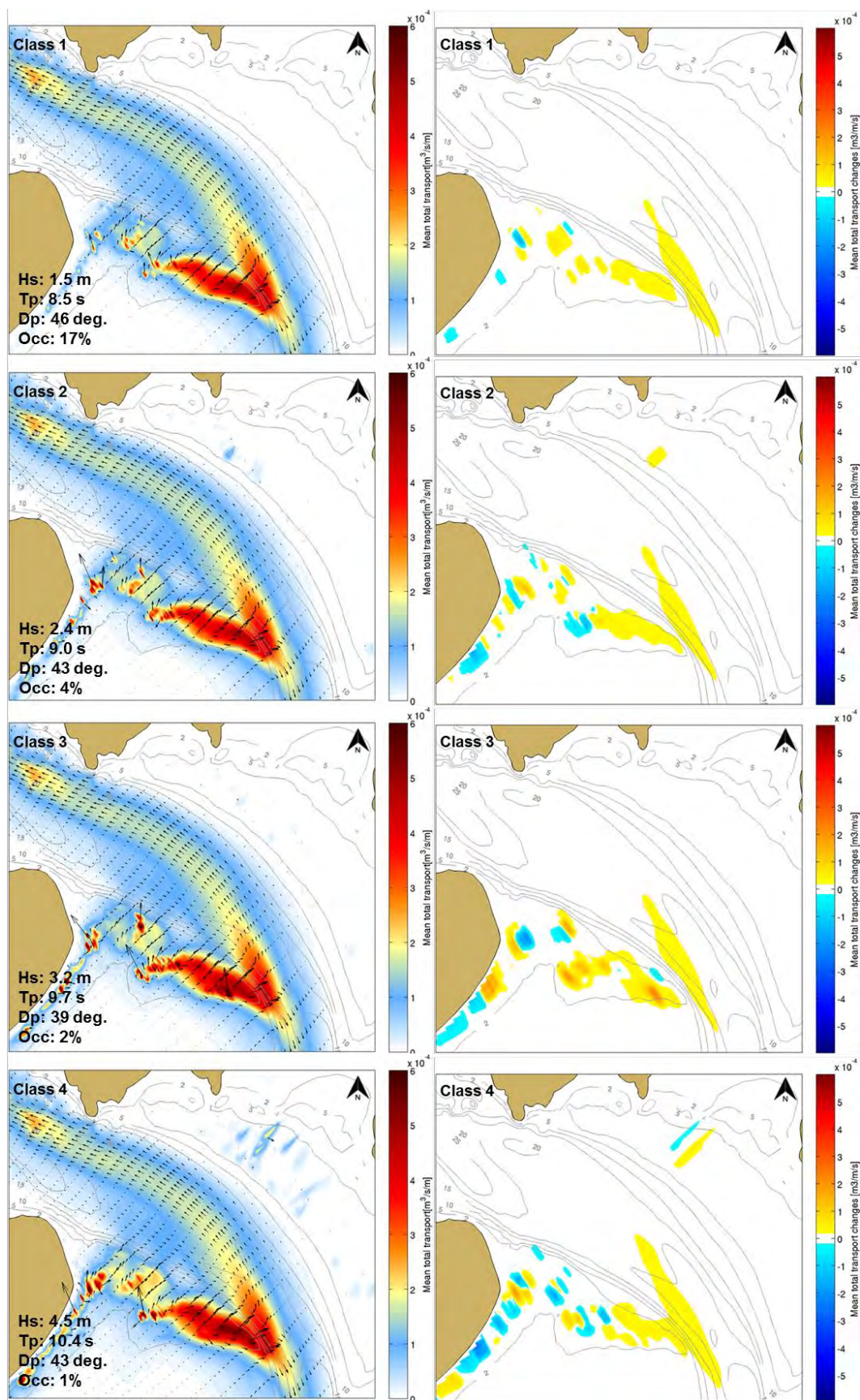


Figure 7.11 Mean net transport fluxes (left) and mean net transport differences (right) between pre- and post-dredge scenarios over one tidal cycle for Classes 1 to 4. A positive magnitude represents an increase.

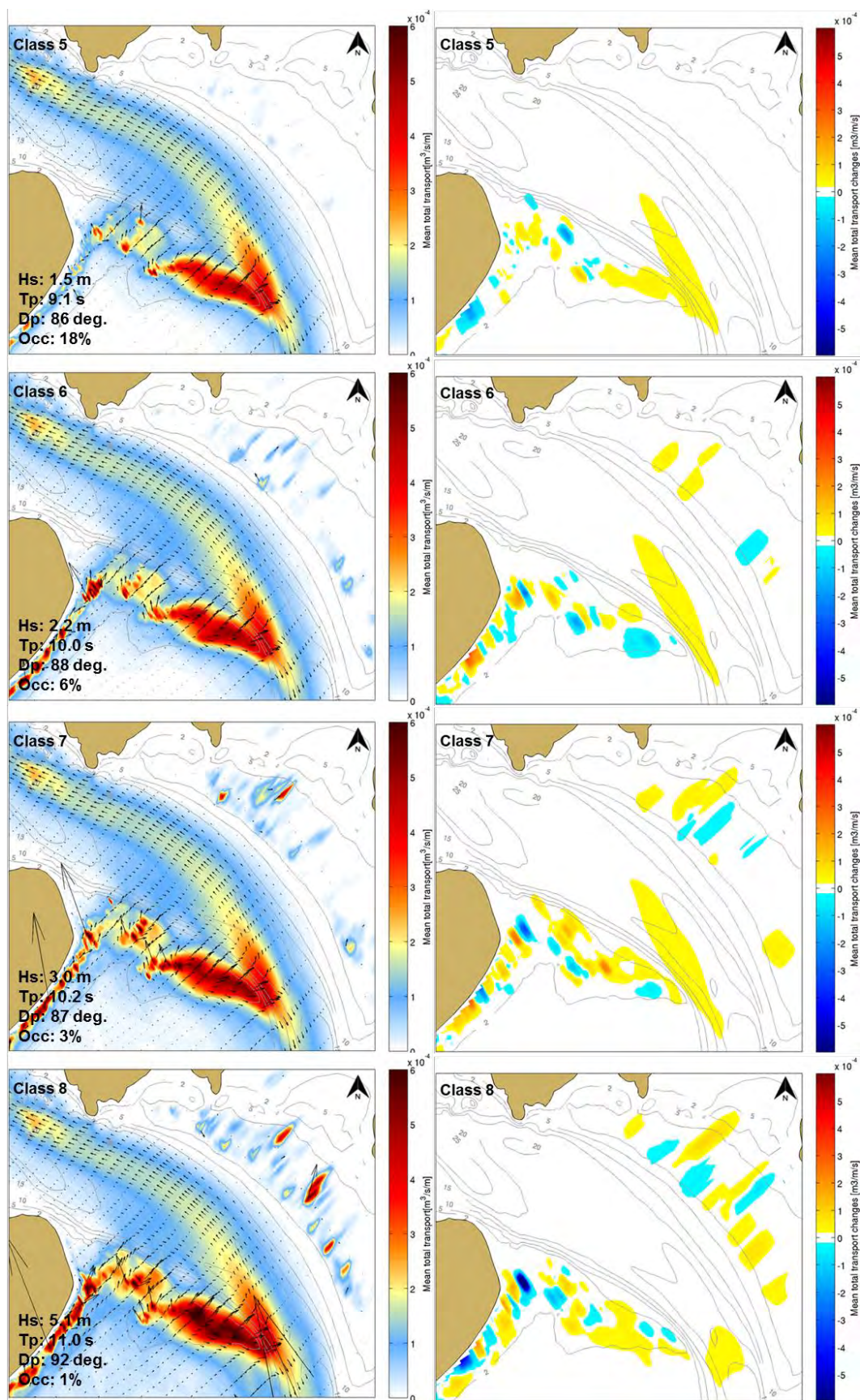


Figure 7.12 Mean net transport fluxes (left) and mean net transport differences (right) between pre- and post-dredge scenarios over one tidal cycle for Classes 5 to 8. A positive magnitude represents an increase.

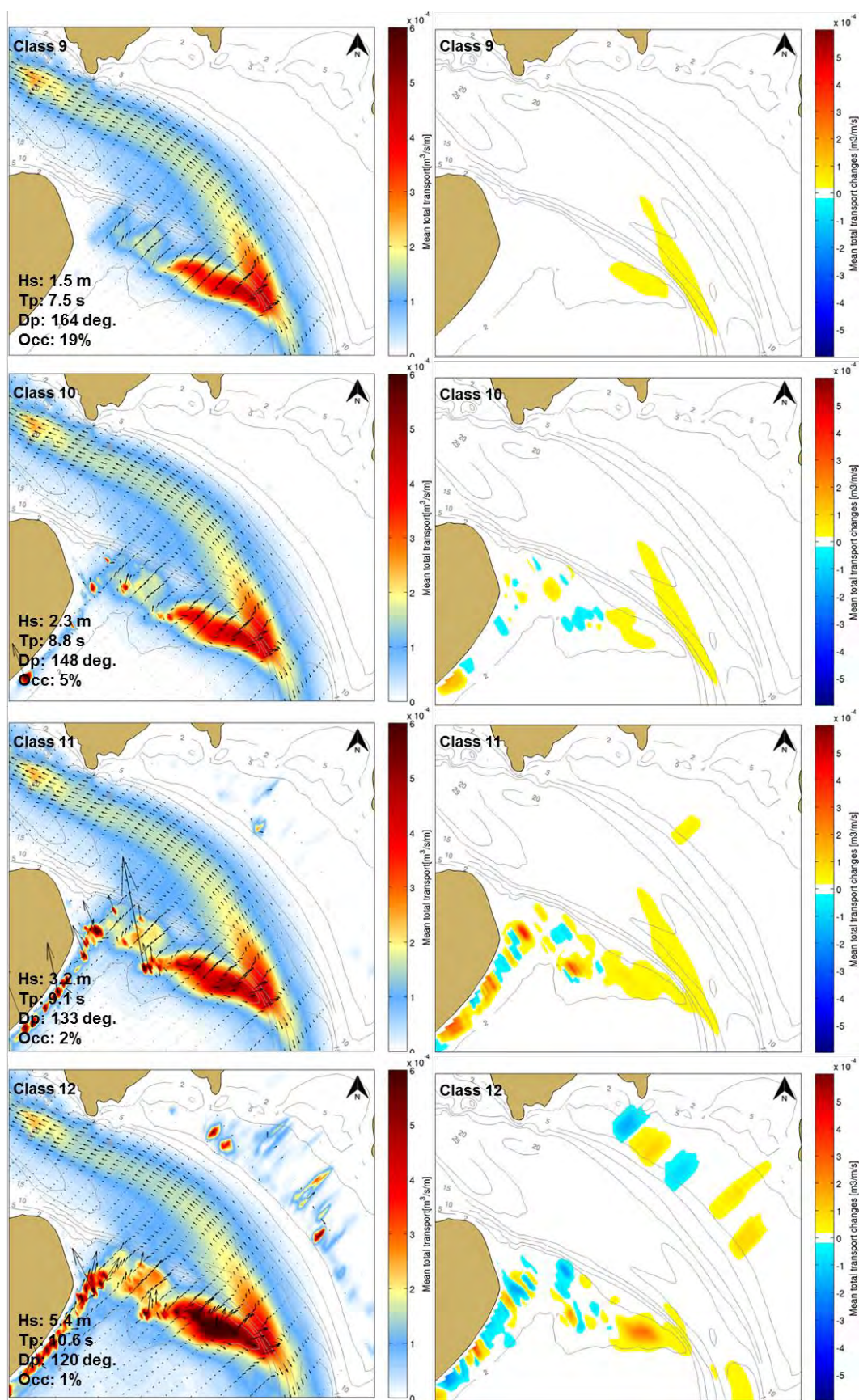


Figure 7.13 Mean net transport fluxes (left) and mean net transport differences (right) between pre- and post-dredge scenarios over one tidal cycle for Classes 9 to 12. A positive magnitude represents an increase.

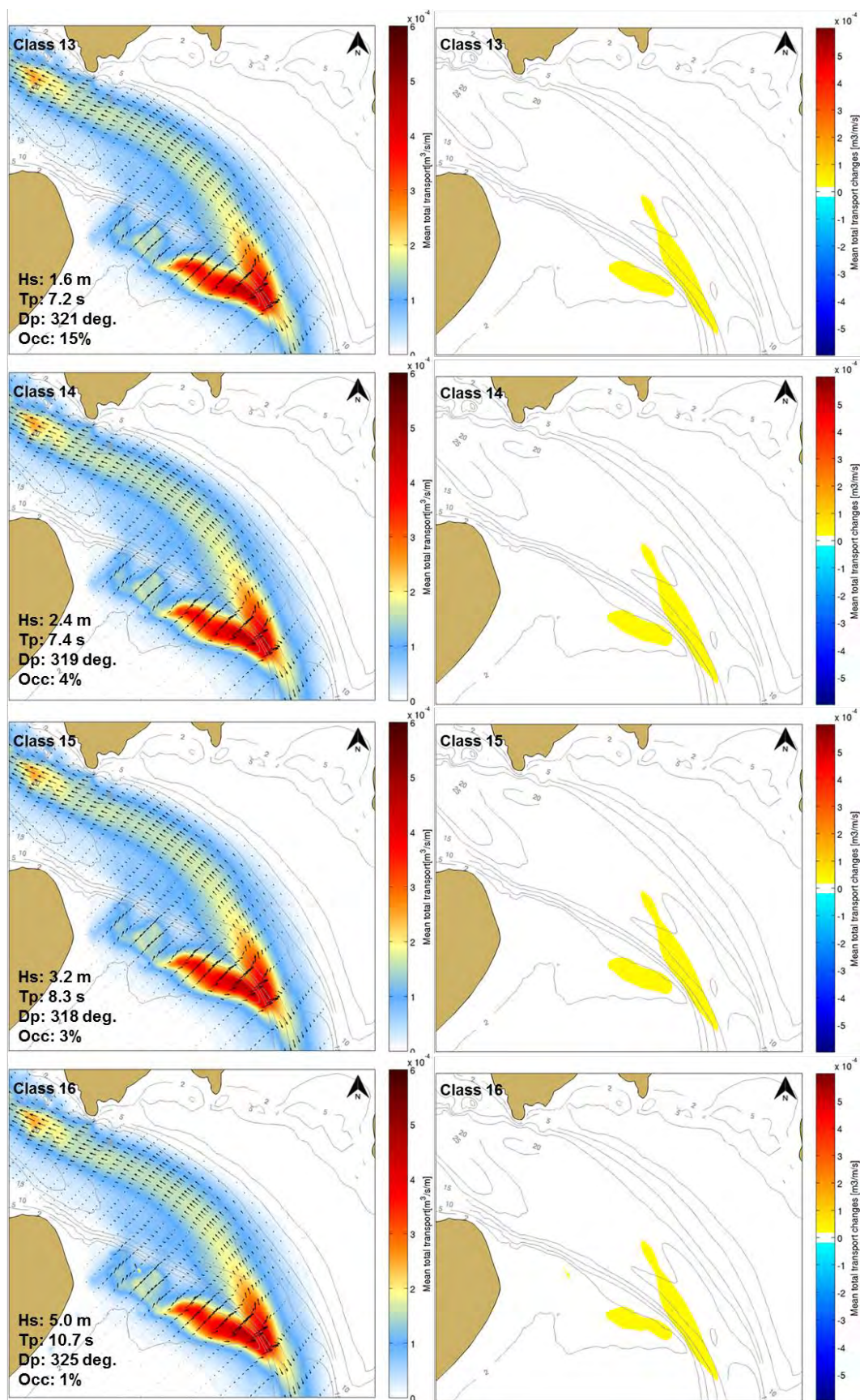


Figure 7.14 Mean net transport fluxes (left) and mean net transport differences (right) between pre- and post-dredge scenarios over one tidal cycle for Classes 13 to 16. A positive magnitude represents an increase.

### 7.3. Sediment dynamics

The adequate initialisation of spatially varying grain size distribution of bottom sediment in a process-based model is often constrained by a lack of appropriate field data for the entire model domain. In the present study, a synthetic simulation was initiated with a uniform sediment type distribution over two bed layers using 6 sediment fractions to replicate a realistic bed composition over the entire domain and thus avoid the problem of data constriction. This “sedimentological spin-up” was performed over a 6-month fair-weather period to promote the vertical and horizontal redistribution of sediment grain size fractions in response to the combination of tide-induced currents and low energy wave conditions, and thus recreate a realistic bed composition. The purpose of this technique was to provide the realistic bed composition required to initialise both the pre- and post-dredging simulations. The same bed composition was used for both configurations to allow comparison of model results. Note, however, that the “sedimentological spin-up” was also performed using the post-dredging bathymetry to investigate the resultant changes in the sedimentology due to potential changes in the tide-induced currents and wave conditions.

This section details firstly the final sediment grain-size distributions obtained for the existing configuration and some qualitative comparisons with the sediment sampling results over the navigation channel. Secondly, the pre- and post-dredging bed compositions were compared to assess the potential changes caused by the channel deepening on the sedimentology at the entrance to Whangarei Harbour.

#### 7.3.1. Bed composition generation (BCG) simulation

Sediment distributions for each fraction generated by the BCG run (i.e. 100, 150, 200 $\mu$ m...) are presented in Figure 7.15 to Figure 7.21. Note that this BCG run corresponds to the existing bathymetry. The BCG technique is fully described in MSL Report P0297-01.

The surficial sediment grain size distribution shown in Figures 7.15-7.21 illustrate a significant coarsening within the main channel. Most of the sandy material (between 100 and 500  $\mu$ m) is actively washed away from the channel. Fine sand is deposited at the outermost ebb-tidal delta lobe where ebb-directed current velocities decrease due to increasing water depths. This is supported by the sediment sampling results, where the fine sand fraction increases to 17% in the furthest offshore section of the channel.

The modelled channel bed was initially composed of medium and coarse sand particles. Field data showed the medium sandy sediment fraction to dominate the channel bed composition (~60%; Tonkin and Taylor, 2016) while modelled sediment distribution suggested a higher fraction of coarse sediments. This is probably related to the low frequency of sediment grain sizes between 500 and 1000  $\mu$ m in the bed composition initialisation. The presence of 500  $\mu$ m grain size material in the channel indicates that the overall bed shear stress exerted by tidal flows in the inlet throat is not much higher than the critical bed shear stress corresponding to medium to coarse sediment grain size. Adding fractions of grain size in the range of 500 – 800  $\mu$ m may limit the overestimation of the coarse sediment fraction within the bed composition of the channel. However, the BCG run was limited to seven sediment fractions because of the computational expenses related to the implementation of the bed stratigraphy module and the 3D mode in the model. Note that the shell fragment layers found in the sediment samples (Tonkin and Taylor, 2016b) were not considered in these simulations. Shell

fragments may shelter the underlying grains from the flow and thus reduce the erosion of medium grained sediments. The interactions between the biological, morphological and hydrodynamic components in the model do not allow a full reproduction of the frictional forces acting on the surface transport layer. This bias is nevertheless compensated to some degree by the morphological spin-up process which modifies the bed composition based on the modelled friction fields. However, the model reproduces the relative stability of the fine sediment layer observed over the southern bottom edge of the channel section located north of Mair Bank well. Measured data indicated the presence of 16% fine sand in the bed composition, which agrees qualitatively with the modelled top layer composition shown in Figure 7.15.

The dredged area adjacent to NorthPort berths was shown by the model to be particularly favourable for the deposition of medium grain size sediments. In the vicinity of the berth, medium and coarse sediment fractions dominated the bed composition in the channels while fine sediments were largely present over the different shoals. The overall modelled sediment pattern was consistent with the configuration described in Longdill and Healy (2007).

The high bed shear stress fields over the intertidal area of Mair Bank lead to rapid redistribution of sediments in this type of simulation. Over subtidal areas of the shoal, fine sediments entrained by tidal flows are transported offshore through the harbour. Medium grain size sediments are washed away from Mair Bank and deposited offshore. These results are not consistent with the sediment sampling reported in Williams and Hume (2014) which indicated a predominance of fine sand (~50%). Such discrepancies can be expected as the reduction of the bed shear stress provided by the shell hash layer and the biomass of pipi on the seabed cannot be reproduced in the model. The discrepancies clearly illustrate the morphological stability provided by the biological component on Mair Bank. The model showed a substantial amount of fine and medium sand sediments located along the harbour flank of the bank controlled by the flood-tidal flows. The southern margin of Mair Bank was predicted to show the largest range of sediment grain sizes from 100 to 1000  $\mu\text{m}$ , with a predominance of coarse sand.

The overall qualitative validation of the bed composition over the particular areas of the domain where sediment samples were available highlighted that it was difficult for the model to recreate the existing bed composition. Most of the results obtained with this technique were nevertheless coherent with the observations, although some differences were identified over specific sections of the channel or over Mair Bank. The armouring of both the channel and Mair Bank provided by the shell layer and the biomass of pipi is not fully resolved by the morphological model. However, the implementation of the “morphodynamic spin-up” technique introduces balancing mechanisms through the adaptation of the bed composition to the model bed shear stress, thus avoiding the occurrence of very large erosion processes in further simulations initiated with this synthetic bed composition. The main purpose of the BCG run is not to replicate the real sea bed composition but rather a sea bed composition that will allow realistic replication of sediment fluxes and depth changes over the domain, including the effect of the processes not implicitly resolved by the model.

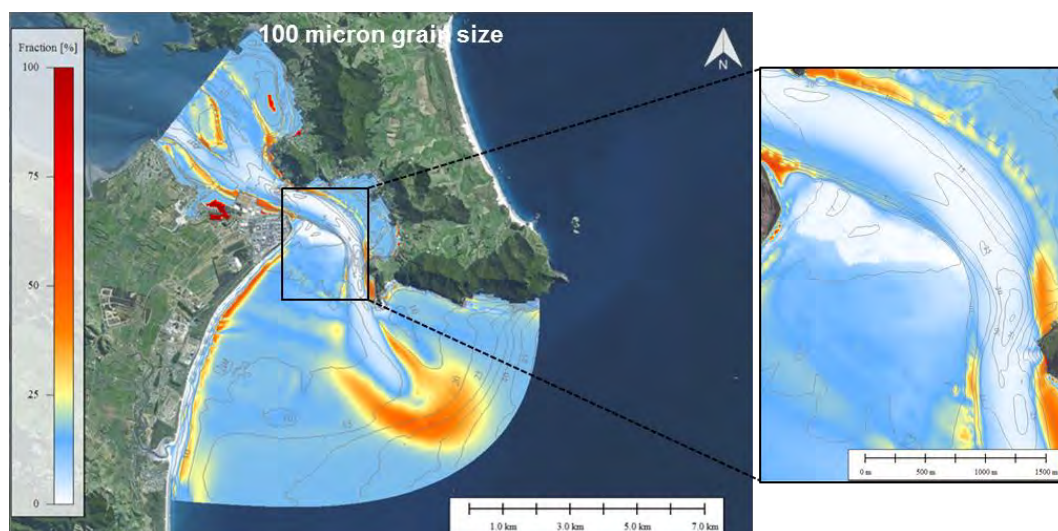


Figure 7.15 Distribution of 100  $\mu\text{m}$  grain size sediments in the active layer generated by the BCG run for a 6-month fair-weather period.

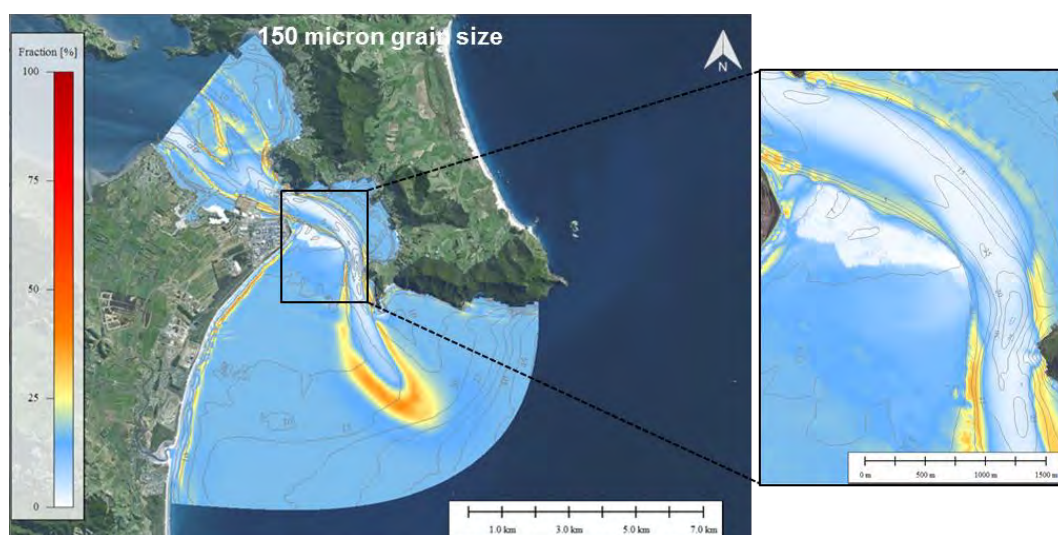


Figure 7.16 Distribution of 150  $\mu\text{m}$  grain size sediments in the active layer generated by the BCG run for a 6-month fair-weather period.

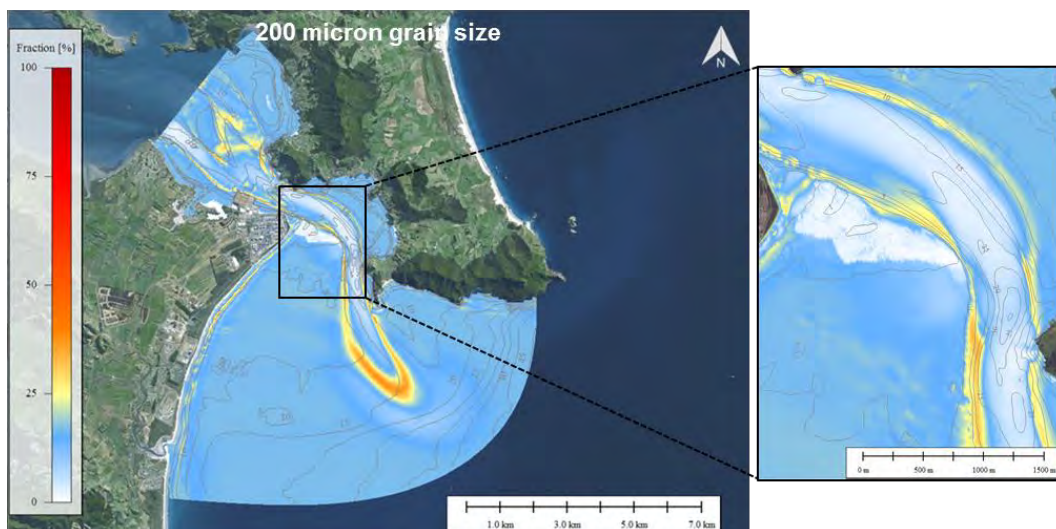


Figure 7.17 Distribution of 200  $\mu\text{m}$  grain size sediments in the active layer generated by the BCG run for a 6-month fair-weather period.

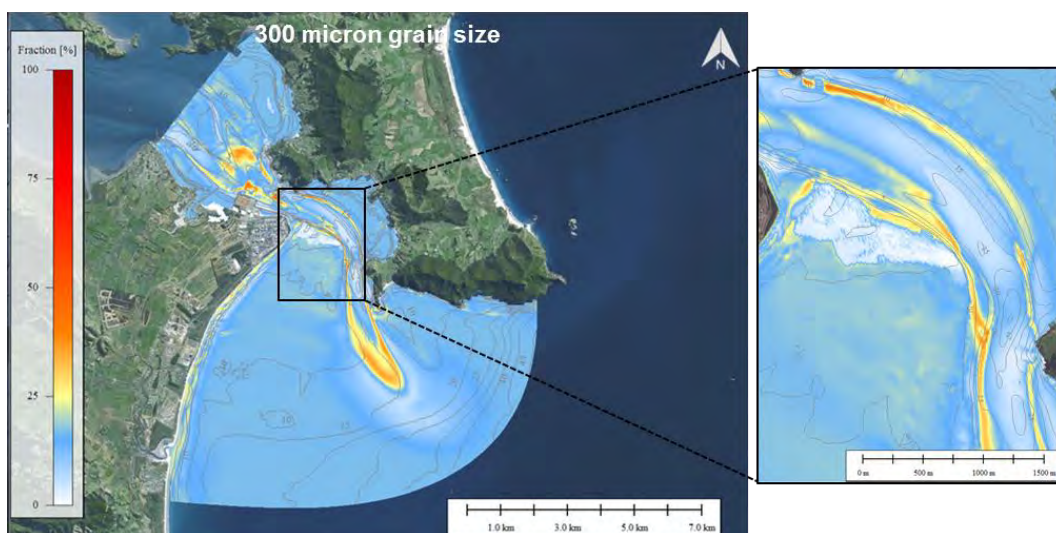


Figure 7.18 Distribution of 300  $\mu\text{m}$  grain size sediments in the active layer generated by the BCG run for a 6-month fair-weather period.

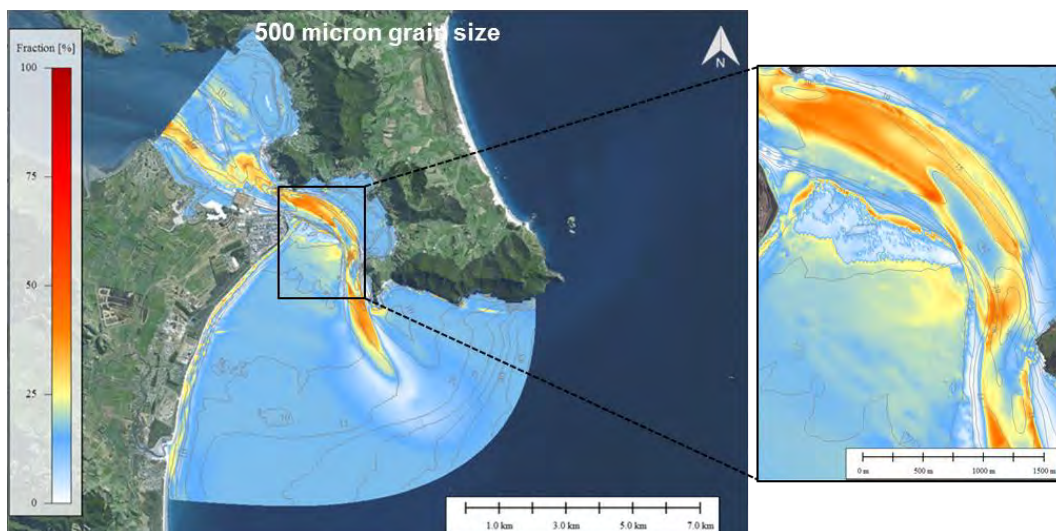


Figure 7.19 Distribution of 500  $\mu\text{m}$  grain size sediments in the active layer generated by the BCG run for a 6-month fair-weather period.

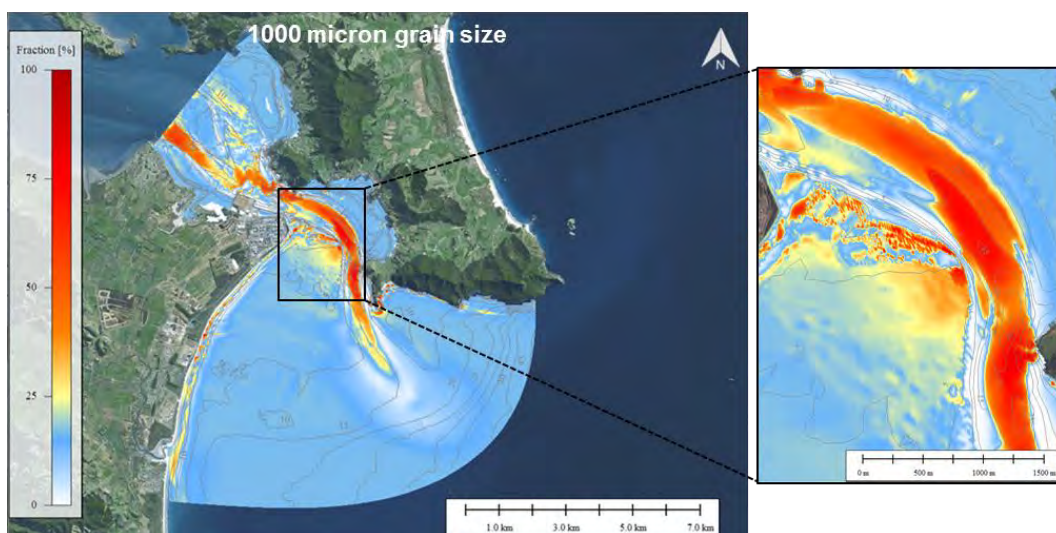


Figure 7.20 Distribution of 1 mm grain size sediments in the active layer generated by the BCG run for a 6-month fair-weather period.

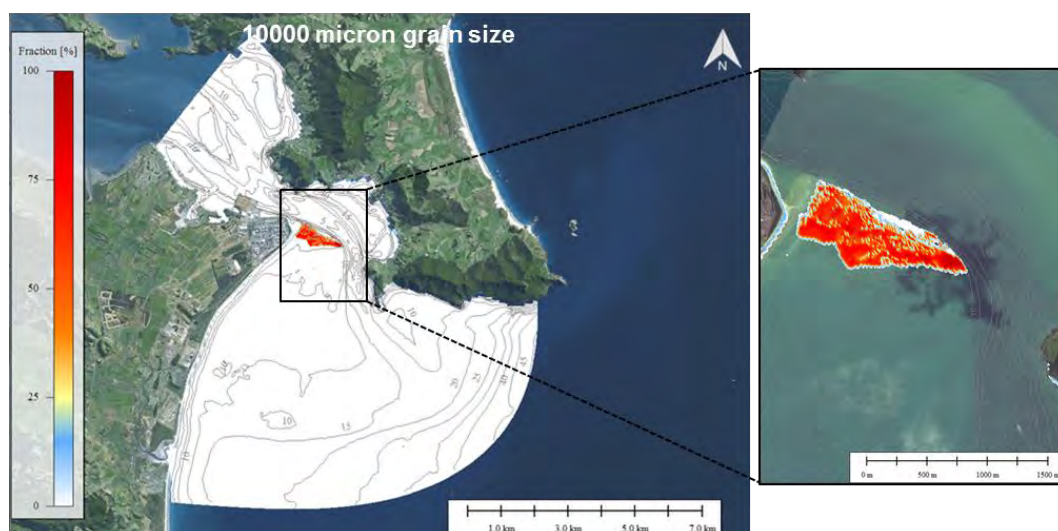


Figure 7.21 Distribution of 10 mm grain size sediments in the active layer generated by the BCG run for a 6-month fair-weather period.

### 7.3.1. Predicted changes in the spatial distribution of sediment fractions

The complex interplay of tidal and wave driven forces in the entrance region leads to characteristic spatial changes in the sediment grain-size distributions. Some of this has been described in the field report on the seabed survey (Tonkin and Taylor, 2016b). In this section the numerical model was used to examine the underlying processes that lead to grain-size sorting, applying the same technique to the existing state and the deepened channel scenario. A comparison of the results of those simulations is provided in Figure 7.22 for the various sediment grain size fractions. The results indicate that the overall changes in grain size sorting are very subtle and less than about 5%. Isolated areas with larger changes in grain sorting correlate directly with the magnitude of the deepening. For example, within the outer part of the channel the increased depth is predicted to increase the finer (100  $\mu\text{m}$ ) grain size fraction due to the reduced tidal flows. The realignment and deepening near Busby Head has a similar effect on the 200  $\mu\text{m}$  fraction. Conversely, the slight changes to the wave climate due to refraction on the channel margins reduce the fine fractions in some areas and increase them in other. These subtle changes in the sedimentology described in this section are predicted to be constricted to discrete zones within the entrance system and are not expected to be discernible in the context of long-term morphological changes.

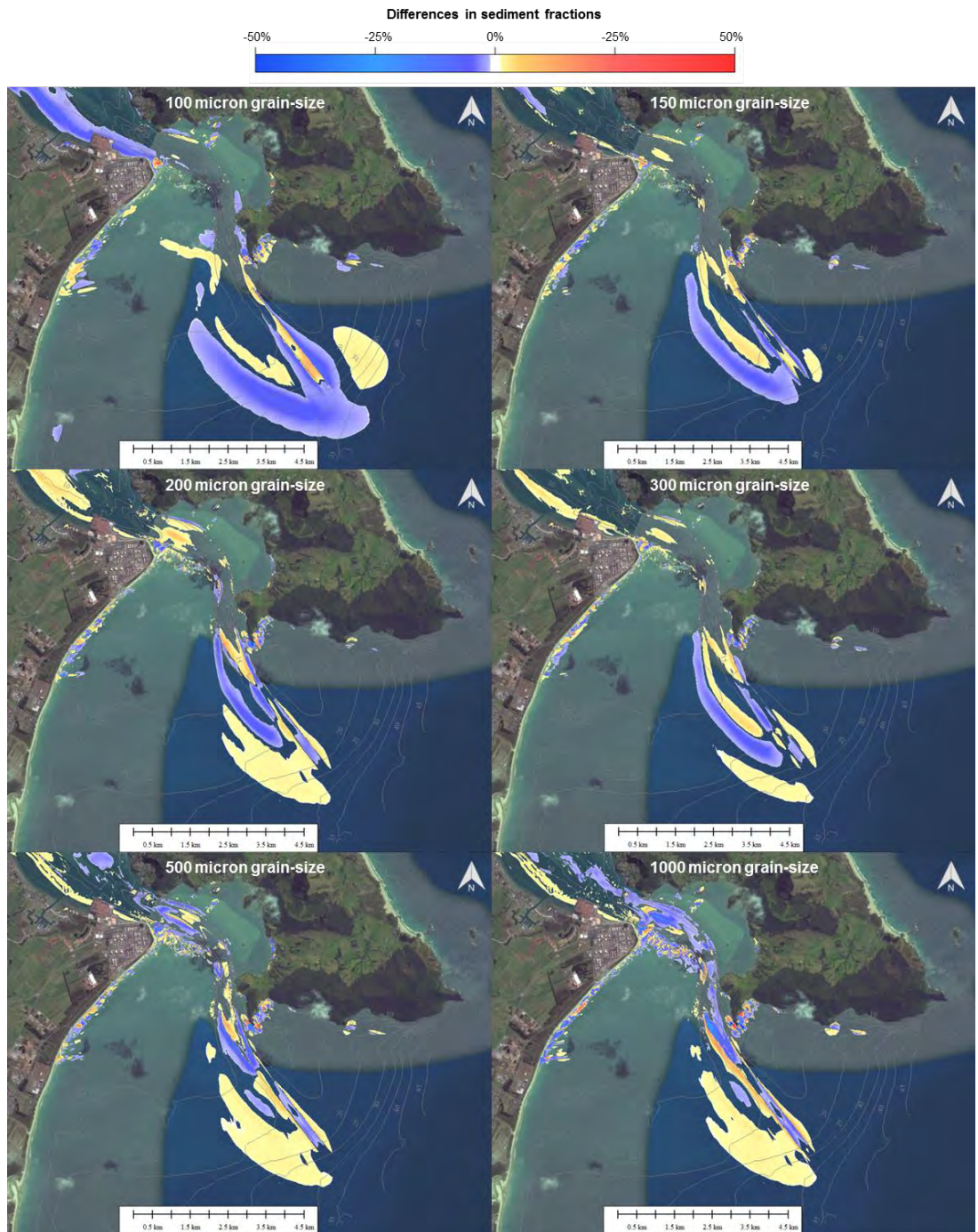


Figure 7.22 Differences in spatial sediment fraction distributions. Positive amplitude indicates an increase of the given sediment fraction in the post-deepening configuration.

## 7.4. Predicted morphological changes

A sequence of storm and fair-weather conditions was used to examine the evolution of the sea bed at the harbour entrance. An historical 21-day period was used for this purpose.

During storm wave conditions (i.e. peak conditions for the existing environment shown in Figure 7.23), significant morphological and sedimentological adjustments occur along Ruakaka Beach and east of Busby Head due to increased sediment transport fluxes (Figure 7.24) generated by refracted waves. This is clearly highlighted by the patterns of accretion (red colour) and erosion (blue colour) along Ruakaka Beach and at Busby Head in Figure 7.25. The residual bed load transport is predominantly directed southward. The erosion of the northern section of Ruakaka Beach during episodic storm events is counteracted by the replenishment of the nearshore regions during the fair-weather conditions (Figure 7.26). Within the channel itself, however, the model predicts more influence from the tidal flows under the fair weather condition than under stormy conditions. This indicates the dominance of the tidal regime on the sediment dynamics. Modelled morphodynamic results exhibit subtle change (in the order of cm) in the channel. Lag deposits of shell effectively armour the seabed and change the hydraulic roughness and the model can only mimic that with an increased grain size in defined areas. Nonetheless, the model remains a useful tool for the integration of the highly non-linear aspects of the sediment transport dynamics, and the direct comparison of the deepened channel with the existing environment is a valid technique to identify potential effects.

Comparison of the predicted morphological changes from the storm and fair weather simulations are presented in Figure 7.27 to Figure 7.32. The results show:

- The outermost section of the channel to the southeast of Busby Head is predicted to infill in the order of few cm over the 21-day period under the sequence of stormy and fair-weather conditions.
- Adjacent to Busby Head, the morphological changes suggest increased critical bed shear stress due to an increase in wave energy directed at this area in a storm caused by enhanced refraction along the eastern margin of the dredged channel. This environment is occasionally subjected to 4-m wave heights during storms. However, photos of the sea bed presented in the Kerr & Associates Report - Ecology Stage One Pilot Study (2016) indicate the seabed comprises coarser sediment than modelled, with a sandy / shelly / gravel sediment top layer near Busby Head. Considering such bed composition, changes in wave height due to the channel deepening are not expected to have a significant influence on the morphodynamics near Busby Head.
- Morphological changes along the northern section of Ruakaka Beach suggest that the migration patterns of shore-oblique sand bars during storm events will be modified, but this is a minor spatial adjustment and not a fundamental change to the overall sediment budget.
- Increased tidal flows between Marsden Bank and Mair Bank are predicted to limit the accretion of sand in this area. This phenomenon may be of importance given the historical observations have highlighted the formation of a marginal channel in this area.

- Subtle changes in the tidal and wave-driven currents over the eastern part of Mair Bank may result in zones of deposition and erosion on the toe of the Bank. Note that the historical survey data have shown that this area is dynamic and that natural bed variability of the order of 0.5 m already occurs.

Overall the conclusion drawn from the sediment transport simulations is that the channel deepening produces a minor redistribution of the sediments, but does not create a change to the governing dynamics. While storm events produce localised changes, it is the tidal regime that dominates over time, acting to smooth out the storm changes as well as mobilise large areas of the delta. The deepening slightly reduces the peak velocities within the channel and slightly increases the velocities on the areas adjacent to the channel. However, large areas of the channel are presently armoured with shall lag and in these areas the sediment transport flux potential is very high and the mobile sediments are entrained for a high percentage every day (see Figure 7.11 and Figure 7.12).

The short-term erosion/accretion patterns modelled over Mair Bank during storm and fair-weather conditions reflect the general consistency between the model and the observations presented in Section 2. The wave action over the southern margin of Mair Bank appears to lead to a slow landward net transport as described in Morgan et al. (2011). The extended accretion pattern for wave conditions over the intertidal area of Mair Bank is difficult to interpret as the morphodynamics in this region are highly related to the biological component. Indeed, the elevation of the ridges observed in Morgan et al. (2011) were interpreted as the migration of the shell swash bar. The gravel layer defined on the top of Mair Bank in the model to mimic the biological component seems to reproduce this behaviour leading to steeper lee slopes on the northern margin of the bank. The bathymetry changes observed between 2011 and 2015 suggest a strong inter-annual variability of this accretion pattern. This may be due to the impact of cyclones on the wave climate which generate wave heights of up to 1.5 m adjacent to Mair Bank leading to a strong erosion of the sand bank over a very short period of time.

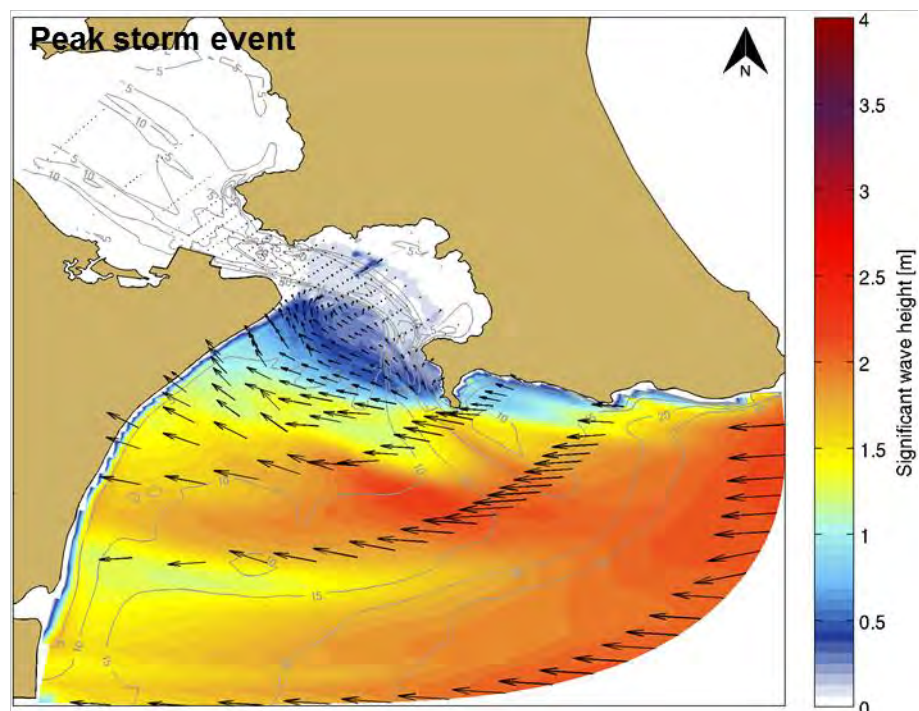


Figure 7.23 Wave height fields during storm event. Black arrows indicate the peak direction.

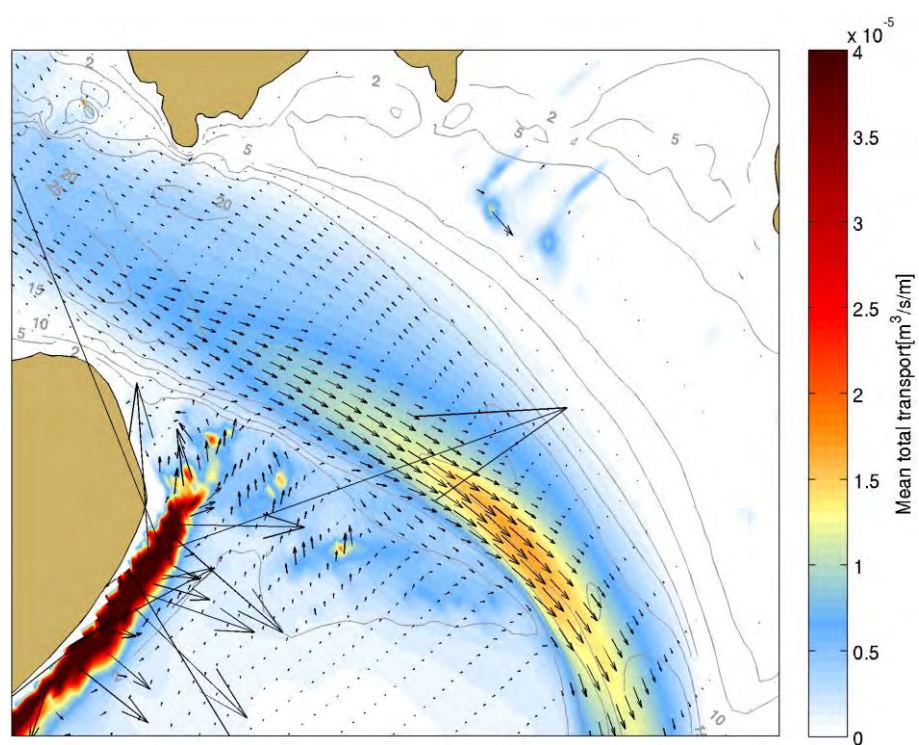


Figure 7.24 Mean total transport calculated during the 5-day storm period. Note that sediment transport was calculated over a complete number of tidal cycles (peak to peak).

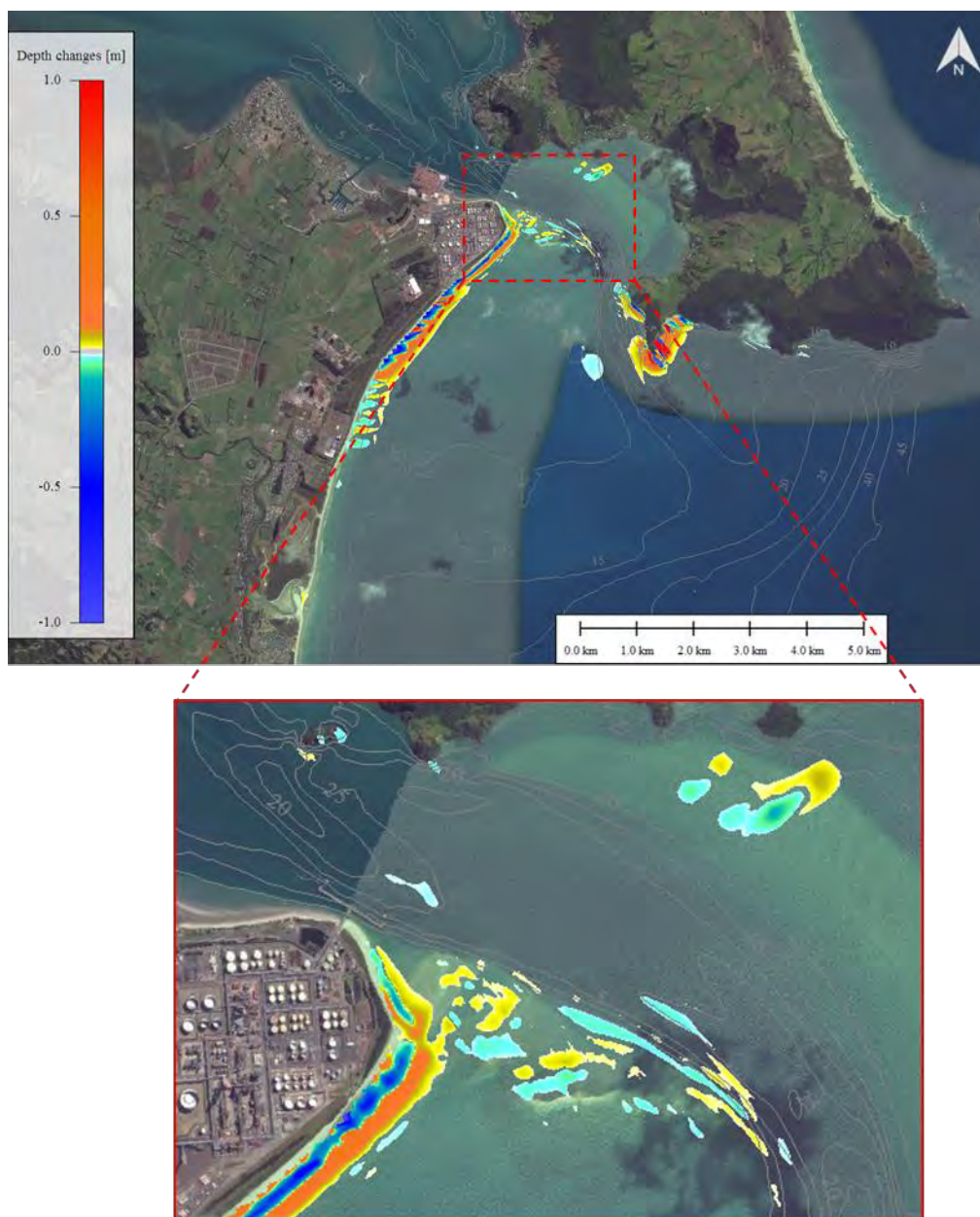


Figure 7.25 Simulated depth changes after 5 days of storm conditions. Positive and negative magnitudes indicate sedimentation and erosion patterns, respectively.

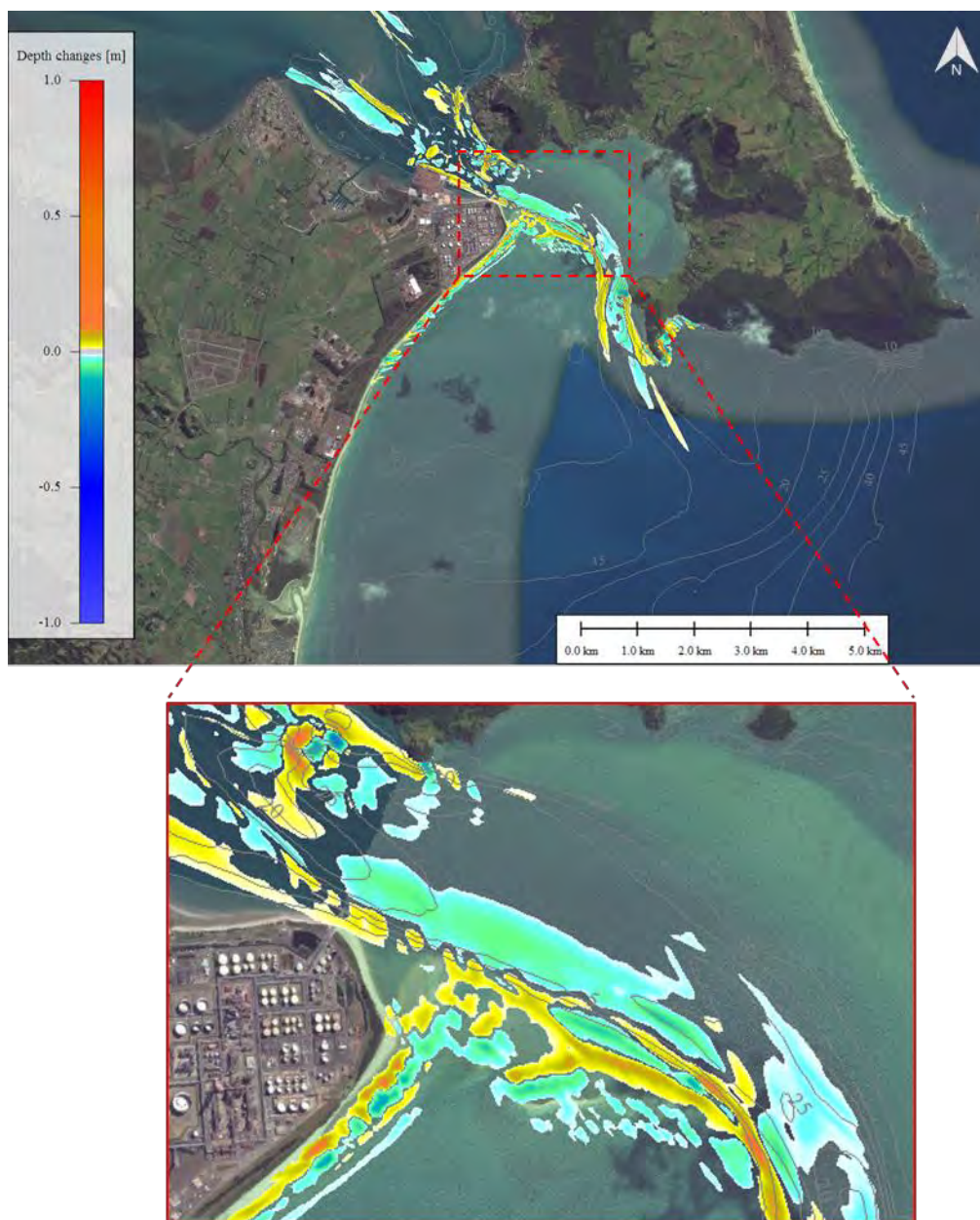


Figure 7.26 Simulated depth changes after 16-day simulation of low energy waves. Positive and negative magnitudes indicate sedimentation and erosion patterns, respectively.



Figure 7.27 Changes in sedimentation and erosion patterns over the study area between the existing and post-deepening configurations over a 5-day storm event.

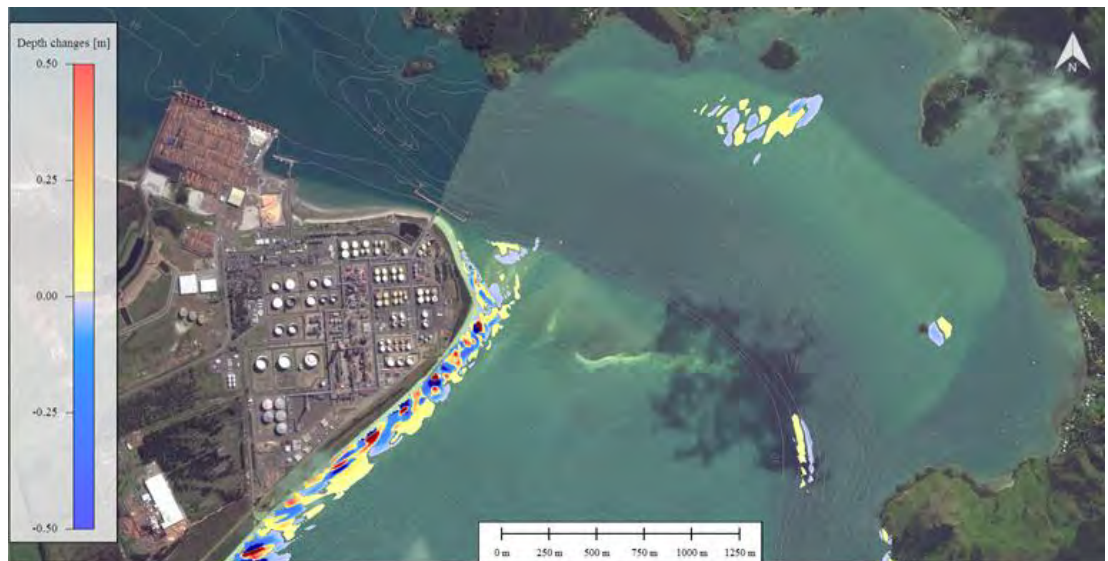


Figure 7.28 Changes in sedimentation and erosion patterns over the entrance to Whangarei Harbour between the existing and post-deepening configurations over a 5-day storm event. Zoom.



Figure 7.29 Changes in sedimentation and erosion patterns over the study area between the existing and post-deepening configurations over a 16-day fair weather event.

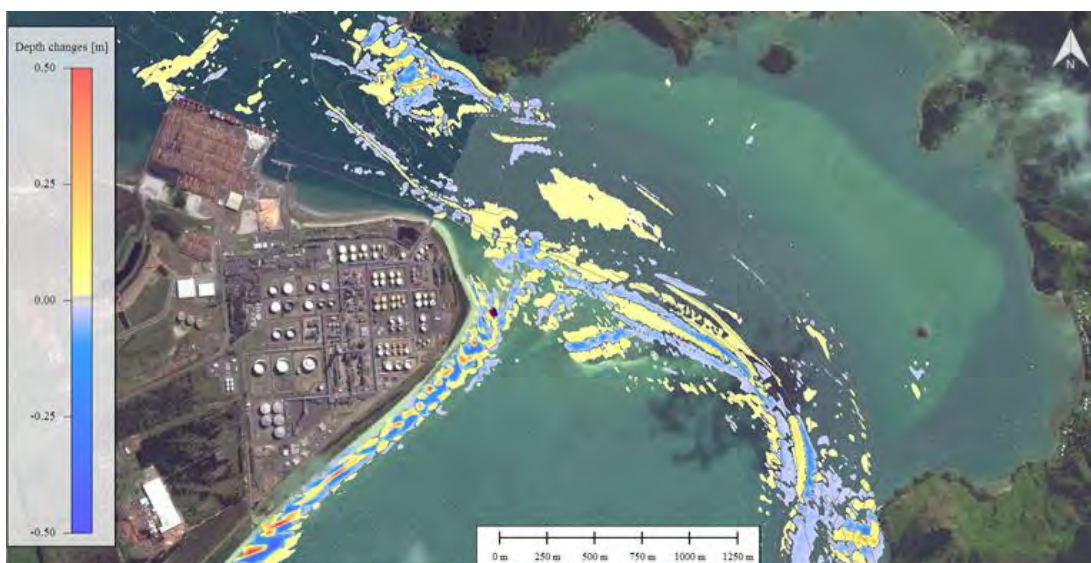


Figure 7.30 Changes in sedimentation and erosion patterns over the entrance to Whangarei Harbour between the existing and post-deepening configurations over a 16-day fair weather event.



Figure 7.31 Changes in sedimentation and erosion patterns over the study area between the existing and post-deepening configurations over a 21-day sequence of storm and fair weather conditions.

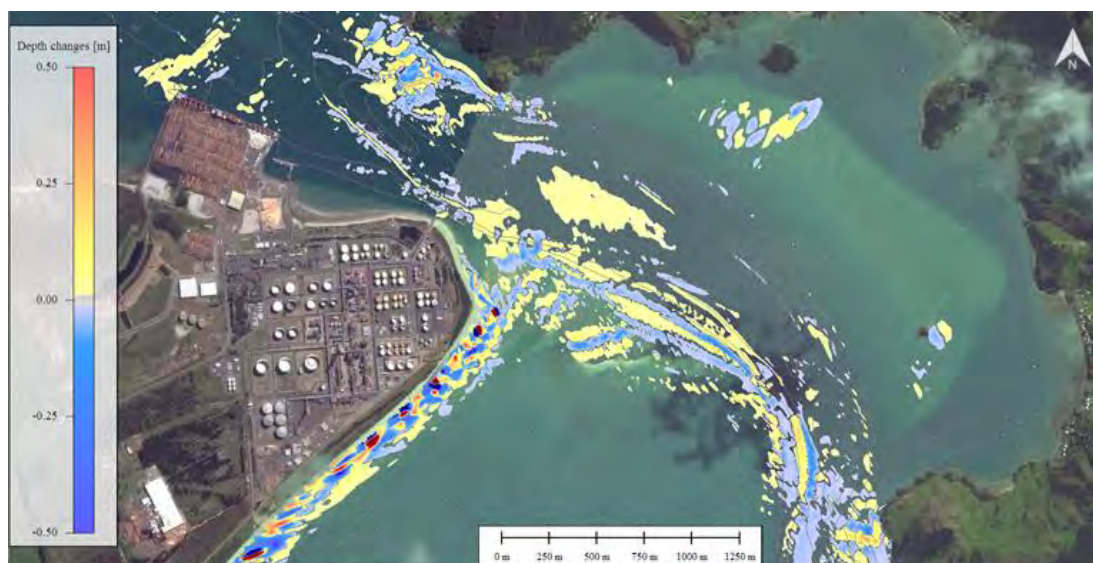


Figure 7.32 Changes in sedimentation and erosion patterns over the entrance to Whangarei Harbour between the existing and post-deepening configurations over a 21-day sequence of storm and fair weather conditions.

## 7.5. Estimates of channel infilling

Infilling of the deepened channel is expected to occur in some areas, and this will likely require a maintenance dredging programme to maintain the navigable design depth over time. While the historical 21-day simulation, which included both stormy and calm weather periods, indicates accretion of the order of a few centimetres in discrete parts of the channel, these results cannot simply be multiplied out to infer the annual accretion rate. First, there will be a period of adjustment as the margins of the new channel adjust to the new hydrodynamics. Then, the sequence of storms and daily tidal entrainment will actively redistribute a fraction of the mobile sediments. Finally, the source of sediment for infilling is primarily the adjacent ebb tidal delta. Interpretation of the model simulations and analysis of the historical observations suggest there will be two areas of channel accretion:

The first is the deepened area immediately adjacent to the Marsden Point jetty. Here the tidal flows are predicted to reduce by around  $0.10 \text{ m.s}^{-1}$  and survey data shows over-wash of sediment from the ebb tide shoal. The sedimentation process at this location will be tidally dominated and relatively constant. The likely evolution pattern will be accretion from the southern shore of the ebb tidal delta outward into the main channel. This is different to the ebb tide migration of sand waves within the central channel, which is a phenomenon reported in the contemporary survey data. Based on the results provided by the short- and medium-term simulations, such accretion within the central channel is not expected to exceed 10 - 15 cm per year.

The second is the area within the offshore extent of the channel, south of Busby Head toward the distal margin. Here, the deepened channel is exposed to diffusive infilling from wave action but notably there are no strong cross-channel fluxes to drive rapid asymmetric infilling, as observed at other ports such as the Otago Harbour entrance (Weppe et al., 2015) and Port Taranaki (McComb et al., 1999). However, a change in the location and focussing of the ebb tide jet is predicted, and also in the magnitude of wave-driven currents near Busby Head. The source of infilling material to the channel is the immediate channel margins and the adjacent delta, and the rate of accretion is expected to decrease over time until equilibrium is reached.

A simulation of the annual infilling for the outermost section of the channel (i.e. from Busby Head to the distal margin) was made for the existing and the deepened channel. The difference in infilling is presented in Figure 8.33, and it highlights the two infilling processes in operation. Over this region, the interactions between biology and physics are not as critical as observed for other parts of the harbour entrance, thus allowing a more accurate medium-term prediction of the infilling processes. For the southern half of this section of channel, the accretion pattern is symmetrical and caused by diffusive sedimentation under wave action, with material being sourced from the adjacent areas of the delta. For the section immediately south of Busby Head, the accretion pattern is highly asymmetrical, with infilling occurring on the eastern side in response to the increased wave driven flows in storm conditions, as described in Section 4.2.

The anticipated post-dredging infilling rate over the section of the channel between Busby Head and the distal margin is  $86,000 \text{ m}^3$  per year (based on a 0.4 - 0.8 m infilling along the flank of the channel and 0.1 m at the centre), with a margin of error of  $\pm 36,000 \text{ m}^3$  per year. This margin was derived from the infilling predicted by the model for the existing channel, which in fact is stable and has not shown historical accretion. A practical volumetric estimate following establishment of an

equilibrium after several years would be 50,000- 100,000 m<sup>3</sup> per year, which corresponds approximately to 1 – 3 % of the total capital dredging volume.

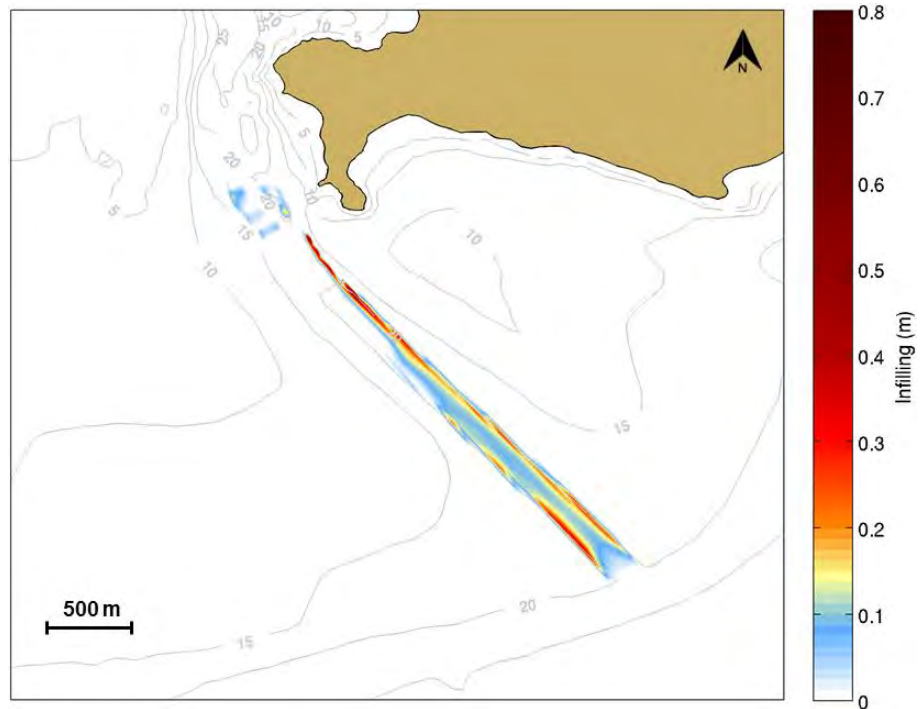


Figure 7.33 Predicted infilling in the outermost section of the channel between Busby Head and the distal margin to the delta estimated from a 1-year simulation including the post-dredging bathymetry.

## 7.6. Summary of effects on sediment transport

Several techniques were used to investigate the potential changes to the harbour entrance as a result of deepening. The first technique was to use a sediment transport pathway approach in which the spatial distribution of the important sediment fractions was simulated over a 6-month period. The second technique was to estimate the effect of a deeper channel on the potential sediment fluxes for a single representative sediment grain size. The third technique consisted of running a sequence of storm and fair-weather conditions over a 21-day historical period to simulate the cumulative morphological changes with a realistic seabed composition. Using these numerical techniques, changes in the erosion and accretion patterns were examined to allow a qualitative estimate of the effects of channel deepening. The findings are as follows:

- The sediment dynamics of the harbour entrance, controlled by the tide-induced currents and waves, are not expected to be fundamentally modified by the channel deepening project. The anticipated changes in the sediment transport fluxes are predicted to occur in spatially discrete zones and are expected to appear negligible compared to the total net sediment transport fluxes occurring through the main channel between the harbour and the open-ocean region.
- The morphodynamics of Mair Bank are largely influenced by the bio-stabilisation provided by live shellfish and their residual shell fragments. This bio-stabilisation is expected to have a more significant effect on future evolution of the Bank than the effect predicted by the proposed channel

deepening. The numerical model results infer that the shell armouring allowed Mair Bank to prevail in the presence of an energetic tidal regime and large temporal and spatial gradients in wave energy, consistent with historical observations and the wealth of previous investigations of this area. While the complexity of the interactions between the biological, morphological and hydrodynamic components do not allow quantitative predictions to be made with confidence, the model studies have confirmed the significance of the biomass of shellfish on the enduring stability of Mair Bank. Inside the high flow areas of the main channel the coarsening of the seabed by shell lagged sediments provides significant armouring and resistance to erosion. Within this context, and constrained by the model limitations, the simulations have reproduced the overall stability of the channel and the ebb tide delta. The stability of Mair Bank is largely controlled by the bio-stabilisation provided by the inhabiting populations of shellfish. The studies undertaken do not indicate that deepening within the channel will significantly change the sedimentary outcomes on Mair Bank.

- The sedimentary stability of Ruakaka Beach is not expected to be influenced by the slight variation in the wave conditions caused by channel deepening.
- Enhanced wave refraction along the eastern ridge of the channel may increase the potential "erodibility" of the seabed around Busby Head. However, this effect is likely to be mitigated by the sandy shelly-gravel top layer of the seabed, rendering it relatively high resistance to suspension and bedload transport processes. This assertion is further supported by the fact that Busby Head is currently occasionally subjected to 4-m wave height suggesting a relative high degree of stability of the sea bed.
- Sedimentation is expected to occur immediately adjacent to the Marsden Point jetty. Here, the tidal flows are predicted to reduce and the tidal asymmetry is expected to promote infilling of the deepened areas over time at a relatively constant rate. While a reliable volumetric estimate is difficult to provide, the likely evolution pattern will be accretion outward from the southern shore.
- A degree of infilling at the toe of Mair Bank may occur where the channel has been realigned.
- A 1-year simulation of the infilling of the channel south of Busby Head toward the distal margin was made. The results confirm a programme of maintenance dredging will likely be required for ongoing navigability. At this location, the deepened channel is exposed to diffusive infilling from wave action and there is a predicted change to the location and width of the ebb tide jet along with an increase in the sediment flux from the adjacent channel margins. The source of infilling material to the channel is the adjacent delta, and the rate of accretion is expected to decrease over time until equilibrium is reached. The infilling of this area is predicted by the model to be 86,000 m<sup>3</sup> per year with a margin of error of ±36,000 m<sup>3</sup>/year. A practical estimate of infilling rates after several years is 50,000-122,000. m<sup>3</sup>/year.

## 8. DREDGING PLUMES

The dispersion of a plume caused by dredging activities was simulated at several sites along the dredged channel design using the ERCORE lagrangian particle modelling technique developed by MSL, forced by tidal currents provided by the SELFE tidal nearshore model. A detailed description of the processes that give rise to a plume for each dredger is provided in MSL Report P0297-01. The model settings considered include the typical type and size range of dredging vessels that might be used on the Crude Shipping Project. The plume dispersion associated with two different (large and small) trailing suction hopper dredgers (TSHD), one cutter suction dredger (CSD) and one Backhoe Dredger (BHD) was simulated in the present study. Different production and discharge rates were used for each dredger, leading to differences in the predicted plume dispersion. In this section, probabilistic assessments of the dispersion dynamics are provided for the dredging and overflow scenarios during the channel deepening operations.

As discussed in MSL Report P0297-01, the TSHD is the preferred option for the dredging operations. The use of a CSD at the jetty pocket and within the inner section of the channel was included in the present study for completeness in case it is required as an option. BHD operations will be restricted to the jetty pocket. Consequently, from the nine sites tested for the TSHD dredge plume modelling, only one site located in the proposed jetty pocket was set up, examining the potential effects of using a CSD and a BHD. The sediment release associated with the CSD was predicted to be confined to the near bottom layer due to the effect of the rotating cutter head. No overflow or propeller source terms were considered for this dredger (see methodology in MSL Report P0297-01). The large TSHD configuration was considered a worst case scenario, which is why only one site was tested for the CSD as the CSD generated plumes were proven to fall within the small and large TSHD plume effect ranges.

### 8.1. Dredging plume modelling results

A large number of scenarios were simulated representing typical conditions. A selection is provided here, while all the results are included in Appendix D. Specific areas including Marine Management Areas (as identified within the Operative Regional Coastal Plan), Marine Reserves and sensitive areas have been considered (see Figure 8.1) to show the limited impact of the dredging on the environment.

The results for the TSHD dredging and overflow stages in the present section are based on a 3% production rate for the drag head source and the maximum period of overflow (79 or 95 minutes depending of the size of the dredge). This is a conservative approach which aims to provide results for the “worst case” outcome. The modelled plume dispersions considering a 1.5% of production rate for the drag head source are provided in Appendix D.

The discharge rate associated with the rotating cutter head (CSD) was set up based on a 5% production rate near the bottom. This corresponds to the upper value of the range proposed in the literature. The bucket source term associated with the BHD was defined using a 4% discharge rate over the entire water column due to the excavation, hoisting and slewing phases during the dredging operations.

The exact timing of the dredging operations is unknown and will depend on a range of factors such as weather conditions, tides, or other time-dependent factors (e.g.

travel to and from disposal site, maintenance etc.). In that sense it is not meaningful to predict a suspended sediment concentration (SSC) time history over a defined period. Instead, a more informative way is to employ a probabilistic approach whereby the entire range of hydrodynamic forcing conditions are considered and from this produce a robust description of the range of SSC plumes that could be expected at a given site, for a given aspect of the operation.

Sediment releases associated with dredging and disposal operations may cause a significant increase of the turbidity over the adjacent areas affecting the light penetration, and consequently the adjacent ecological communities. In this context, a complementary literature review of the existing ecological systems and water quality was undertaken in Brian T. Coffey and Associates Limited (2016a) to provide a solid background for the environmental impact assessment of the Crude Shipping Project. Different levels of disturbance associated with the proposed dredging and spoil disposal activities were provided in Brian T. Coffey and Associates Limited (2016b) to support the interpretation of the dredge and disposal plume modelling results. On this basis, a minimum 12 mg/L SSC threshold was applied to delimit the plume dispersion. Such threshold corresponds to the difference between the 15 NTU level 2 Response Limit (based on one-hour average) indicated in Brian T. Coffey and Associates Limited (2016b) and the 3 NTU existing background level considering a 1:1 relationship between SSC and Turbidity. This linear relationship was established by Stewart (2017) analysing vibrocore samples from the dredging footprint. This methodology aims to assess the predicted SSC levels based on the level of tolerance for the adjacent communities, and thus to status on the degree of disturbance for the existing ecology. Details about the levels and the methodology applied to determine these thresholds are provided in Brian T. Coffey and Associates Limited (2016b).

In Whangarei Harbour entrance, where tidal forcing dominates, two complete spring-neap tidal cycles were used as a reference period to produce the probabilistic SSC plumes associated with the dredging and overflow phases. The SSC plumes were obtained by overlaying the successive particle clouds throughout the 28-day period and computing the SSC fields based on the combined particle clouds. These were computed for the dredging-only phase (i.e. no overflow) and also the four overflow durations, i.e. 10, 20, 50 and 79 minutes for the large TSHD. For the small TSHD, the overflow durations were 10, 20, 50 and 95 minutes. Probabilistic SSC plumes associated with the TSHD for both the dredging and the overflow phases at sites R0, R1, R5 and R6, for the existing hydrodynamics, are given in Figure 8.2 to Figure 8.5. The locations of the sites are shown in MSL Report P0297-01. Comparison between tidal and residual current velocities at the outermost sites R4 and R5 are provided in Appendix C. Although the non-tidal component is somewhat more significant at the seaward entrance of the delta than inside the channel, the tidal component remains dominant, which justifies the use of the *tide-only* nearshore model to force the particle tracking model. Moreover, the occasional high wind-driven flow acceleration highlighted by the non-tidal time series corresponds to storm events. Periods such as these are typical of storm events associated with high waves and strong winds and would not permit any dredging operations.

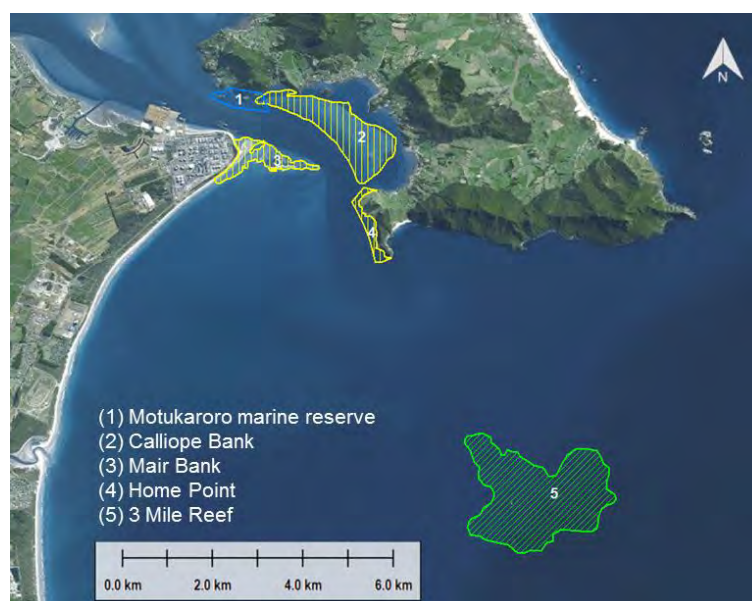


Figure 8.1 Location of the sensitive areas considered for the investigation of the dredging plume dispersion. The blue, yellow and green polygons depict Marine Reserves, Marine 1 (Protection) Management Areas and sensitive areas, respectively, used for the mapping of the dredging plume modelling results.

- Plumes associated with the use of large TSHD

The results show that SSC plumes produced by the drag head are constrained within the lower water column (bottom layer on plots), with negligible SSC levels predicted at mid-water and surface levels. In contrast, the overflow SSC plumes were widely spread across the entire water column, primarily due to the shallower release point and larger quantity of sediment involved.

The plume predictions exhibit considerable variation along the channel; consistent with the tidal flow regime. The plumes follow the channel orientations at sites R0, R1, and R6 while the patterns becomes more elliptical at site R5 where the tidal currents are less bi-directional due to increasing water depth near the delta entrance. Note that the dredging and overflow activities associated with the large TSHD generate larger SSC plumes than with the small TSHD. The maximum extension of the SSC plumes over a 24 h period do not exceed 1200 m at any of the sites examined (considering a minimum threshold of 12 mg/L), and are all constrained within the navigation channel. There is no dispersion of the plume over the adjacent beaches, sand banks, Marine Management Areas and Marine Reserves.

The overflow phase consists in releasing a highly concentrated mixture of water-sediment to maximise the amount of sediment stored in the hopper. The process is generally highly turbulent and will result in suspended sediment within the entire water column. The predicted SSC plumes associated with different overflow periods at sites R0 and R1 are illustrated in Figure 8.6 to Figure 8.9; the overflow duration has a significant effect on the magnitude and extent of the SSC plume.

The difference in the predicted SSC plumes between the existing channel and the post-dredging channel at sites R2 and R3 are illustrated in Figure 8.10 to Figure 8.13. A deeper channel results in a reduced excursion of the plume, as the tidal velocities are slightly decreased. This is particularly evident at site R3 where the

SSC plume dispersion due to the ebb-tidal flows is much more constrained in the post-dredging scenario than in the existing channel one.

The sensitivity analysis undertaken to examine the effect on the predicted plume dispersion of higher silt fraction (10%), lower settling velocity (0.4 mm/s) associated with silt particles and different release extensions (cylinders of 20 m x 100 m and 40 m x 60 m) during overflow did not reveal any fundamental changes in the plume dispersion as shown in Appendix H. The low fraction of silt particles within the tested release (from 5 to 10%) explains largely the relative low impact of these conservative parameters on the plume delimited by the 12 mg/L threshold.

- Plumes associated with the use of CSD

The results show that SSC plumes produced by the rotating cutter head are constrained to the bottom layer of the water column (Figure 8.14), with a relative small horizontal extension (< 200m) due to low current velocities near the seabed. The use of floating pipelines to discharge the sediment sucked up by dredge pumps avoid any sediment losses associated with overflow which tend to considerably limit the plume dispersion within the water column compared to the TSHD. The plume modelling of the CSD was limited to Site R0. The TSHD configuration was considered a worst-case option, and this plume modelling option was used for the other sites in the inner section of the channel, considering that the plume dispersion for the CSD would be always lower in SSC. The use of a CSD is not expected to produce any significant plume extension over Marine Management Areas, Marine Reserve, sand banks or adjacent beaches. The sediment settling is expected to be quick, particularly for the sandy particles.

- Plumes associated with the use of BHD

The use of a BHD is predicted to cause sediment losses over the entire water column at the RNZ Jetty pocket (Site R0). Although the discharge rate is relatively high (up to 4% over the entire water column), the absolute sediment releases dependent on the hourly production rate estimated for the operations using the BHD (source: RHDHV) remains relative low compared to the TSHD configuration. The results show that SSC plumes produced by the excavation, hoisting and slewing phases are expected to create a maximum horizontally extended plume of 210 m after 24 h. The BHD plume dispersion is thus less than that modelled for the TSHD which was considered the worst case scenario in the present study. No sediment depositions over Marine Management Areas, Marine Reserve, sand banks or adjacent beaches were predicted.

### LARGE TSHD: DREDGING MODE

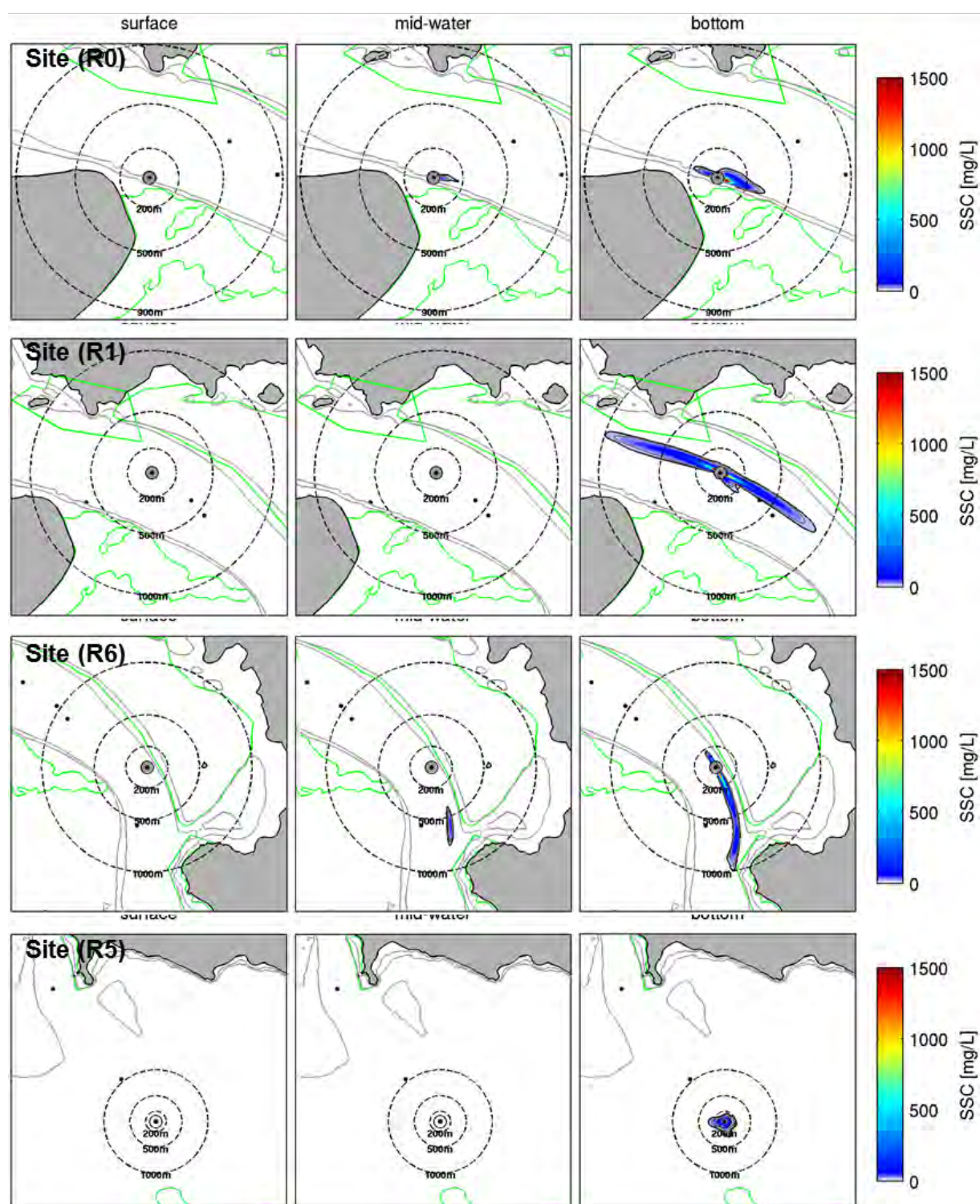


Figure 8.2 Probabilistic SSC plumes during dredging phase (large trailing suction hopper dredger, TSHD) at sites R0, R1, R6 and R5 at three levels of the water column presented in MSL Report P0297-01. The drag head source rate used is 3% and the minimum threshold of SSC is 12 mg/L (black line). The grey contours indicate the 10 and 20 m isobaths delimiting the channel. The green polygons show the area of interest in terms of environment impact.

**SMALL TSHD: DREDGING MODE**

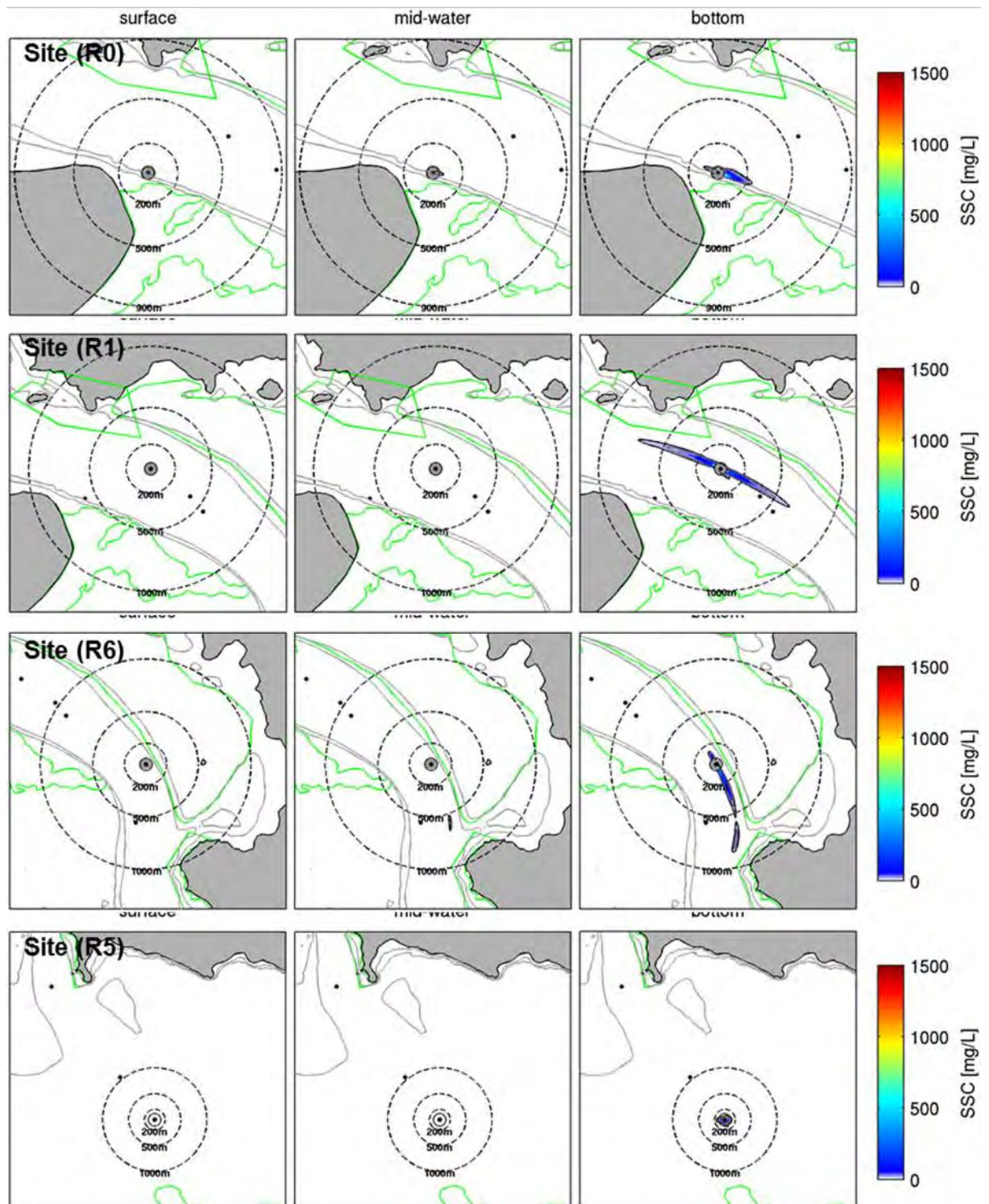


Figure 8.3 Probabilistic SSC plumes during dredging phase (small trailing suction hopper dredger, TSHD) at sites R0, R1, R6 and R5 at three levels of the water column presented in MSL Report P0297-01. The drag head source rate used is 3% and the minimum threshold of SSC is 12 mg/L (black line). The grey contours indicate the 10 and 20 m isobaths delimiting the channel. The green polygons show the areas of interest in terms of environment impact.

**LARGE TSHD: OVERFLOW MODE (79 min)**

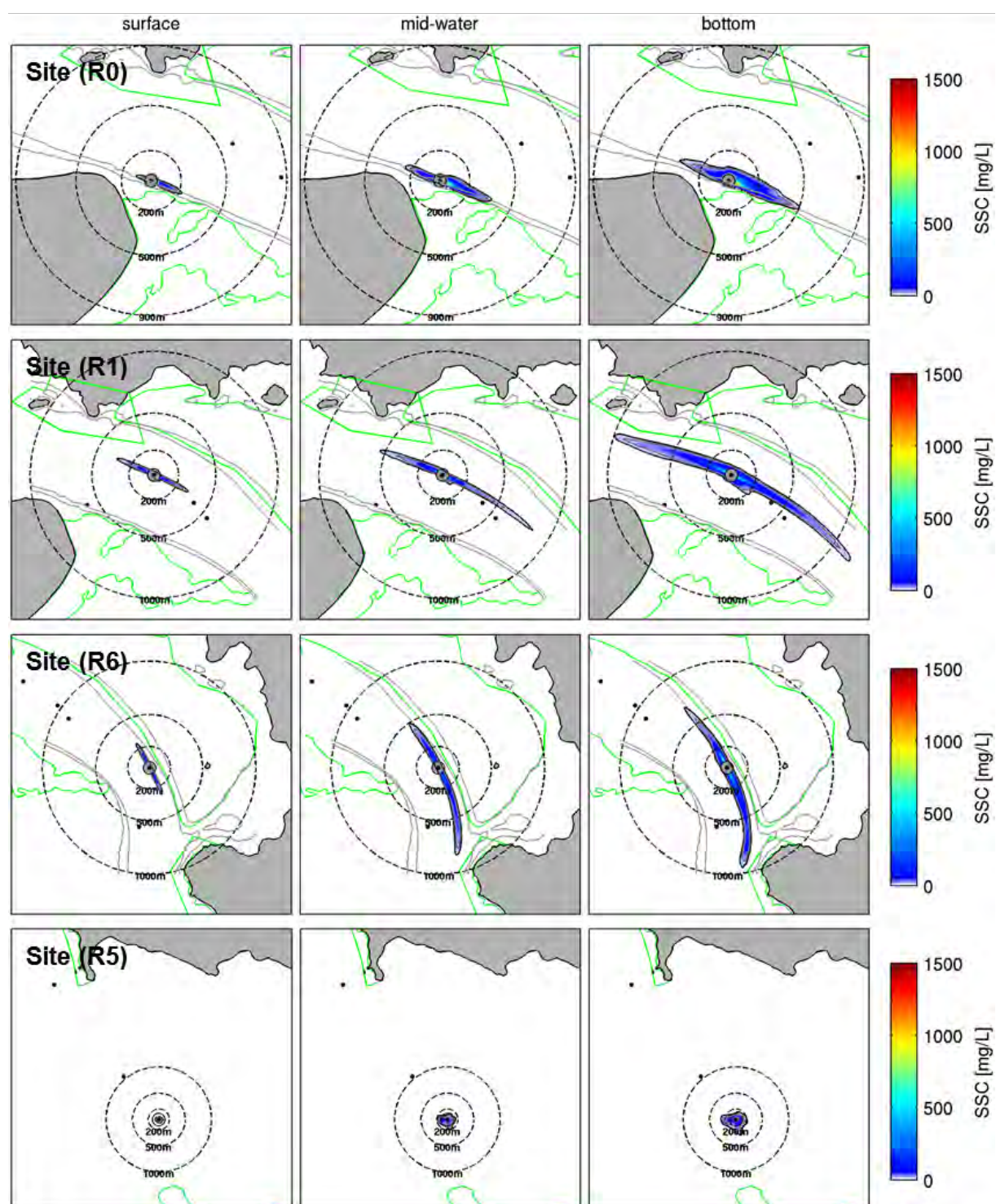


Figure 8.4 Probabilistic SSC plumes during overflow phase (large trailing suction hopper dredger, TSHD) at sites R0, R1, R6 and R5 at three levels of the water column presented in MSL Report P0297-01. SSC plumes are illustrated for a 79 min period. The minimum threshold of SSC is 12 mg/L (black line). The grey contours indicate the 10 and 20 m isobaths delimiting the channel. The green polygons show the areas of interest in terms of environment impact.

**SMALL TSHD: OVERFLOW MODE (95 min)**

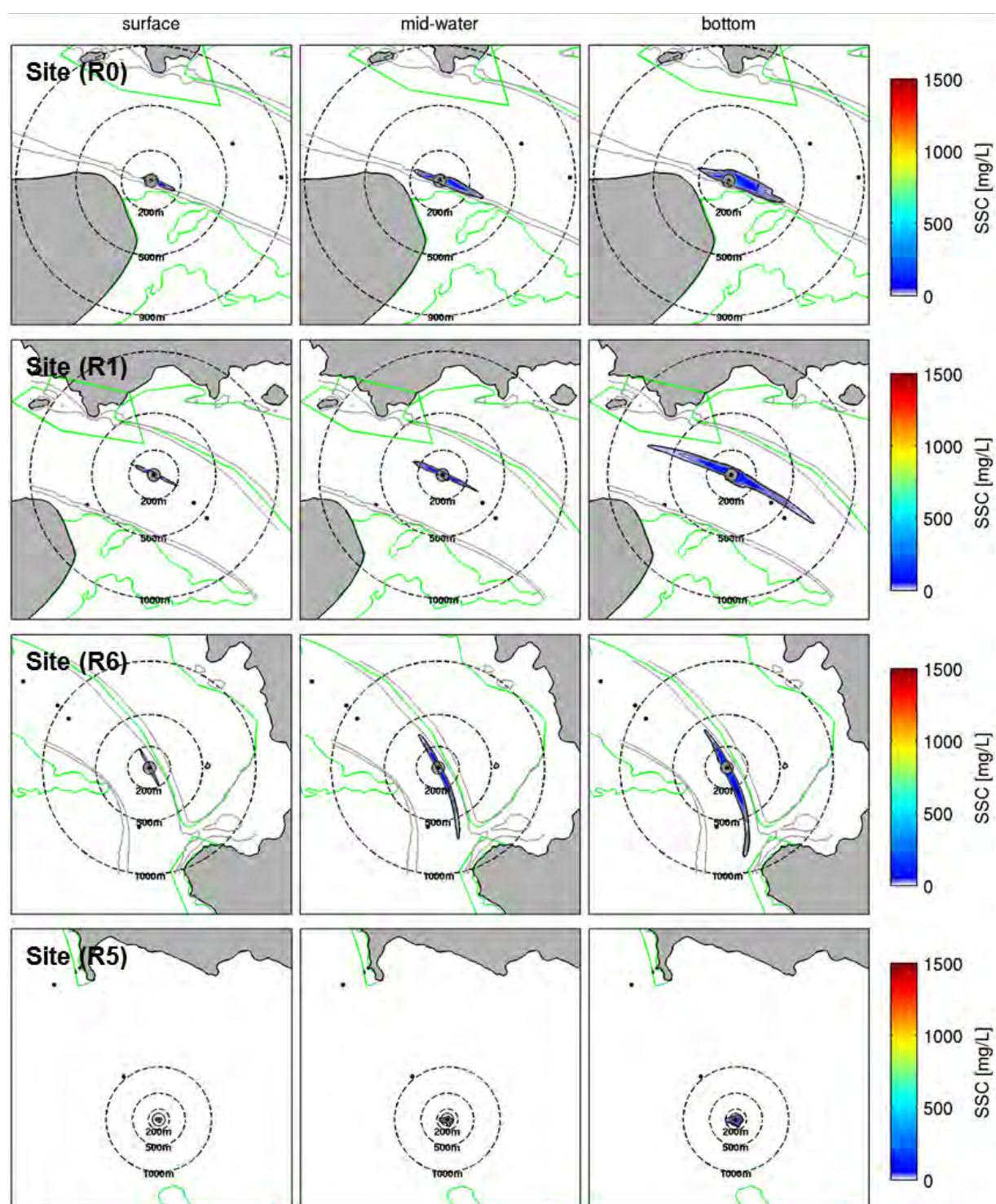


Figure 8.5 Probabilistic SSC plumes during overflow phase (small trailing suction hopper dredger, TSHD) at sites R0, R1, R6 and R5 at three levels of the water column presented in MSL Report P0297-01. SSC plumes are illustrated for a 95 min period. The minimum threshold of SSC is 12 mg/L (black line). The grey contours indicate the 10 and 20 m isobaths delimiting the channel. The green polygons show the areas of interest in terms of environment impact.

**LARGE TSHD: OVERFLOW MODE (SITE R0)**

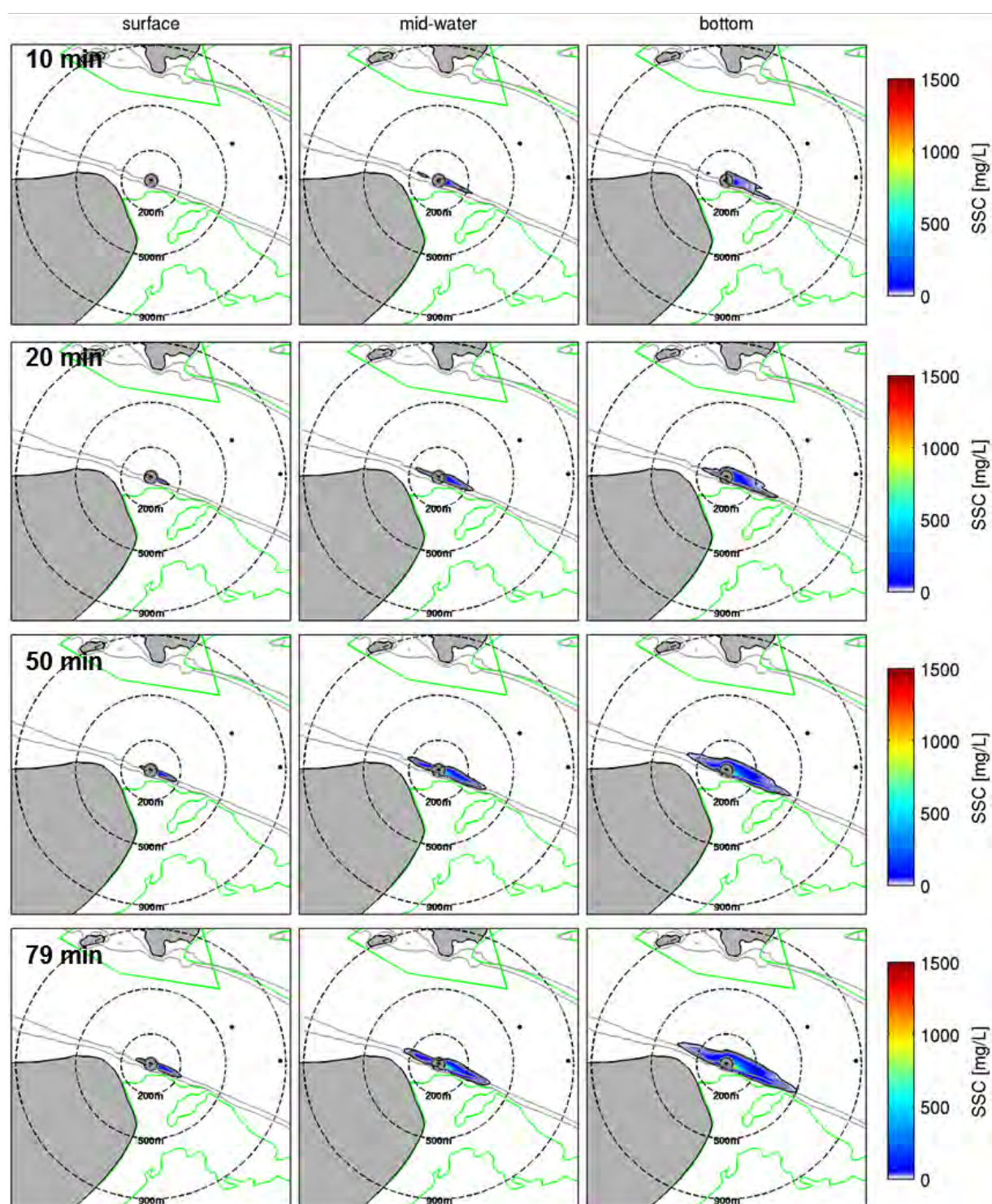


Figure 8.6 Probabilistic SSC plumes during overflow phase (large trailing suction hopper dredger, TSHD) at site R0 at three levels of the water column presented in MSL Report P0297-01. SSC plumes are illustrated for a 10, 30, 50 and 79 min period of overflow. The minimum threshold of SSC is 12 mg/L (black line). The grey contours indicate the 10 and 20 m isobaths delimiting the channel. The green polygons show the areas of interest in terms of environment impact.

**SMALL TSHD: OVERFLOW MODE (SITE R0)**

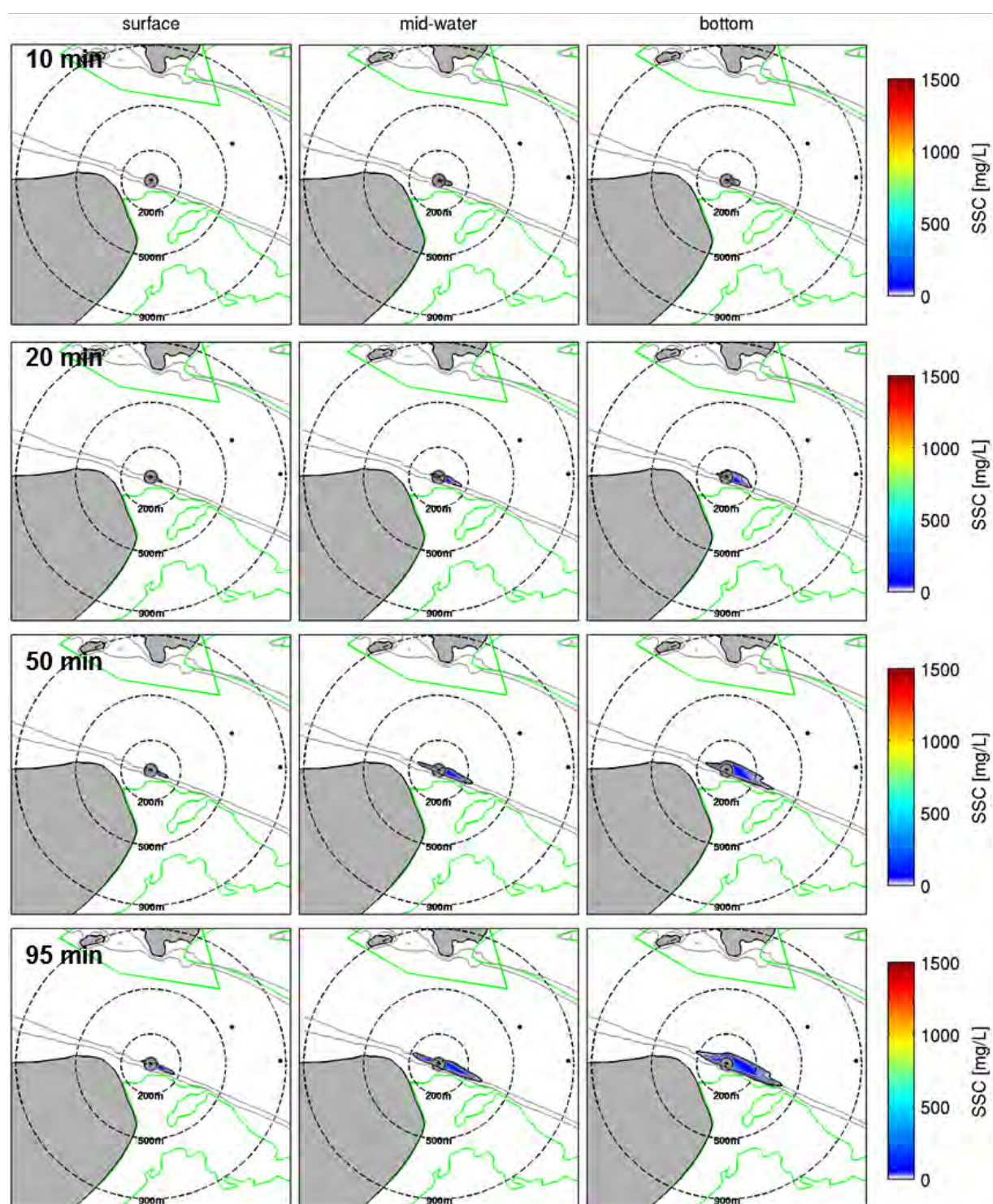


Figure 8.7 Probabilistic SSC plumes during overflow phase (small trailing suction hopper dredger, TSHD) at site R0 at three levels of the water column presented in MSL Report P0297-01. SSC plumes are illustrated for a 10, 30, 50 and 95 min period of overflow. The minimum threshold of SSC is 12 mg/L (black line). The grey contours indicate the 10 and 20 m isobaths delimiting the channel. The green polygons show the areas of interest in terms of environment impact.

**LARGE TSHD: OVERFLOW MODE (SITE R1)**

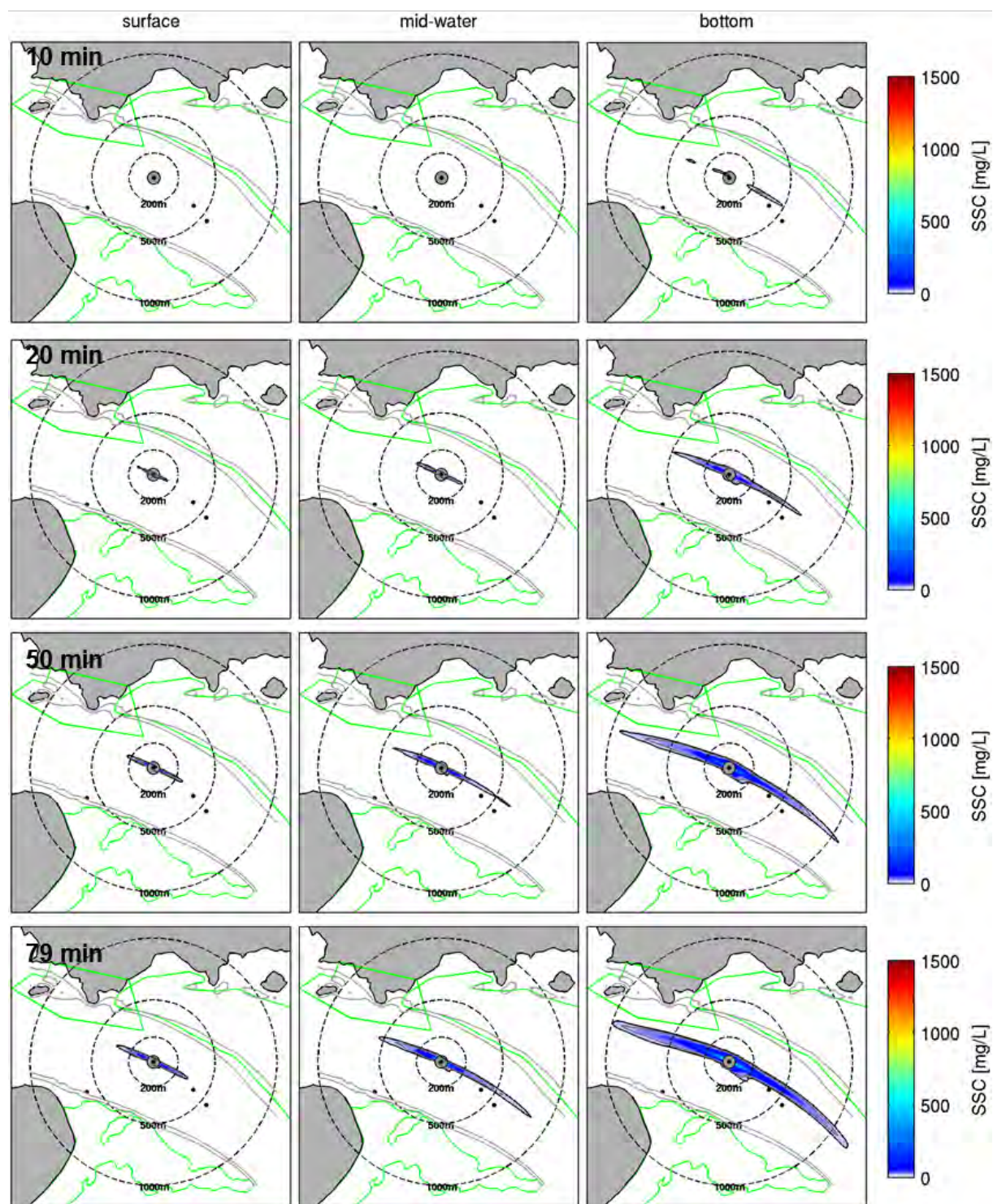


Figure 8.8 Probabilistic SSC plumes during overflow phase (large trailing suction hopper dredger, TSHD) at site R1 at three levels of the water column presented in MSL Report P0297-01. SSC plumes are illustrated for a 10, 30, 50 and 79 min period of overflow. The minimum threshold of SSC is 12 mg/L (black line). The grey contours indicate the 10 and 20 m isobaths delimiting the channel. The green polygons show the areas of interest in terms of environment impact.

**SMALL TSHD: OVERFLOW MODE (SITE R1)**

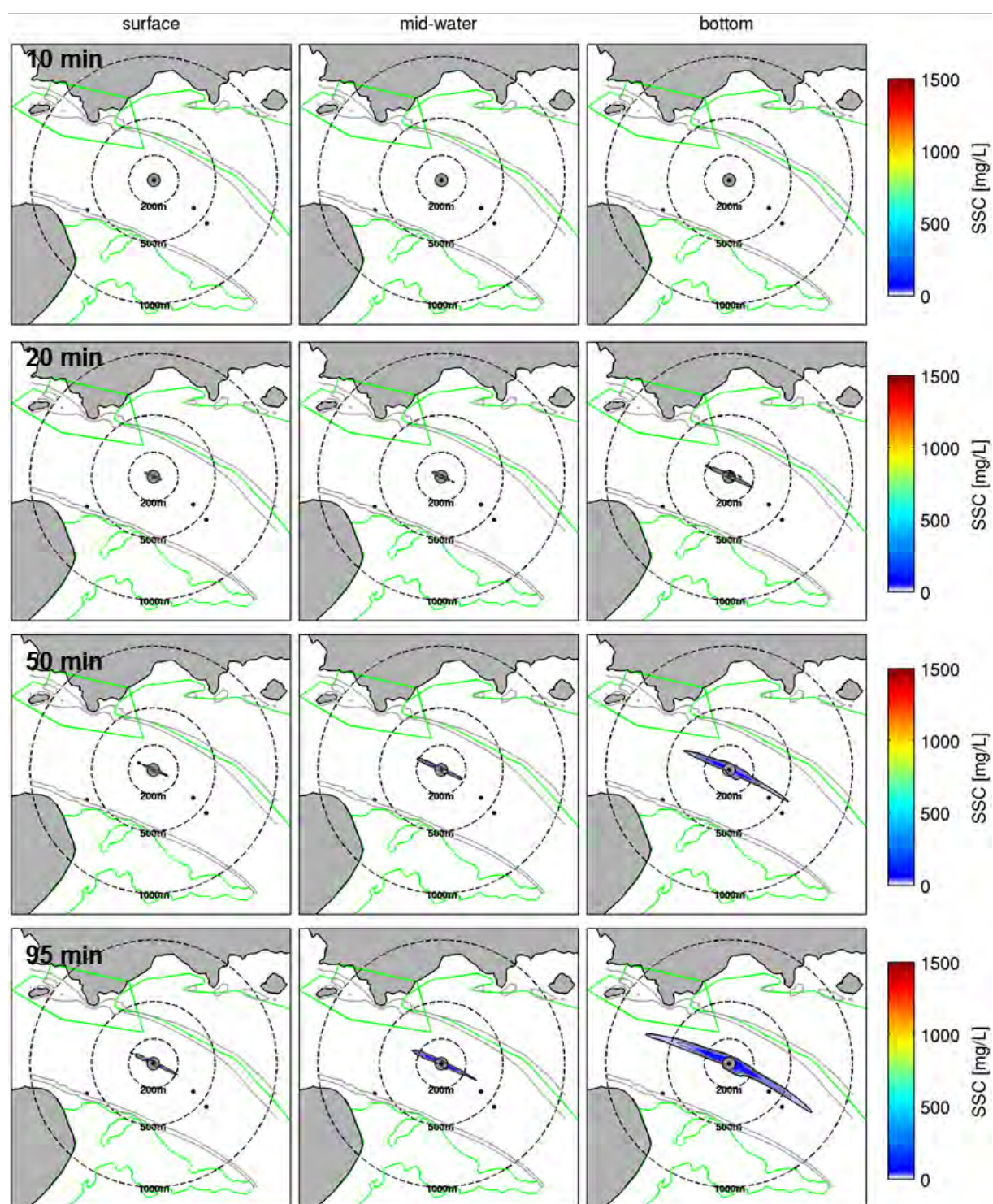
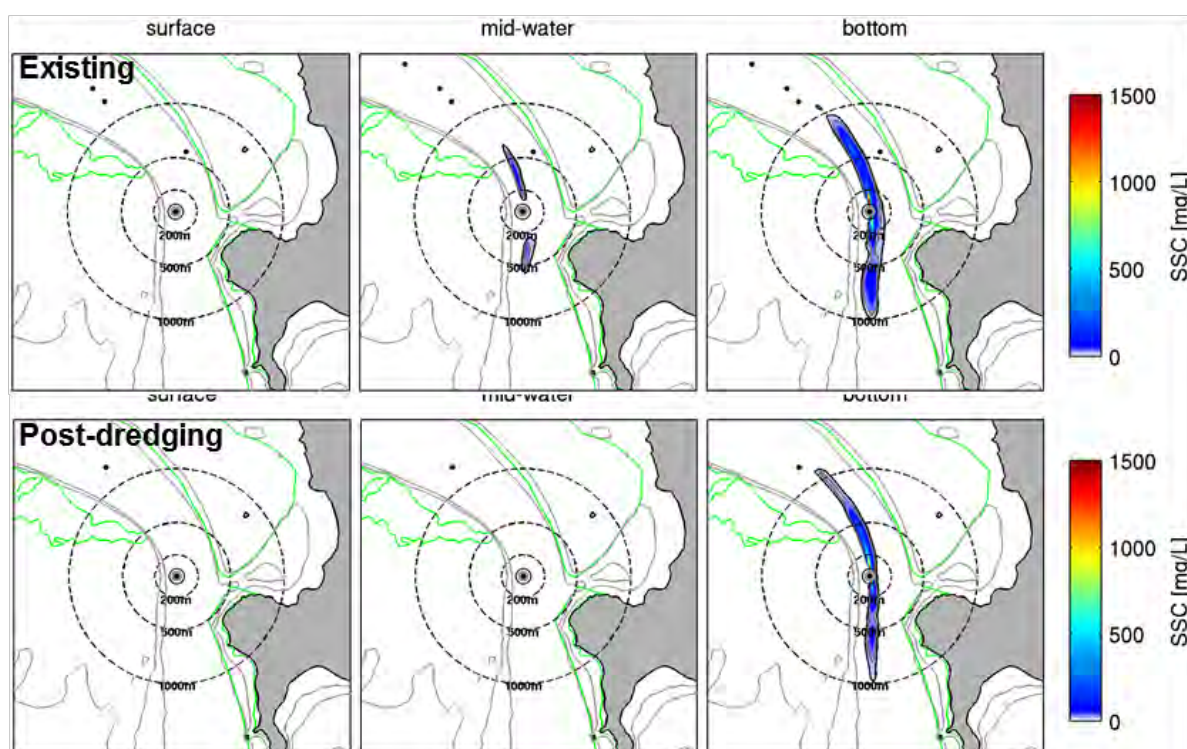


Figure 8.9 Probabilistic SSC plumes during overflow phase (small trailing suction hopper dredger, TSHD) at site R1 at three levels of the water column. SSC plumes are illustrated for a 10, 30, 50 and 95 min period of overflow. The minimum threshold of SSC is 12 mg/L (black line). The grey contours indicate the 10 and 20 m isobaths delimiting the channel. The green polygons show the areas of interest in terms of environment impact.

### LARGE TSHD: DREDGING MODE (SITE R2)



### SMALL TSHD: DREDGING MODE (SITE R2)

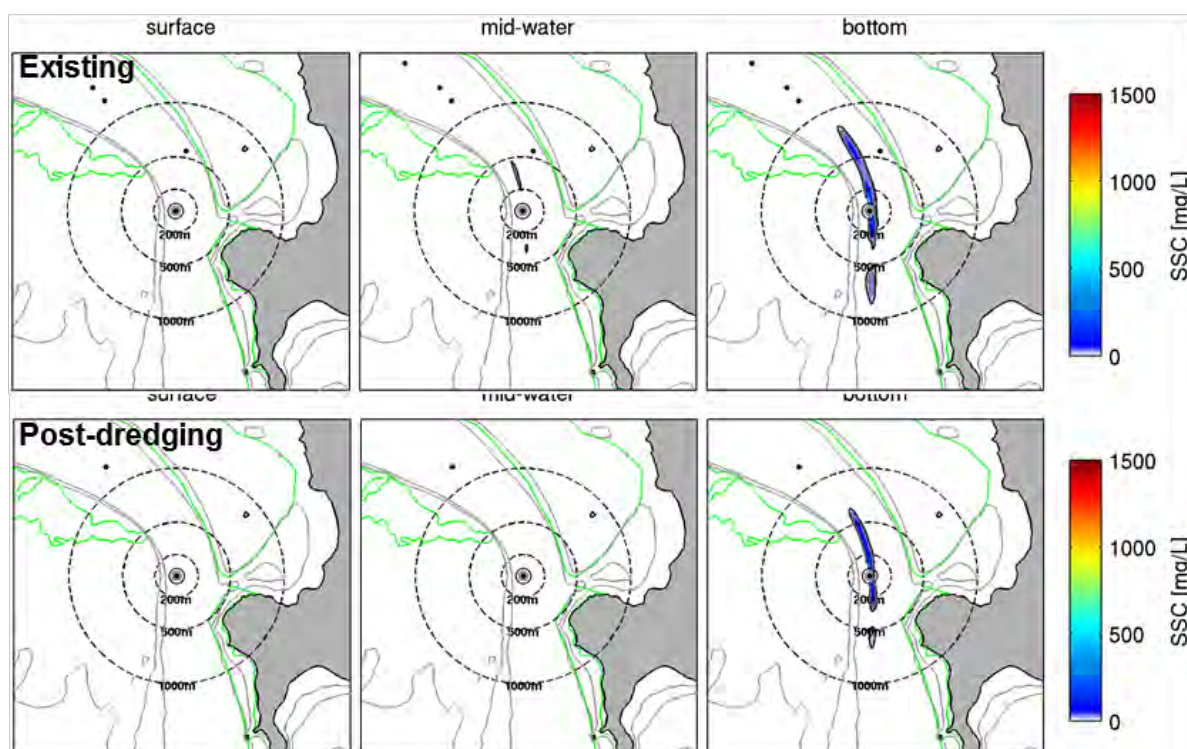
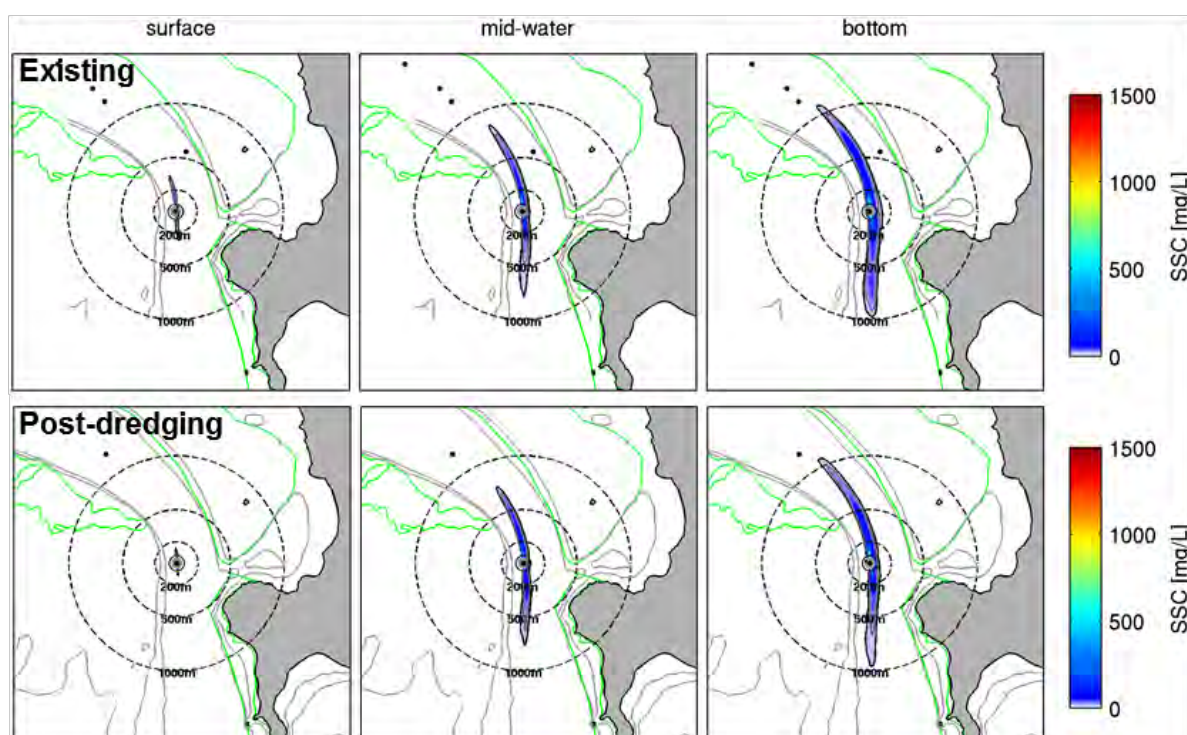


Figure 8.10 Probabilistic SSC plumes during dredging phase at site R2 for both the large (top) and the small (bottom) trailing suction hopper dredger (TSHD) considering the existing and the post-dredging configurations. The minimum threshold of SSC is 12 mg/L (black line). The grey contours indicate the 10 and 20 m isobaths delimiting the channel. The green polygons show the areas of interest in terms of environment impact.

**LARGE TSHD: OVERFLOW MODE 79 MIN (SITE R2)**



**SMALL TSHD: OVERFLOW MODE 95 MIN (SITE R2)**

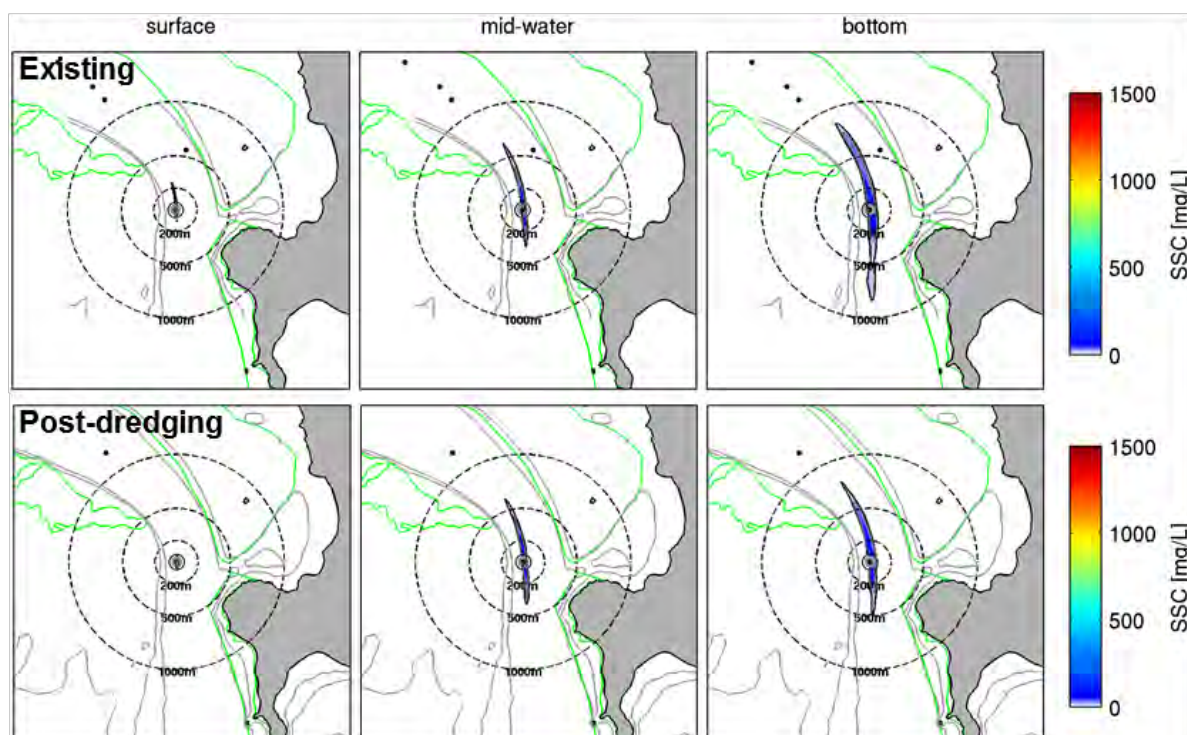
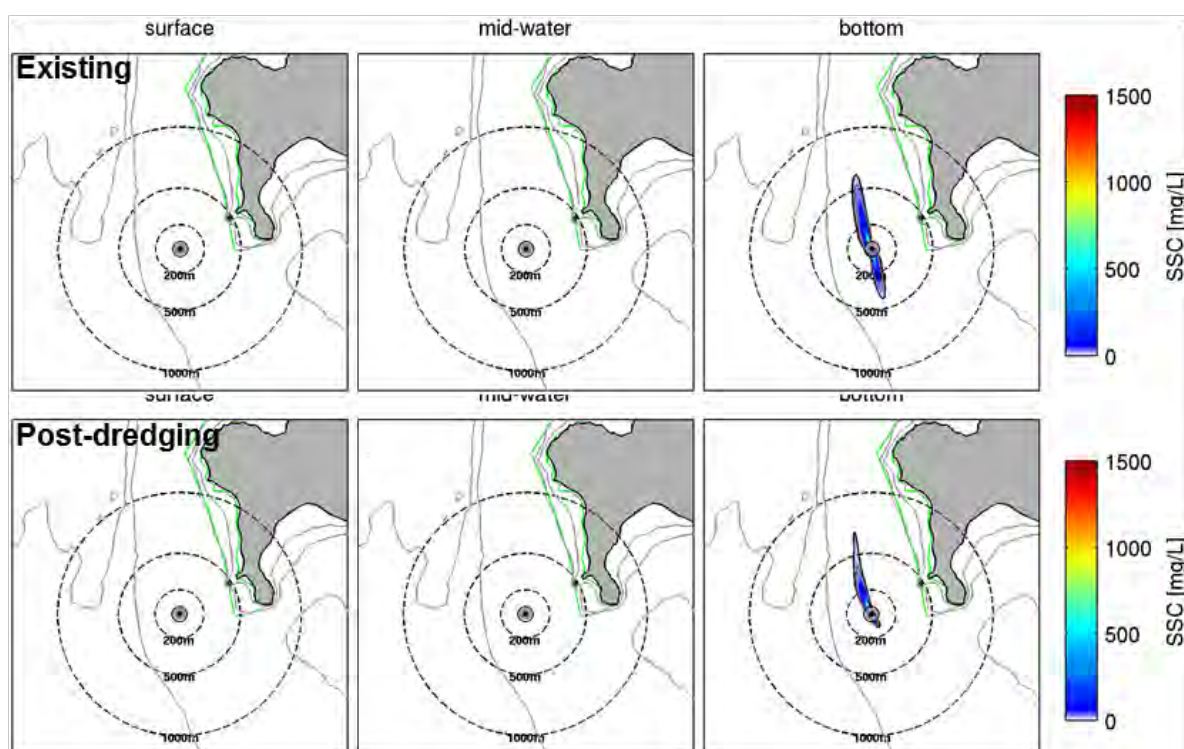


Figure 8.11 Probabilistic SSC plumes during overflow phase at site R2 for both large (top) and small (bottom) trailing suction hopper dredger (TSHD) considering the existing and the post-dredging configurations. SSC plumes are illustrated for a 79 min and 95 min period of overflow depending on the barge. The minimum threshold of SSC is 12 mg/L (black line). The grey contours indicate the 10 and 20 m isobaths delimiting the channel. The green polygons show the areas of interest in terms of environment impact.

### LARGE TSHD: DREDGING MODE (SITE R3)



### SMALL TSHD: DREDGING MODE (SITE R3)

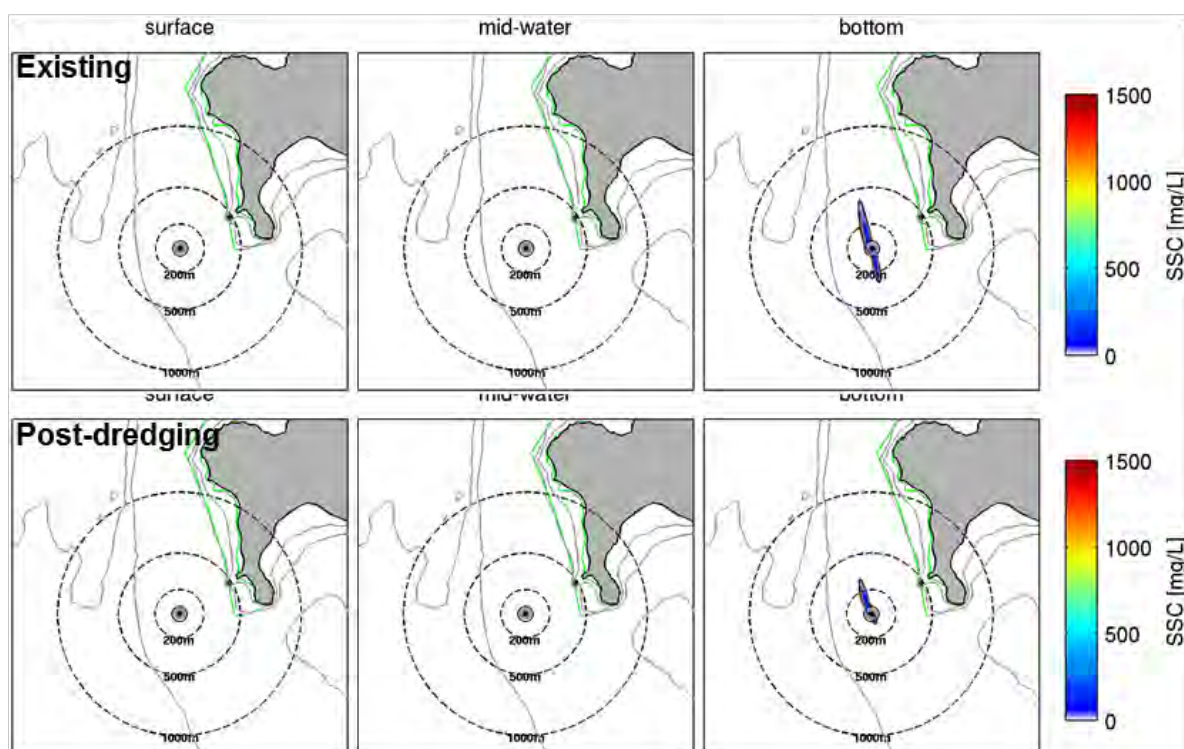
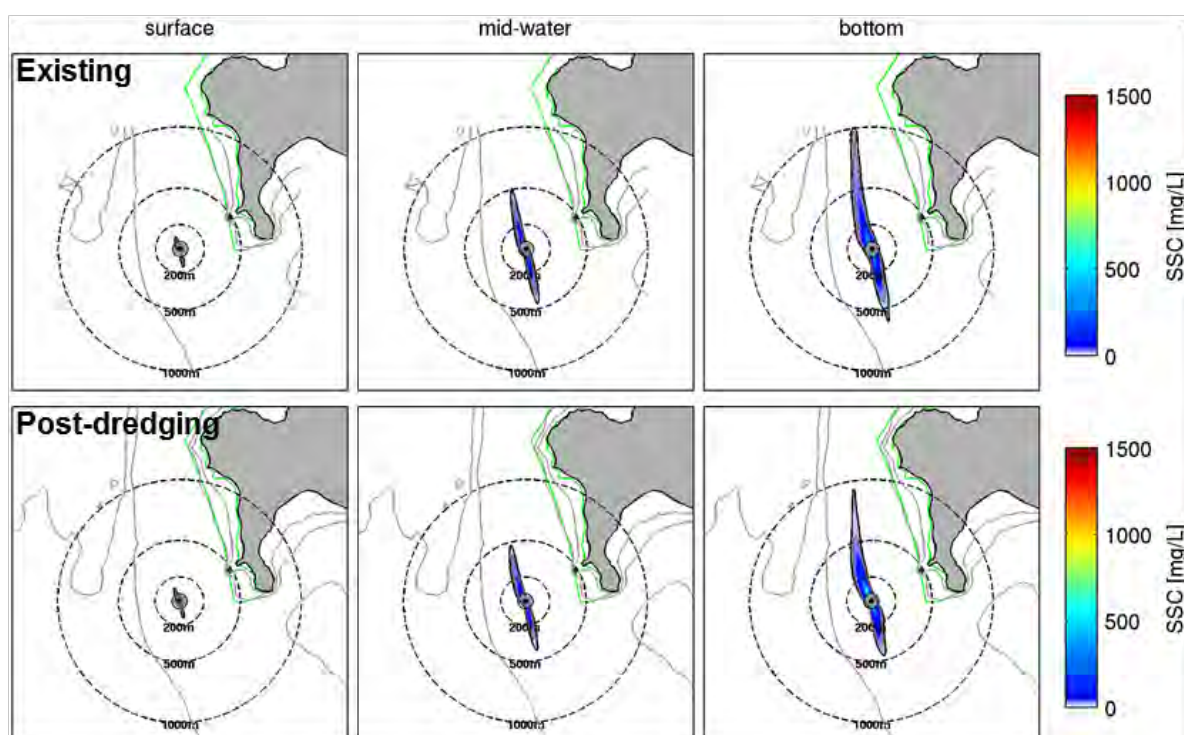


Figure 8.12 Probabilistic SSC plumes during dredging phase at site R3 for both the large (top) and the small (bottom) trailing suction hopper dredger (TSHD) considering the existing and the post-dredging configurations. The minimum threshold of SSC is 12 mg/L (black line). The grey contours indicate the 10 and 20 m isobaths delimiting the channel. The green polygons show the areas of interest in terms of environment impact.

**LARGE TSHD: OVERFLOW MODE 79 MIN (SITE R3)**



**SMALL TSHD: OVERFLOW MODE 95 MIN (SITE R3)**

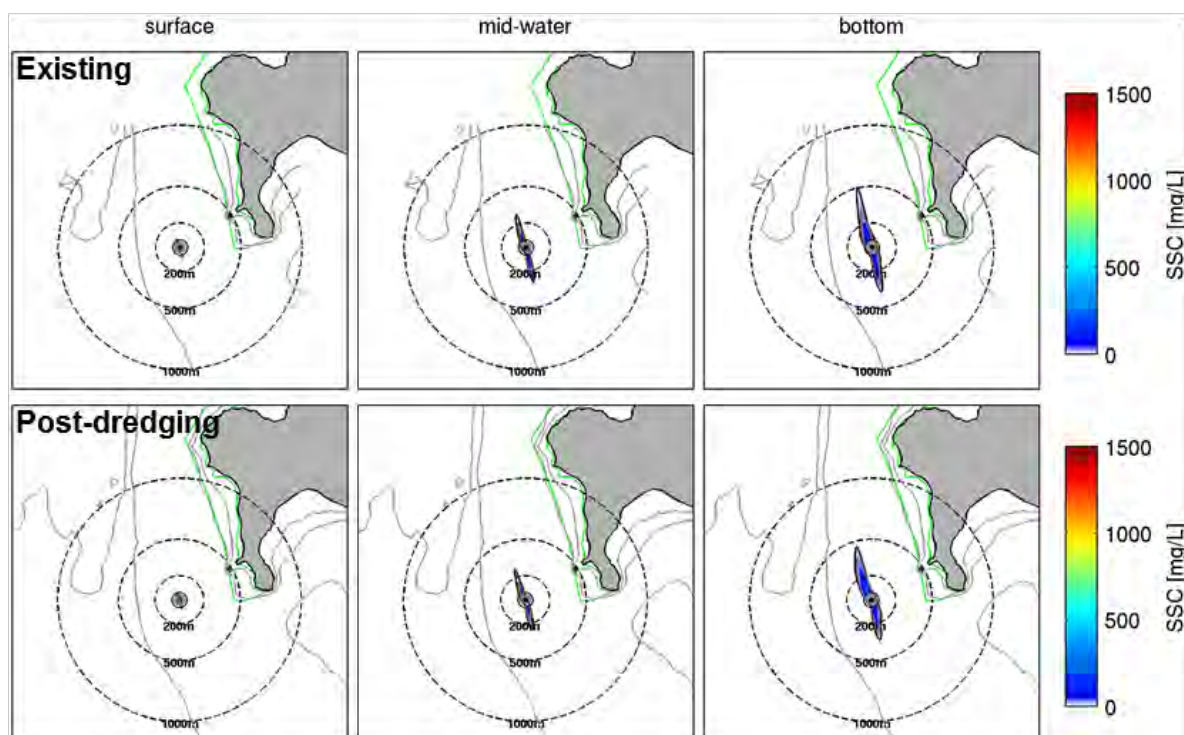


Figure 8.13 Probabilistic SSC plumes during overflow phase at site R3 for both large (top) and small (bottom) trailing suction hopper dredger (TSHD) considering the existing and the post-dredging configurations. SSC plumes are illustrated for a 79 min and 95 min period of overflow depending on the barge.

**CSD: DREDGING MODE**

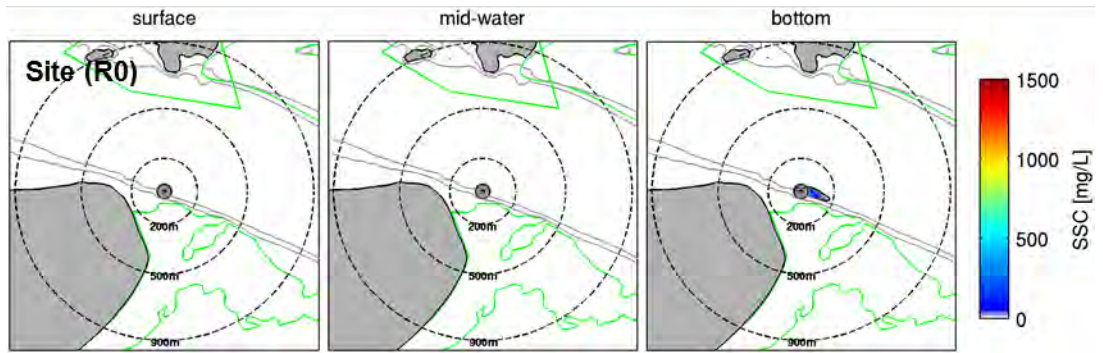


Figure 8.14 Probabilistic SSC plumes during dredging at site R0 for cutter suction dredger (CSD) considering the existing configuration.

**BHD: DREDGING MODE**

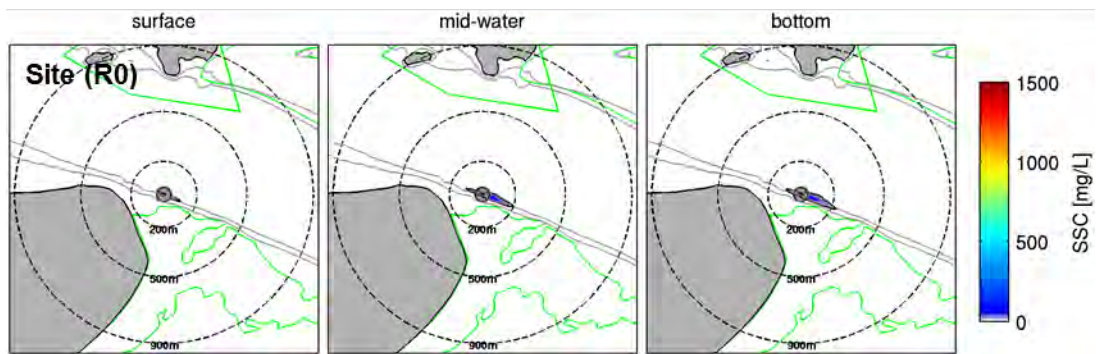


Figure 8.15 Probabilistic SSC plumes during dredging at site R0 for backhoe dredger (BHD) considering the existing configuration.

**8.2. Summary of dredging plumes**

The modelling of the dredging plumes has showed that:

- The sediment plumes associated with dredging and caused by the action of the drag head (TSHD) are predicted to remain constrained within the lower water column, with negligible expression at mid-water and surface levels. In contrast, the sediment plumes associated with the overflow phase are predicted to be spread across the entire water column.
- The resultant plumes from either source are predicted to follow the general channel alignment, consistent with the tidal currents. The maximum modelled excursion of any plume did not exceed 1200 m, with the plume constrained to the channel. The modelling shows no evidence of plume dispersion to the adjacent beaches, sand banks, Marine 1 (Protection) Management Areas or Marine Reserves. The sensitivity analysis carried out using conservative configurations of the sediment release during dredging did not show any fundamental changes in the plume dispersion.
- The modelling shows that the large TSHD generates more extended and concentrated plumes than the smaller vessel. The overflow duration has a significant effect on the magnitude and extent of the plumes.

- The sediment plumes associated with dredging and caused by the action of the rotating cutter head (CSD case) are predicted to remain constrained within the lower water column, with no expression at mid-water and surface levels.
- The sediment plumes associated with dredging and caused by the excavation, hoisting and slewing phases (BHD case) are expected to generate sediment losses over the entire water column. The low production rate associated with the BHD lead, however, to a low discharge rate compared to the TSHD case.
- Comparisons between plumes generated for the existing channel and the post-dredging scenario indicates that the plume excursions will decrease slightly as the channel becomes deeper due to the slightly reduced tidal velocities.
- No plume dispersion extending to the adjacent beaches, sand banks, Marine 1 Management Areas and Marine Reserves were generated by the dredging plume modelling for any of the dredge scenarios.

## 9. DISPOSAL GROUND DYNAMICS

### 9.1. Wave climate

The region of Bream Bay where the proposed offshore disposal Area 3.2 is located (Figure 1.4) is characterised by a relatively low energy wave climate, occasionally affected by short-duration storms and cyclonic events. The wave rose, calculated at the centre of the ground from 10-year hindcast data and illustrated in Figure 9.1, indicates that the wave propagation over the disposal ground is largely dominated by the north-eastern direction. The site is partially sheltered by Bream Head and the offshore islands from northerly and easterly swells, respectively. The modelled wave height fields shown in Figure 9.3 and Figure 9.4 for different wave scenarios exhibit these features explicitly.

At the disposal ground the water depth exceeds 40 m and therefore the wave orbital velocities near the seabed are generally below the threshold required to initiate sediment transport (i.e. less than 0.2 m/s). During storm events involving wave heights between 4 – 6 m (see Figure 9.2) and peak wave periods higher than 10 – 12 s, the near bed wave orbital velocities exceed  $0.4 \text{ m}\cdot\text{s}^{-1}$  (Figure 9.5 and Figure 9.6) which is strong enough to initiate entrainment and transport of sand particles (in suspension or by bedload), depending on the grain size (see diagrams in Figure 7.3 and Figure 7.4).

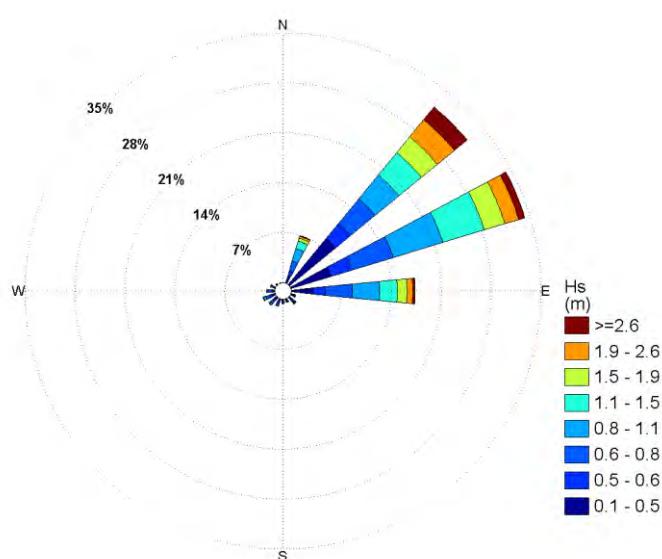


Figure 9.1 Wave rose for the proposed disposal ground from 10-year wave hindcast (2005 – 2014). Wave directions are in the „coming from“ convention.

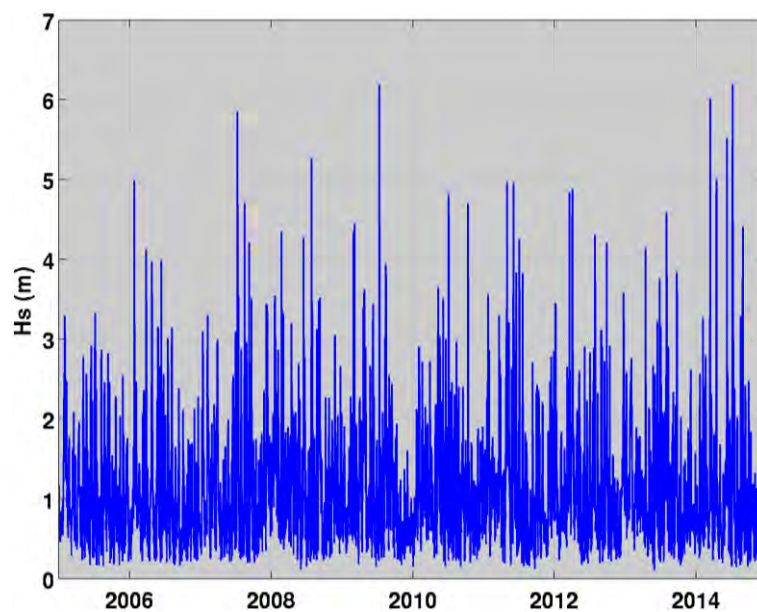


Figure 9.2 Time series (2005 – 2014) of modelled significant wave height (Hs) within the proposed disposal ground.

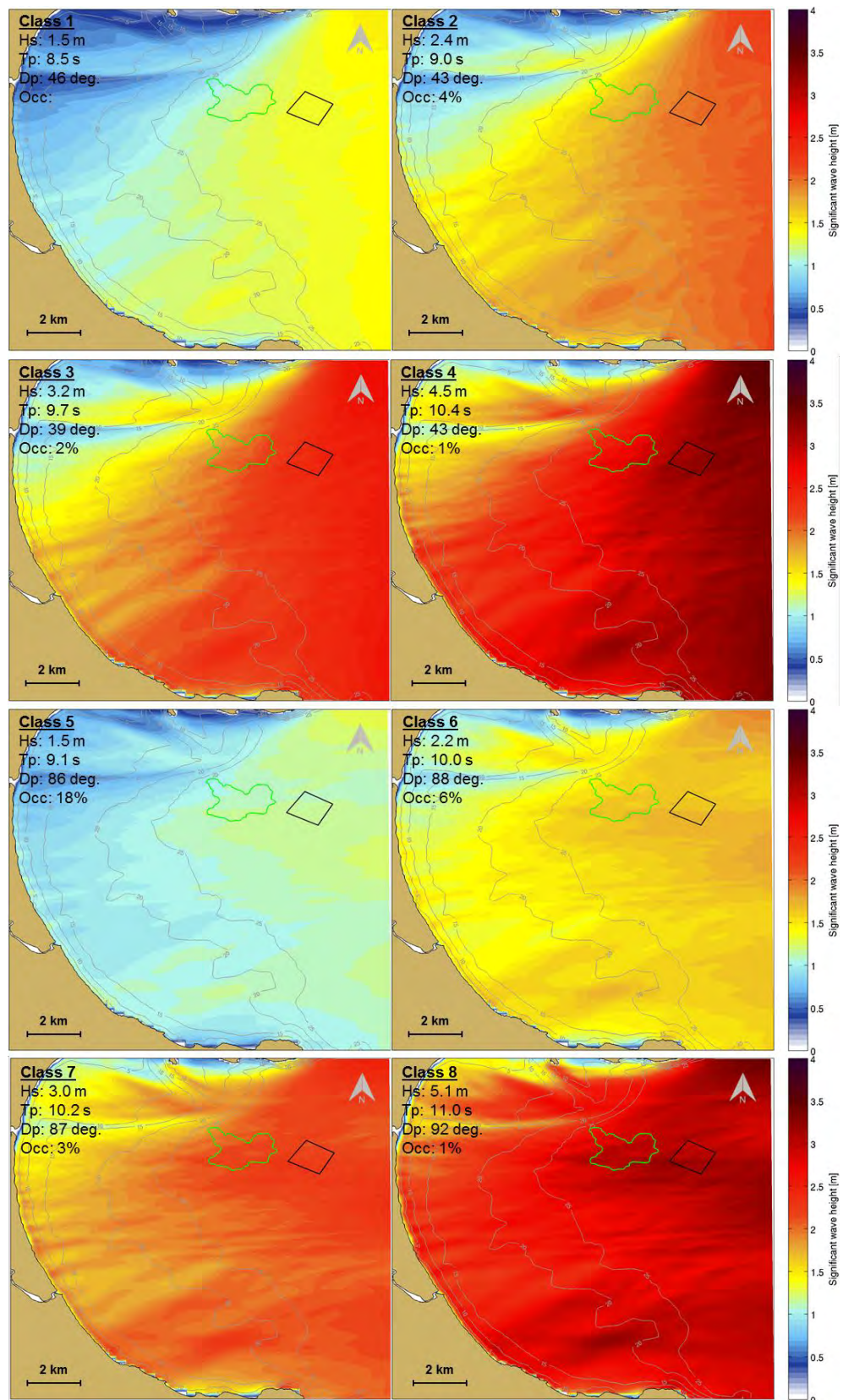


Figure 9.3 Wave height fields over Bream Bay for wave classes 1 to 8. Hs, Tp, Dp and Occ (% Occurrence) presented in the upper left corner indicate the wave conditions at the offshore position BND (see MSL Report P0297-01).

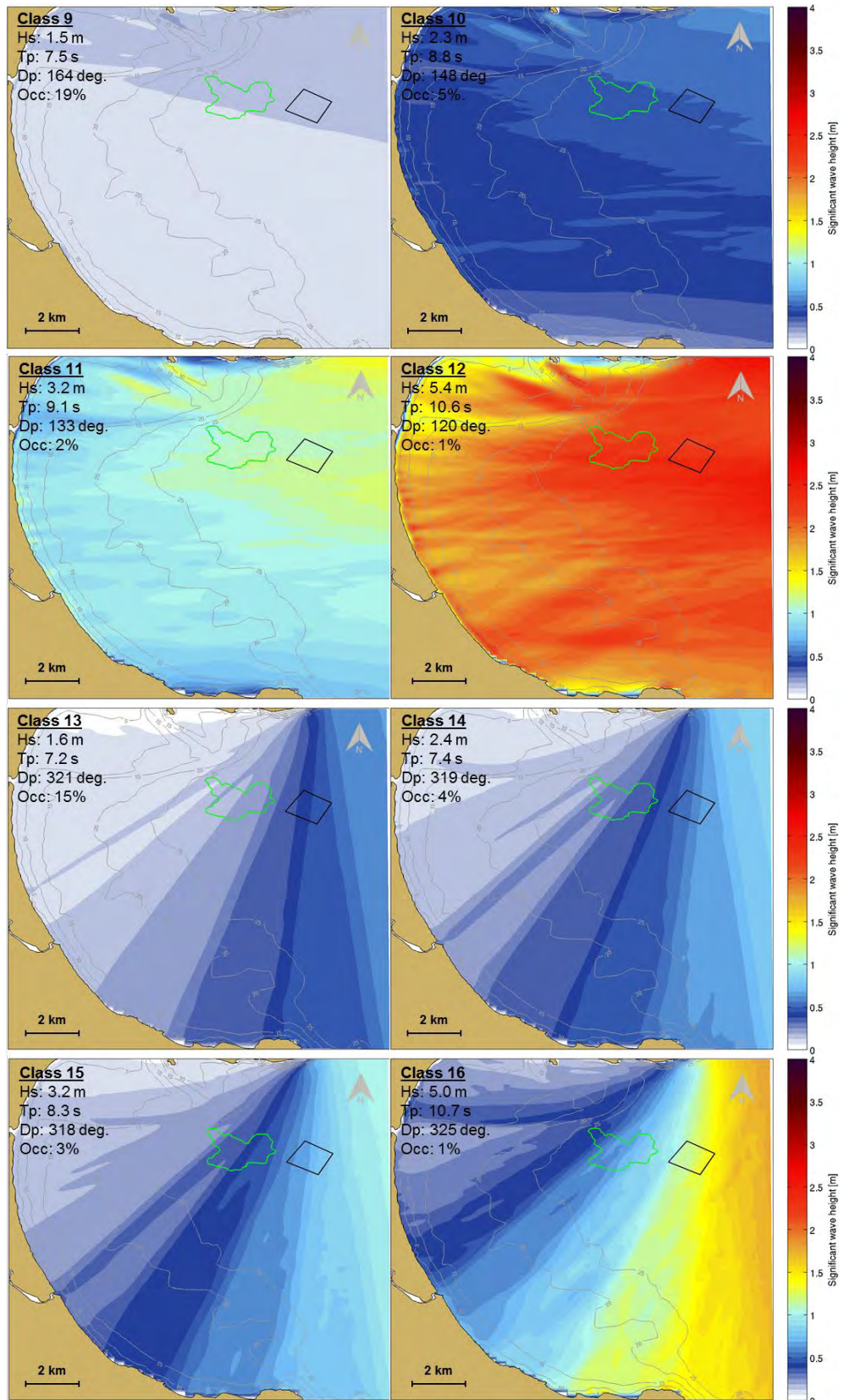


Figure 9.4 Wave height fields over Bream Bay for wave classes 9 to 16. Hs, Tp, Dp and Occ (% Occurrence) presented in the upper left corner indicate the wave conditions at the offshore position BND (see MSL Report P0297-01).

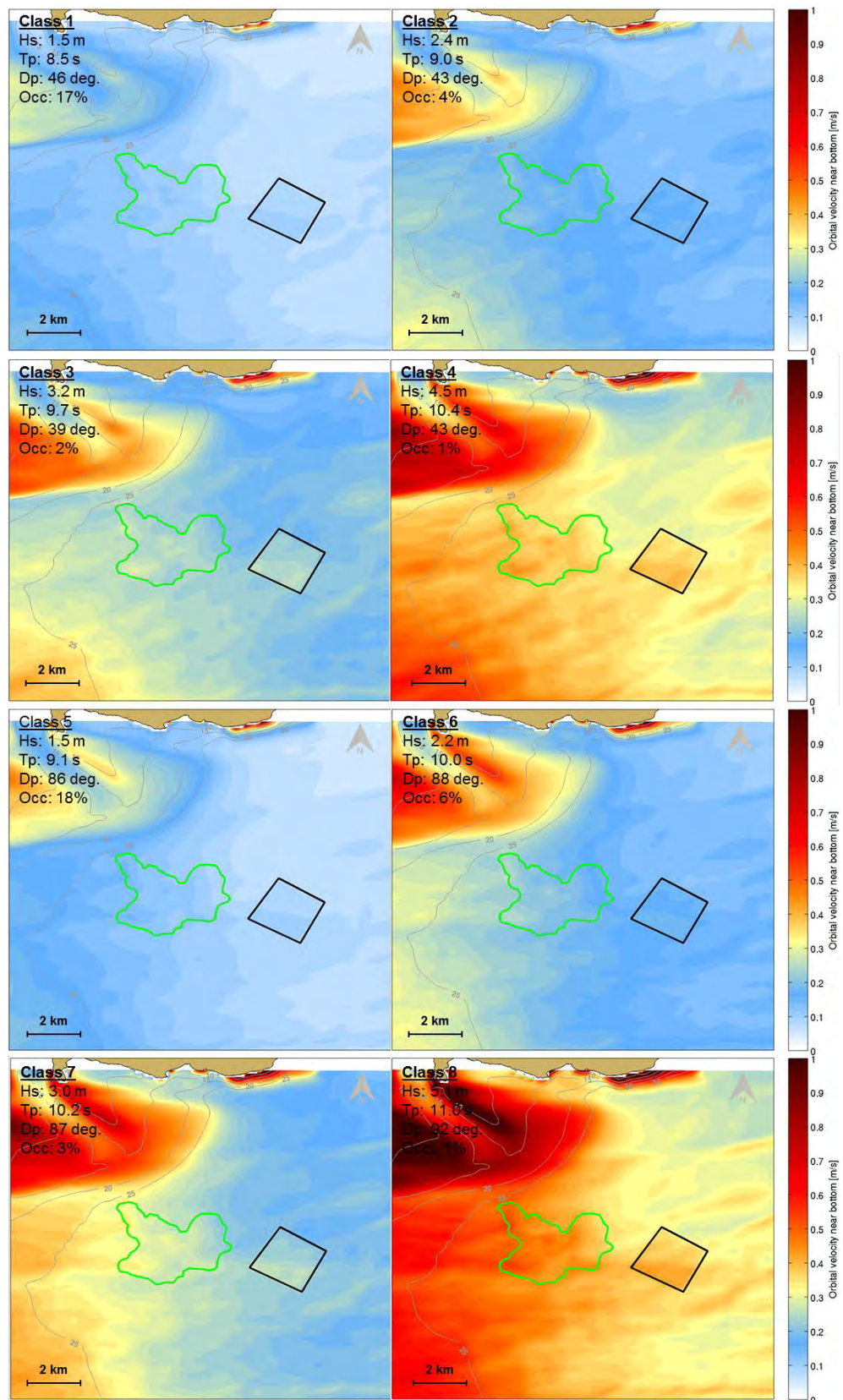


Figure 9.5 Near bottom orbital velocity fields over the disposal ground for wave scenarios 1 to 9. Hs, Tp, Dp and Occ (% Occurrence) presented in the upper left corner indicate the wave conditions at the offshore position BND (see MSL Report P0297-01).

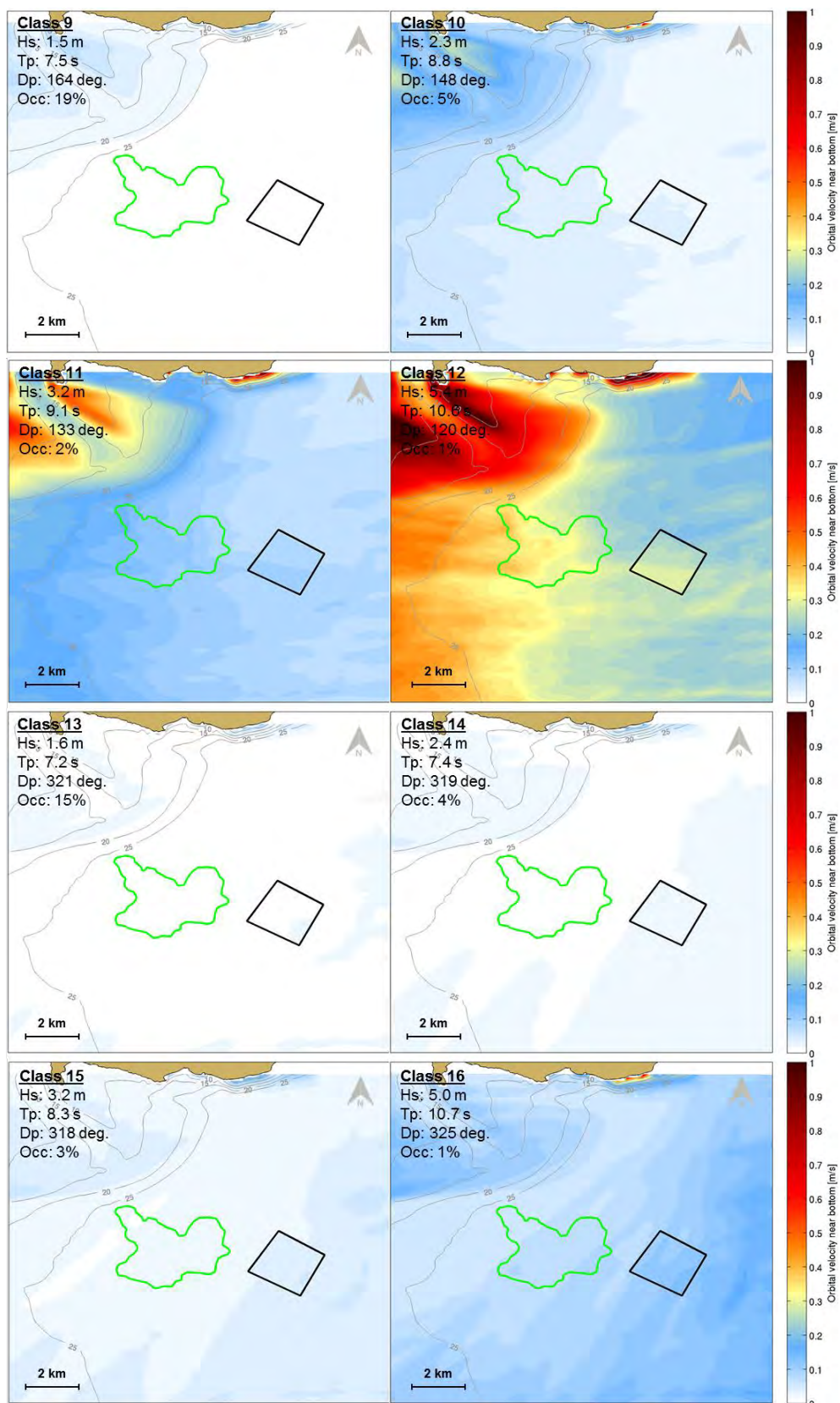


Figure 9.6 Near bottom orbital velocity fields over the disposal ground for wave scenarios 9 to 16. Hs, Tp, Dp and Occ (% Occurrence) presented in the upper left corner indicate the wave conditions at the offshore position BND (see MSL Report P0297-01).

## 9.2. Hydrodynamics

Current roses extracted from a 10-year ROMS hindcast at the centre of the disposal ground and for three different levels (5, 15 and 30 m below sea surface) are presented in Figure 9.7. These data show that the flows (including the tidal and the residual components) are mainly directed toward the south-west, with velocities lower than  $0.3 \text{ m.s}^{-1}$ . During storm events, these velocities may exceed  $0.4 \text{ m.s}^{-1}$  when increased by an intense wind-driven circulation. Note that the current rose near bottom also exhibits a secondary mode in the north-eastern direction with a 10 – 20% of occurrence due to the tidal asymmetry and the westerly wind episodes.

As described in the previous section, current velocities of such magnitudes have the ability to directly initiate the transport of fine grained non-cohesive particles from the disposal ground. Moreover, the validation of the ROMS hindcast at the centre of Disposal Site 3.2 (MSL Report P0297-01) showed that the model was under-predicting the current speed by up to 20%. The consequences of such bias on the model outcomes regarding the predicted disposal ground dynamics are discussed in Sections 9.3 and 9.4.

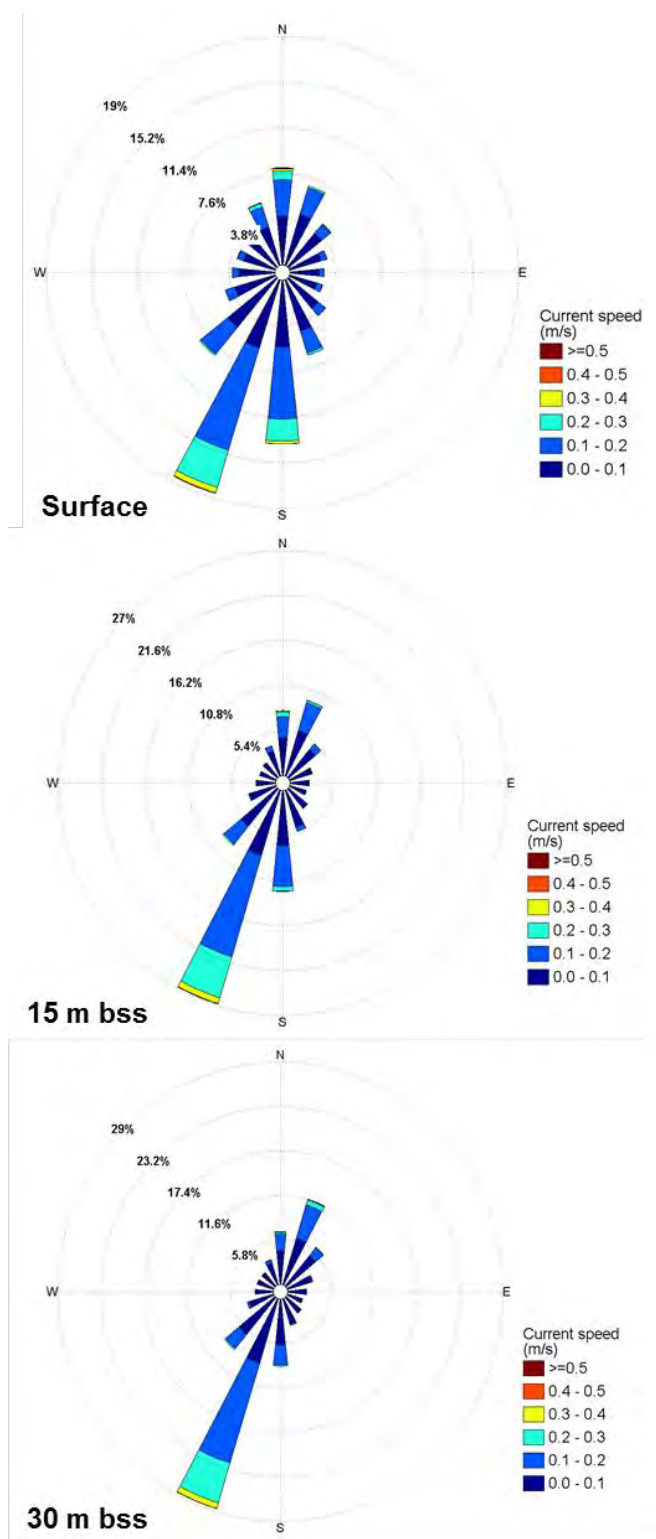


Figure 9.7 Current roses showing total current speed at 0, 15 and 30 m below sea surface (bss) from ROMS hindcast data for the period 2000 – 2010 in the proposed disposal ground. Current directions are in the “going to” convention.

### 9.3. Sediment dynamics for disposal ground 3.2

The characterisation of the wave climate and the near bed hydrodynamic regime at the proposed disposal ground shows that both components were occasionally of sufficient magnitude to initiate sediment transport of the finer fractions in the disposed sediments. A more integrated assessment of the dynamics of the ground was made with the Delft3D model. This model was used to predict the disposal ground 3.2 morphodynamics using an input reduction approach, which is fully described in Section 9 of MSL Report 0297-01. In this technique, a limited number of representative forcing conditions (including tides, waves, residual currents and residual water elevations) are used to reproduce the medium-term residual sediment transport patterns and associated morphological evolutions. The methodology was combined with a morphological acceleration factor based on the occurrence of each scenario to improve computational efficiency by acceleration computed morphological evolution. Using this technique, the disposal ground dynamics were simulated over a 1-year period.

A highly conservative approach was also adopted for the height of the mound in these simulations. A maximum height of 4 m (corresponding to a total volume of 8 million m<sup>3</sup>) was adopted, in order to replicate a scenario in which the disposal operation is constrained to limited areas in order to minimise the footprint of deposition, and being a reasonable upper value to represent some overlapping deposition of the dredged hopper loads. This maximum height of 4 m is less than 10% of water depth at Area 3.2.

The annual morphological changes presented in Figure 9.8 (based on a conservative configuration of the model) show a very slight west-southwest migration of the sediments by bedload transport due to wave effects. The erosion of the disposal mound after 1 year reveals a marked gradient in the transport based on water depth. This suggests that both high energy wave and current conditions are necessary to initiate the entrainment of the disposed sediments. Less than 5% of the disposed material (based on an 8 million m<sup>3</sup> volume) is expected to be eroded and transported over a 1-year period. In this context, under-predicting the current velocity by 5 – 20% at the offshore disposal ground location is not expected to fundamentally change the numerical modelling outcomes. Indeed, the near-bottom current velocities over areas characterised by water depths ranging between 40 – 45 m are relatively low. The high degree of stability highlighted by the 1-year morphodynamic numerical modelling is not expected to be compromised by a ~0.05 m.s<sup>-1</sup> absolute error in the model velocities.

The extent of movement of sediment is very limited and does not reach any sensitive area such as beaches, Marine Reserves, Marine 1 Management Areas or sensitive areas. The adjacent 3 Mile Reef is not expected to receive a detectable amount of sediments from disposal ground 3.2. Given the receiving environment already has a similar grain size composition to the dredged sediments, there will be no material change to the sedimentary character of 3 Mile Reef. Disposal ground 3.2 is expected to be stable over a long-term period given the very low amplitude of transport shown by the model. The ratio of deposited to eroded material indicates that small amounts of fine sediments are transported during storms and spread in undetectable quantities over the adjacent areas.

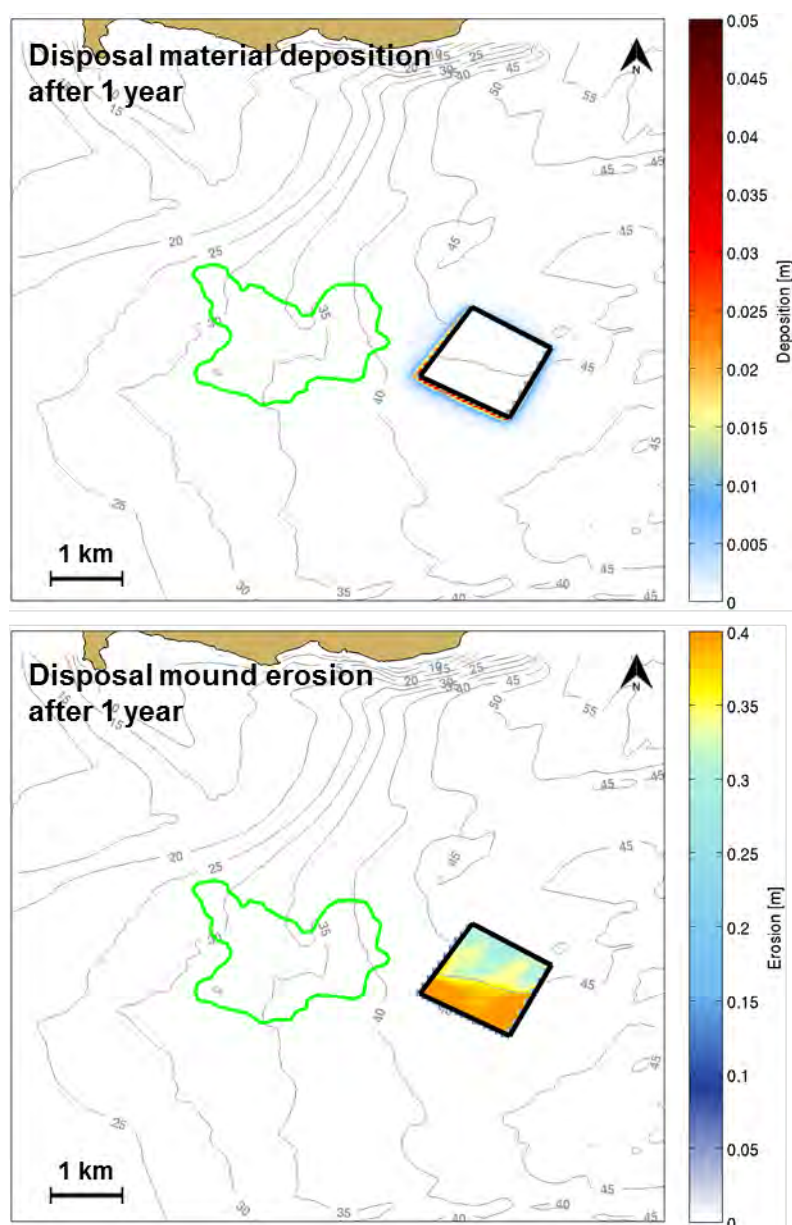


Figure 9.8 Disposal ground 3.2 dynamics simulated for a 1 year period.

#### 9.4. Sediment dynamics for Disposal ground 1.2

For disposal site 1.2, a 0.6-m mound (1.5 million  $\text{m}^3$ ) was considered for the maintenance dredging volume and up to 5% of the capital dredging volume based on the consultation between RNZ and the relevant experts. The site is located over the southern extension of the ebb-tidal delta where depths range from 7 – 15 m. The hydrodynamic study showed that the tidal currents over this region of Bream Bay are not particularly strong, with peak ebb and flood velocities lower than  $0.2 \text{ m}\cdot\text{s}^{-1}$  and oriented northeast. Conversely, the maximum orbital velocities due to the effect of waves over shallow areas are predicted by the model to reach  $0.4 - 0.5 \text{ m/s}$  during storms, making the disposal ground dynamics dominated by waves. This area is exposed to refracted waves propagating in the eastern direction, causing high bottom friction fields over the tidal delta. Results of the 1-year morphodynamic simulation shown in Figure 9.9 clearly confirm the wave-dominated transport of dredged material after disposal. Sediments were predicted to be dispersed in south-western to north-western directions, by waves, and tidal

currents to a lesser extent. The erosion of the disposal mound is predicted to reach approximately 8% of the total volume after 1 year. No connection between the disposed material and the channel is predicted by the model. This disposal site will likely promote the replenishment of the adjacent beach and sand bank areas over years under the effect of waves during storm conditions.

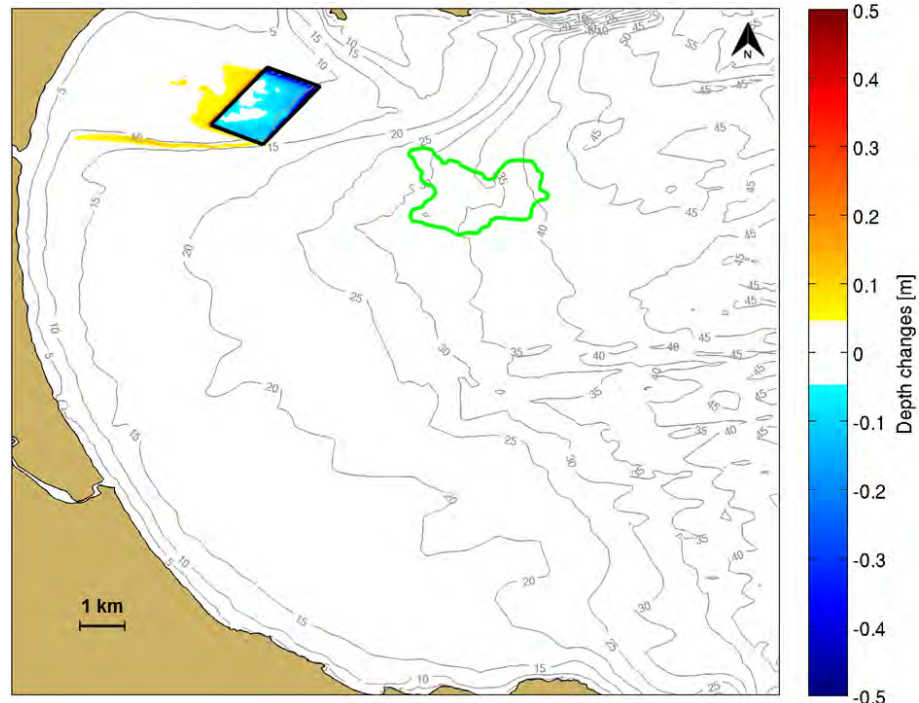


Figure 9.9 Disposal ground 1.2 dynamics simulated for a 1 year period.

## 9.5. Effects of disposal grounds on the wave climate

Changing the shape of the seabed potentially influences the nearshore wave climate through the process of wave refraction. Wave height and direction at the shore can be changed if a disposal mound is of sufficient size, and a local example is the modification of waves by the shape of the ebb tide delta.

To examine this potential, the 16 representative wave classes were simulated with the spectra wave model (DELFT3D – WAVE) to examine the effects of the disposal mounds 1.2 and 3.2 on the wave climate near Ruakaka Beach and over the wider Bream Bay. No hydrodynamic forcing was included. Highly conservative mound heights of 1.75 m and 4 m corresponding to the Disposal grounds 1.2 and 3.2, respectively, were used.

In the case of the Disposal Site 3.2, the results presented in Figure 9.10 and Figure 9.11 for the modelled cases (with incoming waves of 0.5 to 4.0 m in height at the disposal site 3.2) show that the difference in wave height (illustrated by yellow/orange colours for an increase and blue colours for a decrease) is very small (less than 10 cm). Maximum changes are observed near the mound itself while changes along Ruakaka Beach do not exceed 5 cm. These subtle differences in the significant wave height fields are mainly due to the relative high water depth (~40 – 45 m) at the disposal site. The effect near the shore is a slight modulation, with areas of increase and areas of decrease, dependent on the incident wave direction.

Changes in significant wave heights caused by the Disposal Site 1.2 illustrated in Figure 9.12 and Figure 9.13 are not expected to exceed 5 cm and 10 cm along the adjacent beaches and near the mound, respectively. The wave energy is susceptible to be slightly redistributed due to changes in wave refraction and wave breaking, particularly during storm events. The wave height along the adjacent beaches to the north-west of the mound is predicted to increase by less than 10 cm for moderate / high energy wave events. During extreme events characterised by offshore wave height of more than 5 m, the reduction of the water depth due to the presence of the mound may promote wave breaking processes over the disposal Site reducing the wave height along the shoreline by 5 – 10 cm (< 5%). Note that during such exceptional events, the northern area of Ruakaka Beach can be subjected to an increase of a few centimetres in wave heights. The erosion of the disposal mound over years driven by the effect of waves is expected to reduce notably the changes in significant wave heights caused by the mound. The methodology applied in the present study is thus highly conservative as it considers a non-erodible disposal mound over 10 years. The effect of the disposal mound 1.2 on the existing wave climate is largely negligible. Surfing conditions along Ruakaka Beach are therefore not expected to be affected by the disposal mounds 1.2 and 3.2.

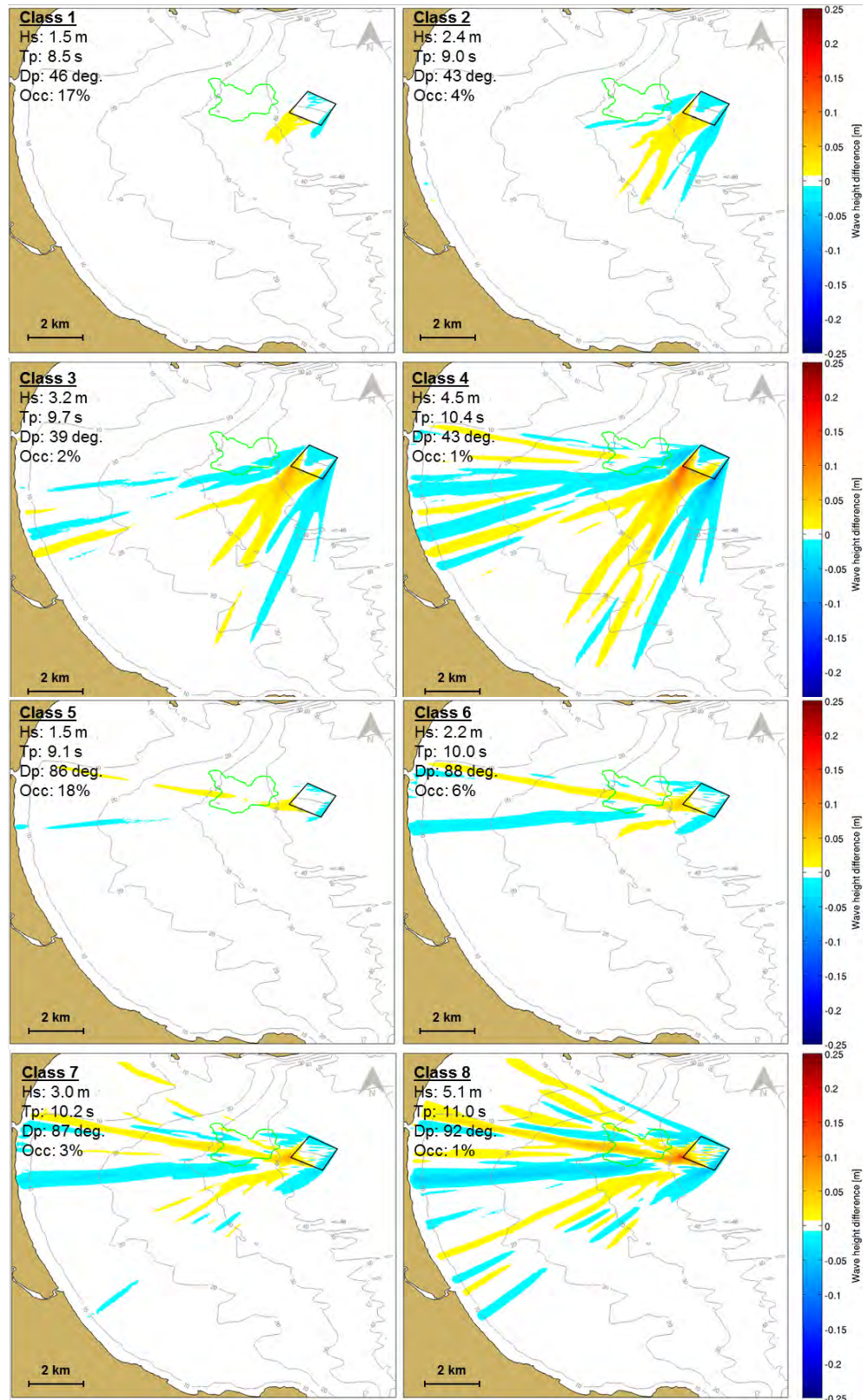


Figure 9.10 Difference in wave height fields caused by the disposal mound 3.2 over Bream Bay for wave scenarios 1 to 8. Hs, Tp, Dp and Occ (% Occurrence) presented in the upper left corner indicate the wave conditions at the offshore position BND (MSL Report P0297-01).

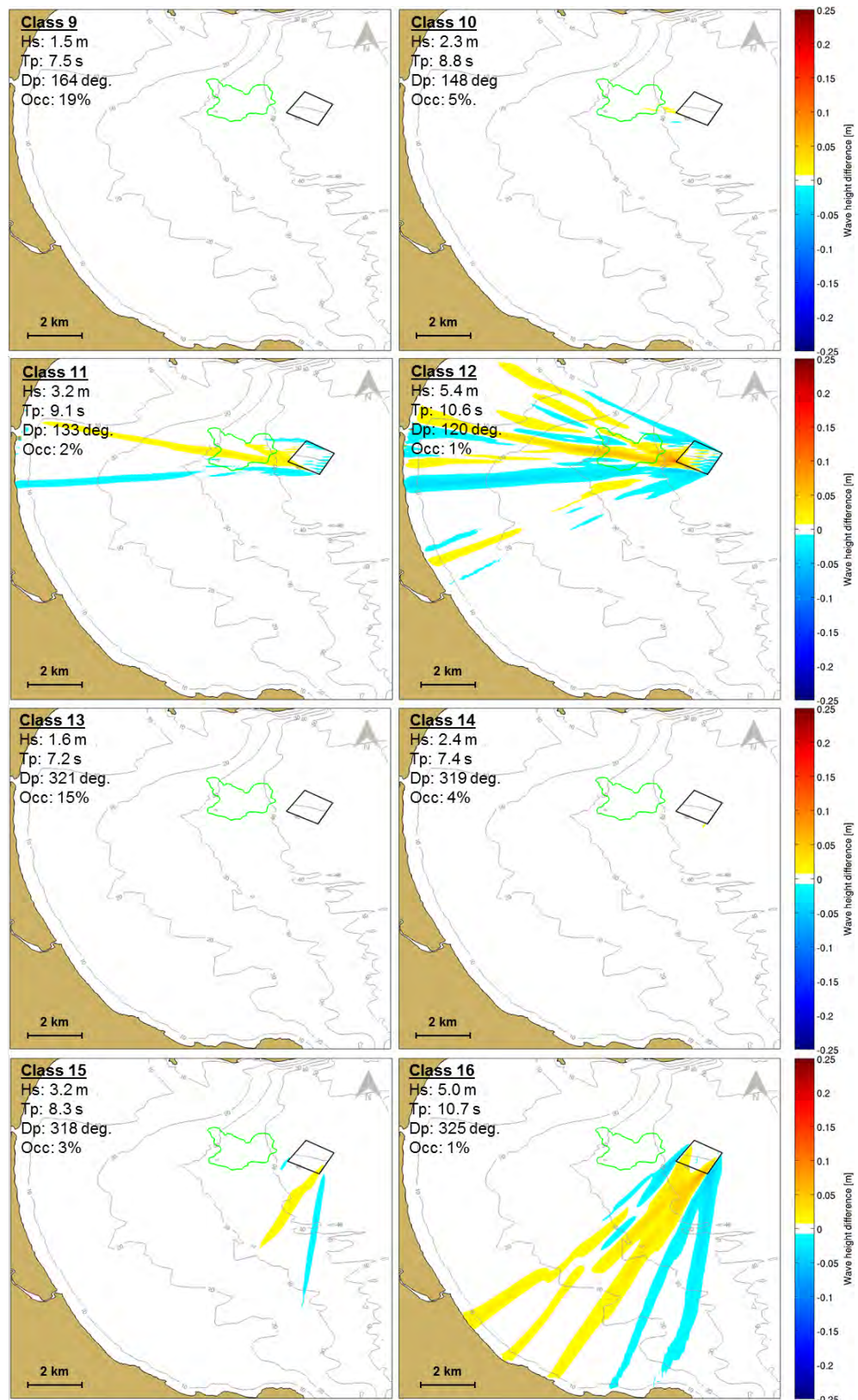


Figure 9.11 Difference in wave height fields caused by the disposal mound 3.2 over Bream Bay for wave scenarios 9 to 16. Hs, Tp, Dp and Occ (% Occurrence) presented in the upper left corner indicate the wave conditions at the offshore position BND (MSL Report P0297-01).

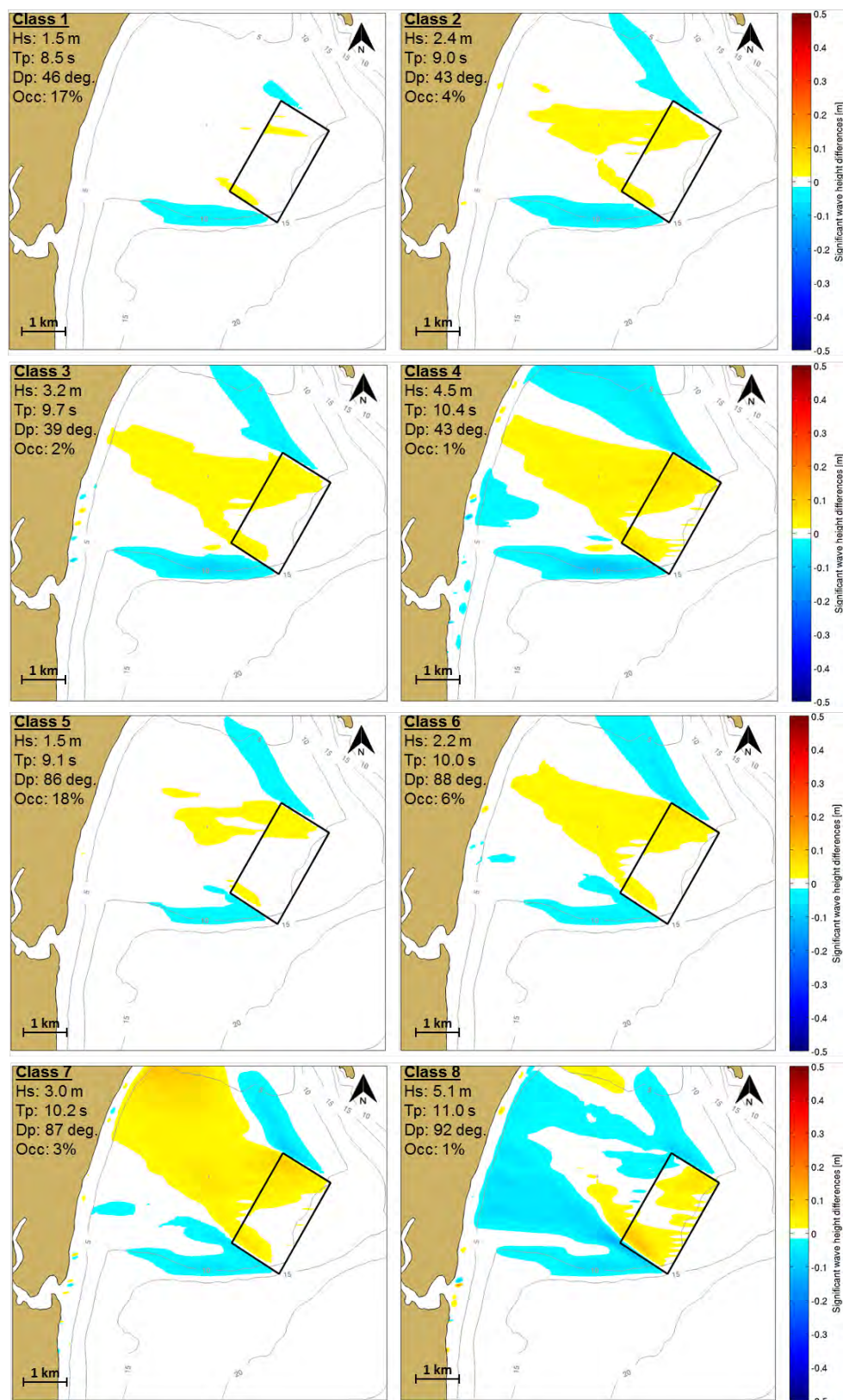


Figure 9.12 Difference in wave height fields caused by the disposal mound 1.2 near Ruakaka Beach for wave scenarios 1 to 8. Hs, Tp, Dp and Occ (% Occurrence) presented in the upper left corner indicate the wave conditions at the offshore position BND (MSL Report P0297-01).

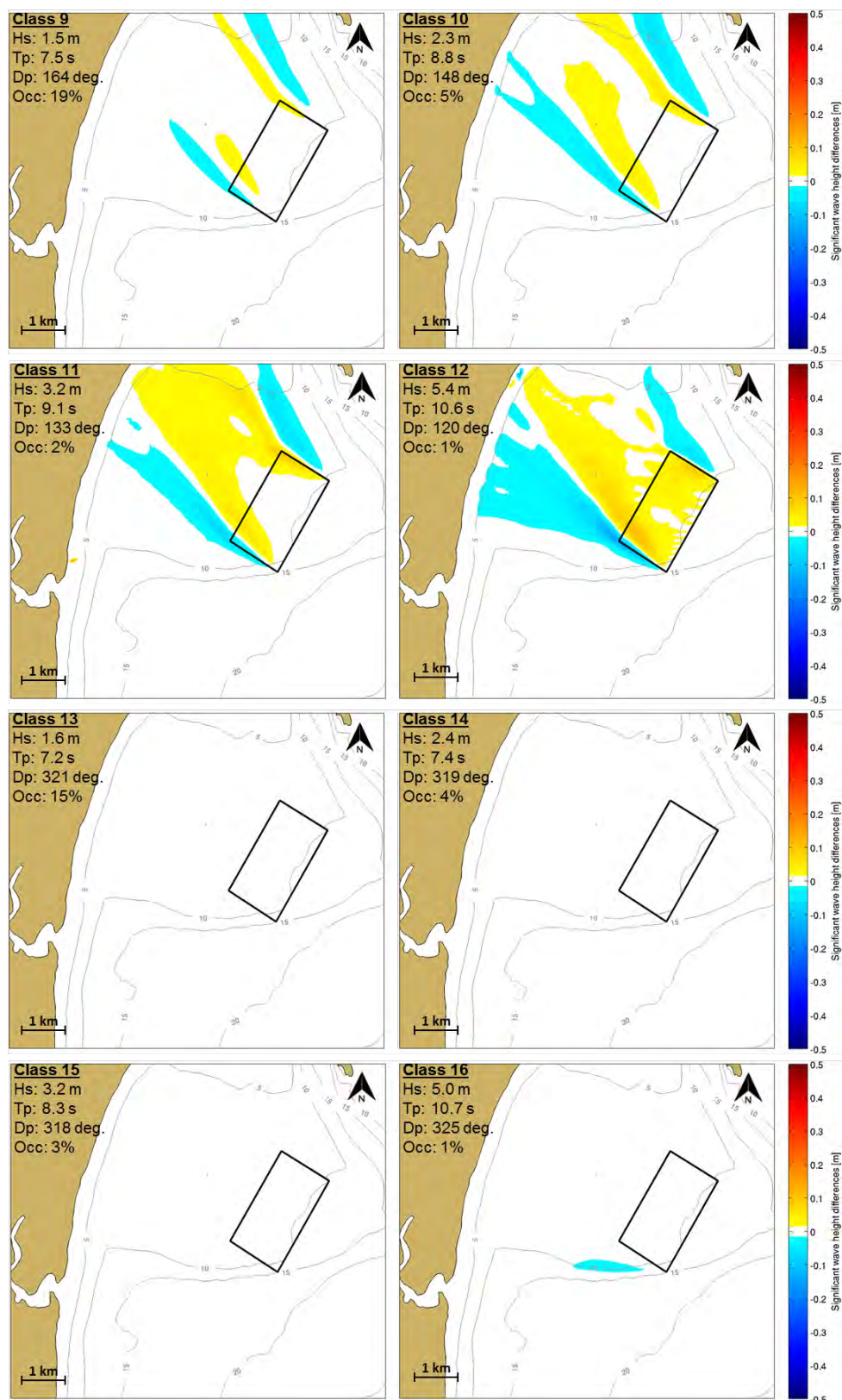


Figure 9.13 Difference in wave height fields caused by the disposal mound 1.2 near Ruakaka Beach for wave scenarios 9 to 16. Hs, Tp, Dp and Occ (% Occurrence) presented in the upper left corner indicate the wave conditions at the offshore position BND (MSL Report P0297-01).

## 9.6. Summary of effects of the disposal grounds

The numerical modelling of the sediment dynamics of the proposed offshore disposal ground in 40-45 m depth in Bream Bay shows that:

- The wave and current regime can occasionally mobilise sediments in this area. This will only occur during more energetic storm conditions, when sediments can be transported in suspension or by bedload processes.
- The predicted rate of movement of sediment from disposal ground 3.2 is very low and essentially omnidirectional, although results suggest a slight bias to the south.
- After one year, the extent of movement from disposal ground 3.2 will have a very limited excursion. This region of Bream Bay is characterised by 40-m water depths, and the erosion of the seabed in the area is not predicted to exceed a few centimetres by current and wave actions. The relative high depth favours a high degree of stability of the disposal mound.
- The adjacent 3 Mile Reef is not expected to receive a detectable amount of sediments coming from disposal ground 3.2. Moreover, given the receiving environment already has a similar grain size composition to the dredged sediments, there will be no material change to the sedimentary character of the 3 Mile Reef.
- The dredged material disposed at Disposal ground 1.2 is predicted to be transported in the south-western and north-western directions over the adjacent beach and sand bank areas by waves. The circulation induced by tidal and wave forcing in this region is not predicted to connect the disposal mound system with the channel system, thus the risk of channel infilling by the dredged material after disposal is limited.
- Predicted maximum changes to the nearshore wave climate by the presence of both the nearshore and the offshore mounds (disposal Site 1.2 and 3.2) are very minor and not expected to exceed +/- 0.05 m along the shoreline under energetic wave conditions. Therefore, no consequences on the beach or nearshore processes are expected. This includes no consequences to the recreational surfing activities along Ruakaka Beach.

## 10. DISPOSAL PLUMES

The dispersion of a plume caused by disposal operations was simulated at several sites within the proposed offshore disposal ground using a lagrangian particle modelling technique (ERcore model) nested within the hindcast regional 3D hydrodynamic flow fields. A detailed description of the methodology is provided in MSL Report P0297-01. As with the dredging plumes, a probabilistic modelling approach has been adopted to capture the range of possible plume outcomes.

### 10.1. Disposal plume modelling results

The mean suspended sediment concentrations (SSC) after 24h of continuous disposal for two different sizes of dredger (small and large trailing suction hopper dredger, TSHD) were determined from a 6-month simulation using the combined tidal and non-tidal currents as the environmental forcing. The results are presented in Figure 10.1 and Figure 10.2. The same conservative 12 mg/L SSC threshold used and discussed in the dredging plume section was applied in the disposal plume modelling.

The predicted SSC plumes clearly follow a northeast-southwest axis, which was expected given the current climate at the disposal ground (see Figure 9.1). Surface plumes are constrained to the mixing zone around the boat and do not extend more than 50 m from the release location. The SSC progressively increases with increasing depth due to the rapid settlement of the sediments through the water column. The simulations suggest that the mid water plume may extend about 500 m from the release location for both the small and the large dredge, to the minimum concentration threshold of 12 mg/L. However, most of the plume is constrained within a radius of 50 and 100 m for the small and the large dredge, respectively. Notably, the highest SSC levels within the lower water column are predicted to the southwest of the disposal ground; consistent with the flow regime being biased to this octant. The plumes do not show significant differences in extent or direction between sites inside the disposal ground. At site PW, the closest to the 3 Mile Reef, it is important to note that the plume does not intersect with the reef area, and the probability of a plume reaching the reef is considered very low.

As a form of corroboration, a disposal plume modelling scenario was also undertaken using the current velocity profiles recorded inside the proposed disposal ground from 15 January to 5 March, 2016. For this scenario, the plume results for both the large and the small vessels over a 24 h period exhibit a different behaviour (Figure 10.4), likely due to the shorter duration and the particular weather patterns at the time. Nonetheless, the results show less dispersion than the longer term modelling and no evidence of trajectory over the reef to the west of the disposal ground. These results confirm that the 5 – 20% bias identified in the model depth-averaged current velocities at the offshore disposal site has no significant impact on the plume dispersion. We therefore conclude that even taking into account this bias there is a very low probability of the plume reaching 3 Mile Reef.

Another useful metric for assessing the disposal plumes is the percentage of time a certain SSC level is exceeded. Exceedance time estimations were undertaken relative to reference SSC levels of 10, 50 and 100 mg.L<sup>-1</sup>. Two specific 48 h periods involving strong west surface and bottom currents were selected and results are provided in Figure 10.5 to Figure 10.8 for the large and small dredges. Also, two month-long simulations (January and August, 1995 – selected at random

to illustrate the summer and winter conditions) were run to investigate the seasonal variability of the exceedance time estimations. The results are presented in Figure 10.9 to Figure 10.12.

The exceedance time estimates suggest that plume dispersion and elevated SSC levels are not expected over the reef. The scenario corresponding to the disposal activities with the large vessel during overall strong westerly-directed currents on surface (Figure 10.5) indicate that even during a short-term non-favourable event, no dispersion over the reef is predicted to occur. Most of the fine sand particles were transported northward (within 3000 m for  $>10 \text{ mg.L}^{-1}$ ) on the surface while the medium sands settle quickly over a limited area (of less than 50 m radius). Note that the relatively strong westerly-directed bottom current scenario exhibits very similar results. The hydrodynamic conditions in summer do not promote large scale dispersions. The northward maximum extension of the exceeding time area considering a  $12 \text{ mg.L}^{-1}$  threshold is not predicted to exceed 1000 m over a 24 h period. In winter, the exceedance time patterns for thresholds of 12 and  $50 \text{ mg.L}^{-1}$  suggest a southward dominated dispersion within a 1500 m maximum radius.

## 10.2. Disposal plume summary

The disposal plume modelling undertaken for disposal ground 3.2 indicates that:

- The plumes caused by disposal are short lived and not highly dispersive. They typically extend along a northeast – southwest axis, preserving the adjacent reef from settlement, and 99% of the plume material settles to the seabed within 14 hours.
- The disposal plumes calculated from the measured current profiles have a lesser excursion than those determined from the long term current hindcast, and does not show incursion with the adjacent 3 Mile reef to the west of the proposed disposal ground.
- The SSC plumes over the disposal area are not expected to extend more than 550 m from the release locations and should only play a moderate role.

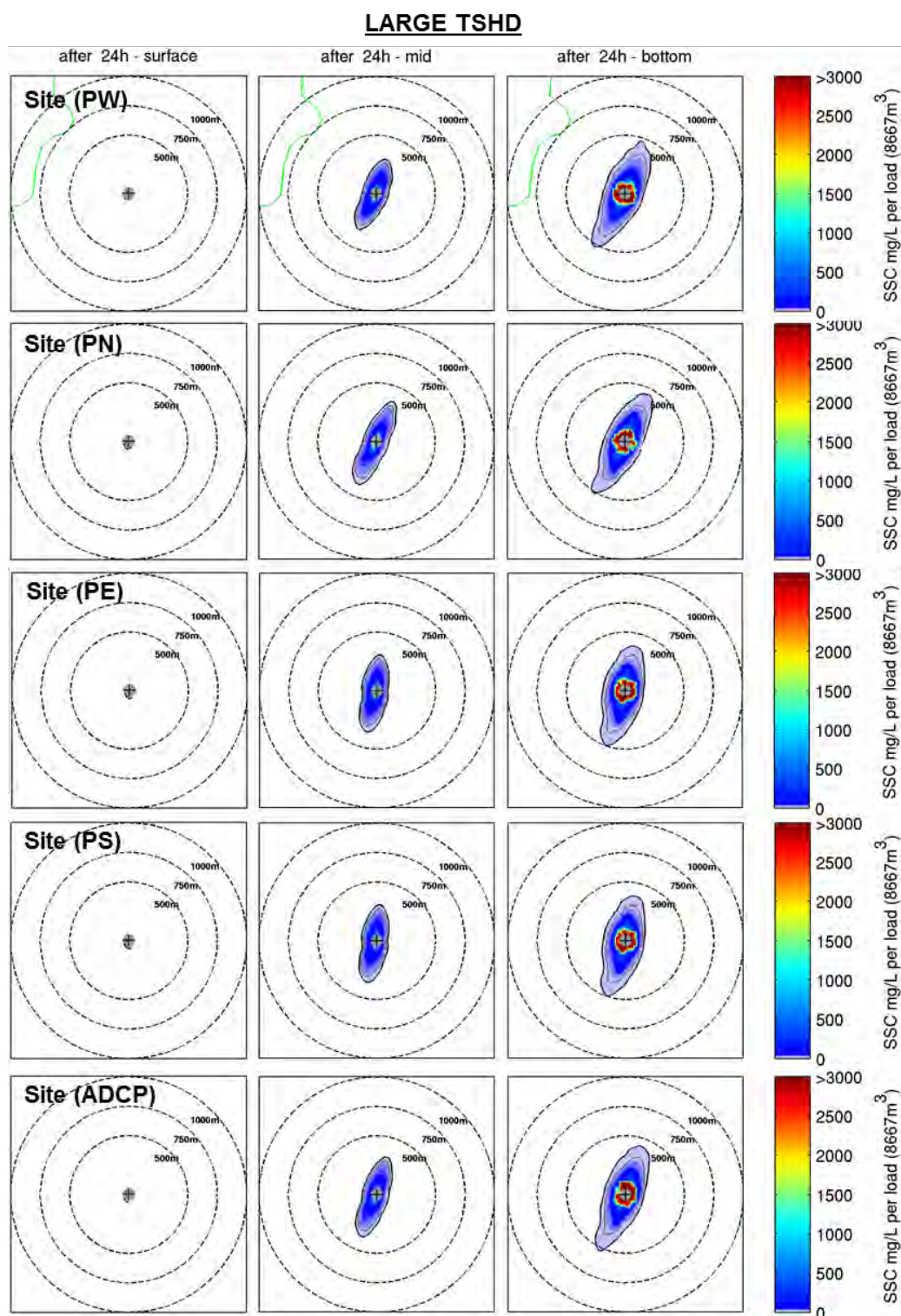


Figure 10.1 Predicted suspended sediment concentrations (SSC) after 24h at bottom, mid water and surface levels for a release at sites PW, PN, PE, PS and ADCP. Note that a large TSHD is considered here for the amount of released sediments. The green polygon indicates the contour of 3 Mile Reef. The black and grey lines indicate the 12- and 20-mg/L SSC threshold corresponding to the critical threshold for rocky reef systems and to the highest background concentration recorded near the entrance to Whangarei Harbour.

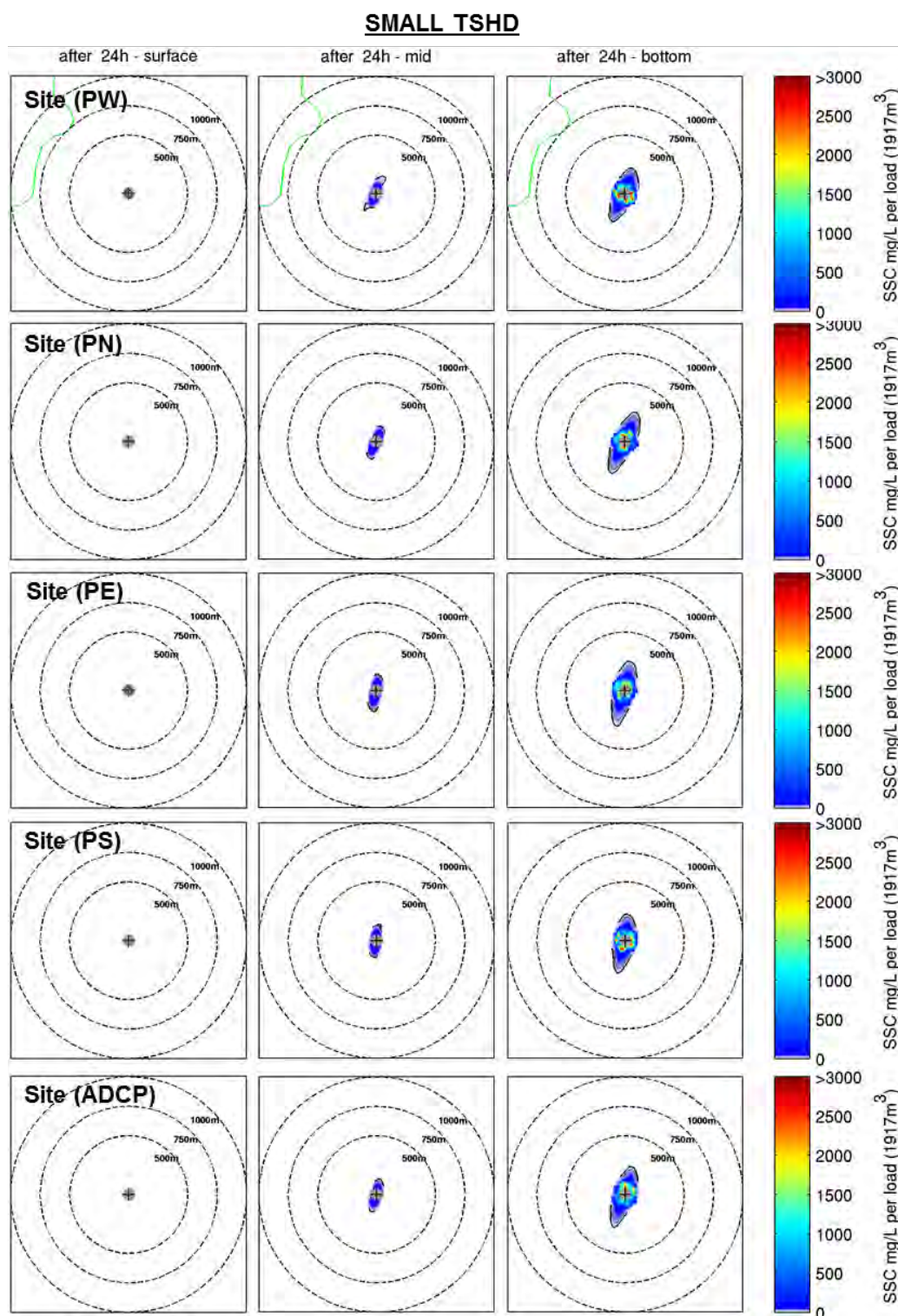


Figure 10.2 Predicted suspended sediment concentrations (SSC) after 24h at bottom, mid water and surface levels for a release at sites PW, PN, PE, PS and ADCP. Note that a small TSHD is considered here for the amount of released sediments. The green polygon indicates the contour of the adjacent reef. The black and grey lines indicate the 12- and 20- mg/L SSC threshold corresponding to the critical threshold for rocky reef systems and to the highest background concentration recorded near the entrance to Whangarei Harbour.

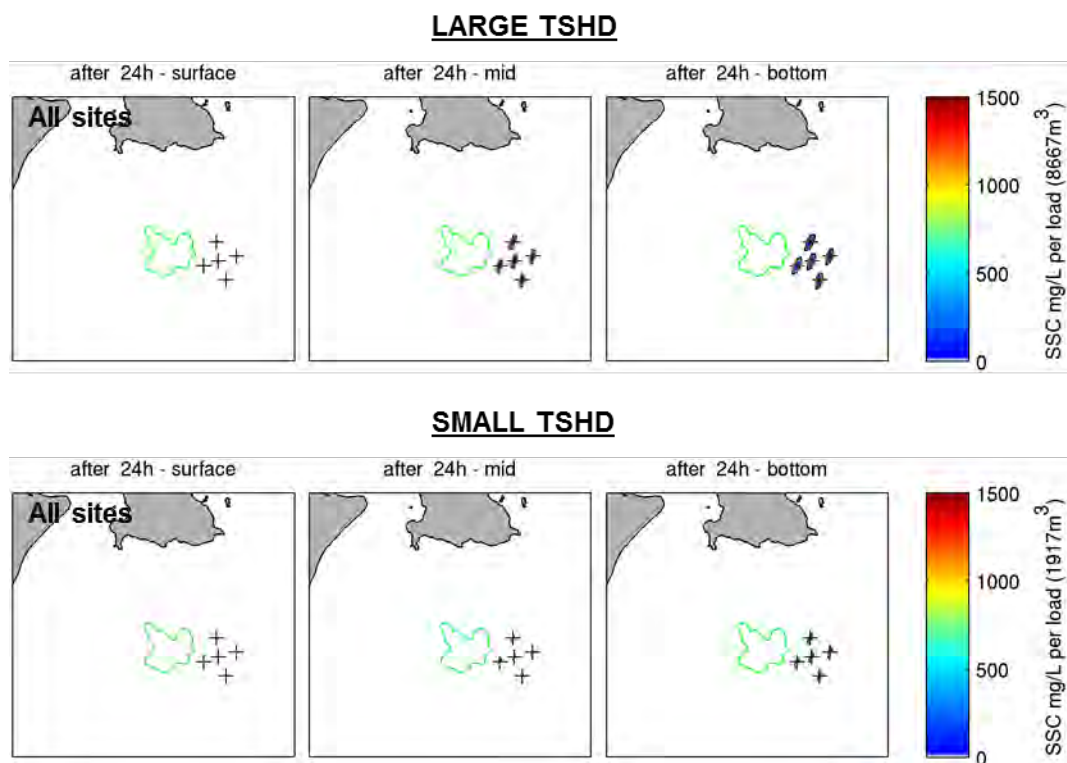


Figure 10.3 Overview of the predicted suspended sediment concentrations (SSC) after 24h at sites PW, PN, PE, PS and ADCP, for both the large and the small TSHD.

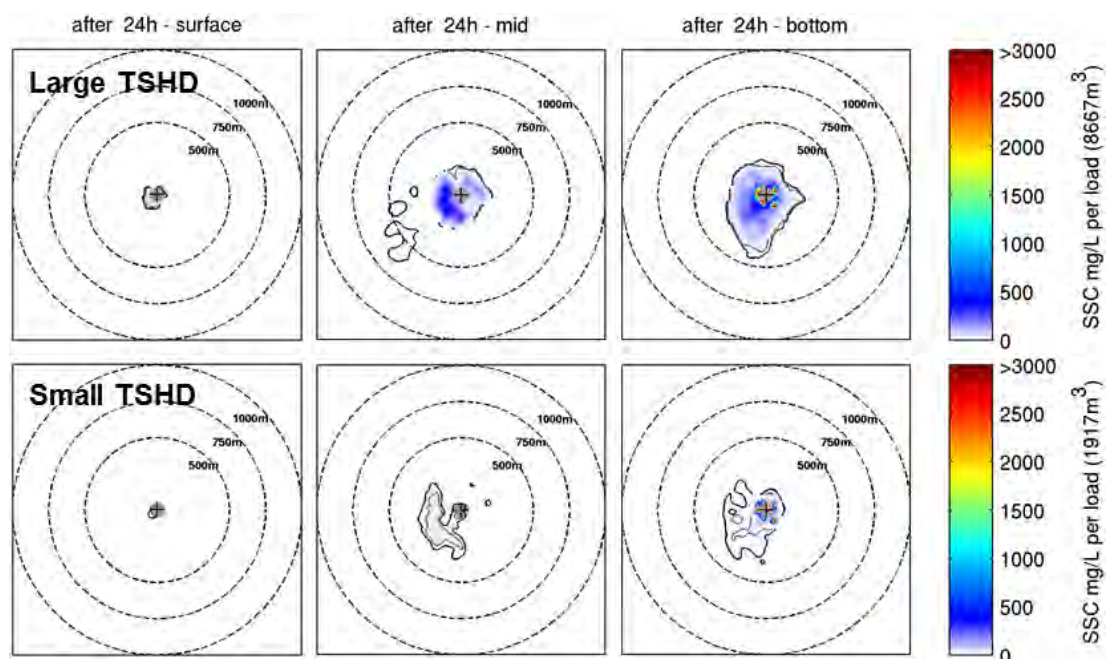


Figure 10.4 Predicted suspended sediment concentrations (SSC) after 24h at bottom, mid water and surface levels for a release at site ADCP forced by measured current data.

**LARGE TSHD - SITE (PW) – 10/12/1995**

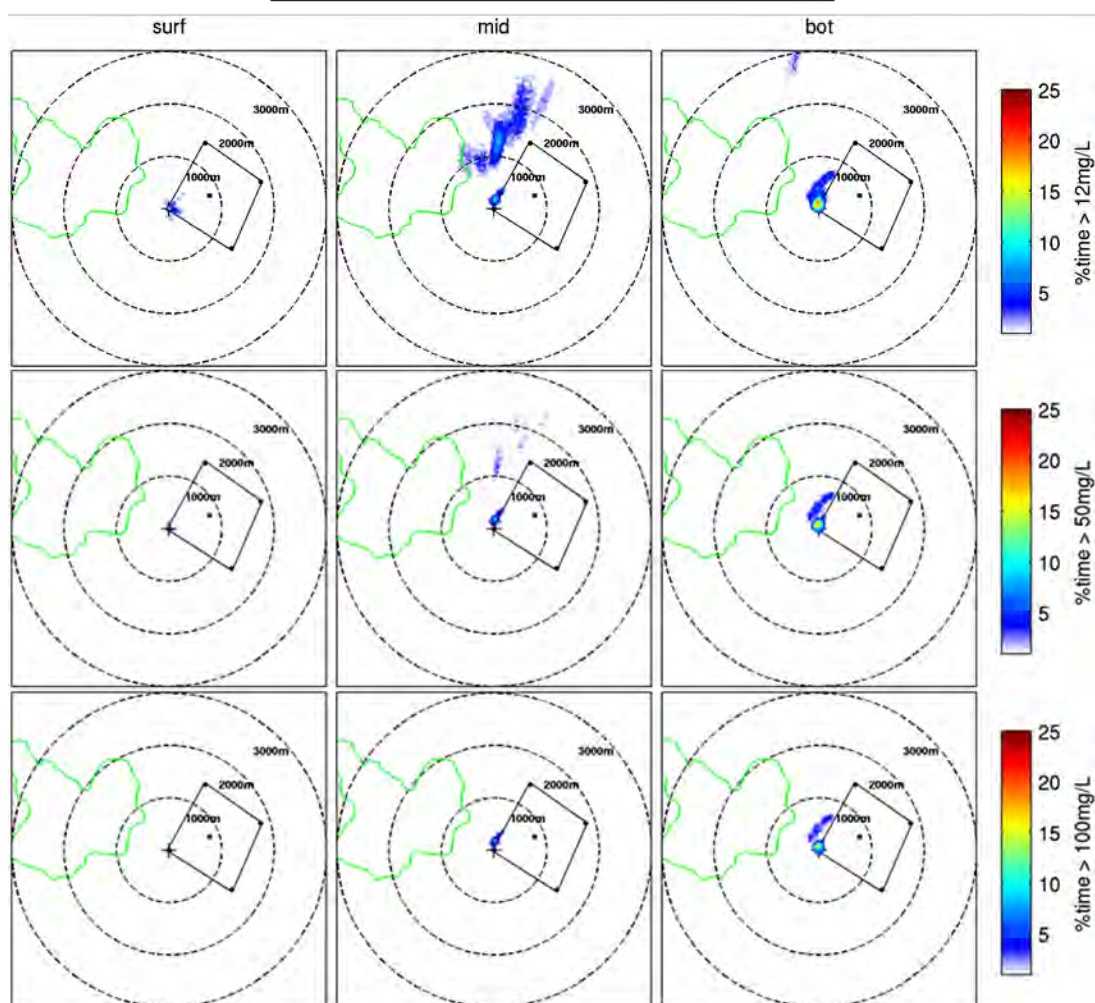


Figure 10.5 Percentage of time SSC thresholds of 12, 50, 100 mg.L<sup>-1</sup> are exceeded between 10/12/1995 12:00 and 12/12/1995 12:00, assuming disposal at site PW with the large TSHD. The green polygon indicates an adjacent reef classified as sensitive.

**SMALL TSHD - SITE (PW) – 10/12/1995**

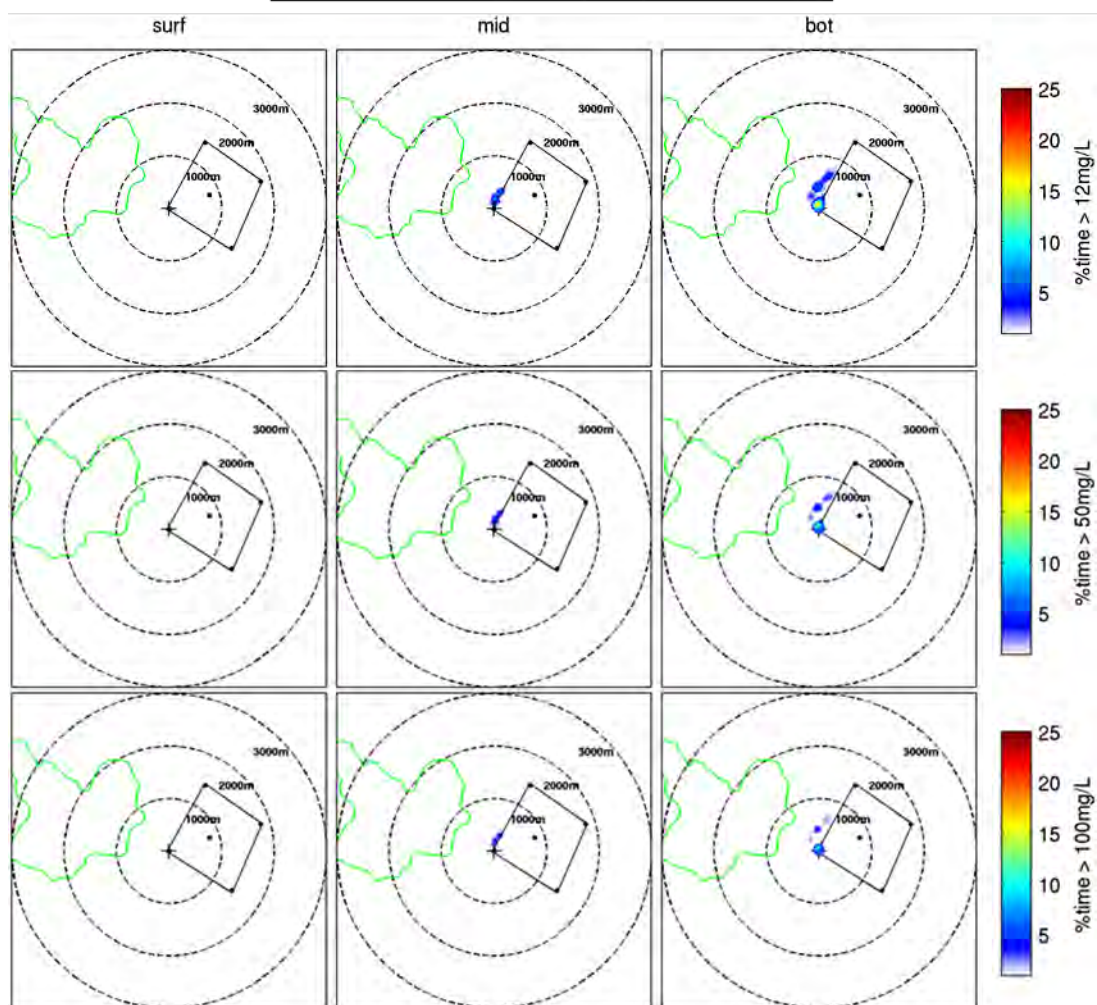


Figure 10.6 Percentage of time SSC thresholds of 12, 50, 100 mg.L<sup>-1</sup> are exceeded between 10/12/1995 12:00 and 12/12/1995 12:00, assuming disposal at site PW with the small TSHD. The green polygon indicates an adjacent reef classified as sensitive.

**LARGE TSHD - SITE (PW) – 06/02/1995**

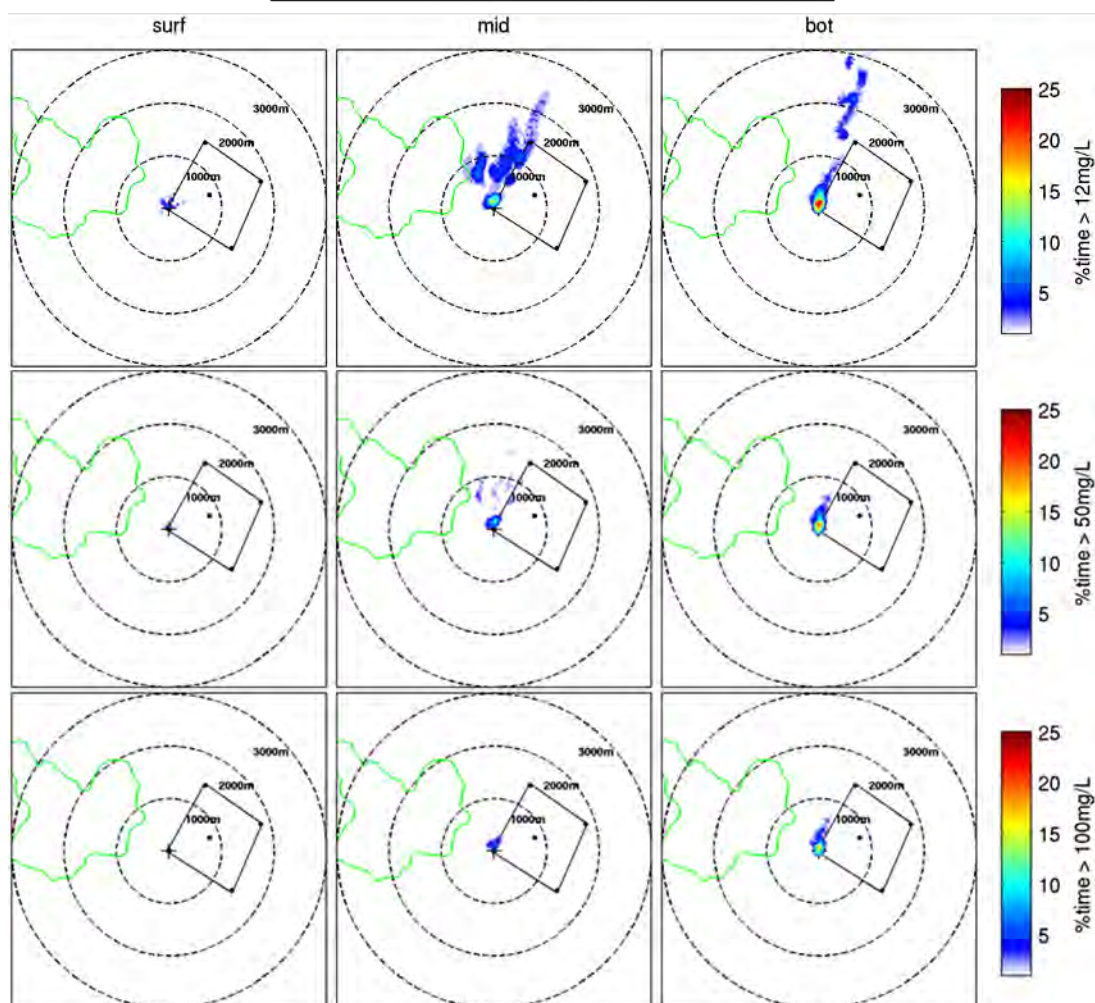


Figure 10.7 Percentage of time SSC thresholds of 12, 50, 100 mg.L<sup>-1</sup> are exceeded between 06/02/1995 12:00 and 08/02/1995 12:00, assuming disposal at site PW with the large TSHD. The green polygon indicates an adjacent reef classified as sensitive.

**SMALL TSHD - SITE (PW) – 06/02/1995**

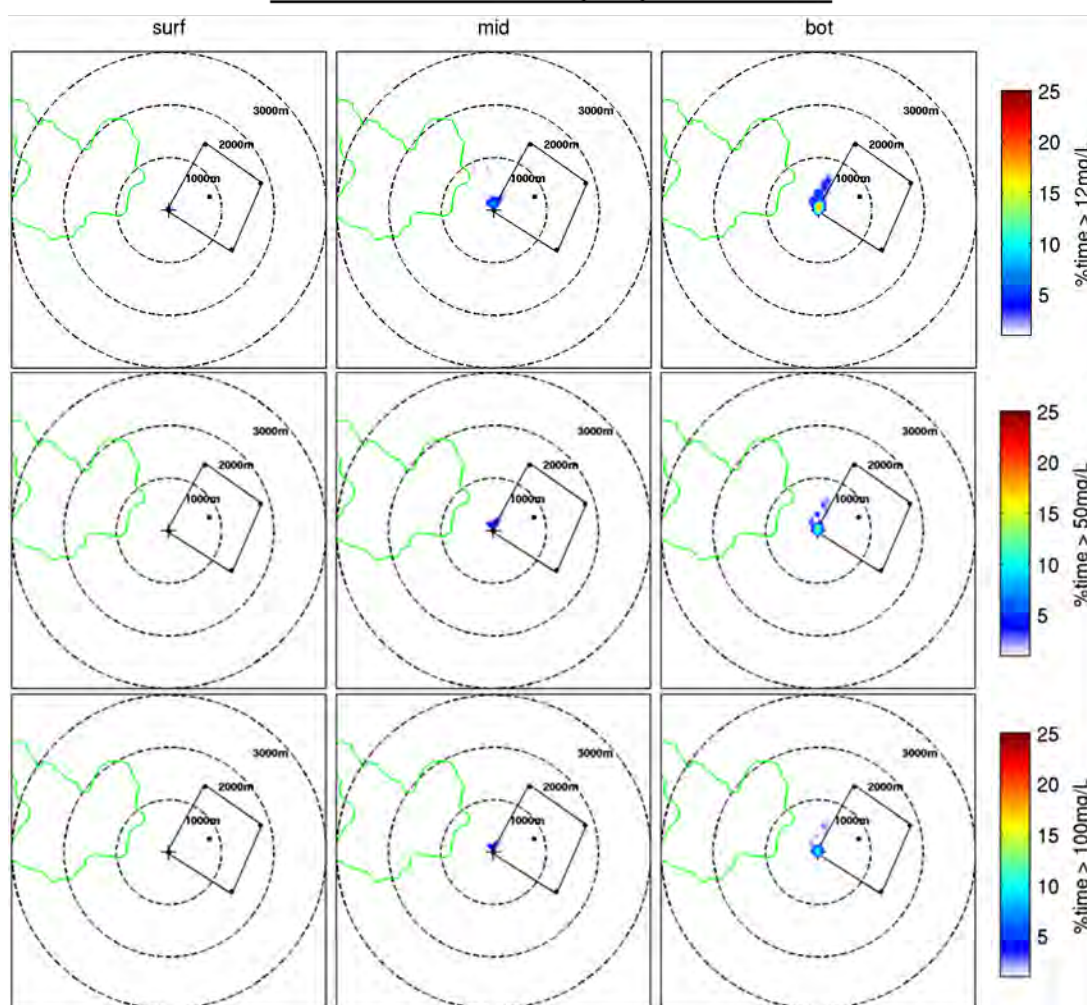


Figure 10.8 Percentage of time SSC thresholds of 12, 50, 100 mg.L<sup>-1</sup> are exceeded between 06/02/1995 12:00 and 08/02/1995 12:00, assuming disposal at site PW with the small TSHD. The green polygon indicates an adjacent reef classified as sensitive.

**LARGE TSHD - SITE (PW) - JANUARY**

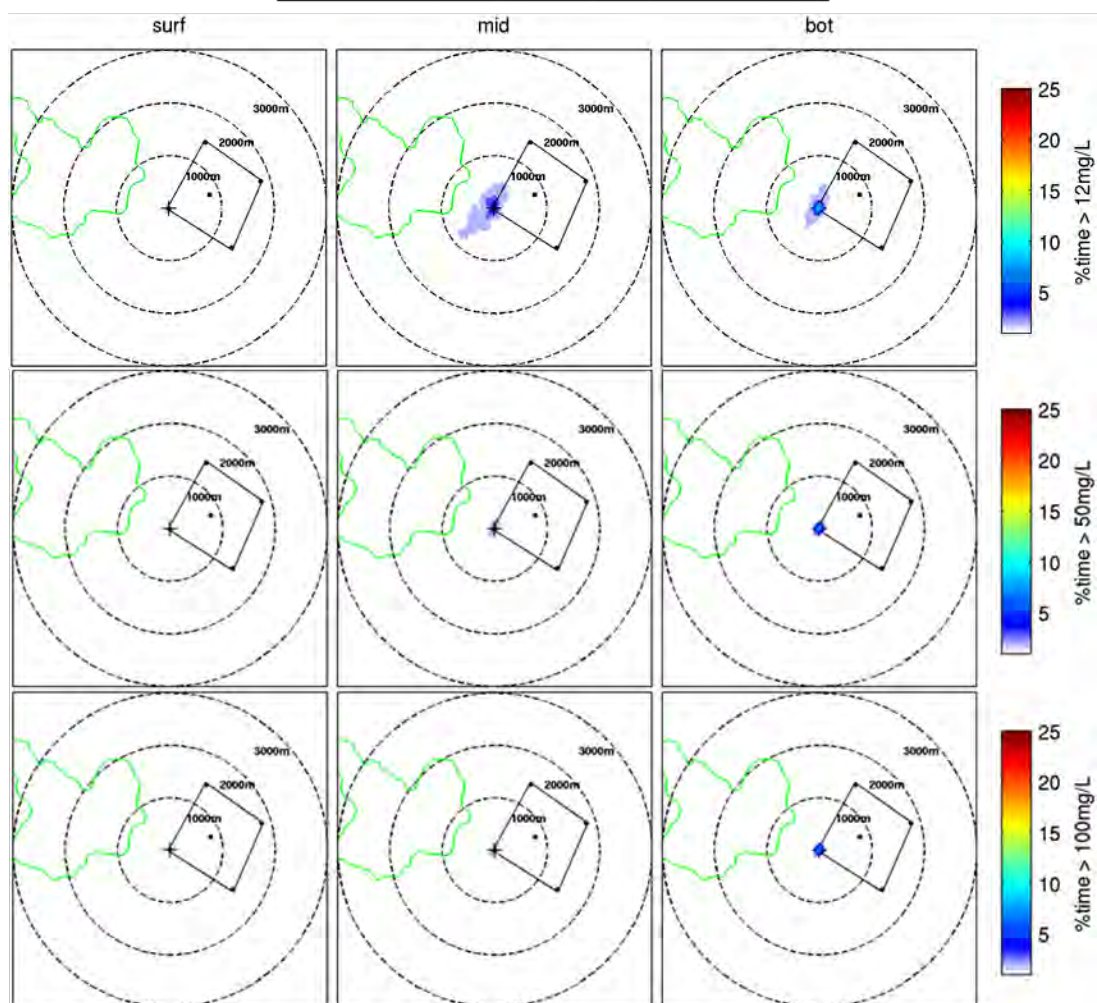


Figure 10.9 Percentage of time SSC thresholds of 12, 50, 100 mg.L<sup>-1</sup> are exceeded during the summer month of January, assuming disposal at site PW with the large TSHD. The green polygon indicates an adjacent reef classified as sensitive.

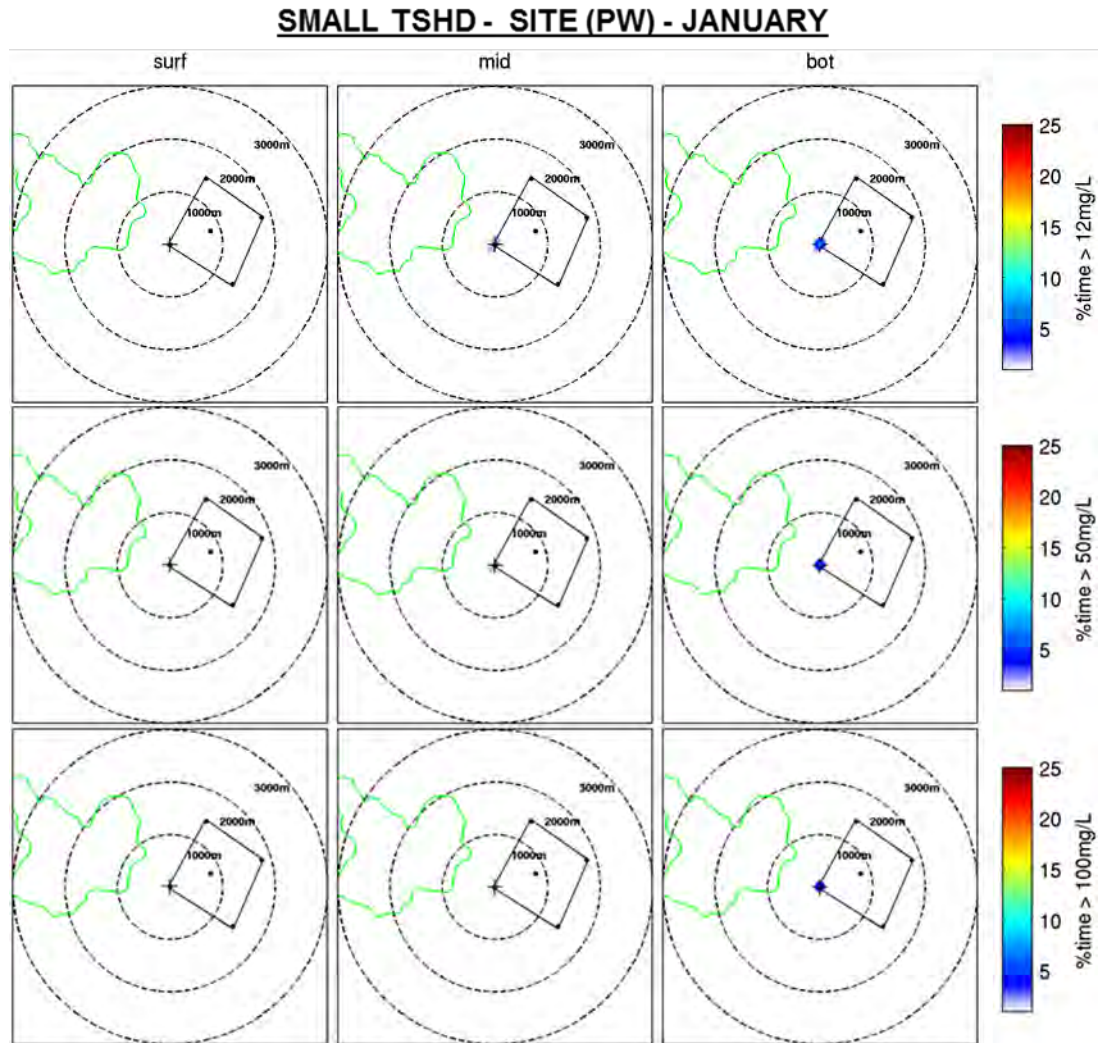


Figure 10.10 Percentage of time SSC thresholds of 12, 50, 100 mg.L<sup>-1</sup> are exceeded during the summer month of January, assuming disposal at site PW with the small TSHD. The green polygon indicates an adjacent reef classified as sensitive.

### LARGE TSHD - SITE (PW) - AUGUST

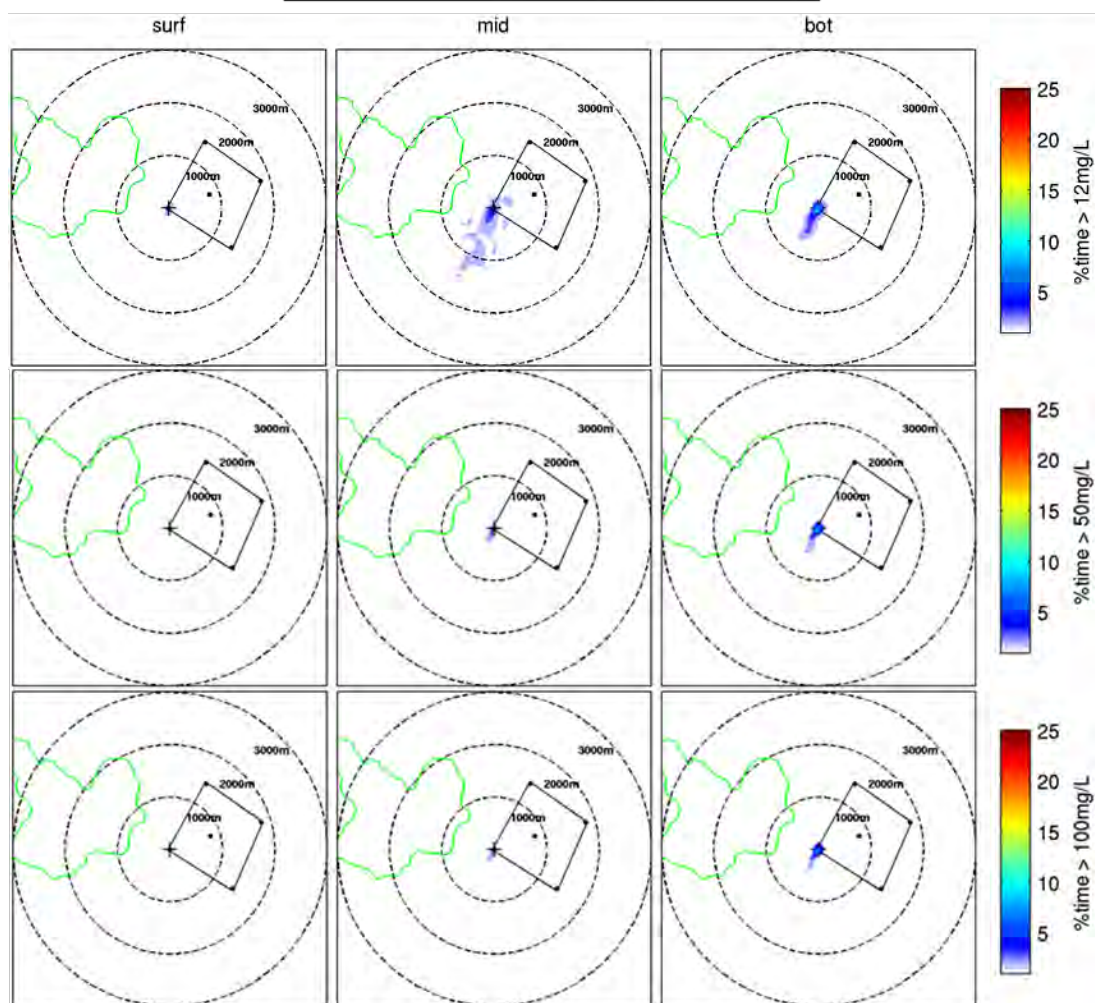


Figure 10.11 Percentage of time SSC thresholds of 12, 50, 100 mg.L<sup>-1</sup> are exceeded during the winter month of August, assuming disposal at site PW with the large TSHD. The green polygon indicates an adjacent reef classified as sensitive.

**SMALL TSHD - SITE (PW) - AUGUST**

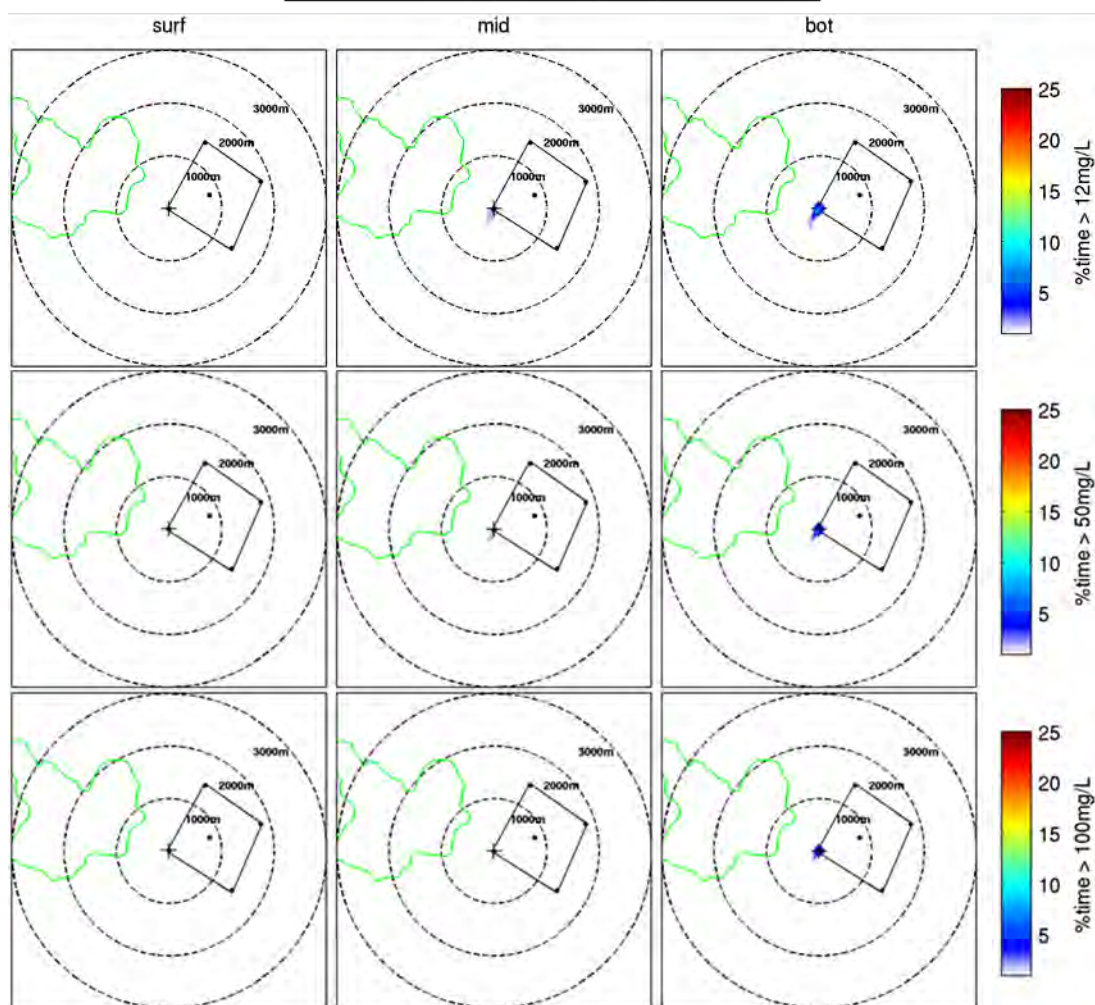


Figure 10.12 Percentage of time SSC thresholds of 102, 50, 100 mg.L<sup>-1</sup> are exceeded during the winter month of August, assuming disposal at site PW with the small TSHD. The green polygon indicates an adjacent reef classified as sensitive.

## REFERENCES

- Brian T. Coffey and Associates Limited, 2016a. Refining New Zealand Crude Shipping Project - Complementary literature review to inform survey work and report requirements to assess the environmental effects of proposed dredging and spoil disposal activities in the approaches to Mardsen Point.
- Brian T. Coffey and Associates Limited, 2016b. Refining New Zealand Crude Shipping Project, Modelling sedimentation effects associated with proposed dredging / Spoil disposal activities - Provisional turbidity / Suspended solids thresholds nominated for the protection of adjacent communities. Prepared for Chancery Green for Refining NZ.
- Folk, R., 1954. The distinction between grain size and mineral composition in sedimentary rock nomenclature. *J. Geol.* 62, 344–359.
- Kerr & Associates Report - Ecology Stage One Pilot Study, 2016.
- Kerr, V.C., 2016. Mair Bank channel edge additional characterisation: Crude Freight shipping project, Bream Bay, Whangarei. For Chancery Green on behalf of Refining NZ by Kerr and Associates.
- Longdill, P.C., Healy, T.R., 2007. Sediment dynamics surrounding a flood tidal delta adjacent to reclamation and a dredged turning basin. *J. Coast. Res.* 1097–1105.
- McComb, P., Black, K., Atkinson, P., Lim, Y.T., Heafy, T., 1999. The accretion of a breakwater-tip shoal following dredging, in: *Proceedings of the 14th Australasian Coastal and Ocean Engineering Conference and the 7th Australasian Port and Harbour Conference*. Australia, pp. 394–399.
- Morgan, K.M., Kench, P.S., Ford, R.B., 2011. Geomorphic change of an ebb-tidal delta: Mair Bank, Whangarei Harbour, New Zealand. *N. Z. J. Mar. Freshw. Res.* 45, 15–28.
- MSL, 2016. Crude Shipping Project, Whangarei Harbour - Establishment of numerical models of wind, wave, current and sediment dynamics.
- OMC International, 2016. Mardsen Point Channel Optimisation.
- Royal HaskoningDHV, 2016a. Shipping Channel - Concept Design Report, prepared for Refining NZ., Refining NZ Crude Freight Project.
- Royal HaskoningDHV, 2016b. Dredging Methodology Assessment. Technical Memo, prepared for Refining NZ., Refining NZ Crude Freight Project.
- Royal HaskoningDHV, 2015. Desktop Simulation Study, prepared for Refining NZ., Refining NZ Crude Freight Project.
- Stewart, 2017. Evaluating TSS/NTU Relationship for CSP, Refining NZ. Ryder Consulting January 2017.
- Tonkin and Taylor, 2016a. Crude Shipping project, Mid-point multi-criteria alternatives assessment. Prepared for ChanceryGreen for Refining NZ.
- Tonkin and Taylor, 2016b. Marsden point Refinery - Crude Freight Project, Vibrocore report (No. 30488.1000). Prepared for Chancery Green on behalf of Refining NZ.
- Tonkin and Taylor, 2010. Coastal Erosion Hazard Zone Review. Prepared for Whangarei District Council.
- Weppe, S., McComb, P., Coe, L., 2015. Numerical Model Studies to Support the Sustainable Management of Dredge Spoil Deposition in a Complex Nearshore Environment, in: *The Proceedings of the Coastal Sediments 2015*. World Scientific.
- Williams, J.R., Hume, T.M., 2014. Investigation into the decline of pipi at Mair Bank, Whangarei Harbour. Prepared for Northland Regional Council (No. AKL2014-022). NIWA.
- Wright, J., Colling, A., Park, D., 1999. *Waves, Tides, and Shallow-water Processes*, 2nd ed. Butterworth-Heinemann and Open University.

## APPENDIX A – WIND STATISTICS

Annual and monthly wind speed statistics at WRB.

Wind speed (m/s))	Parameter					
	Mean (m s <sup>-1</sup> )	Median (m s <sup>-1</sup> )	P90 (m s <sup>-1</sup> )	P95 (m s <sup>-1</sup> )	P99 (m s <sup>-1</sup> )	Max (m s <sup>-1</sup> )
Jan	5.71	5.45	9.28	10.52	13.22	19.24
Feb	5.58	5.35	9.09	10.33	13.33	17.32
Mar	5.75	5.54	9.34	10.71	13.61	23.74
Apr	5.64	5.36	9.25	10.61	13.14	20.01
May	6.10	5.84	10.04	11.21	13.59	19.54
Jun	6.50	6.23	10.60	12.18	14.99	20.09
Jul	6.69	6.26	11.22	13.02	16.14	22.76
Aug	6.46	6.14	10.75	12.09	14.79	20.02
Sep	6.48	6.25	10.44	11.92	14.87	19.88
Oct	6.43	6.24	10.32	11.52	13.65	18.91
Nov	6.17	5.99	9.82	10.95	13.77	20.05
Dec	5.70	5.47	9.31	10.46	13.06	18.56
1979	5.82	5.46	9.60	10.96	13.72	18.91
1980	6.25	6.06	10.26	11.61	14.62	20.08
1981	6.19	5.81	10.37	11.60	13.78	18.11
1982	5.87	5.57	9.62	11.14	13.51	20.39
1983	6.16	5.89	9.76	11.21	14.15	21.08
1984	5.83	5.53	10.03	11.39	14.06	18.49
1985	6.23	6.01	10.35	11.46	14.41	19.63
1986	5.64	5.35	9.39	10.84	13.91	19.24
1987	5.95	5.69	9.86	11.09	13.41	17.13
1988	6.35	6.09	10.34	11.86	15.01	23.74
1989	6.34	5.92	10.59	12.36	15.30	20.02
1990	5.71	5.45	9.34	10.55	13.27	18.49
1991	6.13	6.00	9.65	10.71	12.82	16.61
1992	6.35	6.20	10.10	11.22	14.15	19.20
1993	5.89	5.66	9.71	10.89	13.91	20.07
1994	6.42	6.25	10.20	11.37	13.81	18.30
1995	6.09	5.94	9.64	10.87	13.20	19.88
1996	6.52	6.31	10.33	11.82	14.35	20.09
1997	6.11	5.74	10.05	11.66	14.74	19.21
1998	6.34	5.90	10.70	12.36	15.67	20.05
1999	6.02	5.79	9.87	11.00	13.61	16.56
2000	6.14	5.74	10.09	12.20	14.95	18.20
2001	6.27	6.10	9.92	11.22	14.34	18.08
2002	6.45	6.29	10.16	11.22	13.70	19.58
2003	6.14	5.77	10.03	11.55	14.09	18.51
2004	6.21	6.01	10.07	11.51	13.81	17.13
2005	5.78	5.48	9.65	10.82	14.21	17.98
2006	5.93	5.68	9.66	10.81	14.09	19.58
2007	6.07	5.78	10.12	11.69	14.74	21.62
2008	6.36	6.10	10.19	11.90	14.65	20.83
2009	6.08	5.84	9.87	11.22	14.51	22.76
2010	6.00	5.63	9.94	11.70	14.08	18.89
2011	6.05	5.61	10.27	11.79	14.20	17.27
2012	6.25	6.06	9.99	11.34	13.75	17.29
2013	5.72	5.38	9.63	11.08	13.83	17.39
2014	6.09	5.68	10.15	11.97	15.53	20.85
Annual	6.10	5.83	9.99	11.36	14.27	23.74

Monthly and annual wind speed exceedance probabilities at WRB.

Wind speed (m/s)	Exceedance (%)												
	January	February	March	April	May	June	July	August	September	October	November	December	Year
>2	92.95	92.33	92.53	92.19	93.22	94.07	94.37	94.33	94.21	94.69	94.46	93.18	93.55
>4	70.93	69.37	71.42	70.12	74.10	77.45	78.45	77.18	78.00	78.02	76.81	71.38	74.46
>6	42.44	40.78	43.49	41.48	48.07	52.86	53.24	51.59	53.15	53.42	49.92	42.11	47.75
>8	19.37	17.88	19.44	18.92	24.94	29.84	30.19	29.00	28.91	28.67	24.29	19.05	24.24
>10	6.72	5.94	7.34	6.76	10.22	13.11	15.47	13.65	12.33	12.12	8.85	6.65	9.96
>12	2.51	2.09	2.58	2.23	2.99	5.38	7.43	5.34	4.77	3.77	2.60	2.03	3.65
>14	0.59	0.66	0.72	0.54	0.80	1.86	3.24	1.76	1.66	0.74	0.88	0.50	1.17
>16	0.16	0.14	0.24	0.15	0.15	0.58	1.10	0.43	0.42	0.16	0.24	0.11	0.32
>18	0.04	0.00	0.11	0.03	0.03	0.17	0.38	0.10	0.08	0.04	0.06	0.03	0.09
>20	0.00	0.00	0.07	0.01	0.00	0.02	0.13	0.01	0.00	0.00	0.01	0.00	0.02
>22	0.00	0.00	0.03	0.00	0.00	0.00	0.01	0.00	0.00	0.00	0.00	0.00	0.00

Annual joint probability distribution (parts per thousand) of the wind speed and wind direction at WRB.

Wind speed (m/s)	Wind direction (degT, from)								Total
	337.5-22.5	22.5-67.5	67.5-112.5	112.5-157.5	157.5-202.5	202.5-247.5	247.5-292.5	292.5-337.5	
0 - 2	6.3	6.2	7.0	7.0	8.1	10.5	11.0	8.3	64.4
2 - 4	17.0	19.3	21.9	18.6	22.5	33.0	35.2	23.4	190.9
4 - 6	25.5	26.1	26.3	20.1	26.1	56.1	49.9	37.1	267.2
6 - 8	25.9	20.2	25.8	14.3	16.2	59.9	43.9	28.9	235.1
8 - 10	19.9	12.4	17.3	9.6	7.8	31.1	29.6	15.2	142.9
10 - 12	10.3	8.0	9.6	5.6	2.8	9.8	11.5	5.5	63.1
12 - 14	4.2	4.6	4.7	3.3	1.0	2.5	3.0	1.6	24.9
14 - 16	1.3	1.9	2.4	1.0	0.4	0.5	0.6	0.3	8.4
16 - 18	0.3	0.5	0.7	0.4	0.1	0.1	0.1	0.0	2.2
18 - 20	0.1	0.2	0.3	0.1	0.0	0.0	0.0	0.0	0.7
20 - 22	0.0	0.0	0.1	0.0	0.0	0.0	0.0	0.0	0.1
<b>Total</b>	110.8	99.4	116.1	80.0	85.0	203.5	184.8	120.3	1000.0

## APPENDIX B – WAVE STATISTICS

Annual and monthly total significant wave height statistics at WRB.

$H_s$ (m)	Parameter					
	Mean (m)	Median (m)	P90 (m)	P95 (m)	P99 (m)	Max (m)
Jan	0.82	0.68	1.48	1.89	2.82	3.85
Feb	0.92	0.79	1.63	1.98	2.85	4.51
Mar	0.90	0.75	1.62	1.94	2.74	5.86
Apr	0.86	0.73	1.59	1.93	2.68	4.63
May	0.80	0.67	1.46	1.82	2.64	5.09
Jun	0.81	0.64	1.59	1.98	2.87	4.89
Jul	0.90	0.66	1.88	2.45	3.68	5.35
Aug	0.78	0.61	1.51	2.01	3.08	4.97
Sep	0.74	0.58	1.41	1.80	2.80	4.51
Oct	0.66	0.55	1.22	1.52	2.16	4.29
Nov	0.69	0.54	1.30	1.62	2.56	5.00
Dec	0.75	0.63	1.33	1.62	2.35	3.59
1979	0.81	0.67	1.44	1.84	2.69	3.69
1980	0.73	0.58	1.31	1.72	3.01	4.15
1981	0.88	0.73	1.63	1.97	2.73	4.16
1982	0.75	0.58	1.39	1.91	3.01	4.33
1983	0.76	0.61	1.43	1.83	2.91	4.54
1984	0.88	0.70	1.71	2.00	3.06	5.09
1985	0.94	0.75	1.75	2.09	3.01	3.88
1986	0.71	0.59	1.33	1.62	2.35	3.37
1987	0.73	0.61	1.24	1.66	2.92	3.50
1988	0.84	0.65	1.59	2.05	3.52	5.86
1989	0.99	0.82	1.89	2.28	3.44	4.97
1990	0.68	0.59	1.23	1.46	1.88	2.34
1991	0.70	0.60	1.26	1.56	2.16	2.89
1992	0.70	0.56	1.26	1.65	2.73	4.63
1993	0.71	0.54	1.42	1.81	2.48	4.22
1994	0.75	0.60	1.39	1.79	2.30	3.31
1995	0.78	0.65	1.38	1.64	2.36	3.15
1996	0.78	0.62	1.48	1.93	2.89	4.89
1997	0.77	0.62	1.37	1.85	2.96	4.51
1998	0.95	0.81	1.64	2.10	2.92	5.00
1999	0.88	0.76	1.53	1.87	2.51	2.91
2000	0.85	0.62	1.71	2.14	3.58	4.40
2001	0.90	0.75	1.67	1.97	3.13	4.05
2002	0.73	0.61	1.33	1.71	2.73	4.21
2003	0.86	0.72	1.58	2.09	2.99	4.51
2004	0.72	0.62	1.26	1.51	2.25	2.92
2005	0.79	0.63	1.58	1.91	2.57	3.14
2006	0.71	0.58	1.31	1.82	2.72	3.38
2007	0.83	0.65	1.59	1.93	3.04	5.02
2008	0.87	0.71	1.57	1.98	2.85	4.12
2009	0.79	0.59	1.54	1.91	2.63	5.35
2010	0.80	0.68	1.47	1.77	2.49	4.29
2011	0.87	0.73	1.62	2.07	2.77	3.88
2012	0.85	0.68	1.61	1.91	2.80	4.63
2013	0.83	0.70	1.59	1.92	2.64	3.41
2014	0.80	0.62	1.51	2.08	3.50	4.84
Annual	0.80	0.65	1.50	1.89	2.85	5.86

Annual and monthly significant swell wave statistics at WRB.

$H_s$ (m)	Parameter					
	Mean (m)	Median (m)	P90 (m)	P95 (m)	P99 (m)	Max (m)
Jan	0.50	0.39	1.00	1.39	2.09	3.22
Feb	0.57	0.45	1.17	1.42	2.04	3.24
Mar	0.55	0.41	1.13	1.39	2.00	4.85
Apr	0.53	0.40	1.15	1.44	2.03	3.83
May	0.45	0.31	1.00	1.32	2.10	4.03
Jun	0.43	0.26	1.04	1.40	2.13	4.08
Jul	0.52	0.28	1.36	1.85	2.78	4.28
Aug	0.44	0.28	0.98	1.42	2.39	3.99
Sep	0.40	0.25	0.91	1.25	2.01	3.33
Oct	0.33	0.21	0.77	1.06	1.70	2.96
Nov	0.38	0.25	0.84	1.13	1.95	4.05
Dec	0.46	0.35	0.91	1.14	1.76	3.16
1979	0.46	0.35	0.96	1.23	1.91	2.73
1980	0.37	0.23	0.83	1.15	1.96	3.11
1981	0.51	0.40	1.12	1.41	1.80	3.01
1982	0.42	0.28	0.85	1.35	2.31	3.34
1983	0.44	0.31	0.97	1.28	2.12	3.55
1984	0.55	0.38	1.24	1.50	2.55	4.03
1985	0.55	0.39	1.21	1.50	2.26	3.07
1986	0.40	0.29	0.86	1.13	1.72	2.30
1987	0.40	0.29	0.88	1.21	2.12	2.71
1988	0.50	0.31	1.11	1.43	2.88	4.85
1989	0.60	0.43	1.39	1.76	2.63	3.99
1990	0.36	0.28	0.76	0.97	1.33	1.67
1991	0.37	0.25	0.85	1.08	1.54	2.00
1992	0.34	0.22	0.66	1.02	1.96	3.50
1993	0.39	0.23	0.92	1.19	1.78	2.92
1994	0.40	0.25	0.99	1.29	1.94	2.43
1995	0.43	0.30	0.95	1.19	1.94	2.69
1996	0.43	0.29	0.91	1.27	2.38	4.08
1997	0.43	0.30	0.88	1.24	2.32	3.63
1998	0.60	0.47	1.10	1.47	2.21	4.05
1999	0.53	0.40	1.13	1.31	1.73	2.12
2000	0.52	0.30	1.27	1.69	2.74	3.49
2001	0.54	0.40	1.16	1.49	2.34	3.11
2002	0.36	0.20	0.86	1.17	2.20	3.23
2003	0.52	0.36	1.16	1.55	2.32	3.55
2004	0.39	0.27	0.82	1.14	1.80	2.37
2005	0.47	0.31	1.17	1.43	2.04	2.89
2006	0.40	0.27	0.86	1.24	2.23	2.95
2007	0.48	0.34	1.04	1.34	2.08	4.12
2008	0.48	0.34	1.09	1.39	1.98	2.92
2009	0.47	0.32	1.05	1.33	1.88	4.28
2010	0.47	0.33	1.03	1.27	1.65	2.96
2011	0.54	0.40	1.16	1.45	2.18	2.92
2012	0.52	0.39	1.19	1.46	2.11	3.83
2013	0.55	0.41	1.21	1.55	2.00	2.58
2014	0.49	0.35	1.05	1.56	2.59	3.85
<b>Annual</b>	0.46	0.32	1.03	1.36	2.13	4.85

Annual and monthly significant windsea wave statistics at WRB.

$H_s$ (m)	Parameter					
	Mean (m)	Median (m)	P90 (m)	P95 (m)	P99 (m)	Max (m)
Jan	0.62	0.52	1.13	1.39	2.03	2.76
Feb	0.69	0.60	1.21	1.46	2.10	3.17
Mar	0.68	0.59	1.19	1.45	2.06	3.37
Apr	0.64	0.55	1.14	1.38	1.97	2.68
May	0.62	0.53	1.10	1.35	1.97	3.11
Jun	0.64	0.53	1.19	1.49	2.17	3.03
Jul	0.68	0.53	1.35	1.78	2.54	3.31
Aug	0.60	0.48	1.15	1.51	2.12	3.11
Sep	0.58	0.48	1.06	1.31	2.09	3.05
Oct	0.53	0.46	0.96	1.15	1.65	3.11
Nov	0.55	0.45	1.00	1.21	1.87	2.99
Dec	0.57	0.48	1.03	1.23	1.76	2.73
1979	0.63	0.52	1.12	1.40	2.07	2.74
1980	0.59	0.49	1.09	1.37	2.31	2.88
1981	0.68	0.58	1.19	1.50	2.12	2.97
1982	0.58	0.46	1.07	1.35	2.22	2.88
1983	0.59	0.49	1.08	1.31	2.15	2.85
1984	0.64	0.53	1.17	1.48	2.00	3.11
1985	0.72	0.61	1.34	1.59	2.12	2.61
1986	0.55	0.47	0.97	1.20	1.87	2.76
1987	0.57	0.49	1.00	1.25	2.02	2.53
1988	0.64	0.52	1.23	1.53	2.26	3.37
1989	0.74	0.63	1.28	1.68	2.32	3.11
1990	0.54	0.48	0.96	1.20	1.62	1.85
1991	0.55	0.46	0.99	1.17	1.77	2.51
1992	0.58	0.48	1.05	1.26	2.10	3.31
1993	0.55	0.43	1.11	1.33	2.13	3.05
1994	0.59	0.52	1.03	1.27	1.61	2.45
1995	0.61	0.52	1.05	1.23	1.60	2.38
1996	0.62	0.51	1.17	1.45	2.09	2.84
1997	0.60	0.49	1.09	1.43	2.14	3.04
1998	0.70	0.59	1.26	1.55	2.29	3.04
1999	0.67	0.59	1.18	1.44	1.93	2.55
2000	0.64	0.50	1.18	1.59	2.29	3.07
2001	0.68	0.59	1.18	1.46	2.27	2.65
2002	0.59	0.50	1.04	1.27	1.77	2.94
2003	0.64	0.55	1.12	1.43	2.06	3.17
2004	0.56	0.49	0.96	1.15	1.61	2.32
2005	0.60	0.51	1.10	1.31	1.77	2.17
2006	0.54	0.46	0.96	1.21	1.83	2.62
2007	0.64	0.51	1.21	1.52	2.36	3.05
2008	0.68	0.58	1.23	1.47	2.18	2.94
2009	0.60	0.47	1.10	1.48	2.08	3.21
2010	0.62	0.53	1.09	1.38	2.09	3.12
2011	0.64	0.54	1.23	1.50	2.09	2.65
2012	0.63	0.53	1.21	1.43	2.04	2.77
2013	0.58	0.50	1.04	1.26	1.86	2.65
2014	0.59	0.45	1.11	1.56	2.39	3.06
<b>Annual</b>	0.62	0.51	1.12	1.39	2.09	3.37

Monthly and annual total significant wave height exceedance probabilities at WRB.

$H_s$ (m)	Exceedance (%)												
	January	February	March	April	May	June	July	August	September	October	November	December	Year
>0.5	71.68	79.24	76.61	72.69	69.06	63.54	66.11	62.24	60.01	56.10	55.23	65.57	66.45
>1	24.35	33.68	31.82	30.45	25.18	26.96	29.41	22.61	20.66	16.32	18.52	22.66	25.17
>1.5	9.72	13.21	13.03	11.54	9.33	11.54	15.99	10.09	8.52	5.14	6.27	6.68	10.07
>2	4.22	4.84	4.41	4.24	3.72	4.80	8.40	5.05	3.13	1.69	2.48	2.13	4.09
>2.5	1.95	1.68	1.46	1.56	1.38	1.92	4.82	2.45	1.40	0.35	1.16	0.80	1.75
>3	0.53	0.71	0.73	0.51	0.48	0.83	2.64	1.24	0.72	0.11	0.30	0.36	0.77
>3.5	0.08	0.20	0.40	0.16	0.20	0.42	1.38	0.34	0.31	0.03	0.20	0.02	0.31
>4	0.00	0.02	0.21	0.07	0.08	0.20	0.57	0.13	0.05	0.01	0.14	0.00	0.12
>4.5	0.00	0.01	0.10	0.02	0.03	0.05	0.19	0.02	0.01	0.00	0.08	0.00	0.04
>5	0.00	0.00	0.08	0.00	0.01	0.00	0.03	0.00	0.00	0.00	0.00	0.00	0.01
>5.5	0.00	0.00	0.02	0.00	0.00	0.00	0.00	0.00	0.00	0.00	0.00	0.00	0.00

Annual joint probability distribution (parts per thousand) of the total significant wave height and mean wave direction at peak energy at WRB.

$H_s$ (m)	Wave direction (degT)									Total
	337.5 -22.5	22.5 -67.5	67.5 -112.5	112.5 -157.5	157.5 -202.5	202.5 -247.5	247.5 -292.5	292.5 -337.5		
0 - 0.5	0.2	6.5	269.3	11.9	10.8	17.2	12.5	8.4		336.8
0.5 - 1	0.1	6.8	337.8	15.6	17.0	23.9	6.8	4.0		412.0
1 - 1.5	0.0	0.3	143.6	3.8	1.5	1.4	0.1	0.0		150.7
1.5 - 2	0.0	0.0	58.5	1.1	0.0	0.0	0.0	0.0		59.6
2 - 2.5	0.0	0.0	22.9	0.5	0.0	0.0	0.0	0.0		23.4
2.5 - 3	0.0	0.0	9.8	0.0	0.0	0.0	0.0	0.0		9.8
3 - 3.5	0.0	0.0	4.5	0.0	0.0	0.0	0.0	0.0		4.5
3.5 - 4	0.0	0.0	1.8	0.0	0.0	0.0	0.0	0.0		1.8
4 - 4.5	0.0	0.0	0.8	0.0	0.0	0.0	0.0	0.0		0.8
4.5 - 5	0.0	0.0	0.3	0.0	0.0	0.0	0.0	0.0		0.3
5 - 5.5	0.0	0.0	0.1	0.0	0.0	0.0	0.0	0.0		0.1
<b>Total</b>	0.3	13.6	849.4	32.9	29.3	42.5	19.4	12.4		1000.0

Annual joint probability distribution (parts per thousand) of the total significant wave height and peak wave period at WRB.

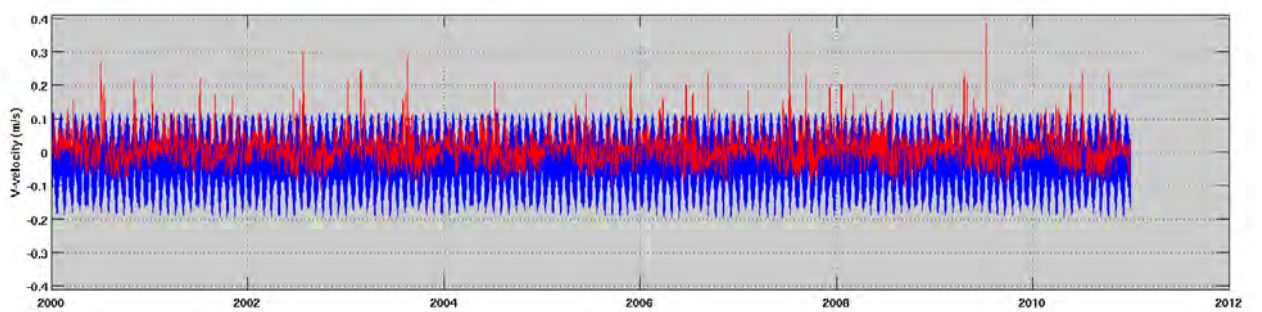
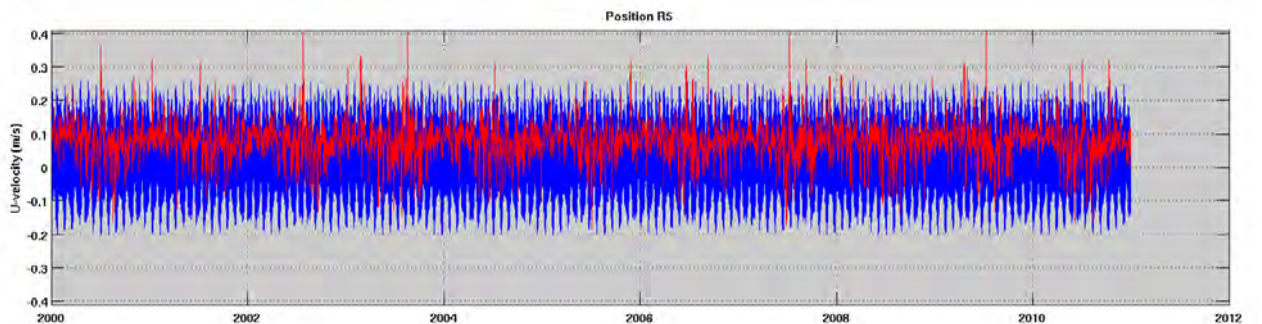
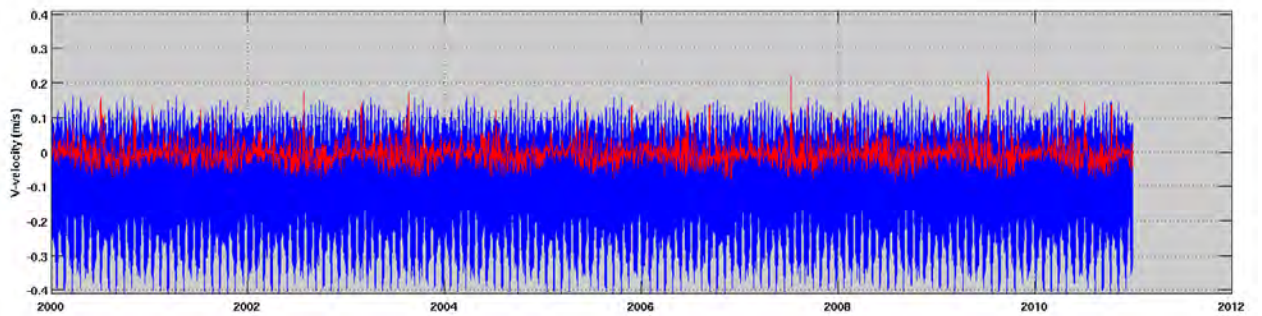
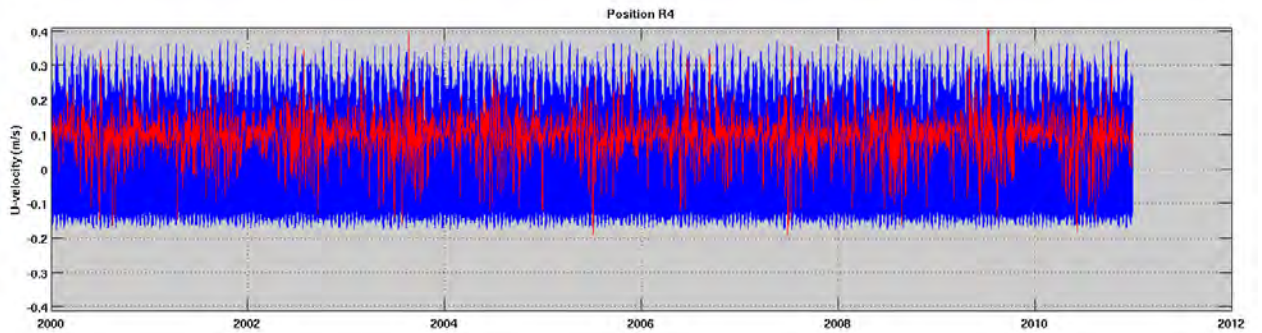
$H_s$ (m)	Peak wave period $T_p$ (s)									
	2-4	4-6	6-8	8-10	10-12	12-14	14-16	16-18	18-20	Total
0 - 0.5	60.0	13.5	27.9	138.2	63.9	19.6	5.7	1.5	0.1	330.4
0.5 - 1	62.8	42.8	61.1	159.2	62.4	19.7	3.5	0.5	0.1	412.1
1 - 1.5	2.1	11.3	37.2	62.7	29.1	7.4	0.7	0.1	0.0	150.6
1.5 - 2	0.0	1.1	11.0	27.6	16.2	3.7	0.2	0.0	0.0	59.8
2 - 2.5	0.0	0.1	4.2	9.9	7.1	2.1	0.0	0.0	0.0	23.4
2.5 - 3	0.0	0.0	0.9	4.7	3.2	0.9	0.0	0.0	0.0	9.7
3 - 3.5	0.0	0.0	0.2	1.8	2.0	0.4	0.1	0.0	0.0	4.5
3.5 - 4	0.0	0.0	0.0	0.7	0.9	0.3	0.0	0.0	0.0	1.9
4 - 4.5	0.0	0.0	0.0	0.3	0.4	0.1	0.0	0.0	0.0	0.8
4.5 - 5	0.0	0.0	0.0	0.1	0.2	0.0	0.0	0.0	0.0	0.3
5 - 5.5	0.0	0.0	0.0	0.0	0.1	0.0	0.0	0.0	0.0	0.1
<b>Total</b>	124.9	68.8	142.5	405.2	185.5	54.2	10.2	2.1	0.2	1000.0

Annual persistence non-exceedance (%) for total significant wave height at WRB.

$H_s$ (m)	Duration (hours)											
	> 6	> 12	> 18	> 24	> 30	> 36	> 42	> 48	> 54	> 60	> 66	> 72
<= 0.5	33.06	32.11	31	29.63	28.29	26.66	25.27	23.51	21.73	20.21	18.71	17.16
<= 1	74.75	74.54	74.2	73.87	73.42	72.93	72.4	71.73	71.18	70.59	69.99	69.37
<= 1.5	89.89	89.83	89.71	89.56	89.32	89.13	88.99	88.86	88.71	88.53	88.33	88.17
<= 2	95.88	95.83	95.8	95.77	95.75	95.69	95.63	95.55	95.5	95.41	95.33	95.28
<= 2.5	98.24	98.22	98.21	98.19	98.19	98.18	98.17	98.12	98.11	98.11	98.11	98.06
<= 3	99.23	99.22	99.21	99.19	99.19	99.18	99.18	99.18	99.18	99.18	99.18	99.18
<= 3.5	99.68	99.68	99.68	99.68	99.67	99.67	99.67	99.67	99.67	99.67	99.67	99.67
<= 4	99.87	99.87	99.87	99.87	99.87	99.87	99.87	99.87	99.87	99.87	99.85	99.85

## APPENDIX C – TIDAL AND NON-TIDAL TIME SERIES

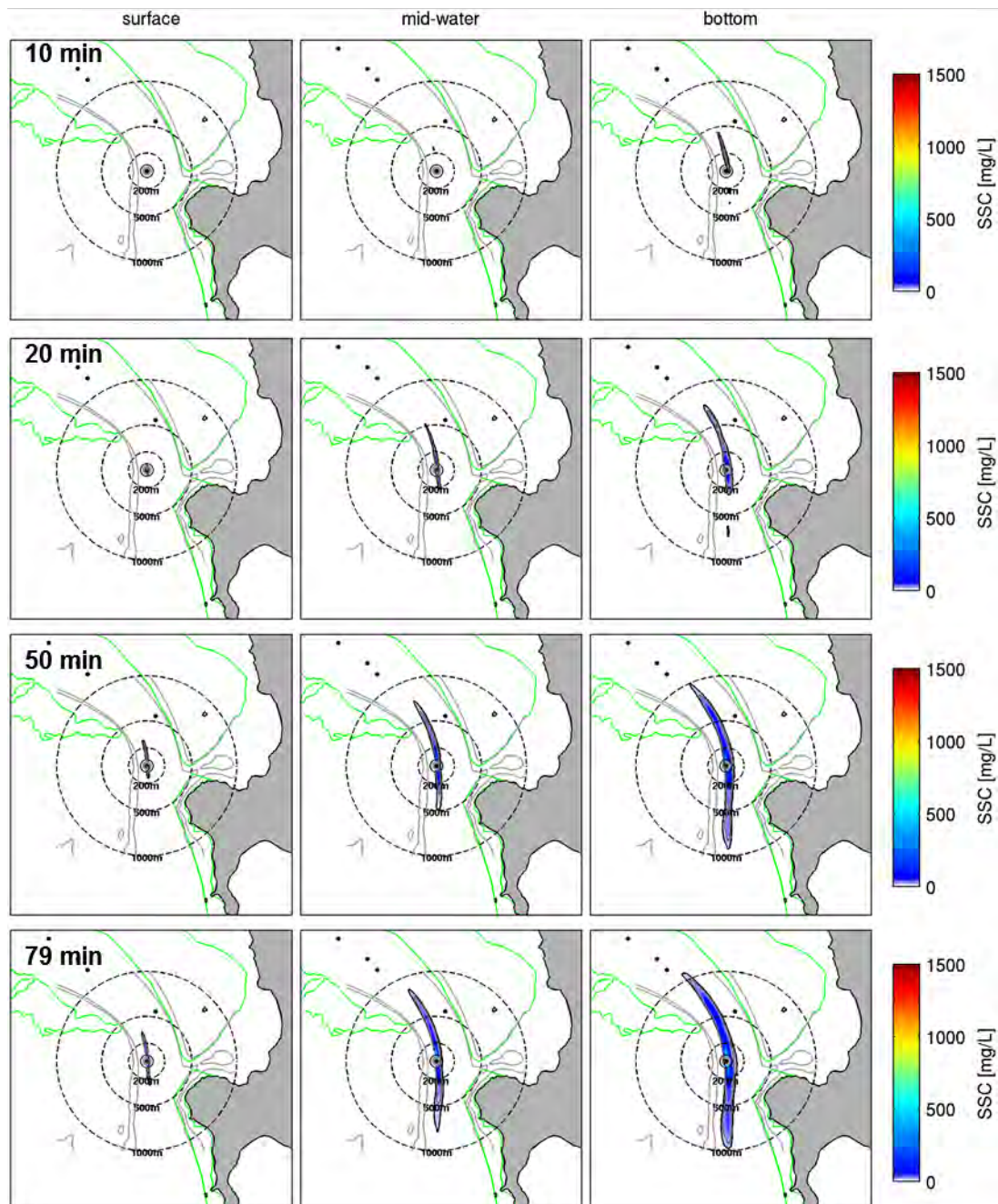
Tidal (blue) and non-tidal (red) time series of the current velocities extracted from SELFE and ROMS, respectively, at the positions R4 and R5 at the seaward entrance of the delta.



## APPENDIX D – ADDITIONAL DREDGING PLUME RESULTS

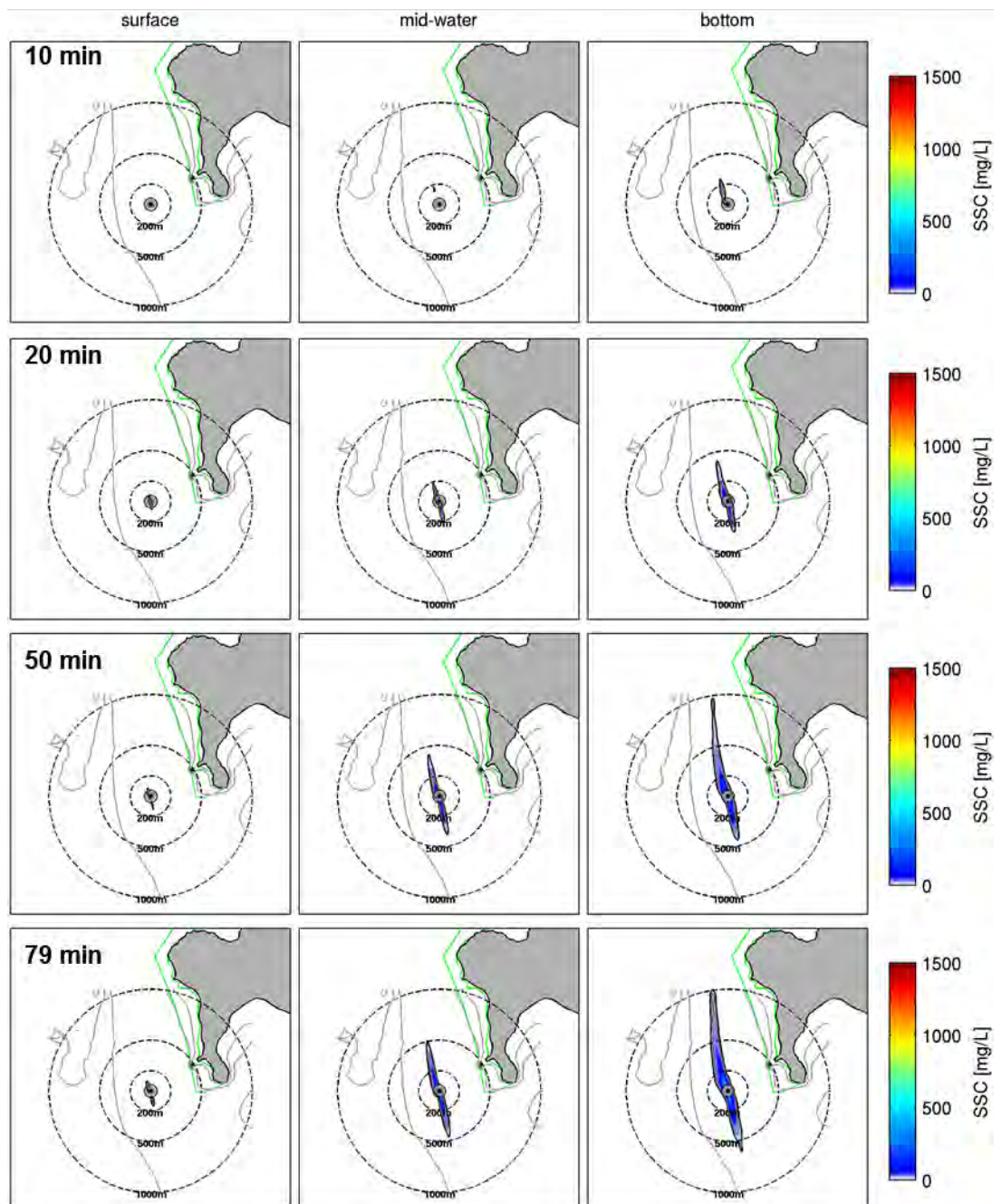
Probabilistic SSC plumes during overflow phase (large TSHD) at site R2 at three levels of the water column. SSC plumes are illustrated for a 10, 30, 50 and 79 min period of overflow.

### LARGE TSHD: OVERFLOW MODE (SITE R2)



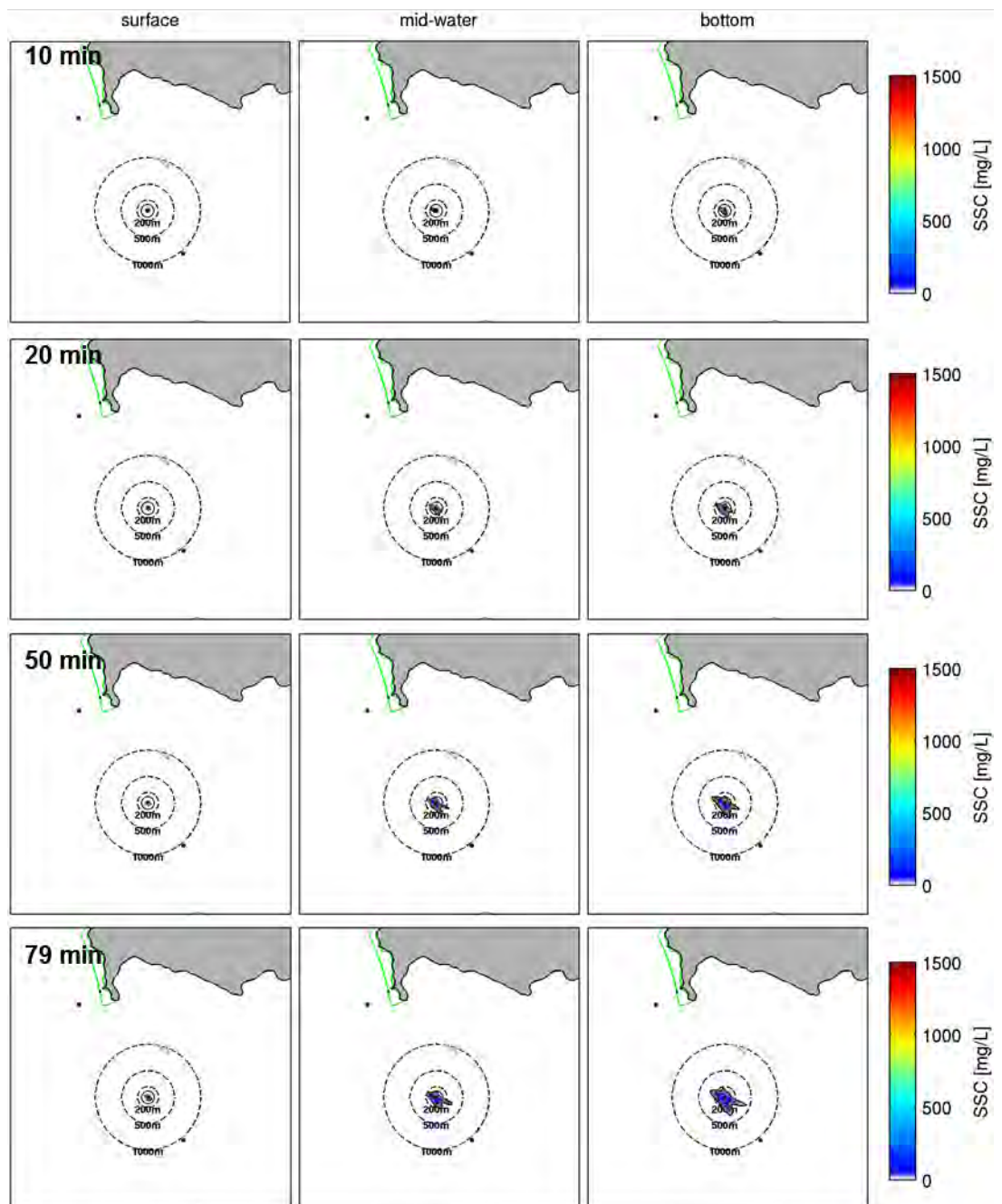
Probabilistic SSC plumes during overflow phase (large TSHD) at site R3 at three levels of the water column. SSC plumes are illustrated for a 10, 30, 50 and 79 min period of overflow.

**LARGE TSHD: OVERFLOW MODE (SITE R3)**



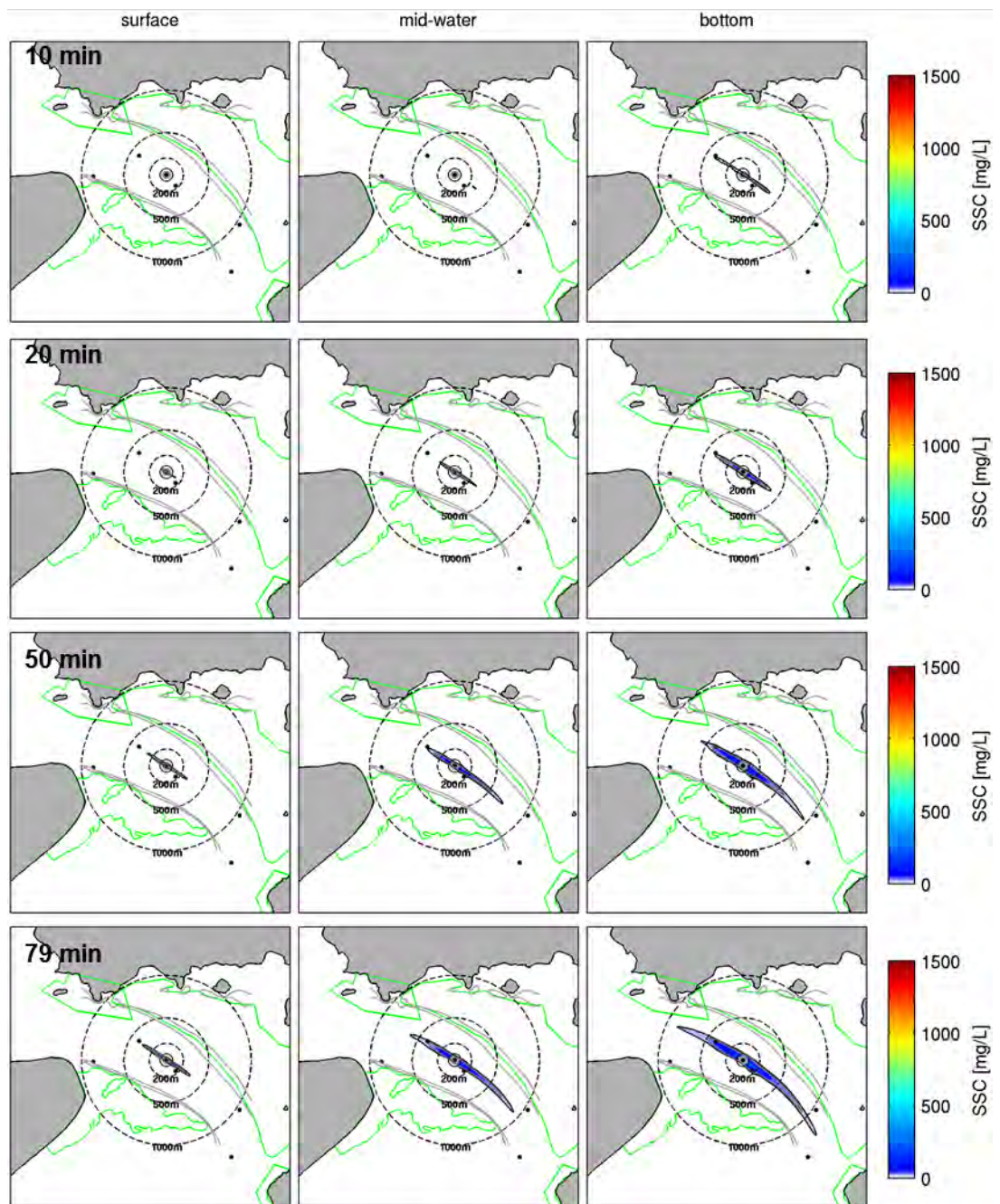
Probabilistic SSC plumes during overflow phase (large TSHD) at site R4 at three levels of the water column. SSC plumes are illustrated for a 10, 30, 50 and 79 min period of overflow.

**LARGE TSHD: OVERFLOW MODE (SITE R4)**



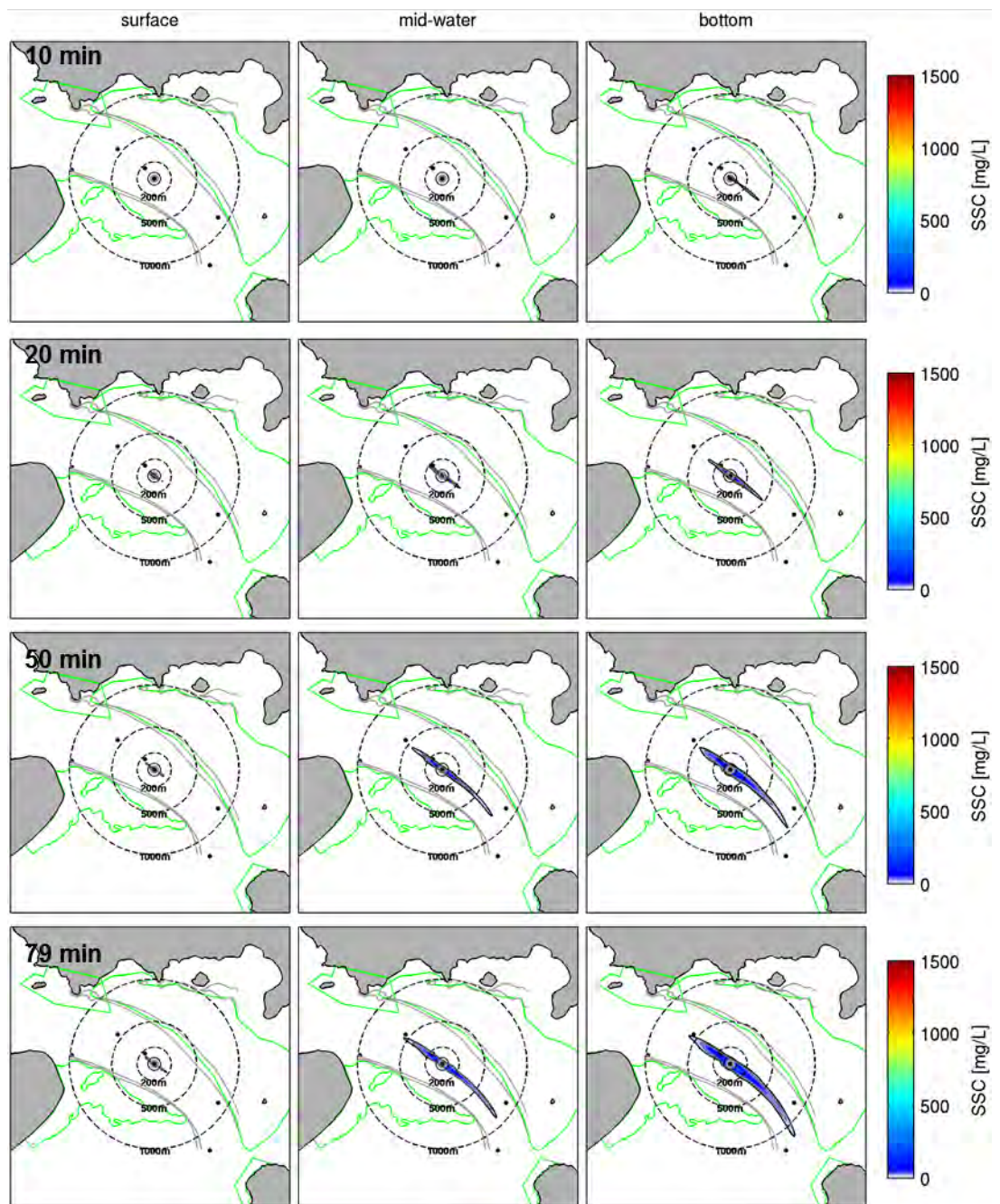
Probabilistic SSC plumes during overflow phase (large TSHD) at site R7 at three levels of the water column. SSC plumes are illustrated for a 10, 30, 50 and 79 min period of overflow.

**LARGE TSHD: OVERFLOW MODE (SITE R7)**



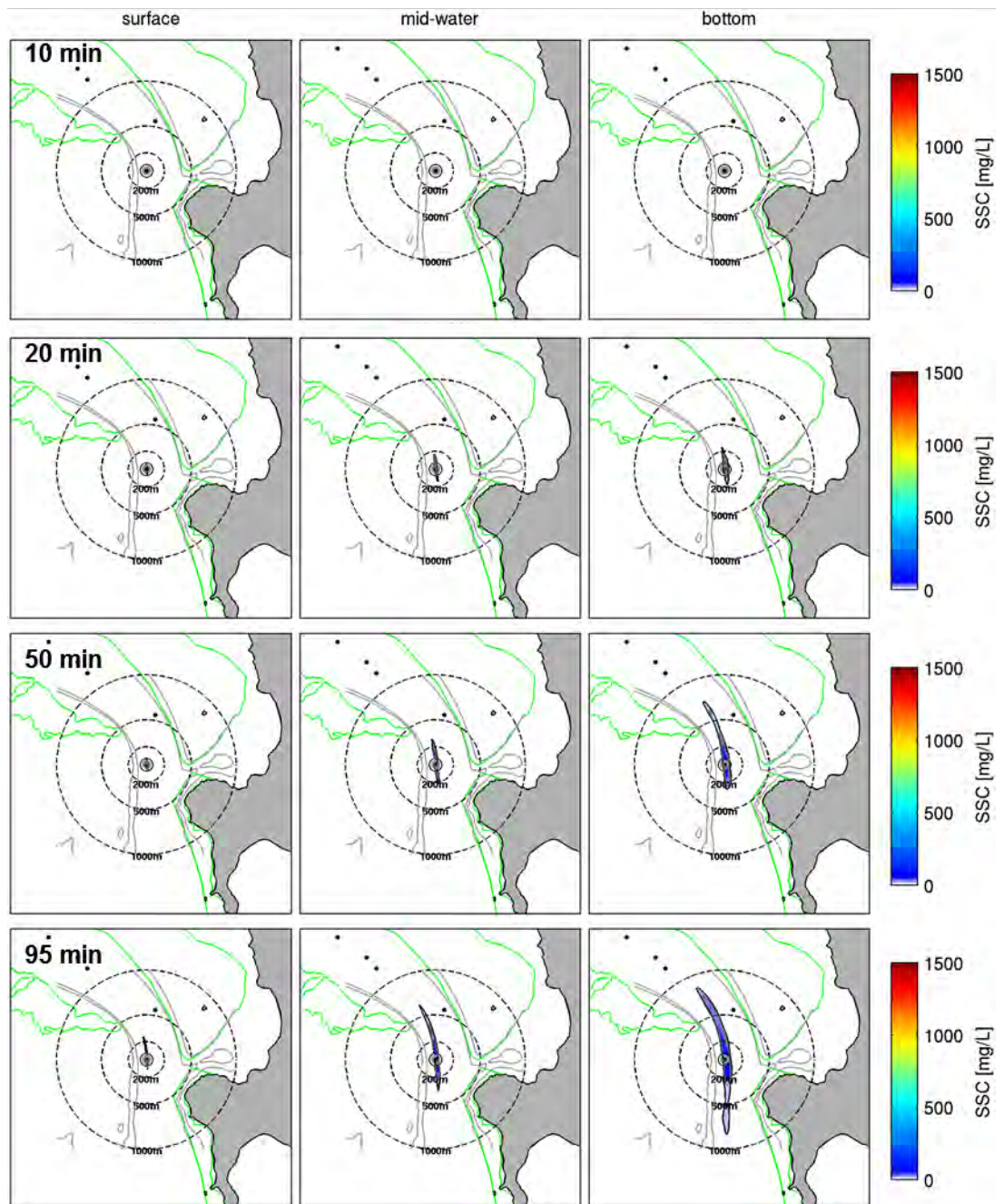
Probabilistic SSC plumes during overflow phase (large TSHD) at site R8 at three levels of the water column. SSC plumes are illustrated for a 10, 30, 50 and 79 min period of overflow.

**LARGE TSHD: OVERFLOW MODE (SITE R8)**



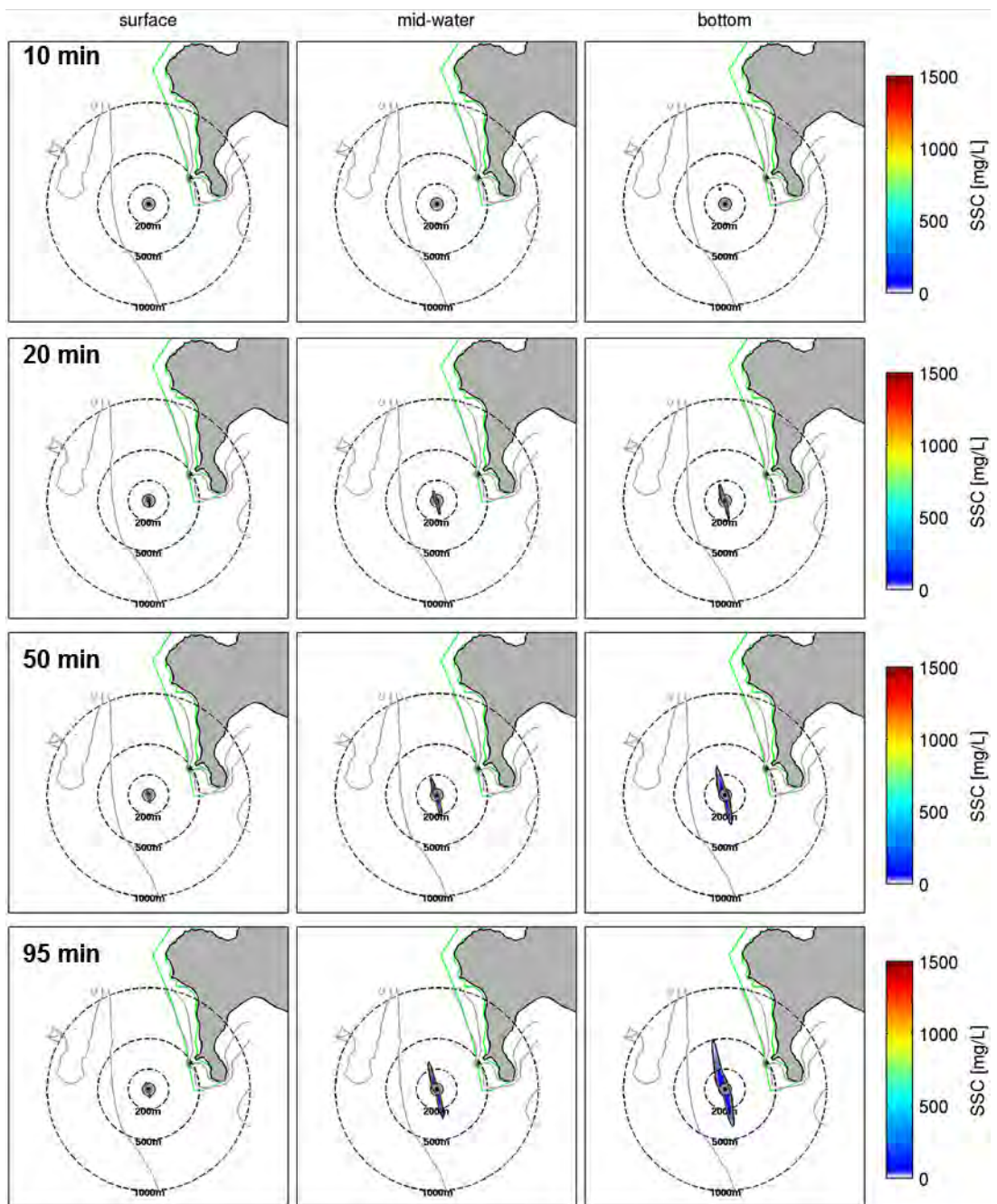
Probabilistic SSC plumes during overflow phase (small TSHD) at site R2 at three levels of the water column. SSC plumes are illustrated for a 10, 30, 50 and 95 min period of overflow.

**SMALL TSHD: OVERFLOW MODE (SITE R2)**



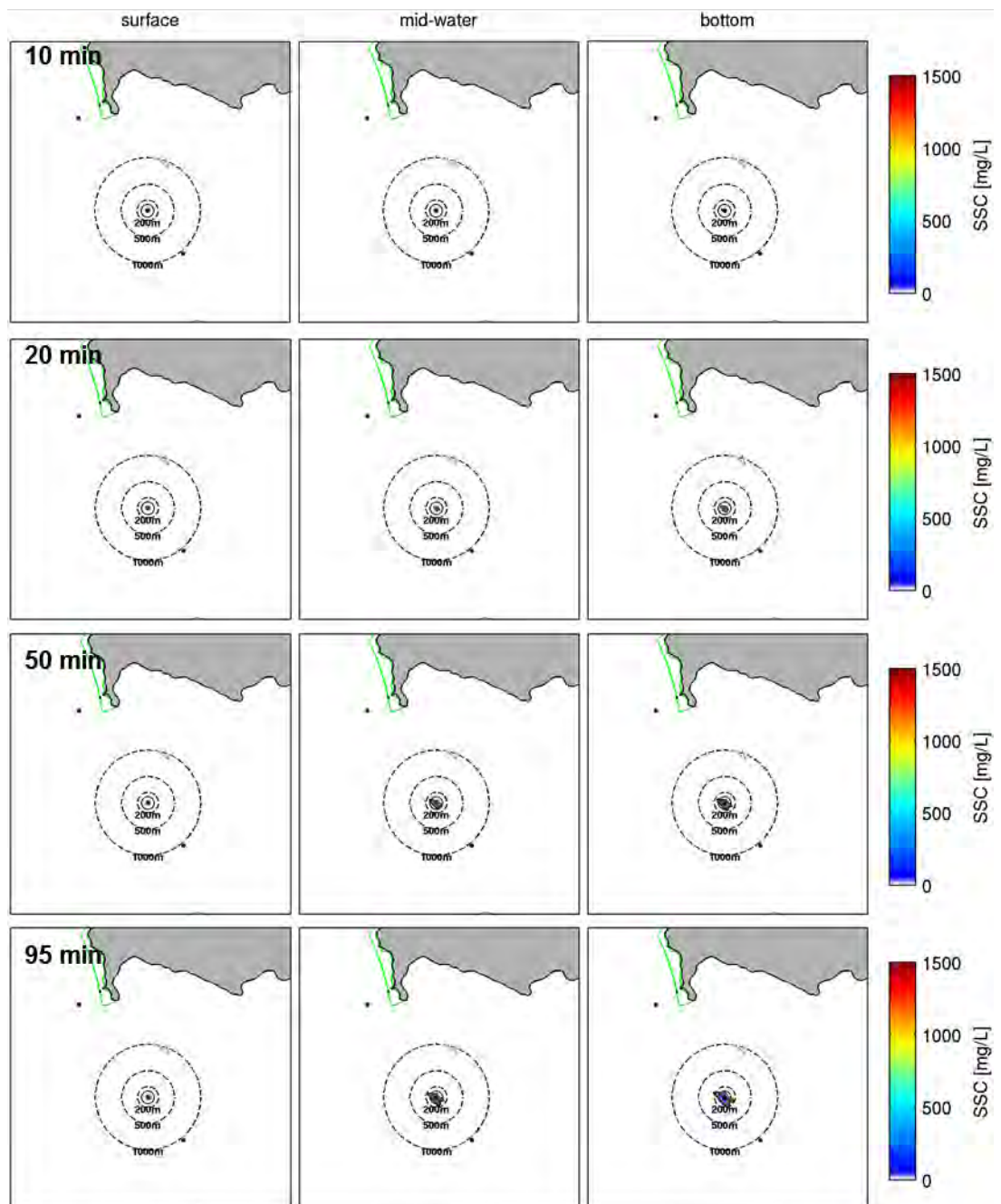
Probabilistic SSC plumes during overflow phase (small TSHD) at site R3 at three levels of the water column. SSC plumes are illustrated for a 10, 30, 50 and 95 min period of overflow.

**SMALL TSHD: OVERFLOW MODE (SITE R3)**



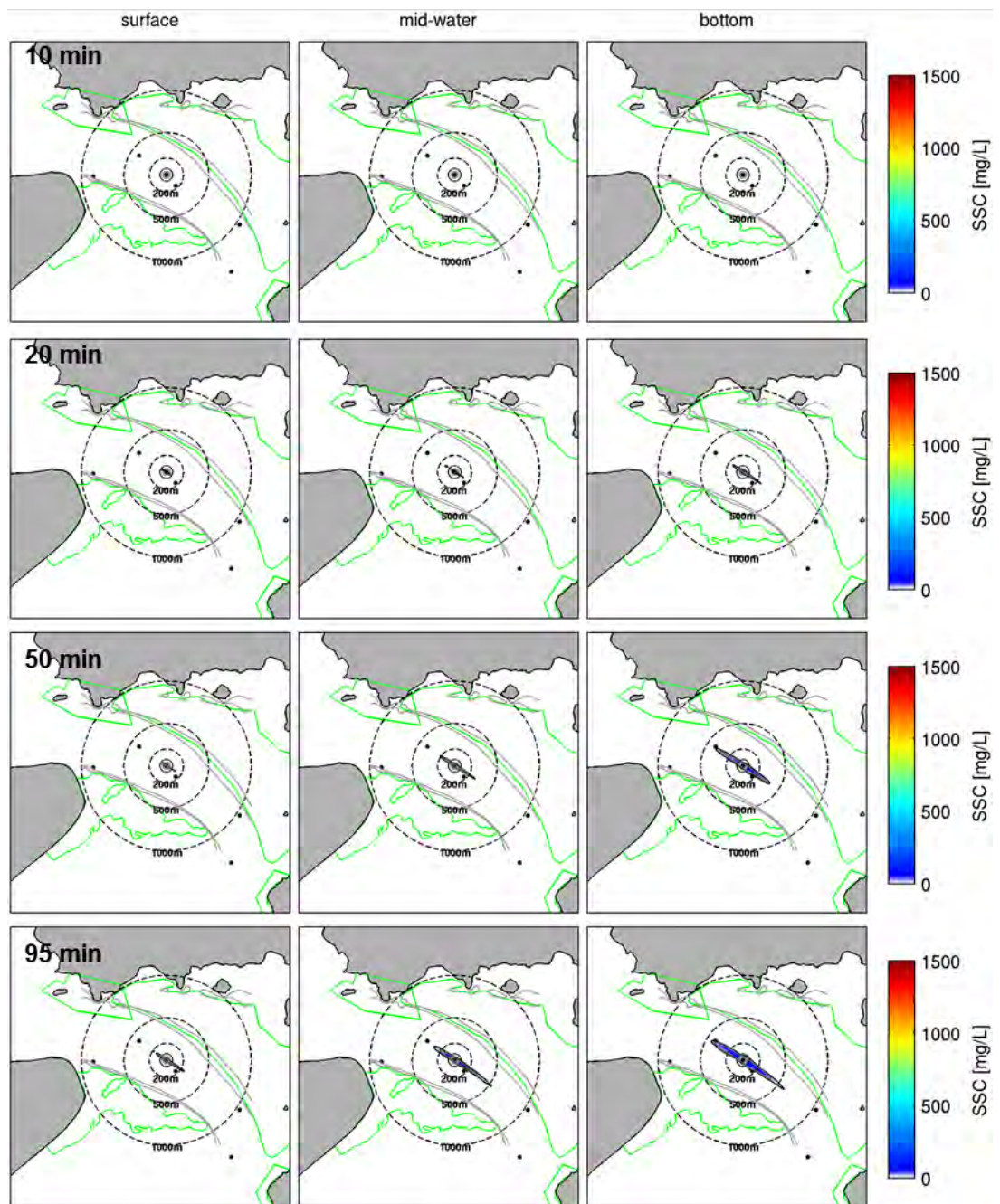
Probabilistic SSC plumes during overflow phase (small TSHD) at site R4 at three levels of the water column. SSC plumes are illustrated for a 10, 30, 50 and 95 min period of overflow.

**SMALL TSHD: OVERFLOW MODE (SITE R4)**



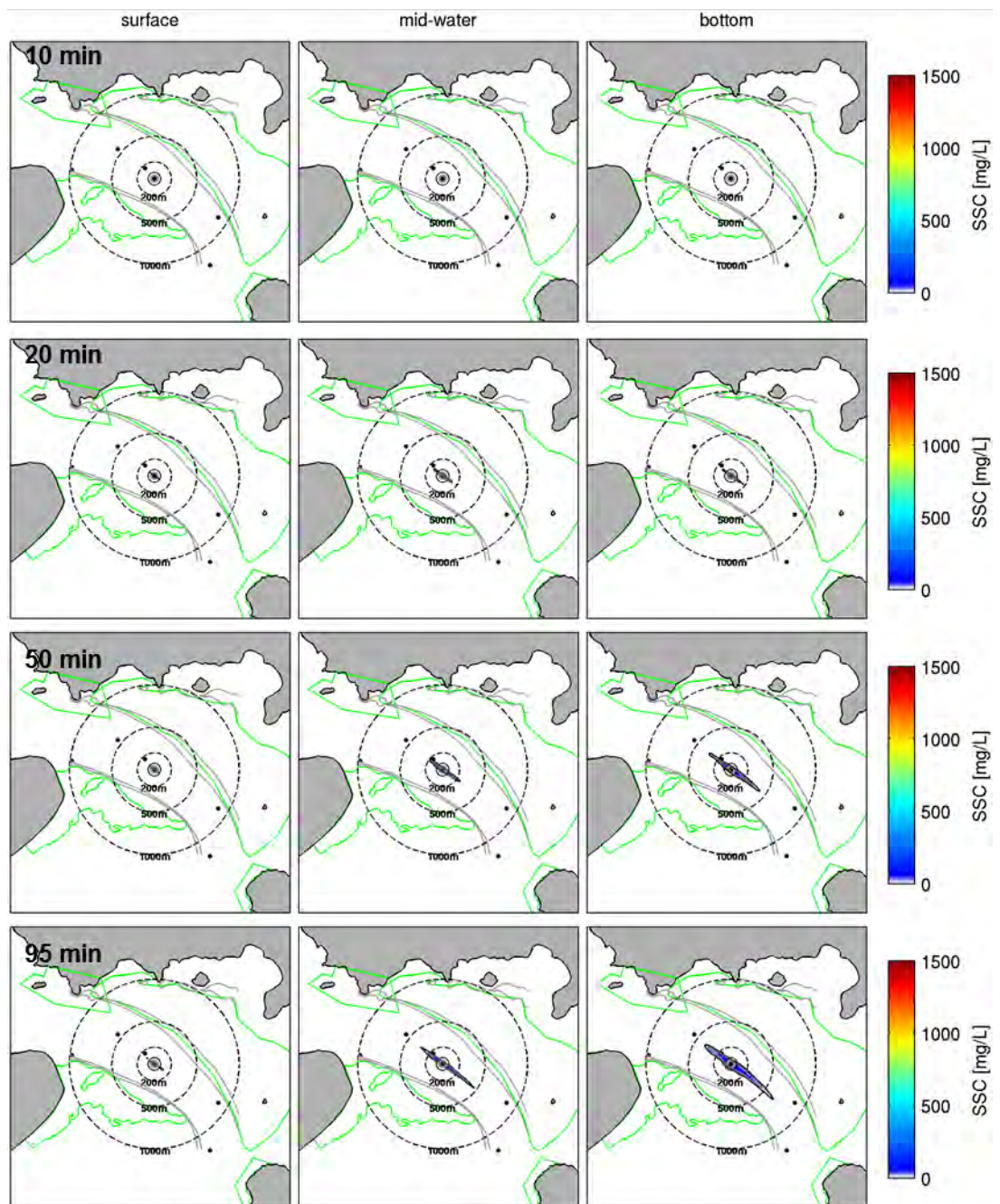
Probabilistic SSC plumes during overflow phase (small TSHD) at site R7 at three levels of the water column. SSC plumes are illustrated for a 10, 30, 50 and 95 min period of overflow.

**SMALL TSHD: OVERFLOW MODE (SITE R7)**



Probabilistic SSC plumes during overflow phase (small TSHD) at site R8 at three levels of the water column. SSC plumes are illustrated for a 10, 30, 50 and 95 min period of overflow.

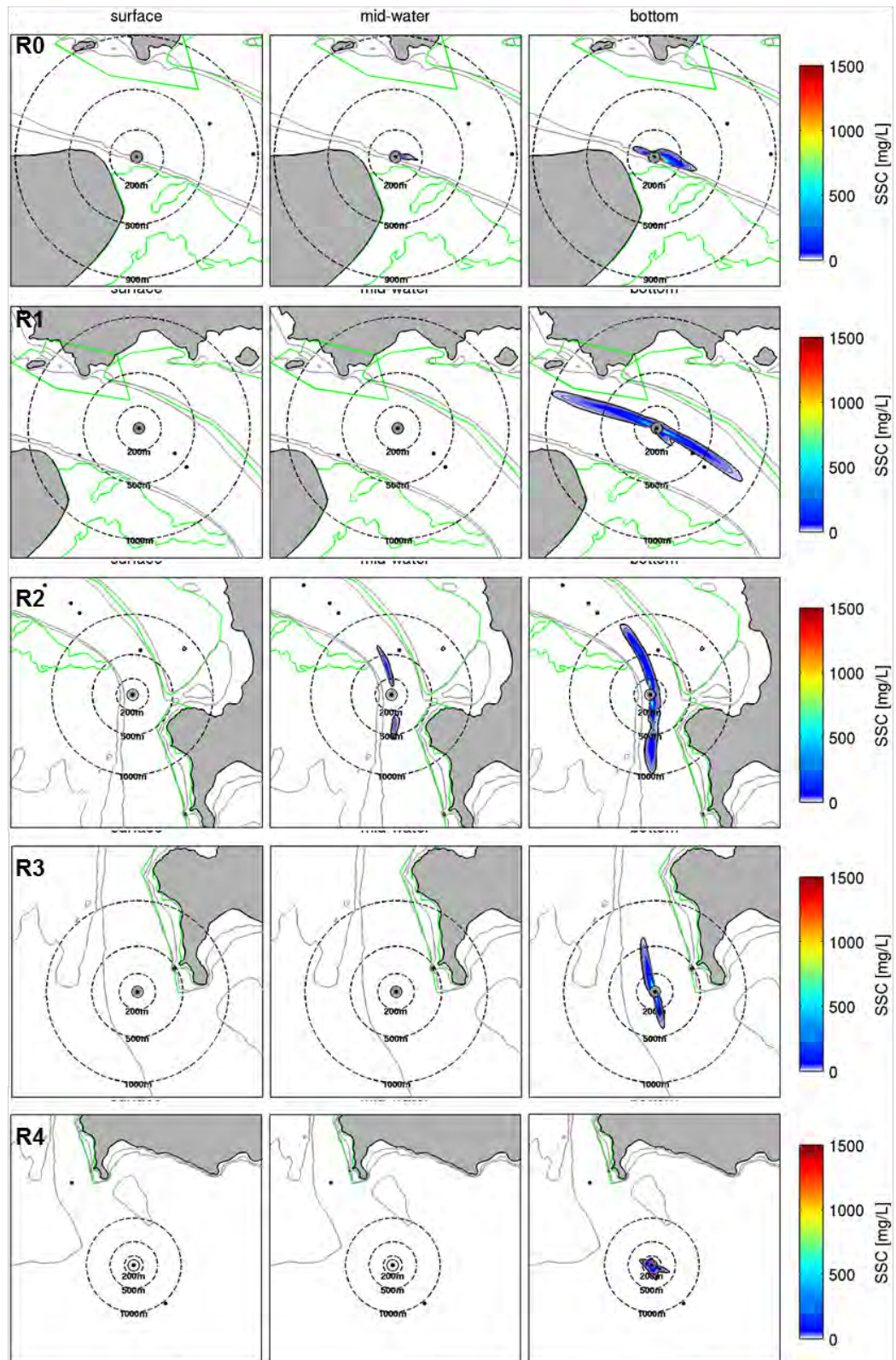
**SMALL TSHD: OVERFLOW MODE (SITE R8)**



## APPENDIX E – ADDITIONAL DREDGING PLUME RESULTS

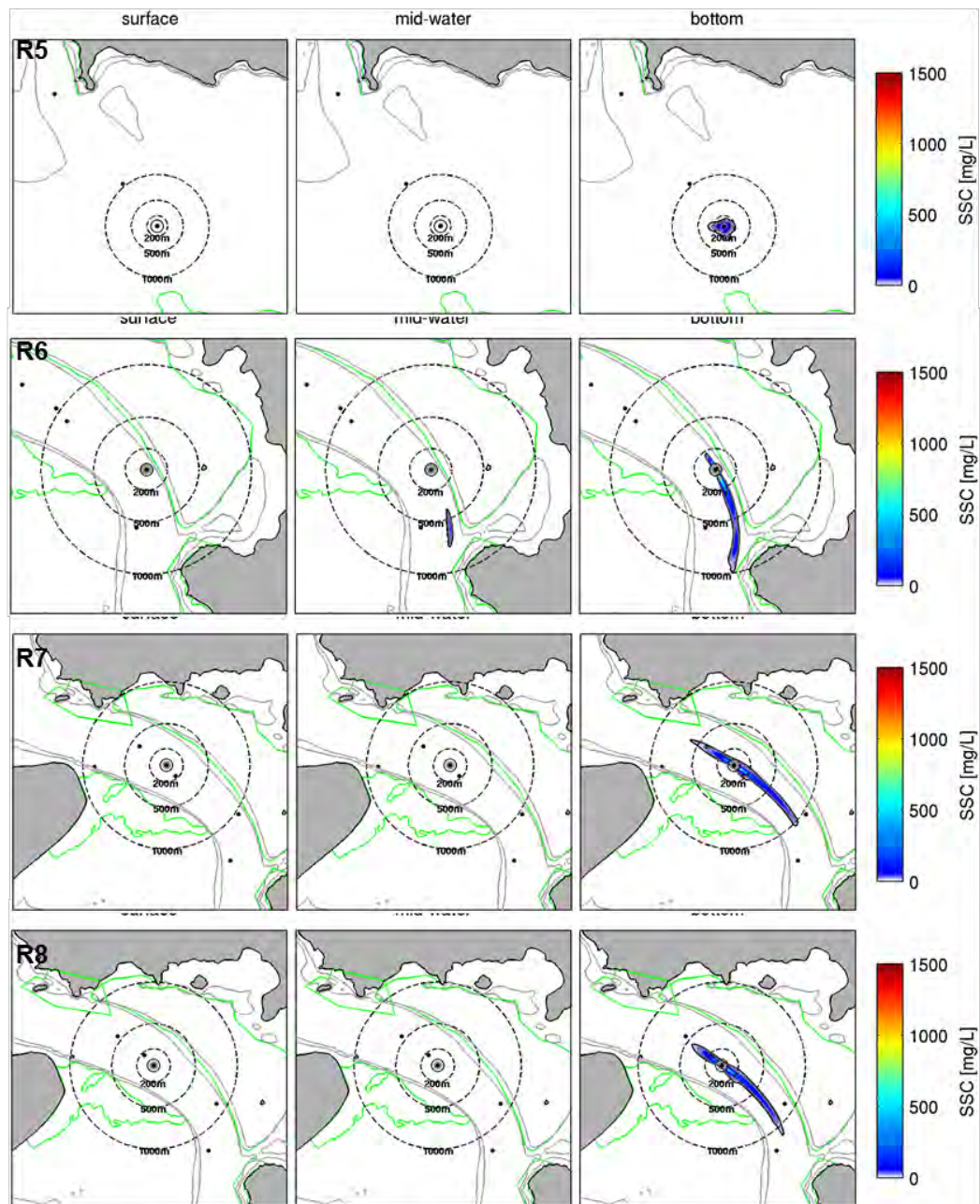
Probabilistic SSC plumes during dredging phase (large TSHD) at sites R0 to R4 at three levels of the water column considering a 1.5 % production rate for the drag head source.

### LARGE TSHD: DREDGING MODE (1.5% PRODUCTION RATE)



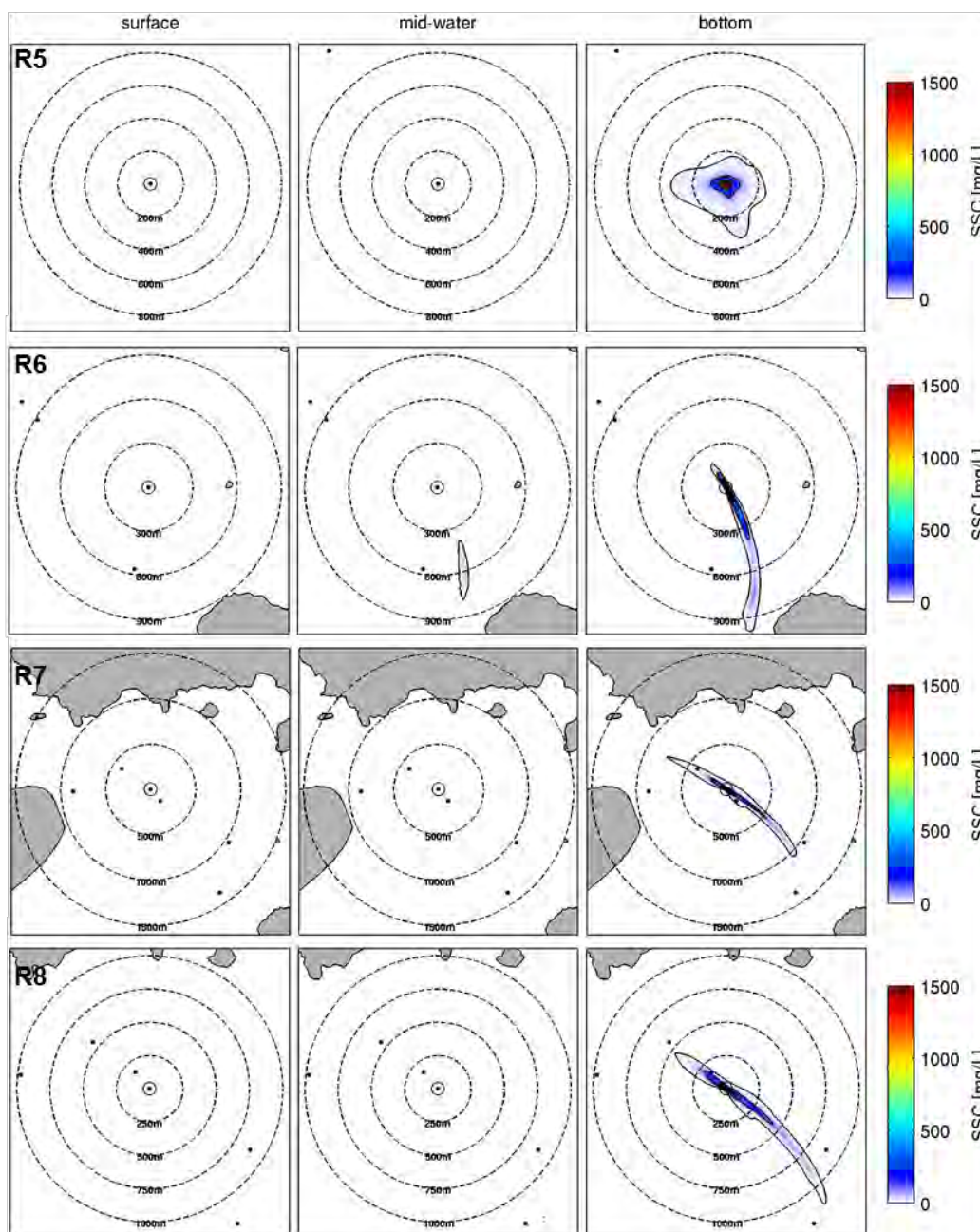
Probabilistic SSC plumes during dredging phase (large TSHD) at sites R0 to R4 at three levels of the water column considering a 3.0 % production rate for the drag head source.

**LARGE TSHD: DREDGING MODE (1.5% PRODUCTION RATE)**



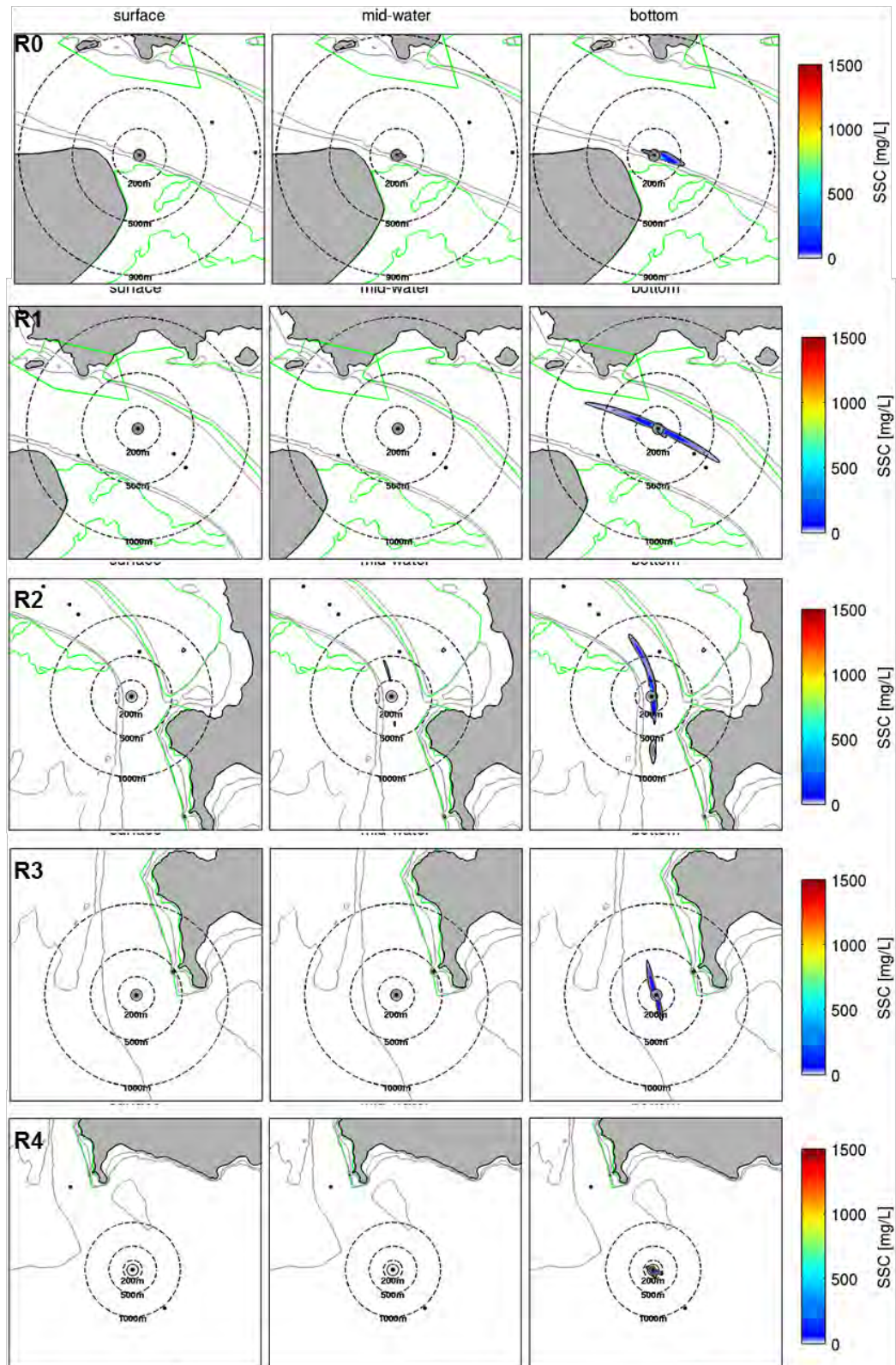
Probabilistic SSC plumes during dredging phase (large TSHD) at sites R5 to R8 at three levels of the water column considering a 1.5 % production rate for the drag head source.

**LARGE TSHD: DREDGING MODE (1.5% PRODUCTION RATE)**



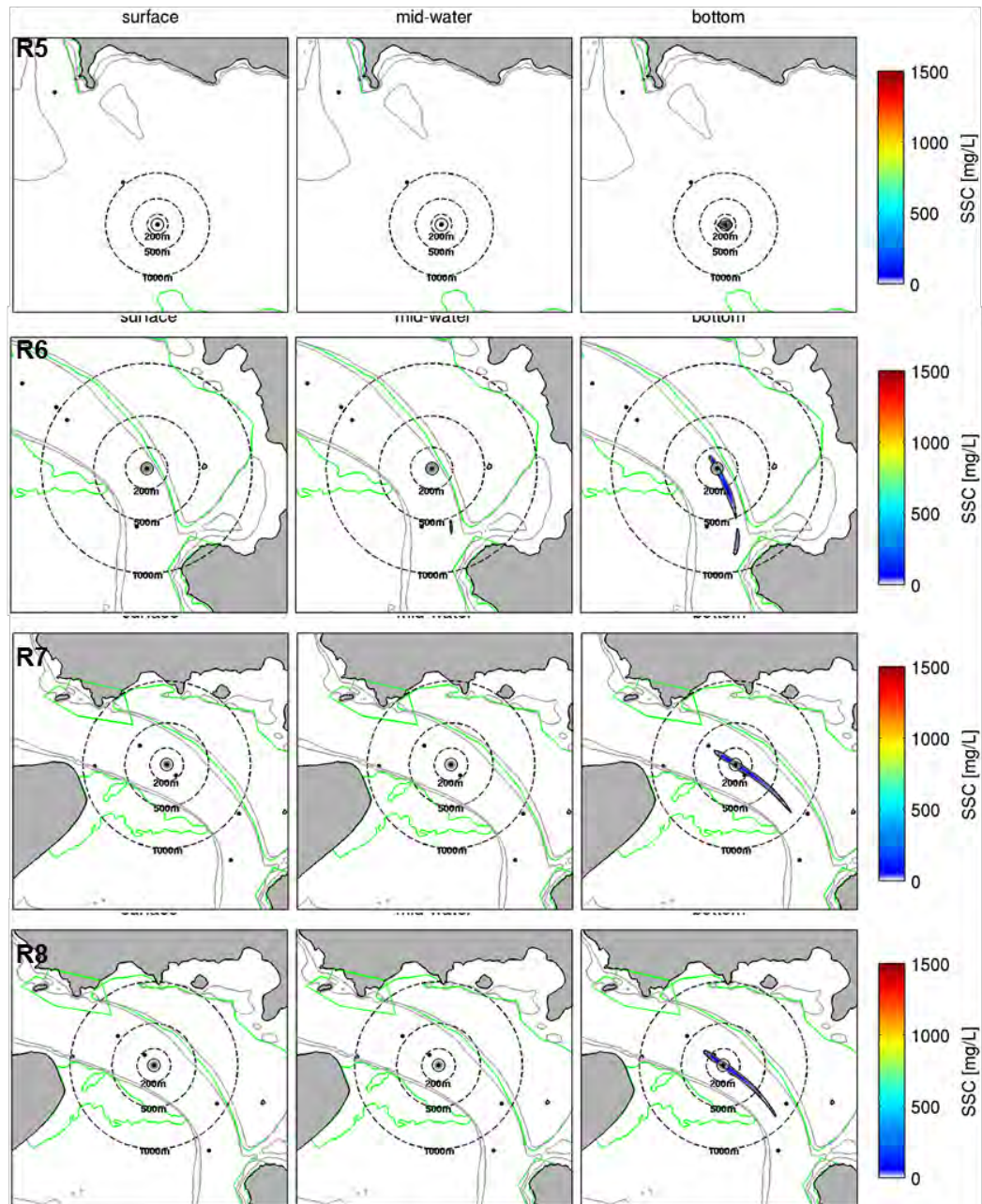
Probabilistic SSC plumes during dredging phase (small TSHD) at sites R0 to R4 at three levels of the water column considering a 1.5 % production rate for the drag head source.

**SMALL TSHD: DREDGING MODE (1.5% PRODUCTION RATE)**



Probabilistic SSC plumes during dredging phase (small TSHD) at sites R5 to R8 at three levels of the water column considering a 1.5 % production rate for the drag head source.

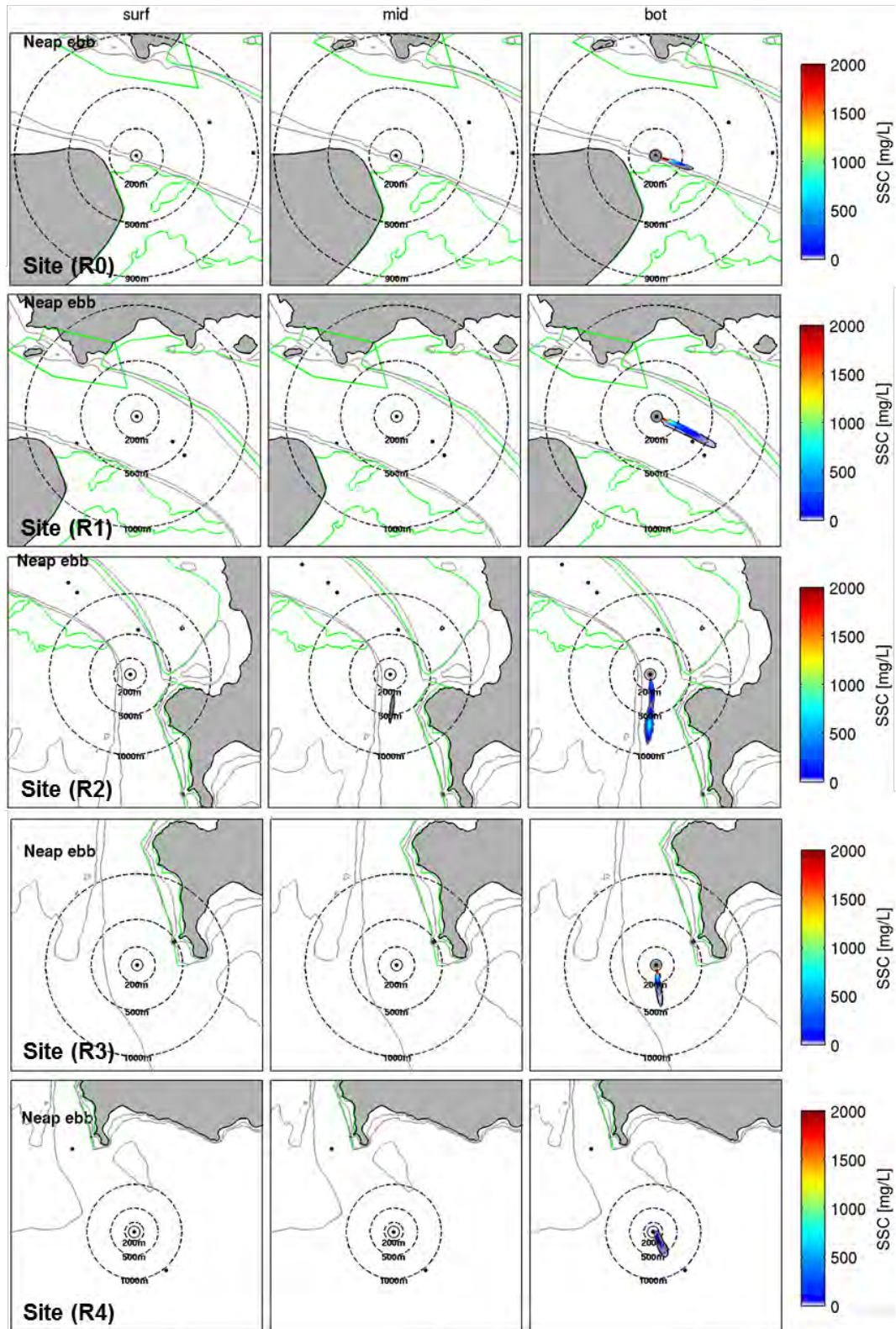
**SMALL TSHD: DREDGING MODE (1.5% PRODUCTION RATE)**



## **APPENDIX F – PLUME MODELLING AT DIFFERENT TIDE STAGES**

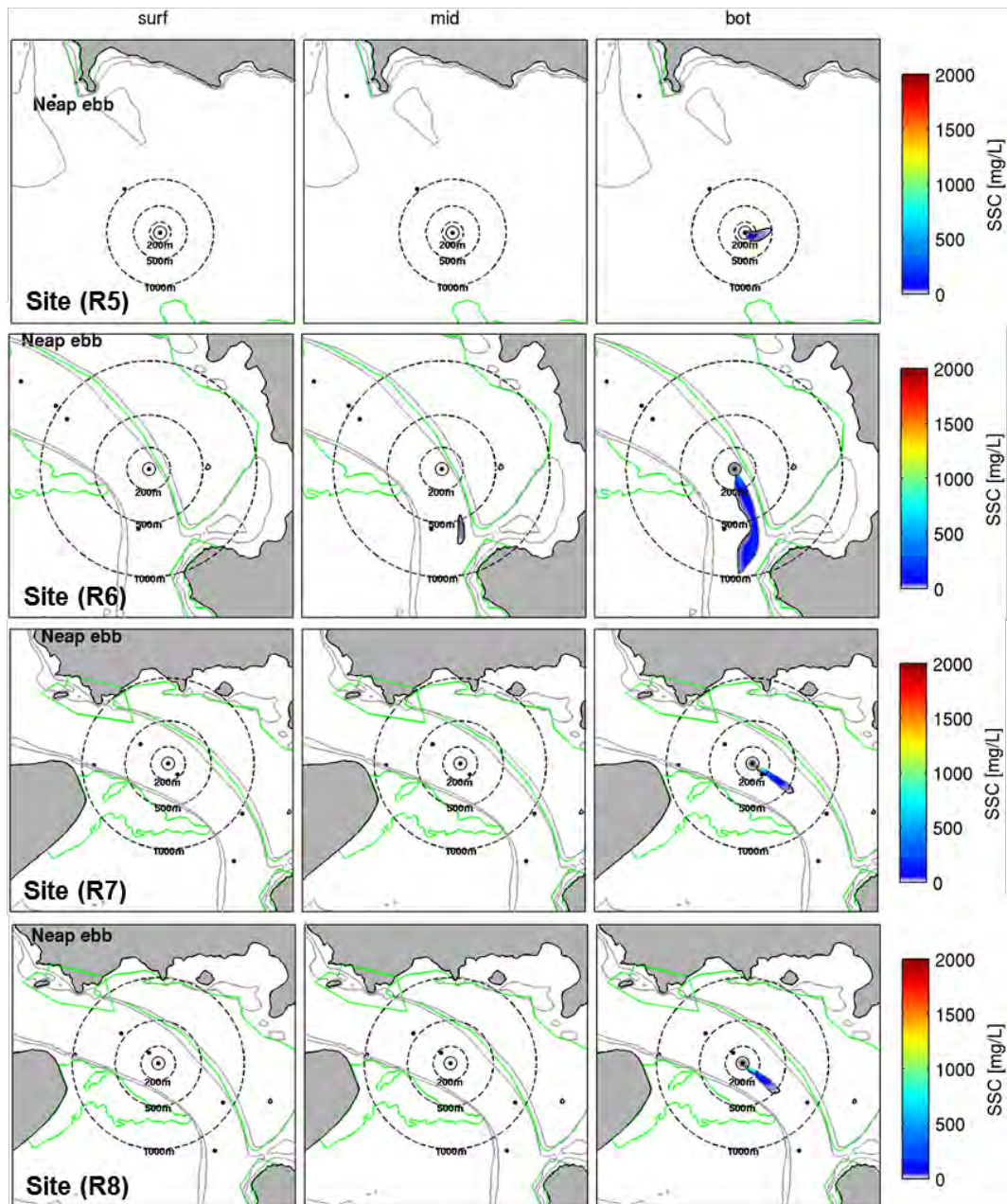
Probabilistic SSC plumes at Neap ebb tide during dredging phase (large TSHD) at sites R0 to R4 at three levels of the water column considering a 3.0 % production rate for the drag head source.

**LARGE TSHD: DREDGING MODE – EBB (NEAP TIDE)**



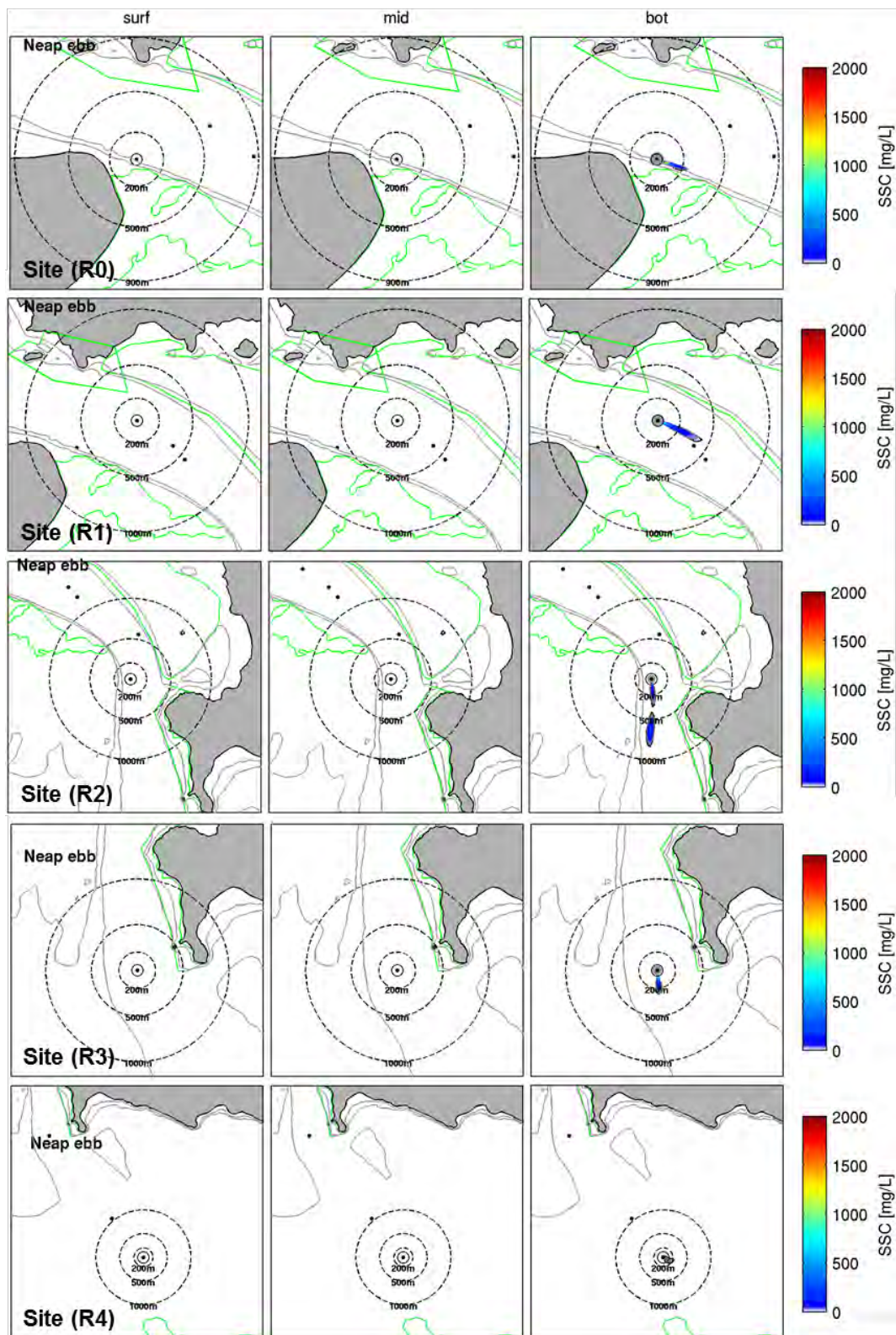
Probabilistic SSC plumes at Neap ebb tide during dredging phase (large TSHD) at sites R5 to R8 at three levels of the water column considering a 3.0 % production rate for the drag head source.

**LARGE TSHD: DREDGING MODE – EBB (NEAP TIDE)**



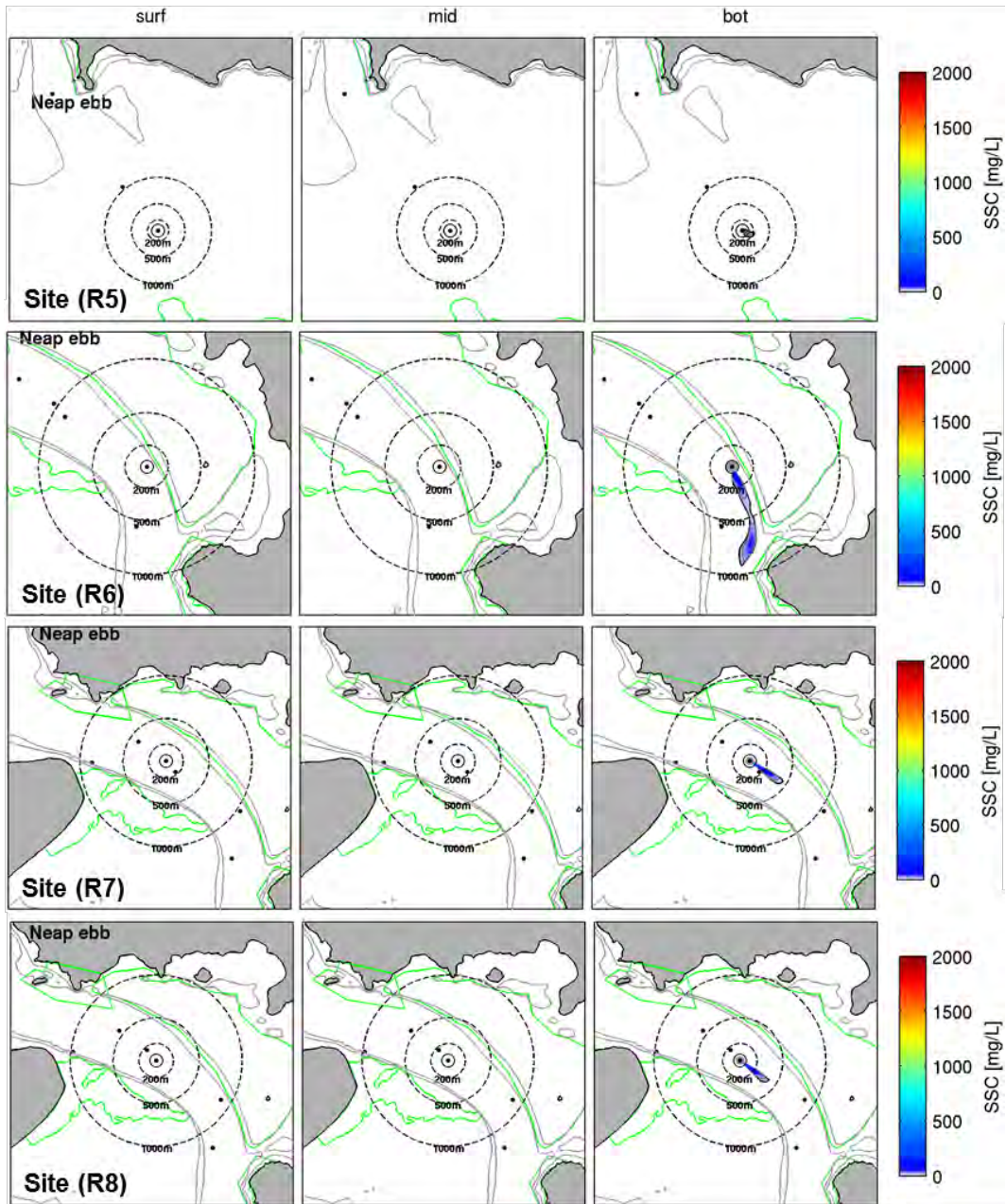
Probabilistic SSC plumes at Neap ebb tide during dredging phase (small TSHD) at sites R0 to R4 at three levels of the water column considering a 3.0 % production rate for the drag head source.

**SMALL TSHD: DREDGING MODE – EBB (NEAP TIDE)**



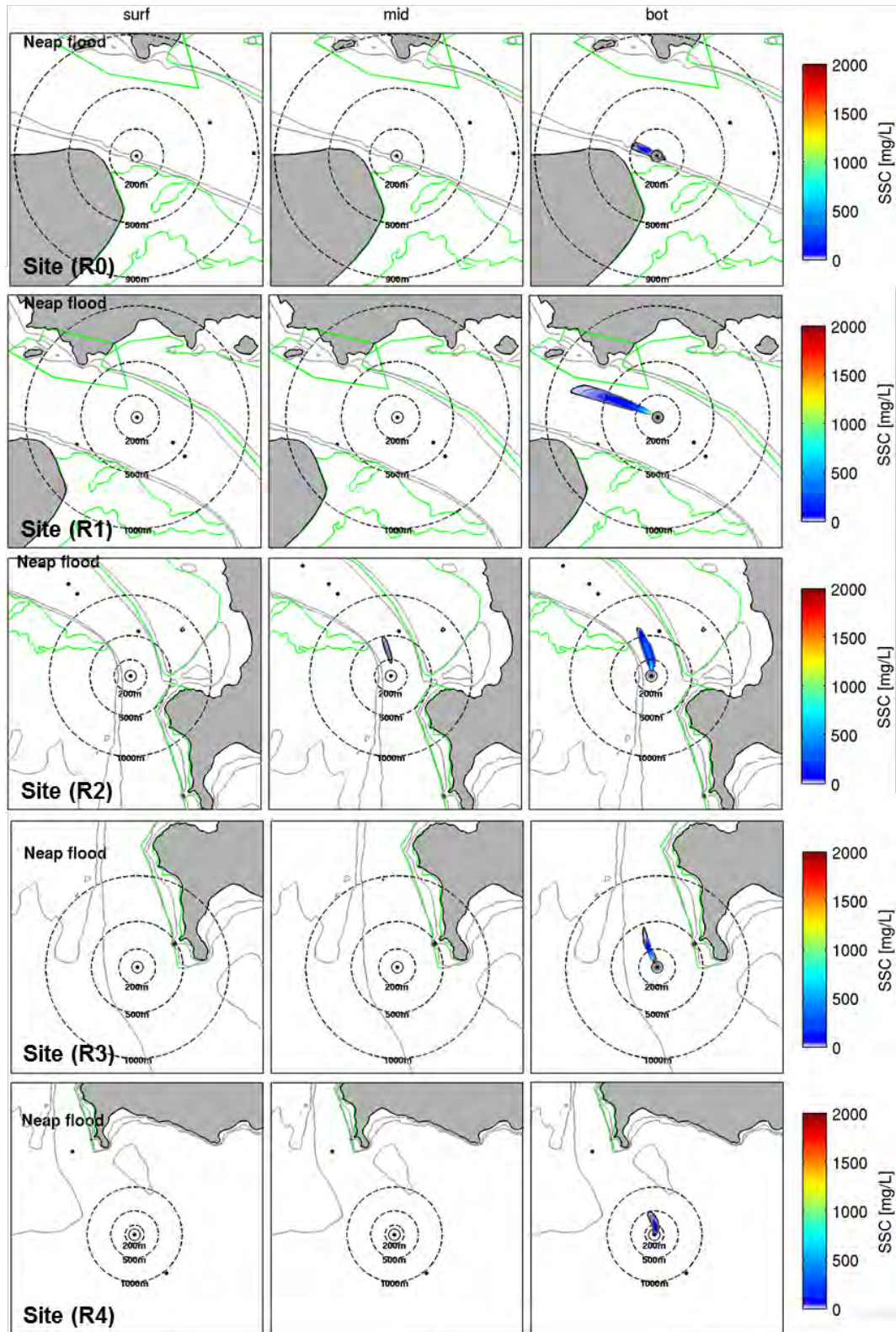
Probabilistic SSC plumes at Neap ebb tide during dredging phase (small TSHD) at sites R5 to R8 at three levels of the water column considering a 3.0 % production rate for the drag head source.

**SMALL TSHD: DREDGING MODE – EBB (NEAP TIDE)**



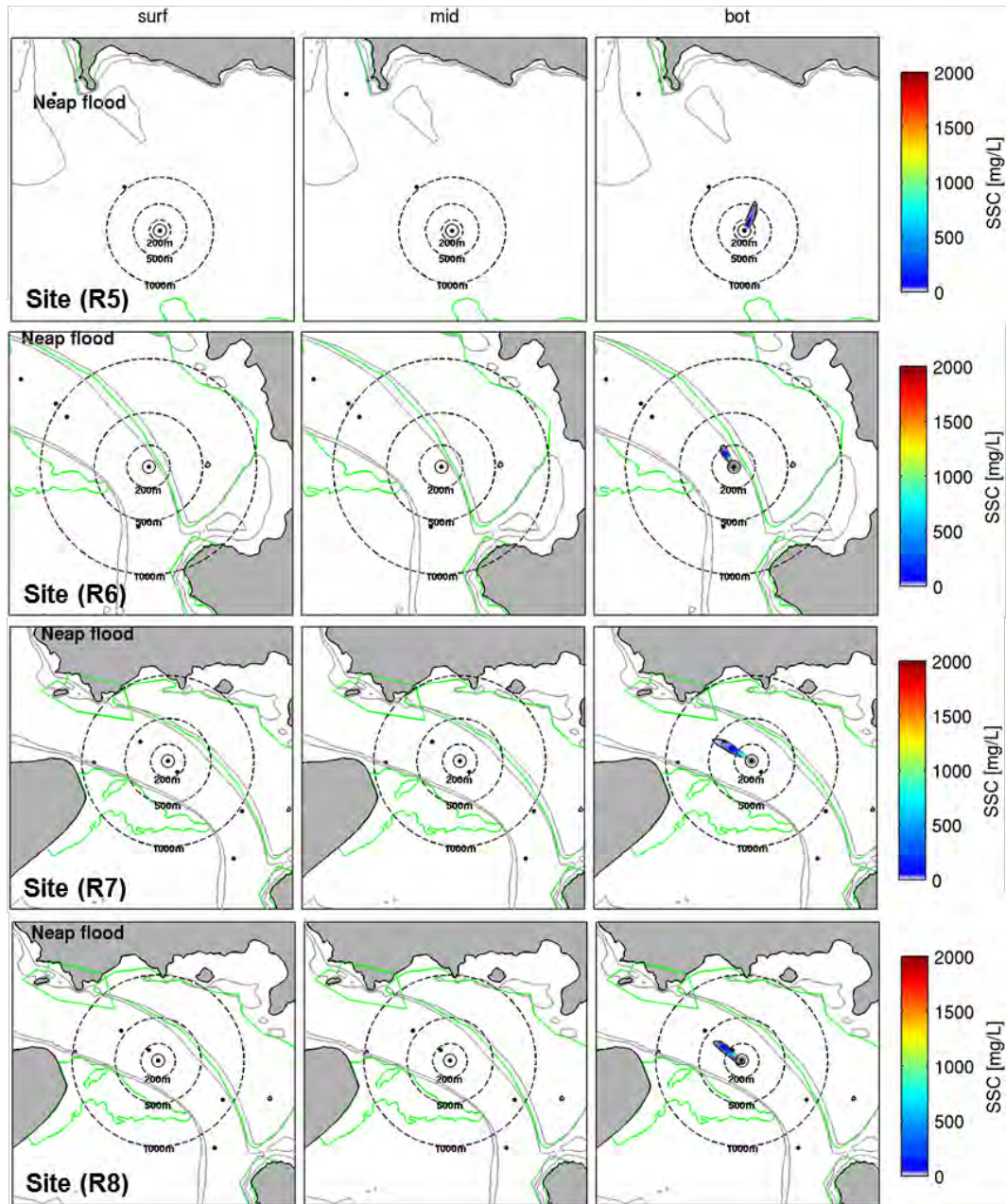
Probabilistic SSC plumes at Neap flood tide during dredging phase (large TSHD) at sites R0 to R4 at three levels of the water column considering a 3.0 % production rate for the drag head source.

**LARGE TSHD: DREDGING MODE – FLOOD (NEAP TIDE)**



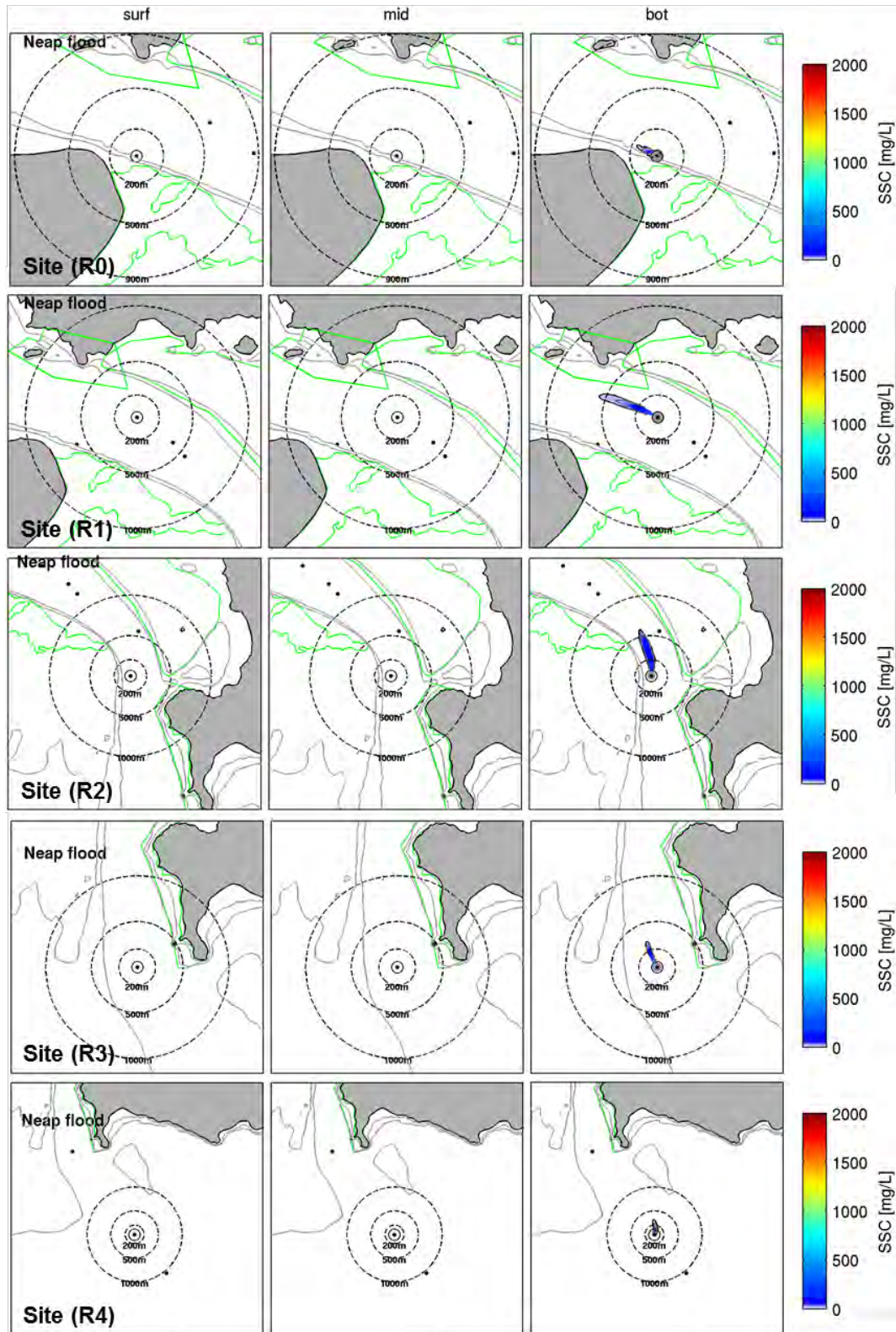
Probabilistic SSC plumes at Neap flood tide during dredging phase (large TSHD) at sites R5 to R8 at three levels of the water column considering a 3.0 % production rate for the drag head source.

**LARGE TSHD: DREDGING MODE – FLOOD (SPRING TIDE)**



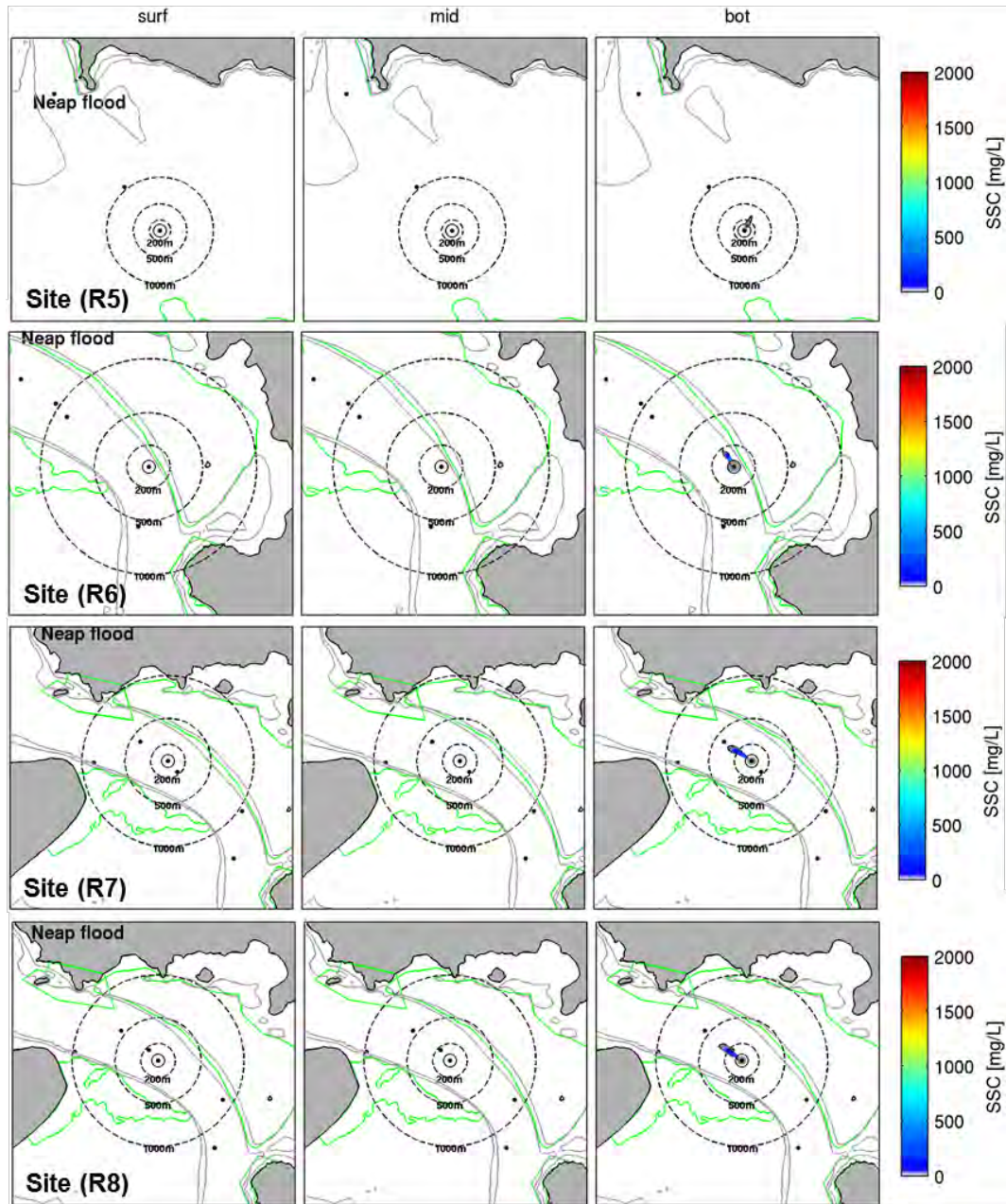
Probabilistic SSC plumes at Neap flood tide during dredging phase (small TSHD) at sites R0 to R4 at three levels of the water column considering a 3.0 % production rate for the drag head source.

**SMALL TSHD: DREDGING MODE – FLOOD (NEAP TIDE)**



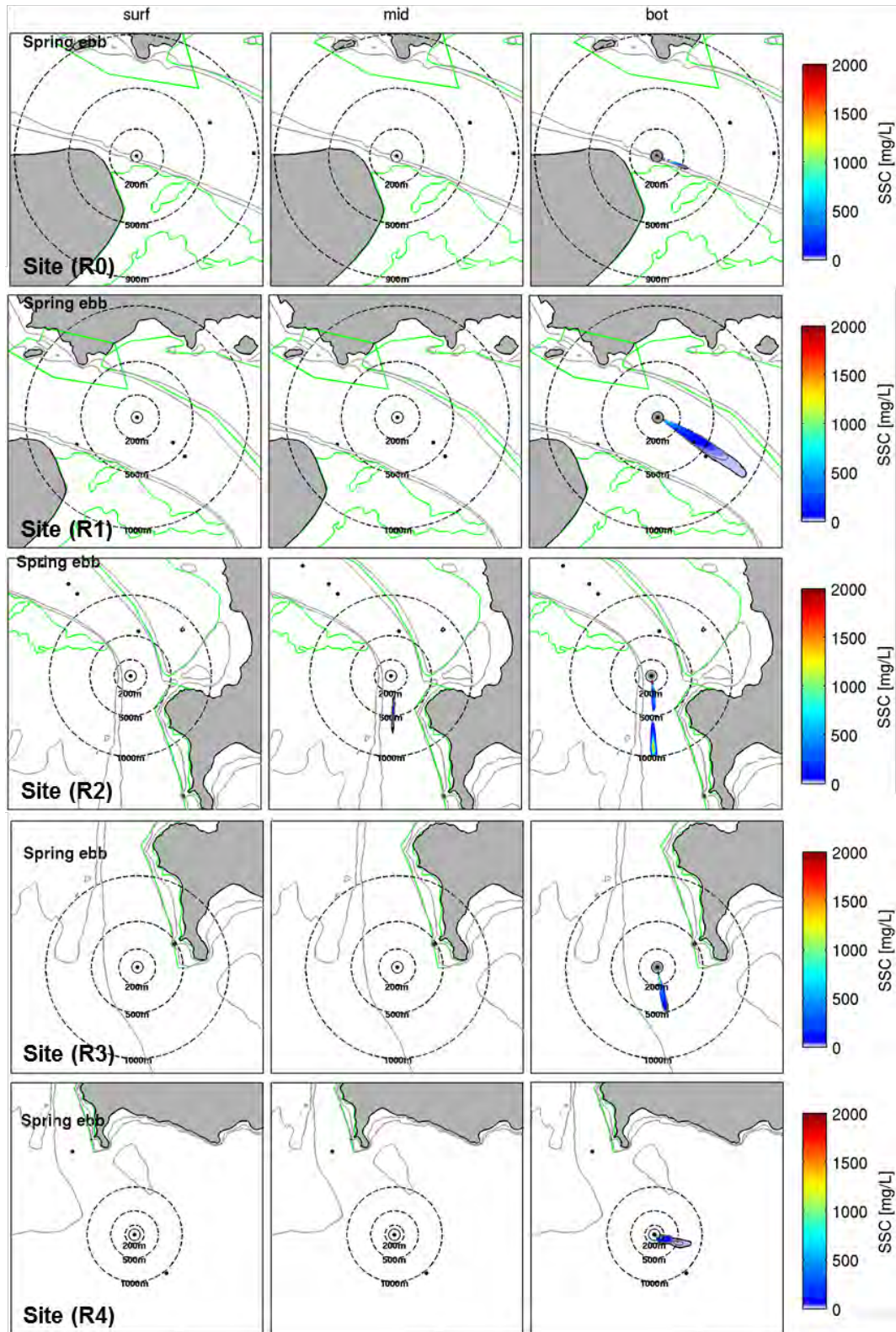
Probabilistic SSC plumes at Neap flood tide during dredging phase (large TSHD) at sites R5 to R8 at three levels of the water column considering a 3.0 % production rate for the drag head source.

**SMALL TSHD: DREDGING MODE – FLOOD (NEAP TIDE)**



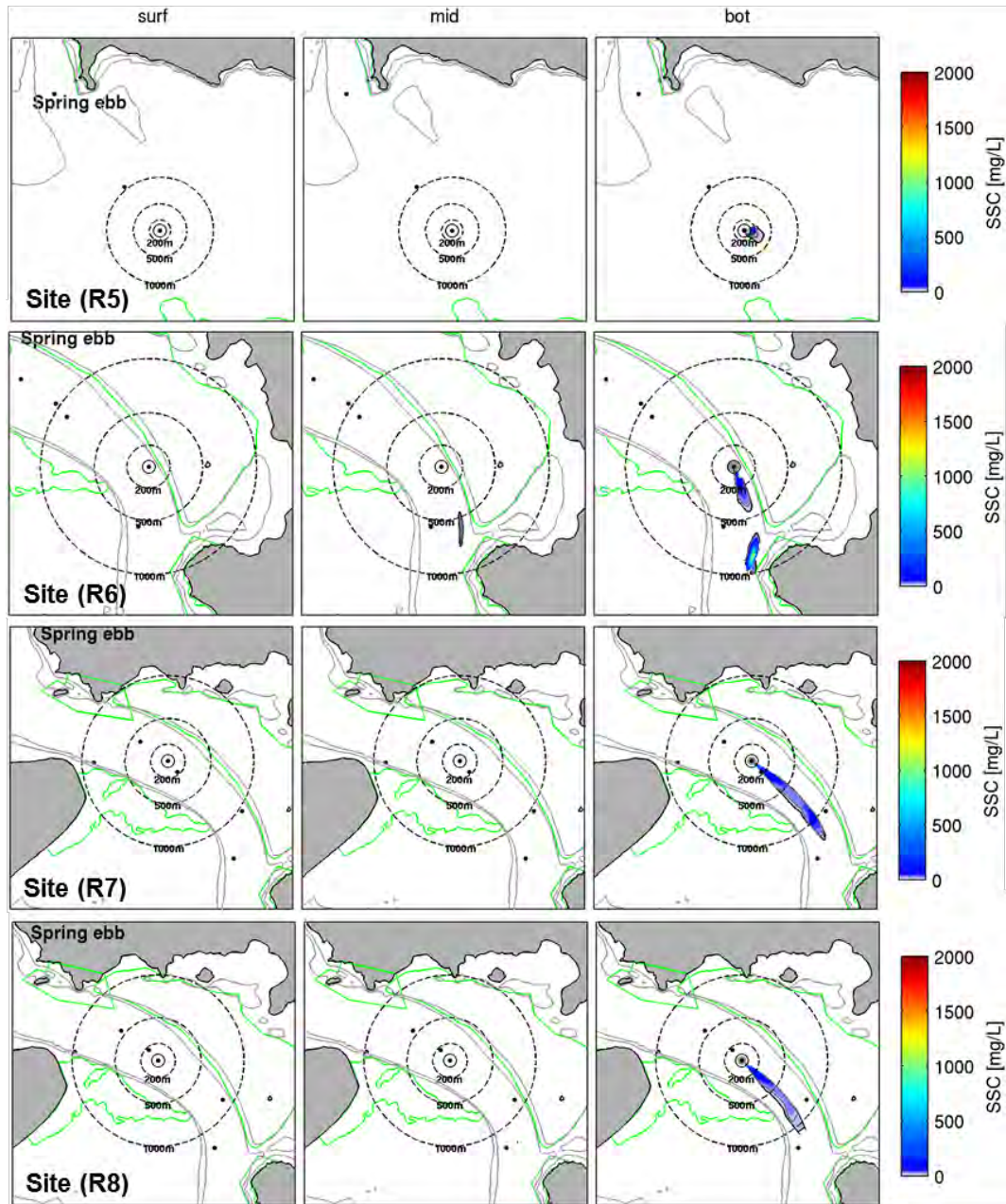
Probabilistic SSC plumes at spring ebb tide during dredging phase (large TSHD) at sites R0 to R4 at three levels of the water column considering a 3.0 % production rate for the drag head source.

**LARGE TSHD: DREDGING MODE – EBB (SPRING TIDE)**



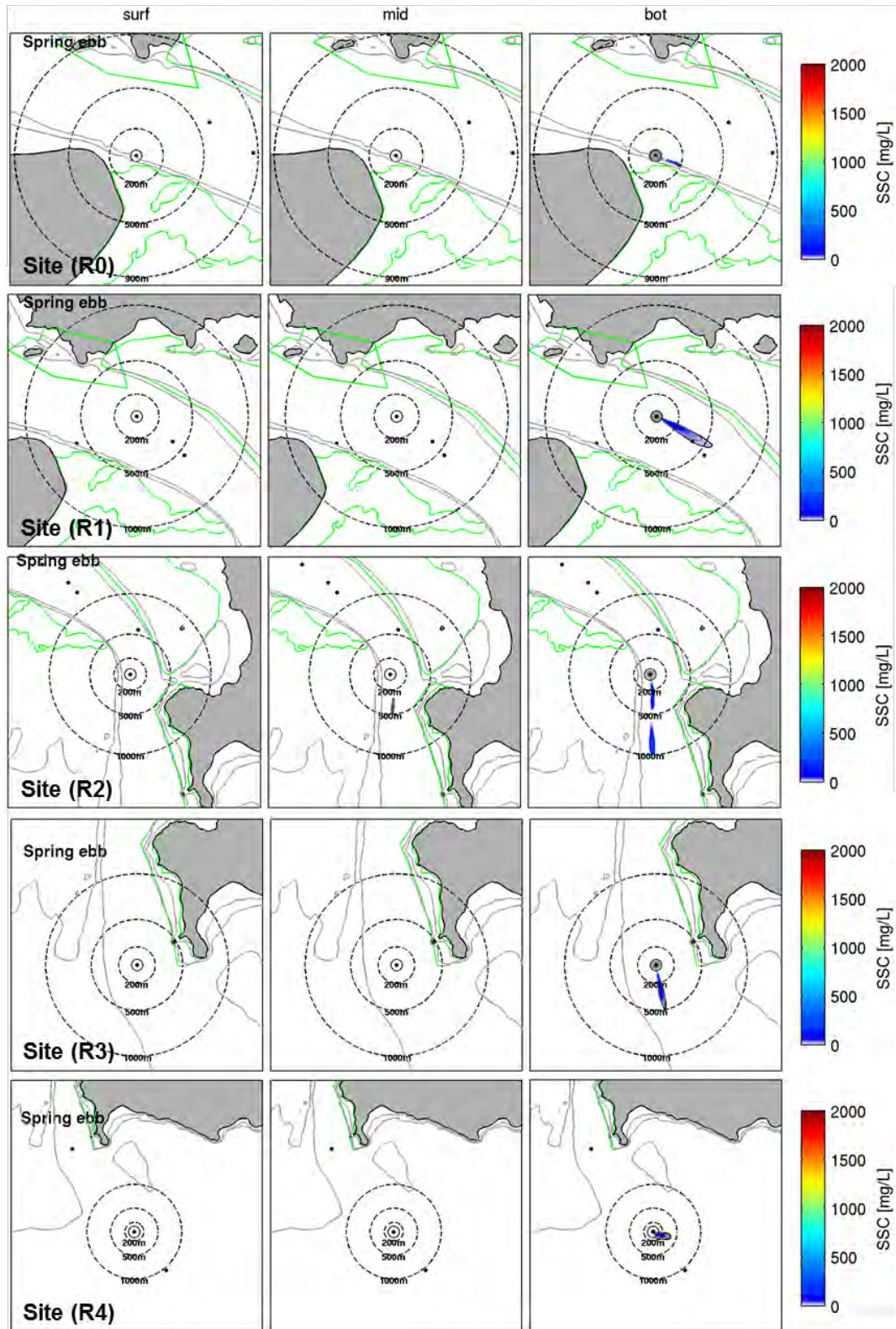
Probabilistic SSC plumes at spring ebb tide during dredging phase (large TSHD) at sites R5 to R8 at three levels of the water column considering a 3.0 % production rate for the drag head source.

**LARGE TSHD: DREDGING MODE – EBB (SPRING TIDE)**



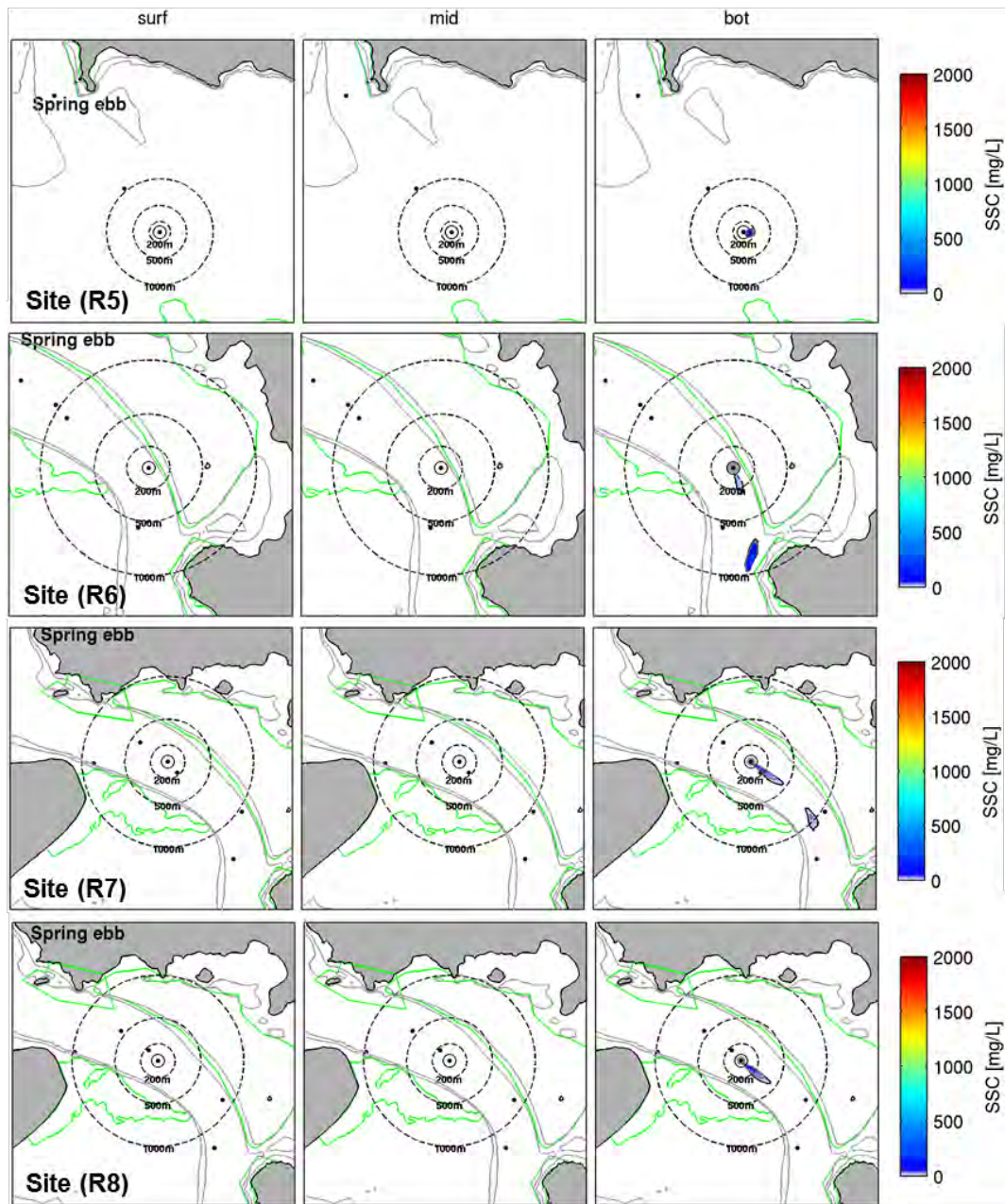
Probabilistic SSC plumes at spring ebb tide during dredging phase (small TSHD) at sites R0 to R4 at three levels of the water column considering a 3.0 % production rate for the drag head source.

**SMALL TSHD: DREDGING MODE – EBB (SPRING TIDE)**



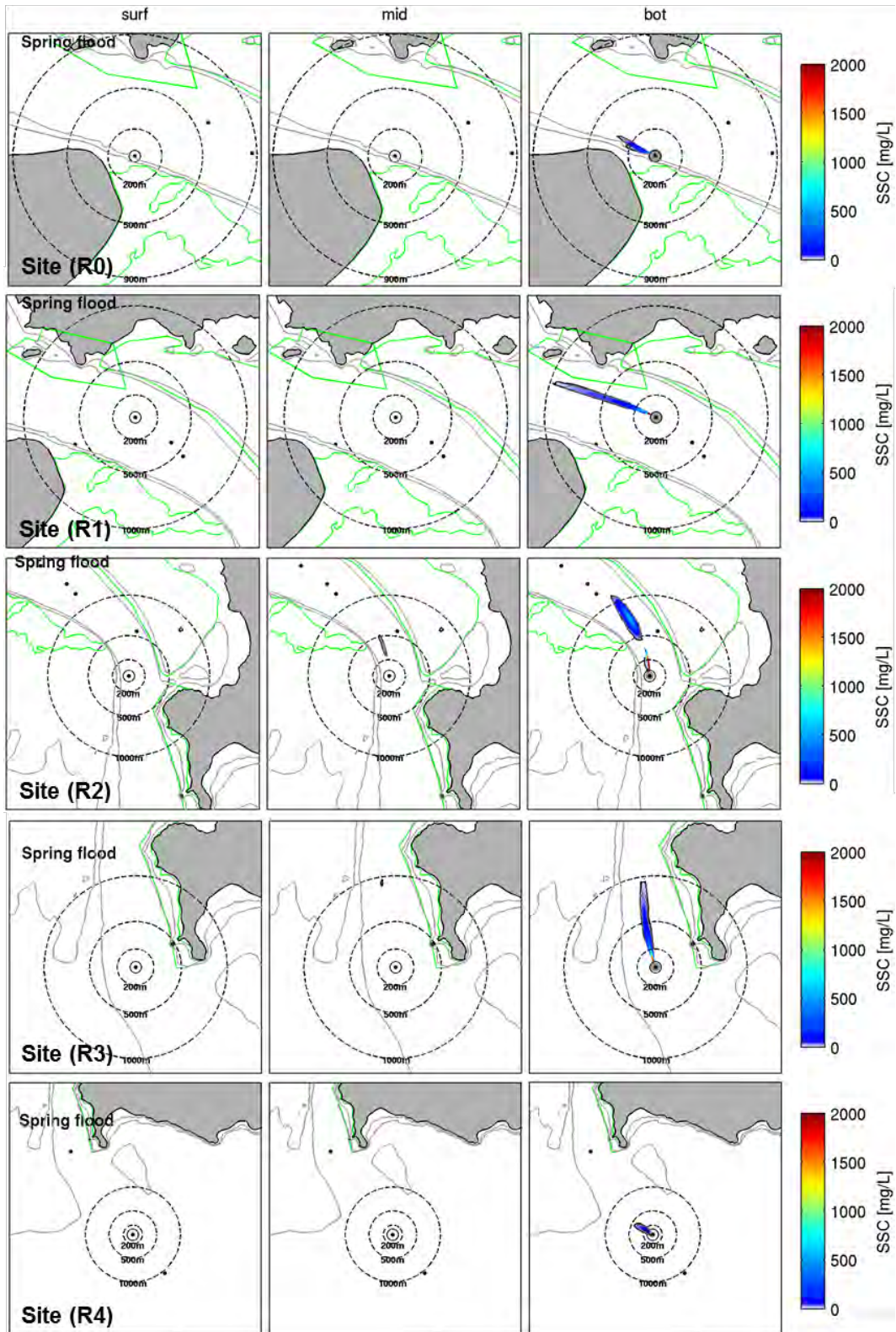
Probabilistic SSC plumes at spring ebb tide during dredging phase (small TSHD) at sites R5 to R8 at three levels of the water column considering a 3.0 % production rate for the drag head source.

**SMALL TSHD: DREDGING MODE – EBB (SPRING TIDE)**



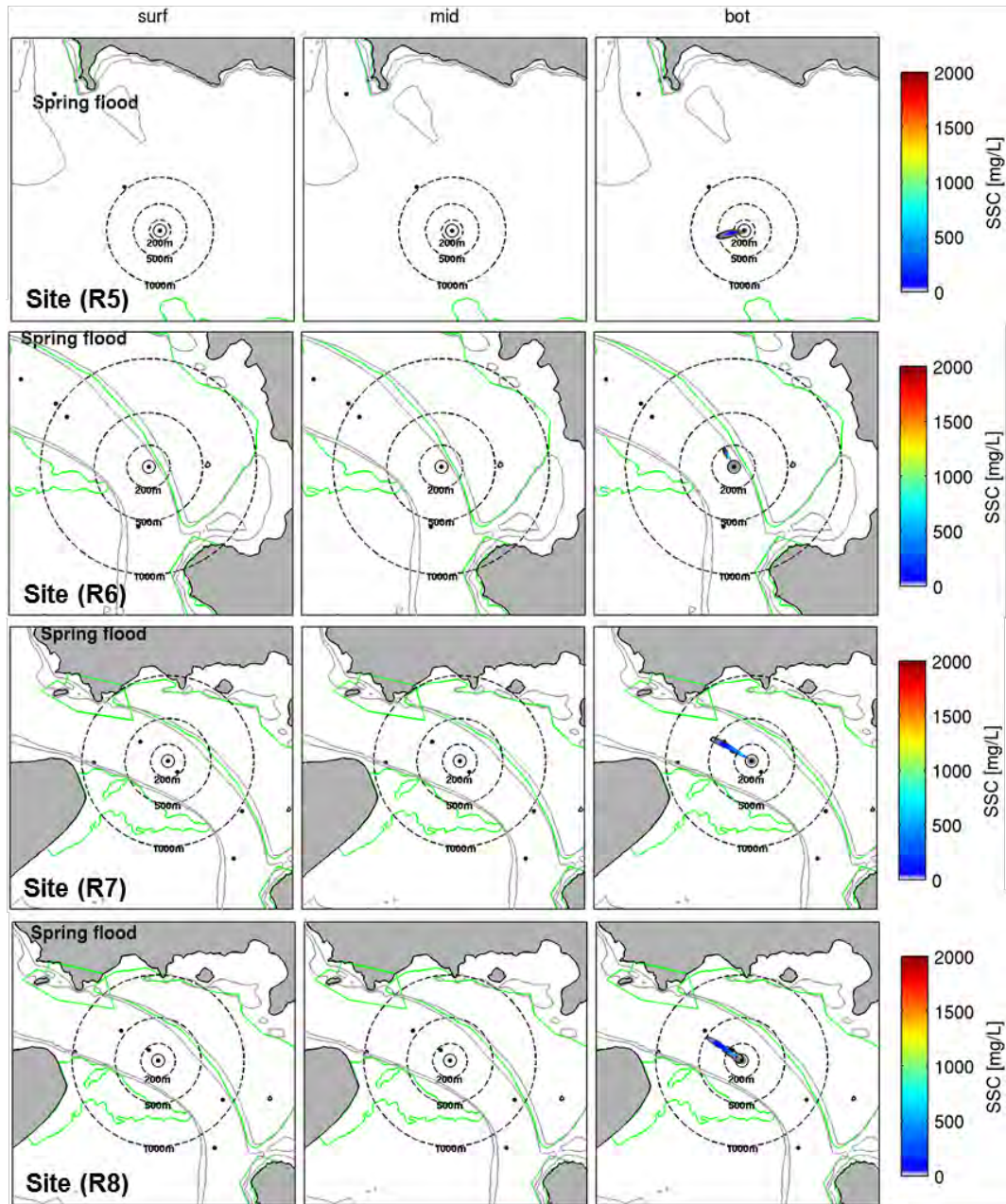
Probabilistic SSC plumes at spring flood tide during dredging phase (large TSHD) at sites R0 to R4 at three levels of the water column considering a 3.0 % production rate for the drag head source.

**LARGE TSHD: DREDGING MODE – FLOOD (SPRING TIDE)**



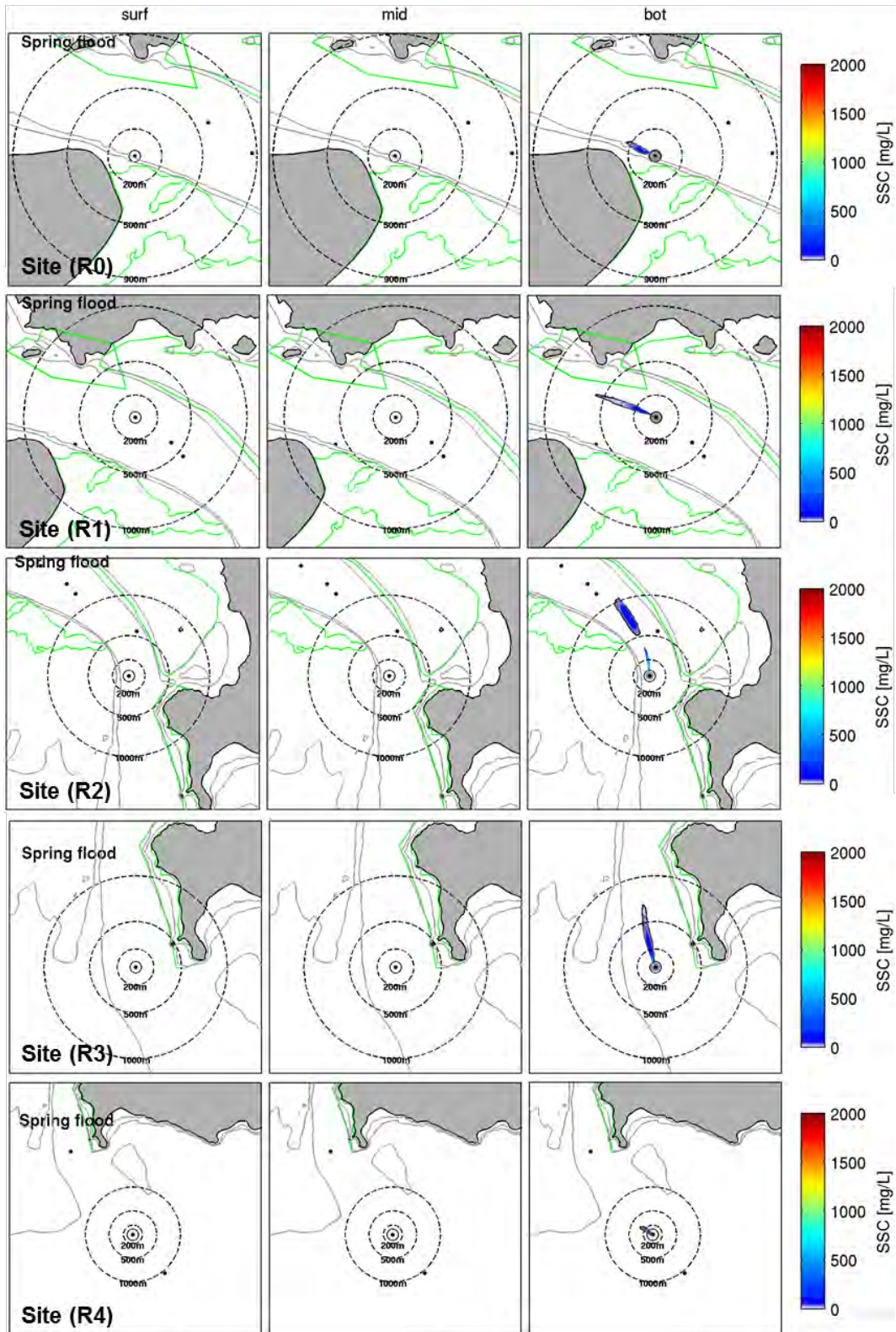
Probabilistic SSC plumes at spring flood tide during dredging phase (large TSHD) at sites R5 to R8 at three levels of the water column considering a 3.0 % production rate for the drag head source.

**LARGE TSHD: DREDGING MODE – FLOOD (SPRING TIDE)**



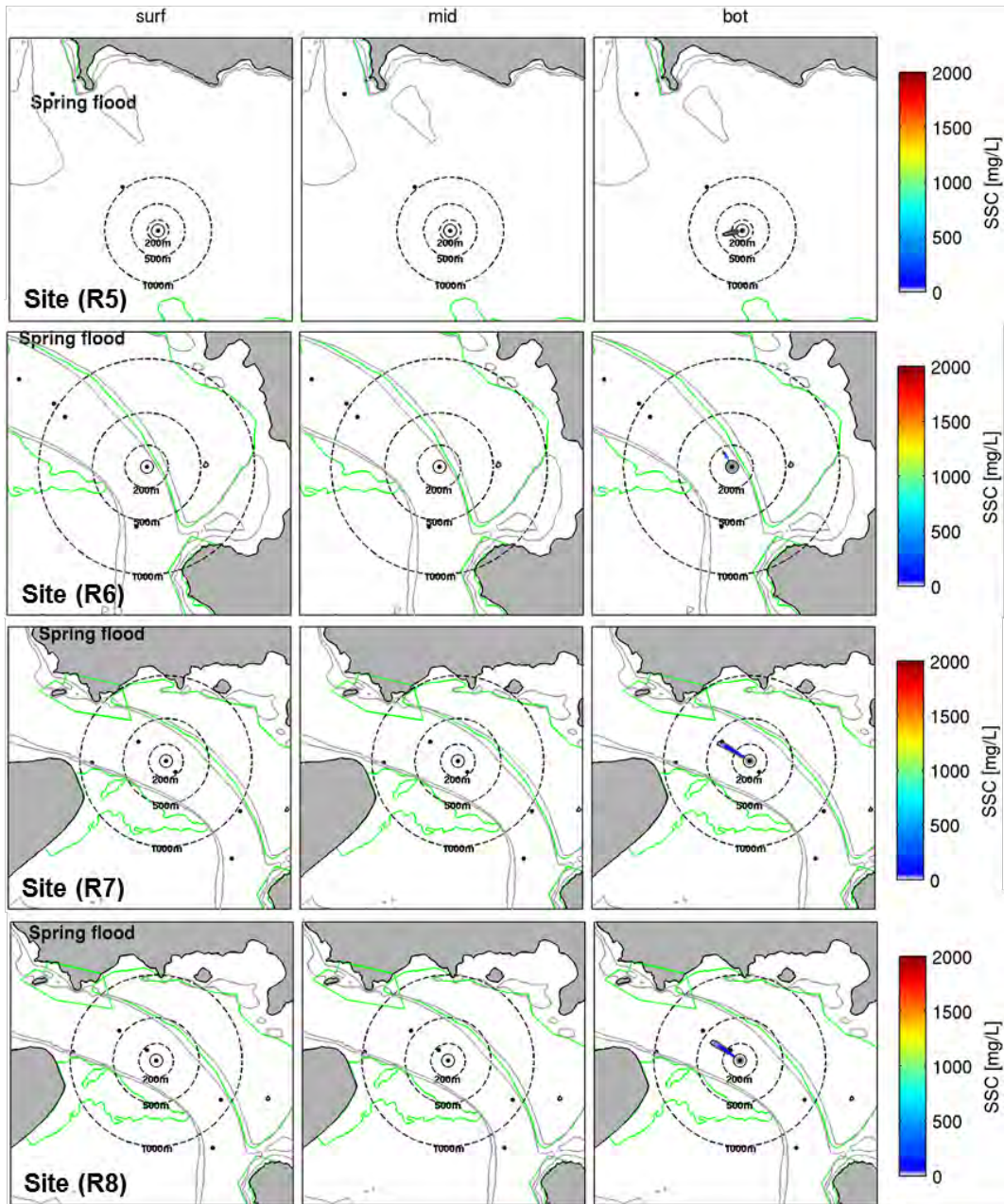
Probabilistic SSC plumes at spring flood tide during dredging phase (small TSHD) at sites R0 to R4 at three levels of the water column considering a 3.0 % production rate for the drag head source.

**SMALL TSHD: DREDGING MODE – FLOOD (SPRING TIDE)**



Probabilistic SSC plumes at spring flood tide during dredging phase (small TSHD) at sites R5 to R8 at three levels of the water column considering a 3.0 % production rate for the drag head source.

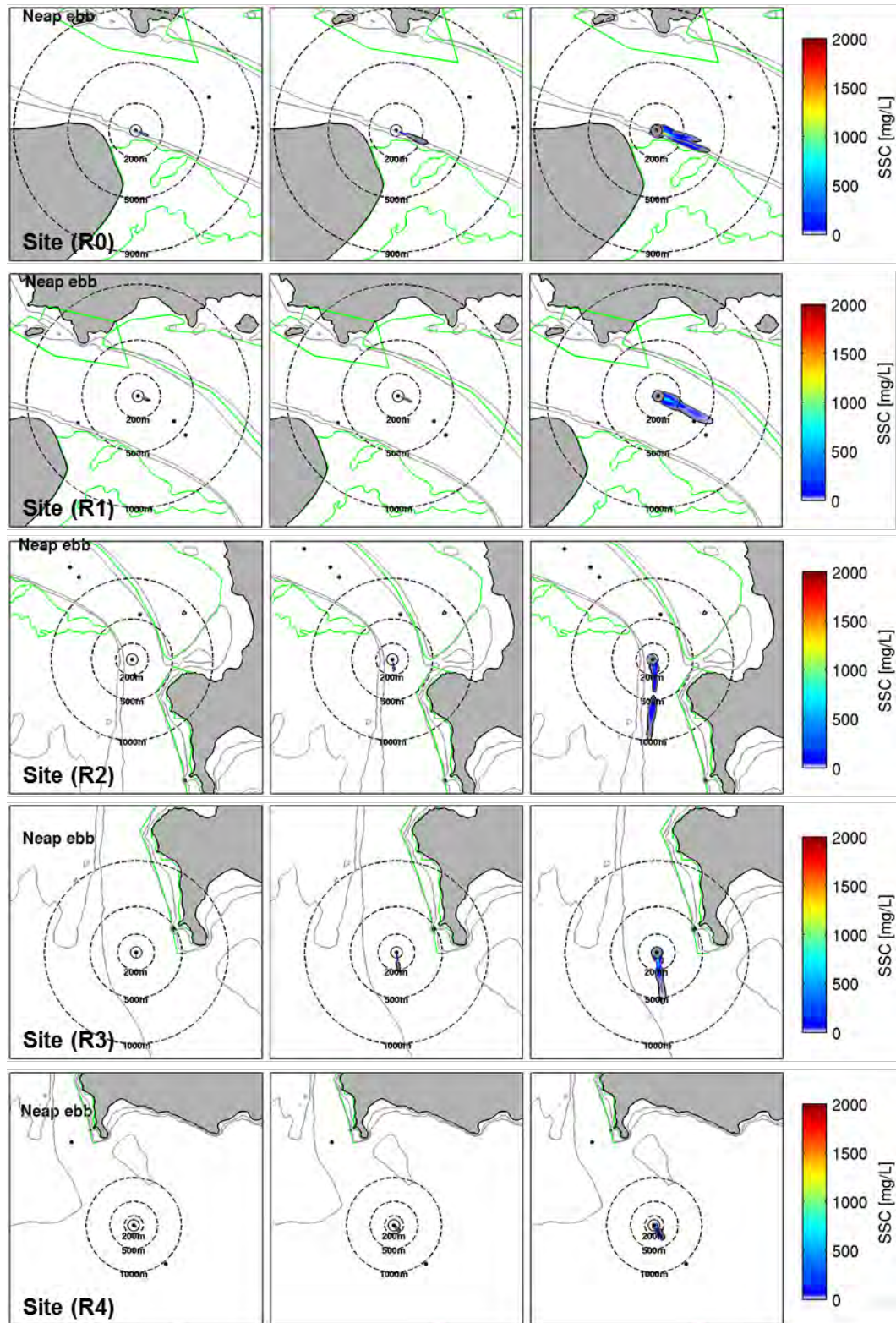
**SMALL TSHD: DREDGING MODE – FLOOD (SPRING TIDE)**



## **APPENDIX G – OVERFLOW MODE AT DIFFERENT TIDE STAGES**

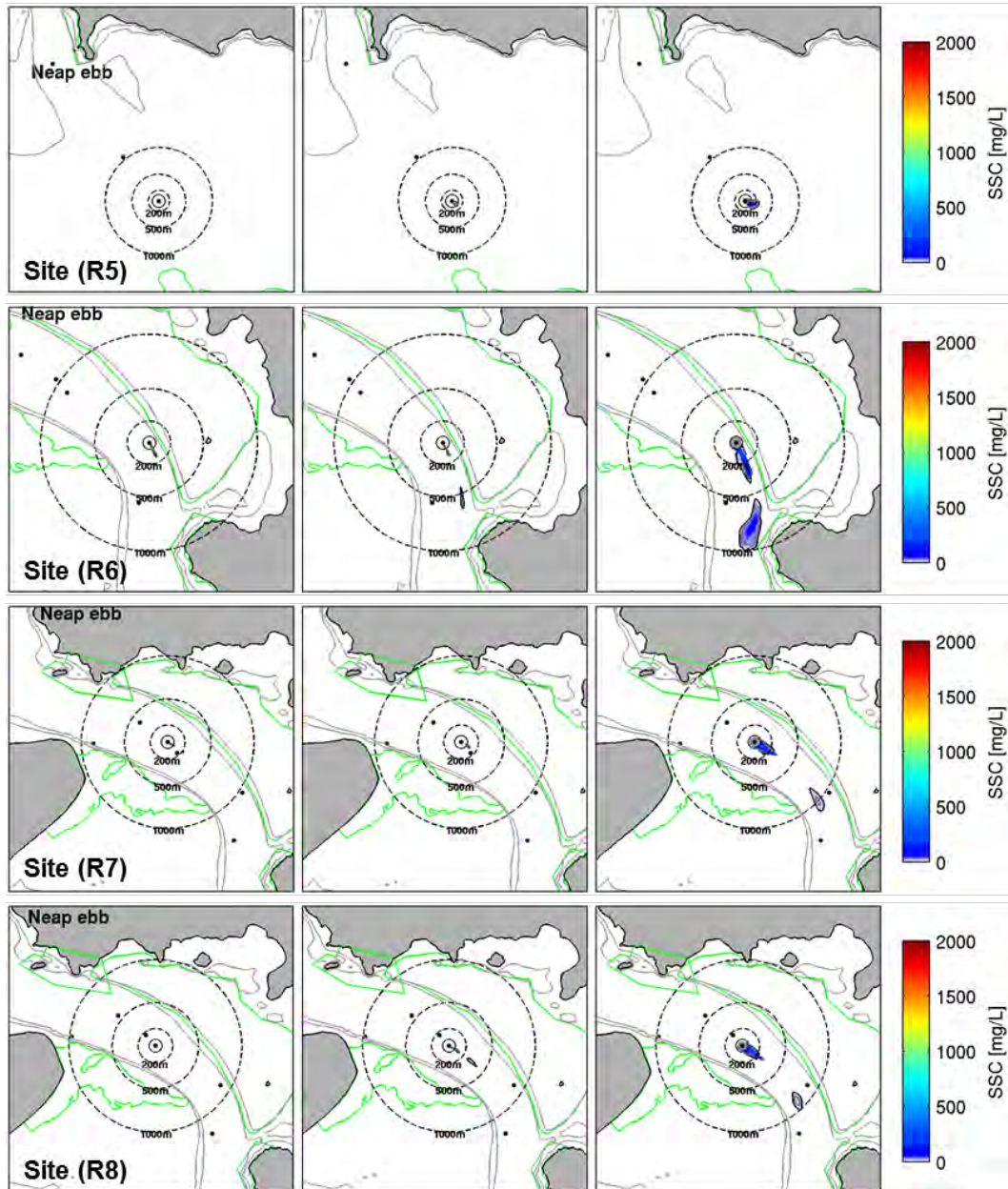
Probabilistic SSC plumes at neap ebb tide during the overflow (large TSHD) at sites R0 to R4.

**LARGE TSHD: OVERFLOW MODE – EBB (NEAP)**



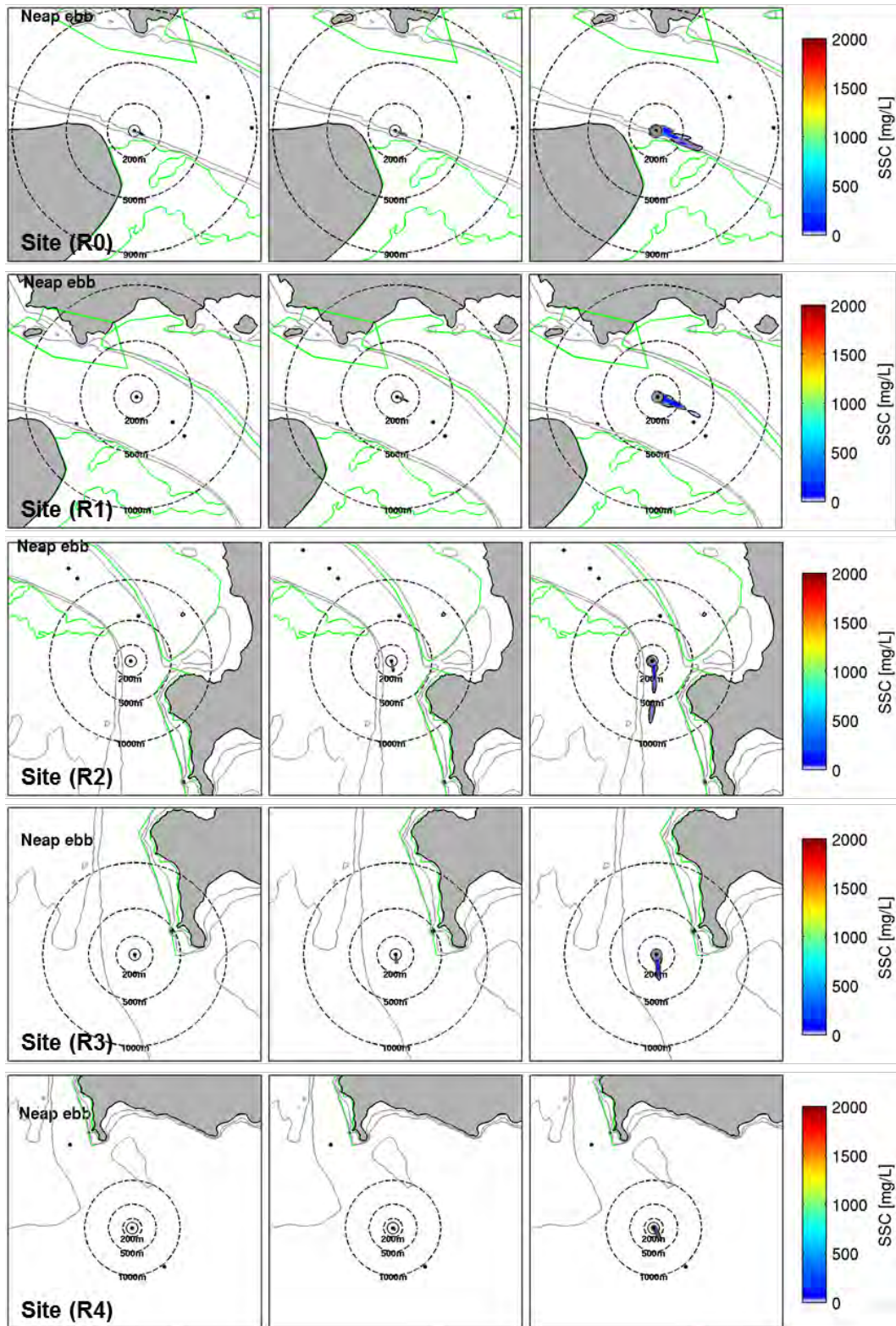
Probabilistic SSC plumes at neap ebb tide during the overflow (large TSHD) at sites R5 to R8.

**LARGE TSHD: OVERFLOW MODE – EBB (NEAP)**



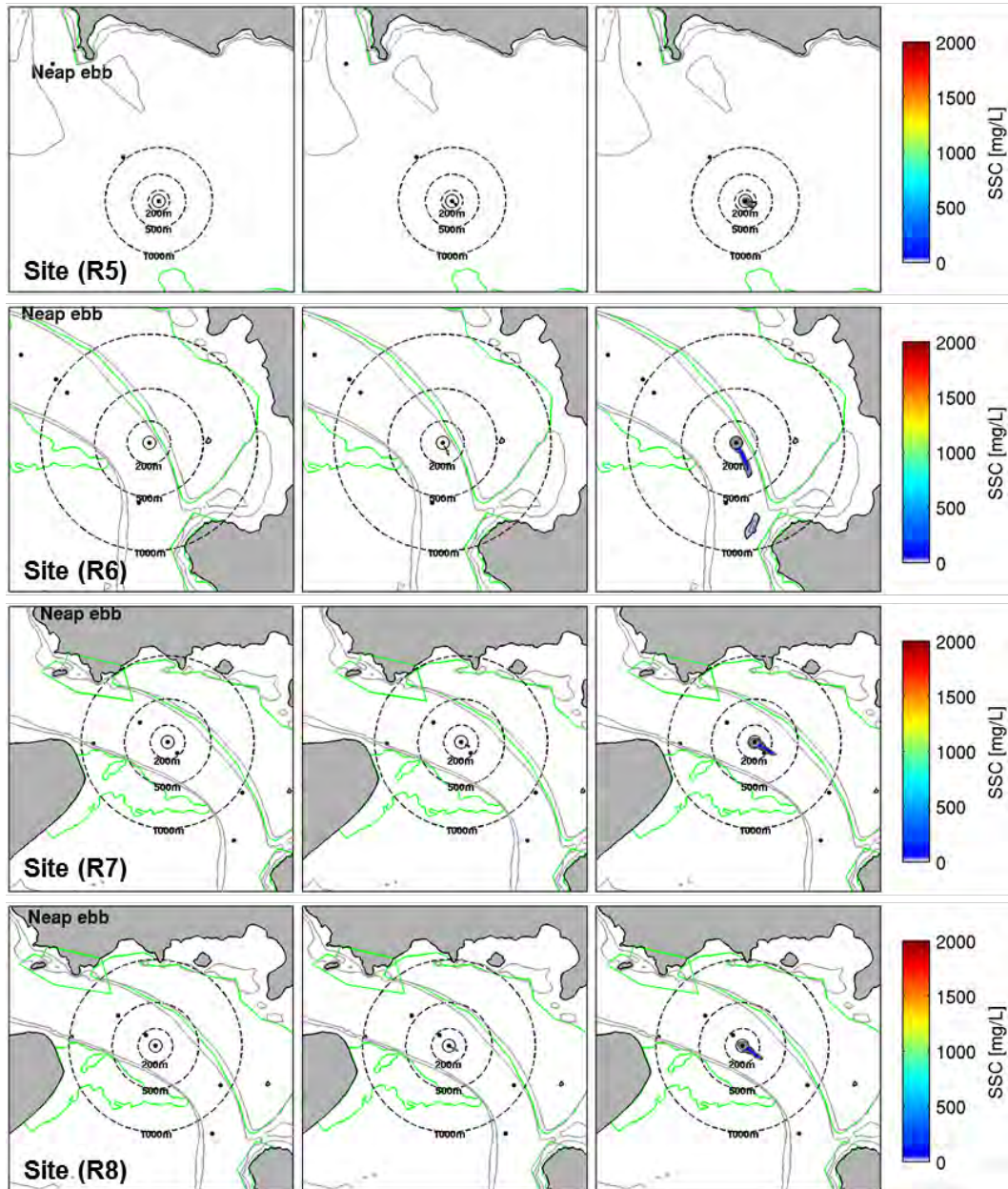
Probabilistic SSC plumes at neap ebb tide during the overflow (small TSHD) at sites R0 to R4.

**SMALL TSHD: OVERFLOW MODE – EBB (NEAP)**



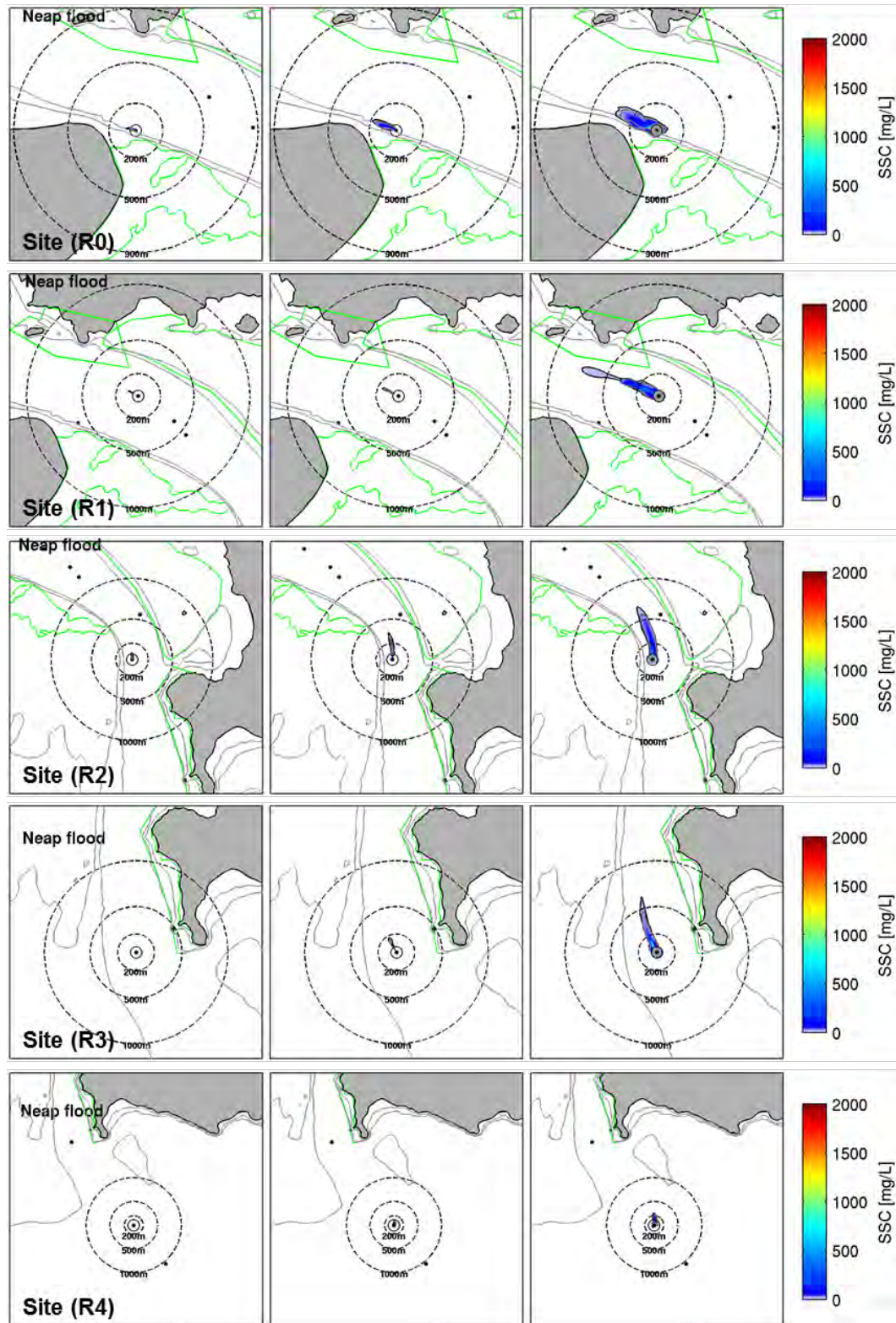
Probabilistic SSC plumes at neap ebb tide during the overflow (small TSHD) at sites R5 to R8.

**SMALL TSHD: OVERFLOW MODE – EBB (NEAP)**



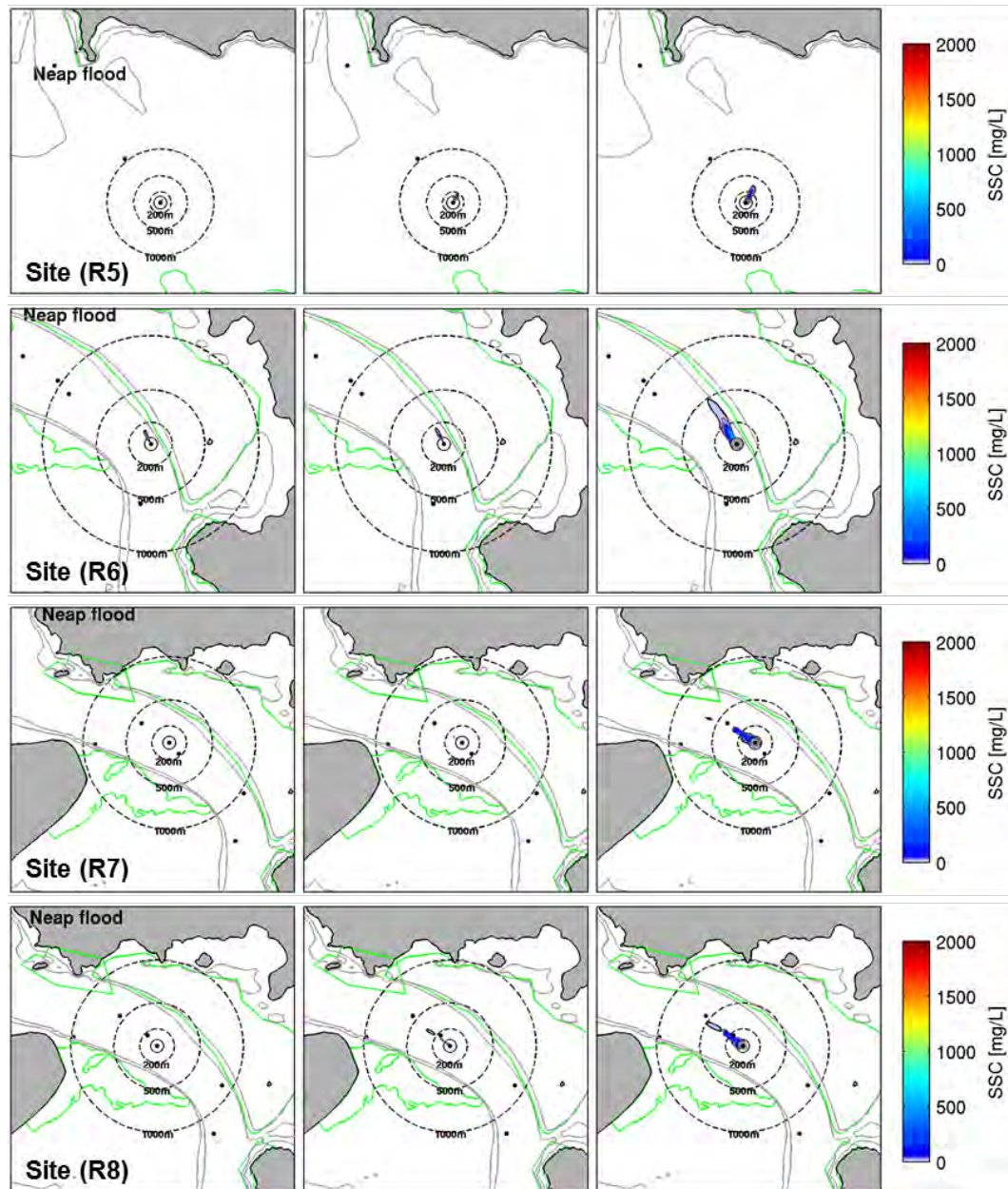
Probabilistic SSC plumes at neap flood tide during the overflow (large TSHD) at sites R0 to R4.

**LARGE TSHD: OVERFLOW MODE – FLOOD (NEAP)**



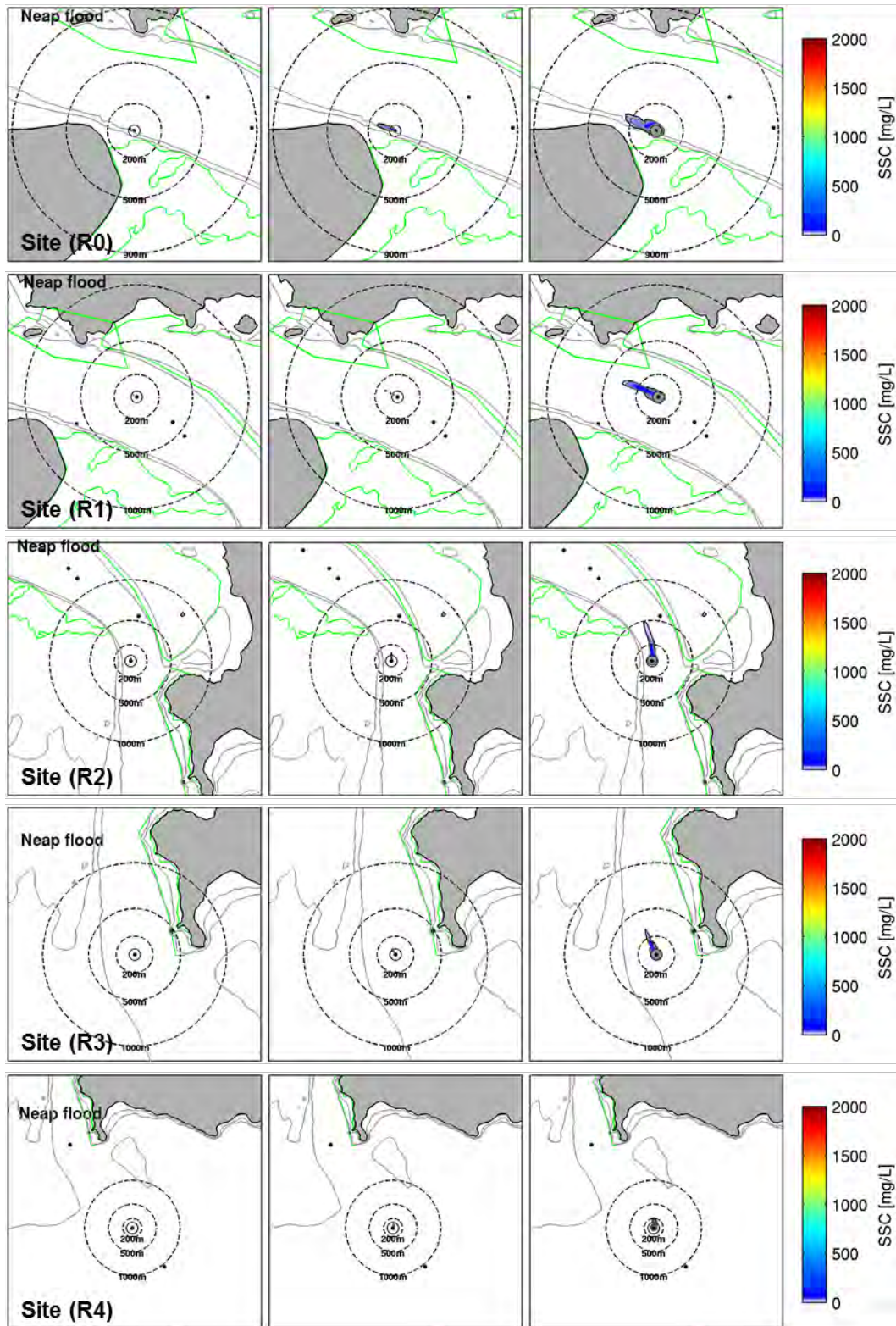
Probabilistic SSC plumes at neap flood tide during the overflow (large TSHD) at sites R5 to R8.

**LARGE TSHD: OVERFLOW MODE – FLOOD (NEAP)**



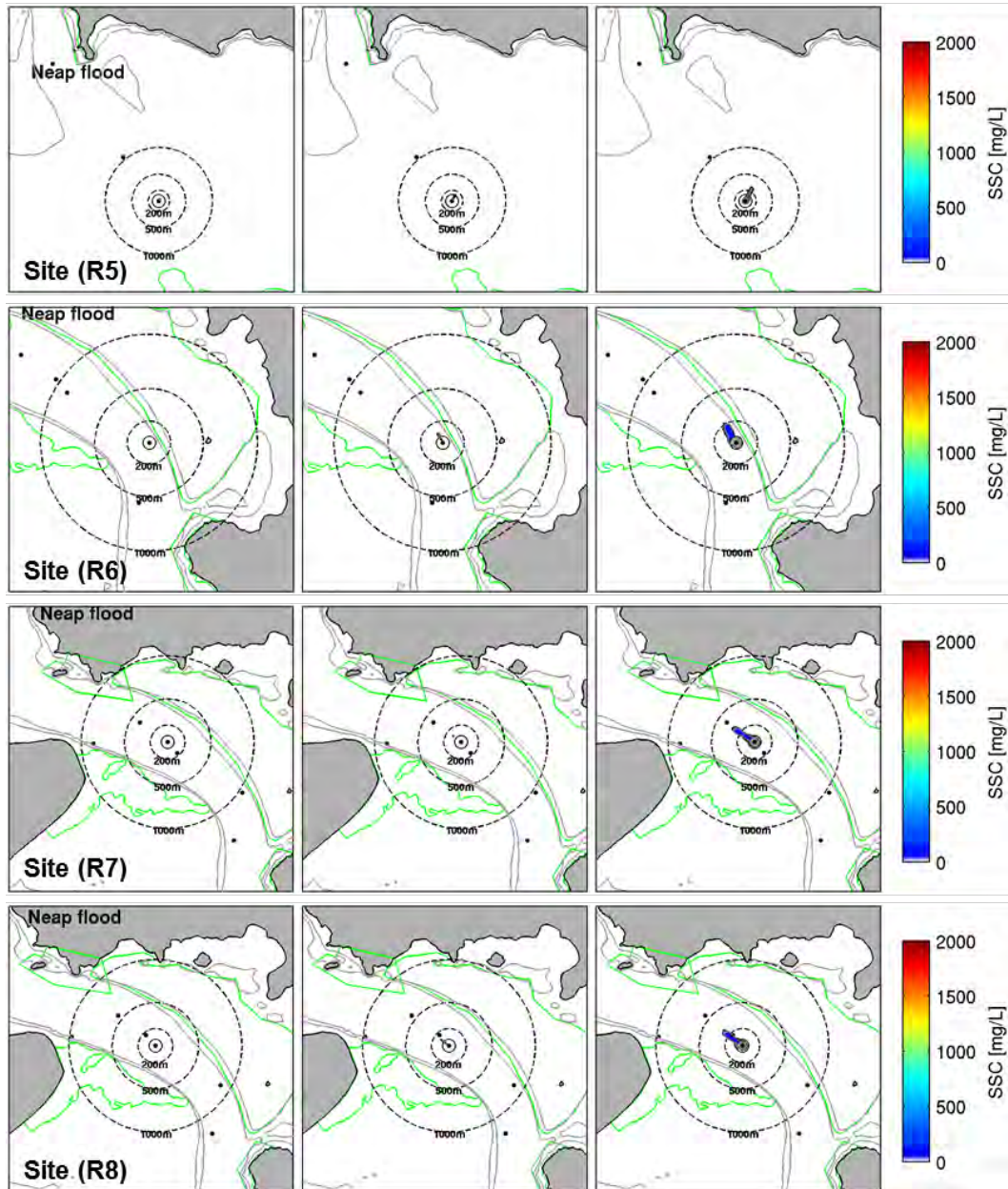
Probabilistic SSC plumes at neap flood tide during the overflow (small TSHD) at sites R0 to R4.

**SMALL TSHD: OVERFLOW MODE – FLOOD (NEAP)**



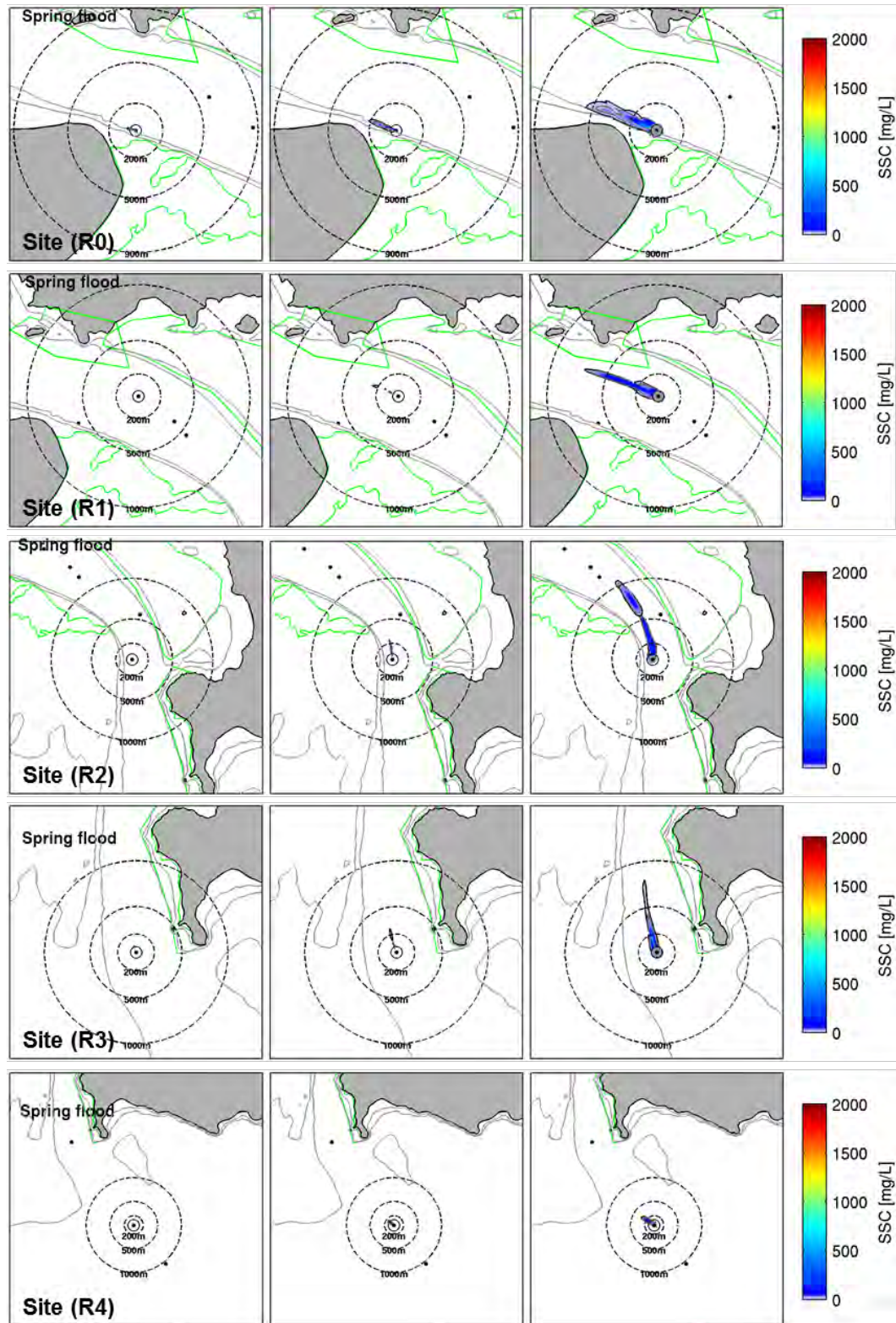
Probabilistic SSC plumes at neap flood tide during the overflow (small TSHD) at sites R5 to R8.

**SMALL TSHD: OVERFLOW MODE – FLOOD (NEAP)**



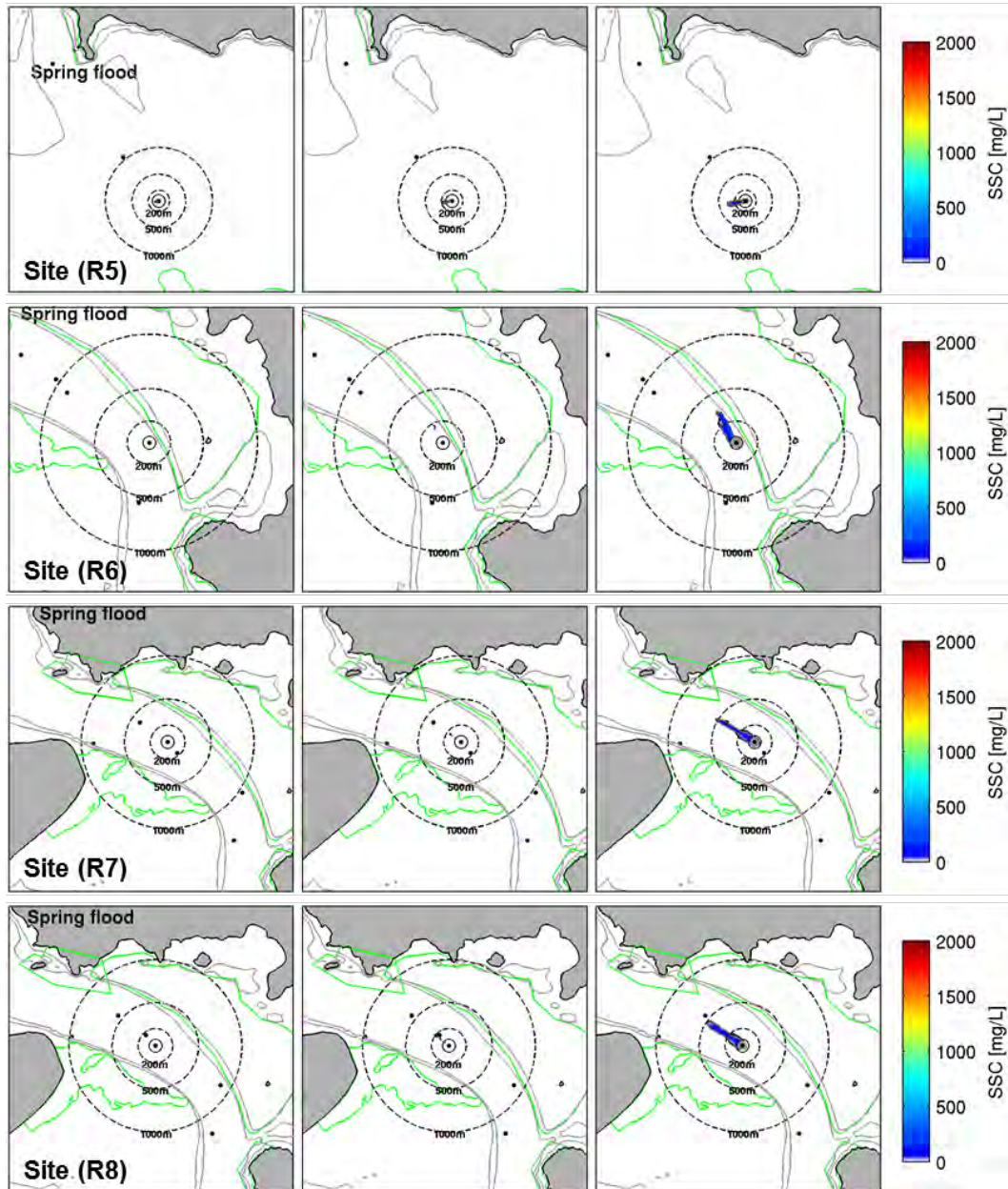
Probabilistic SSC plumes at spring flood tide during the overflow (large TSHD) at sites R0 to R4.

**LARGE TSHD: OVERFLOW MODE – FLOOD (SPRING)**



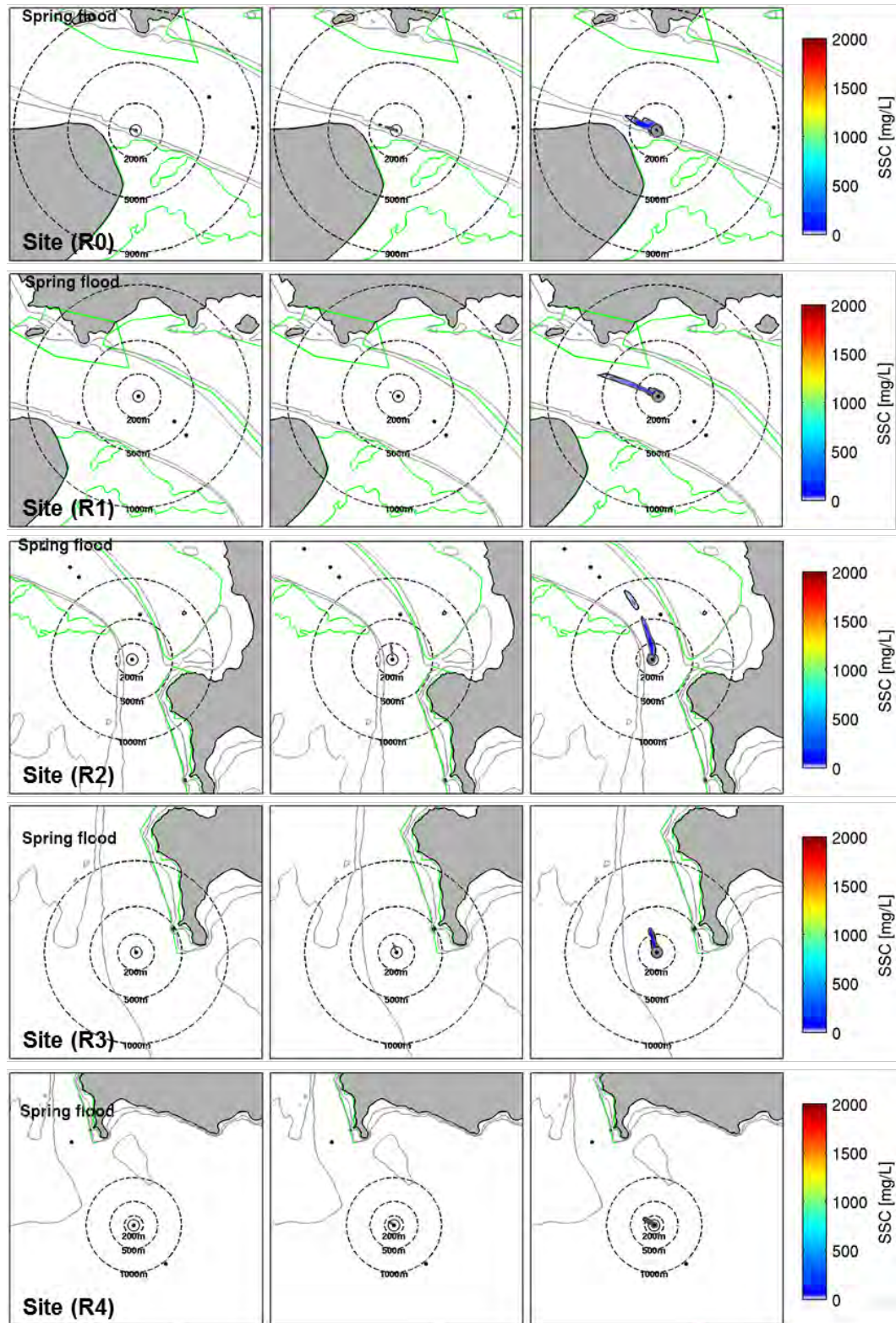
Probabilistic SSC plumes at spring flood tide during the overflow (large TSHD) at sites R5 to R8.

**LARGE TSHD: OVERFLOW MODE – FLOOD (SPRING)**



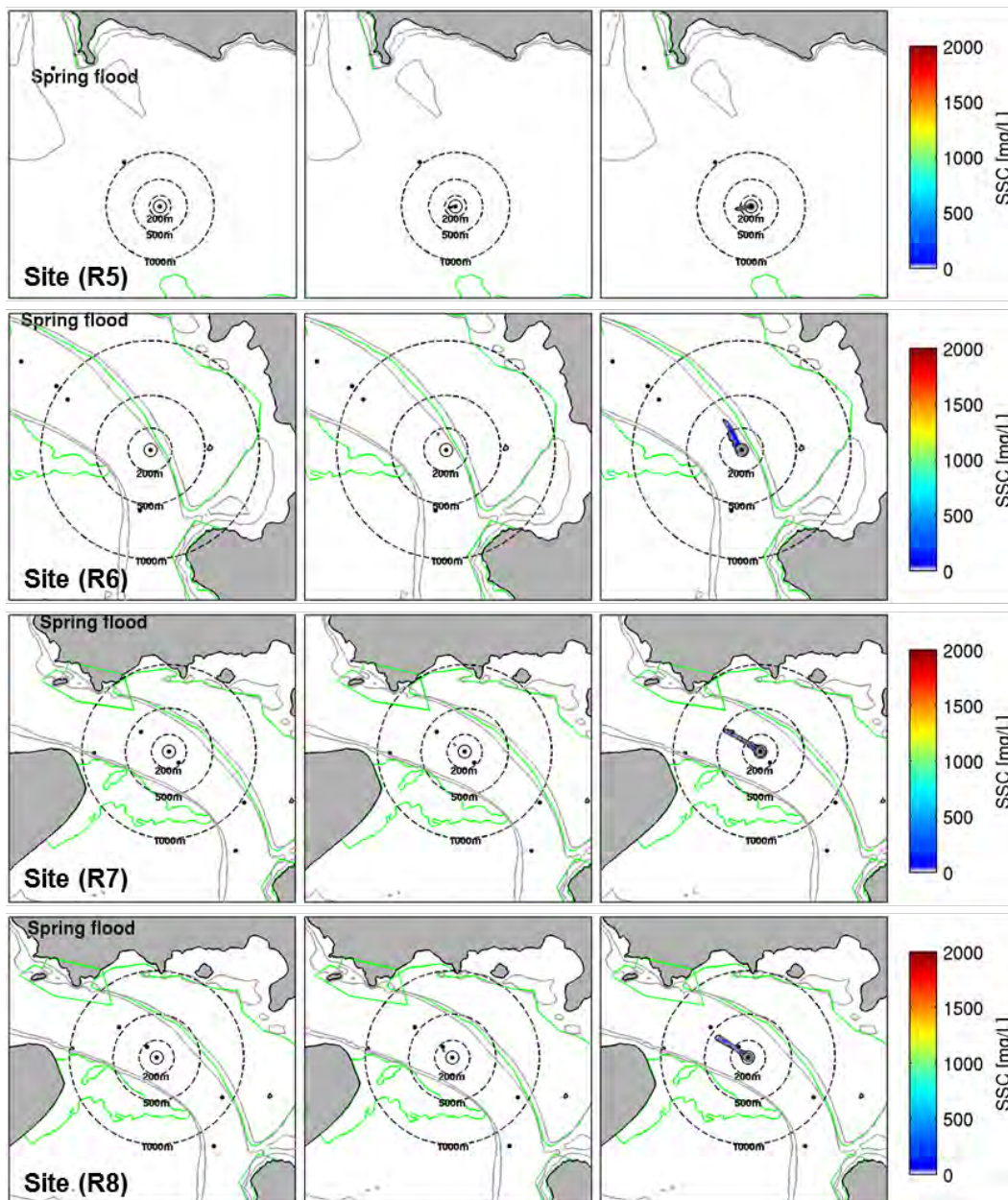
Probabilistic SSC plumes at spring flood tide during the overflow (small TSHD) at sites R0 to R4.

**SMALL TSHD: OVERFLOW MODE – FLOOD (SPRING)**



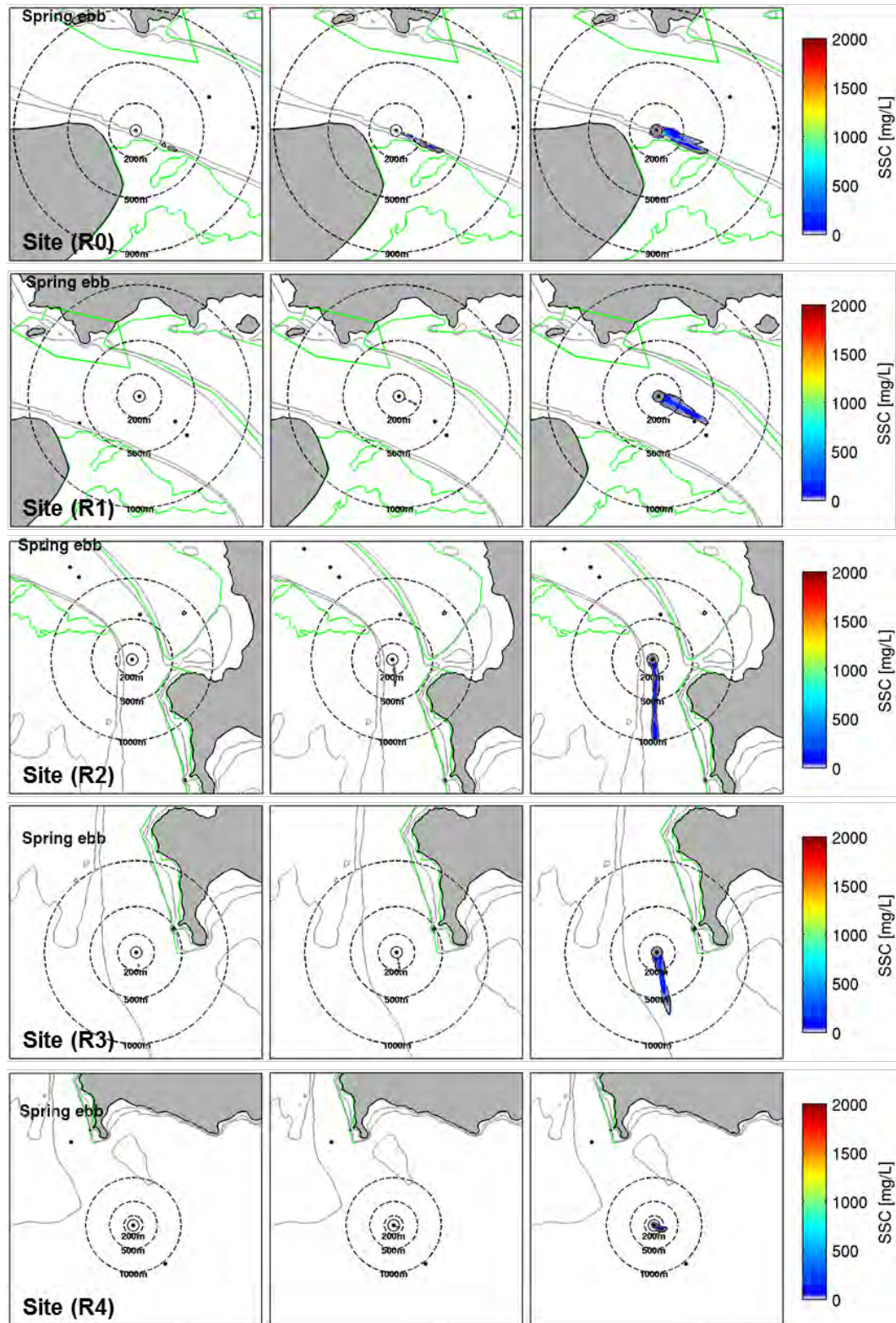
Probabilistic SSC plumes at spring flood tide during the overflow (small TSHD) at sites R5 to R8.

**SMALL TSHD: OVERFLOW MODE – FLOOD (SPRING)**



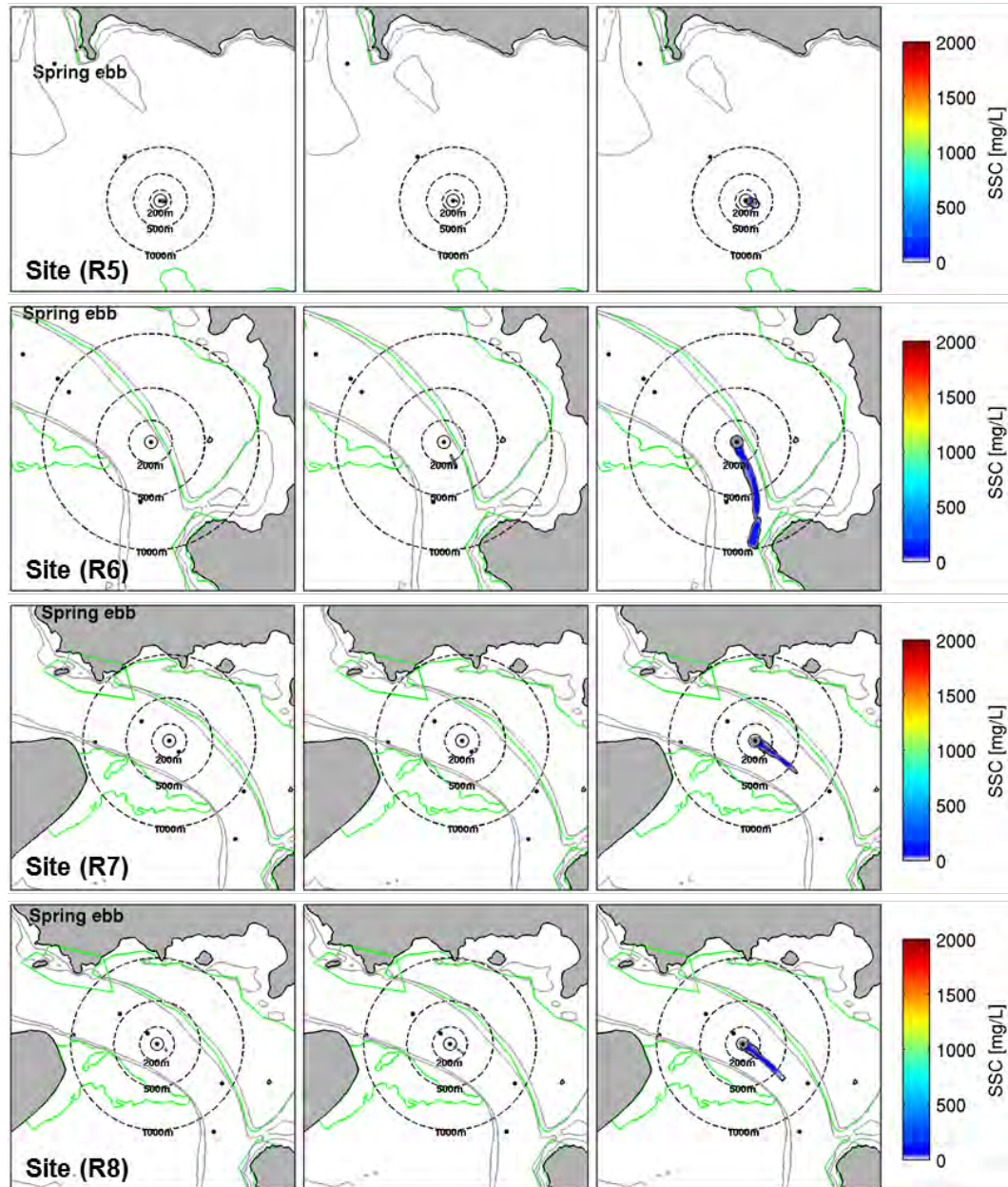
Probabilistic SSC plumes at spring ebb tide during the overflow (large TSHD) at sites R0 to R4.

**LARGE TSHD: OVERFLOW MODE – EBB (SPRING)**



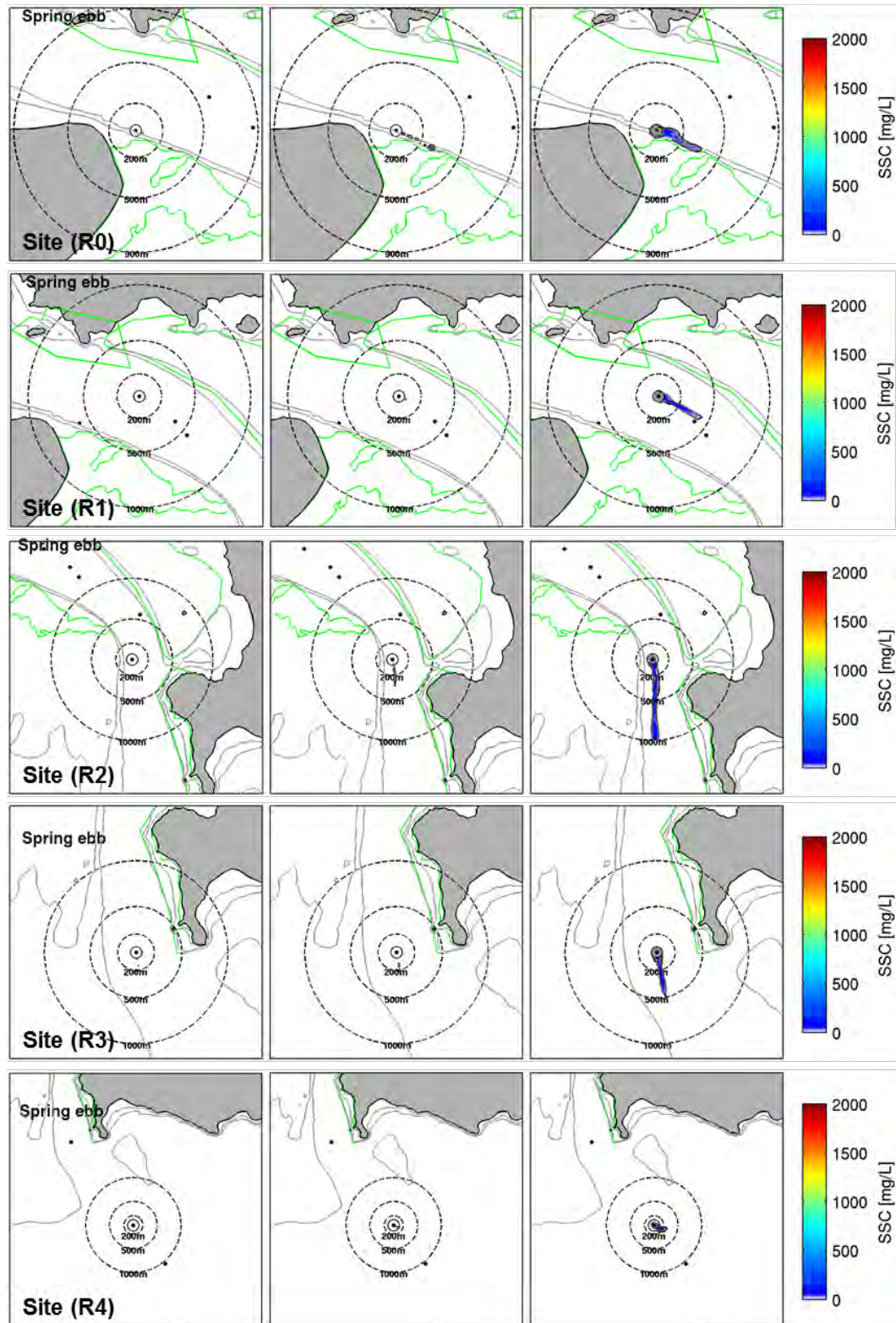
Probabilistic SSC plumes at spring ebb tide during the overflow (large TSHD) at sites R5 to R8.

**LARGE TSHD: OVERFLOW MODE – EBB (SPRING)**



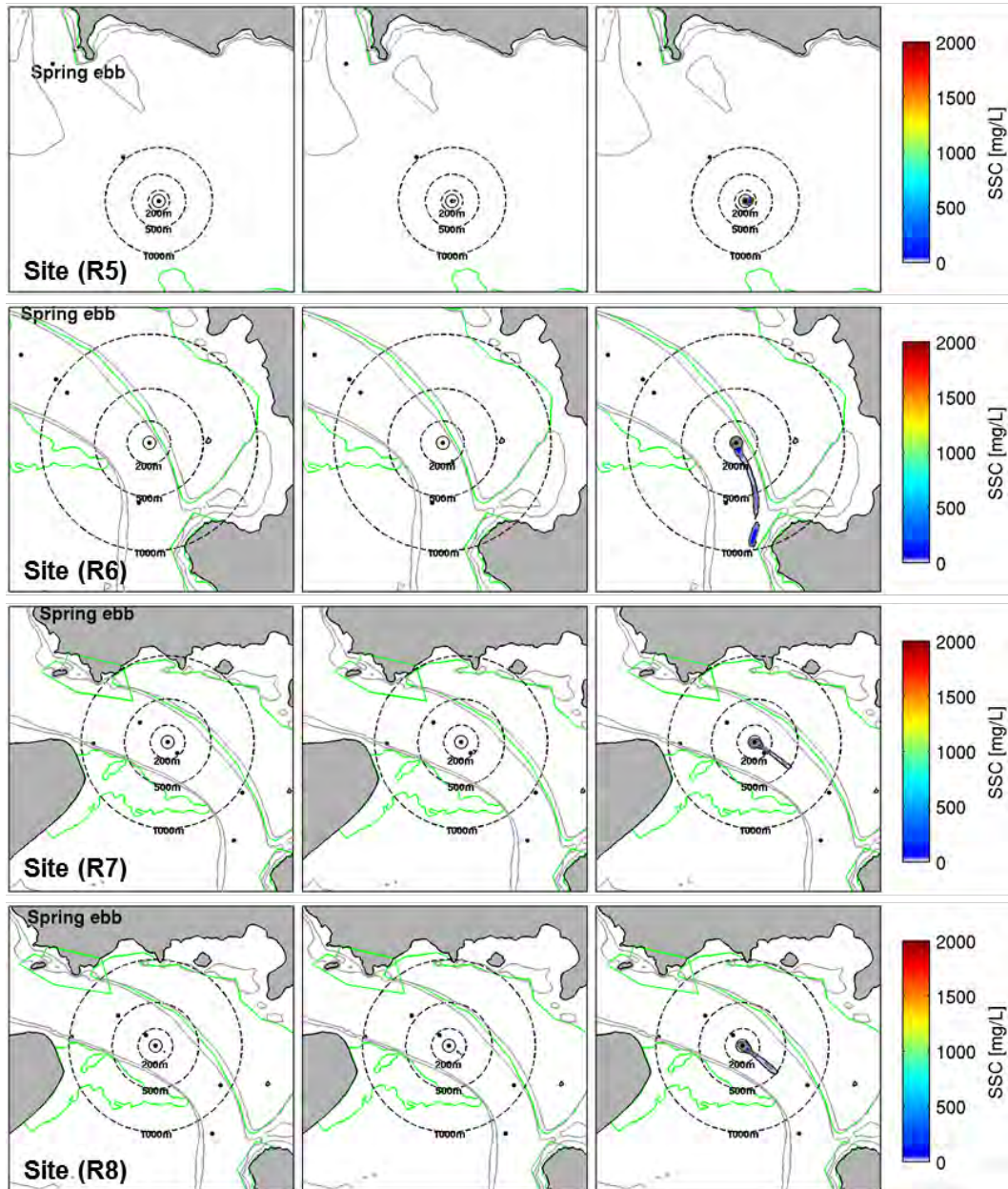
Probabilistic SSC plumes at spring ebb tide during the overflow (small TSHD) at sites R0 to R4.

**SMALL TSHD: OVERFLOW MODE – EBB (SPRING)**



Probabilistic SSC plumes at spring ebb tide during the overflow (small TSHD) at sites R5 to R8.

**SMALL TSHD: OVERFLOW MODE – EBB (SPRING)**

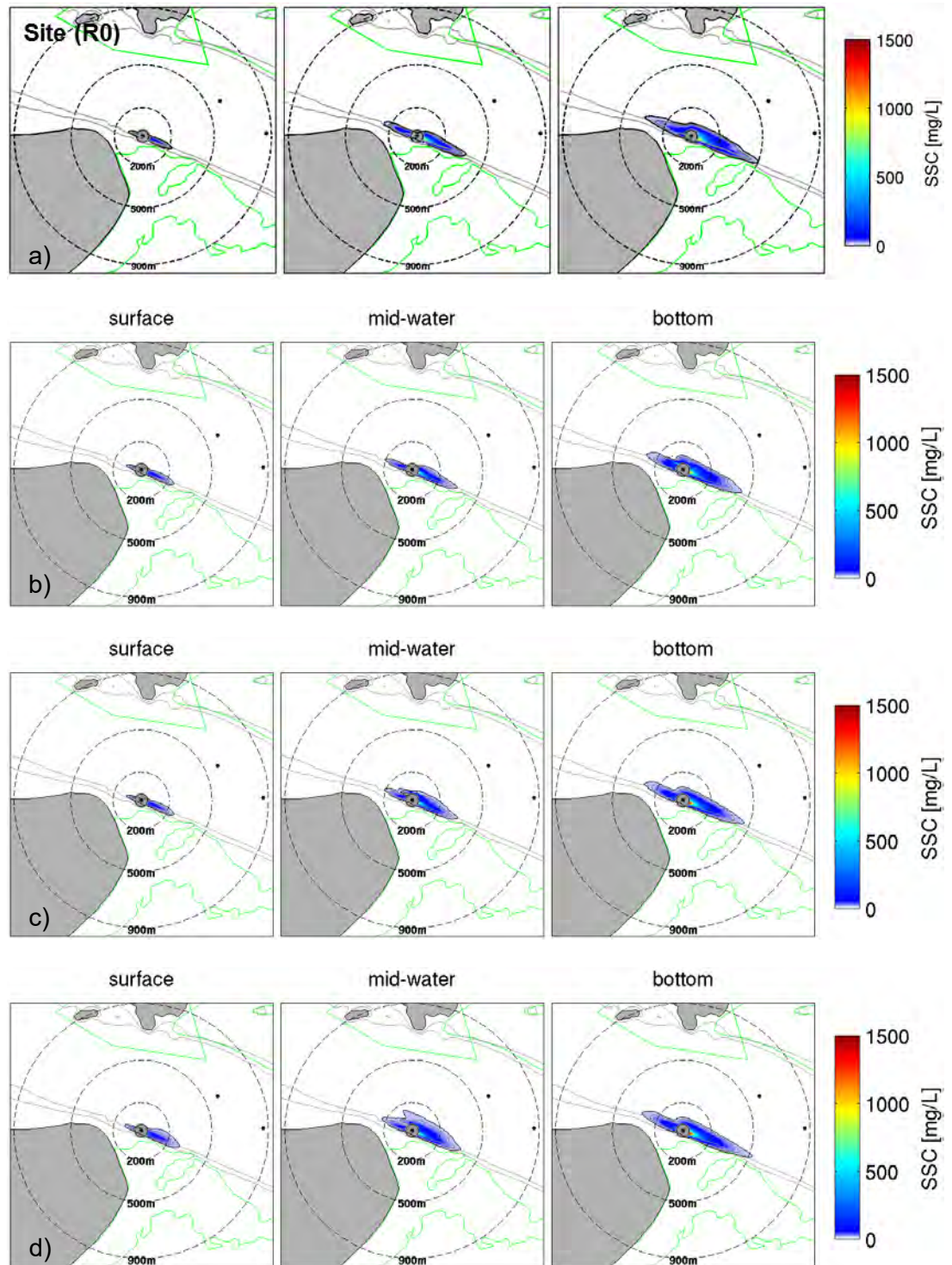


## APPENDIX H – SENSITIVITY ANALYSIS OF THE PLUME MODEL

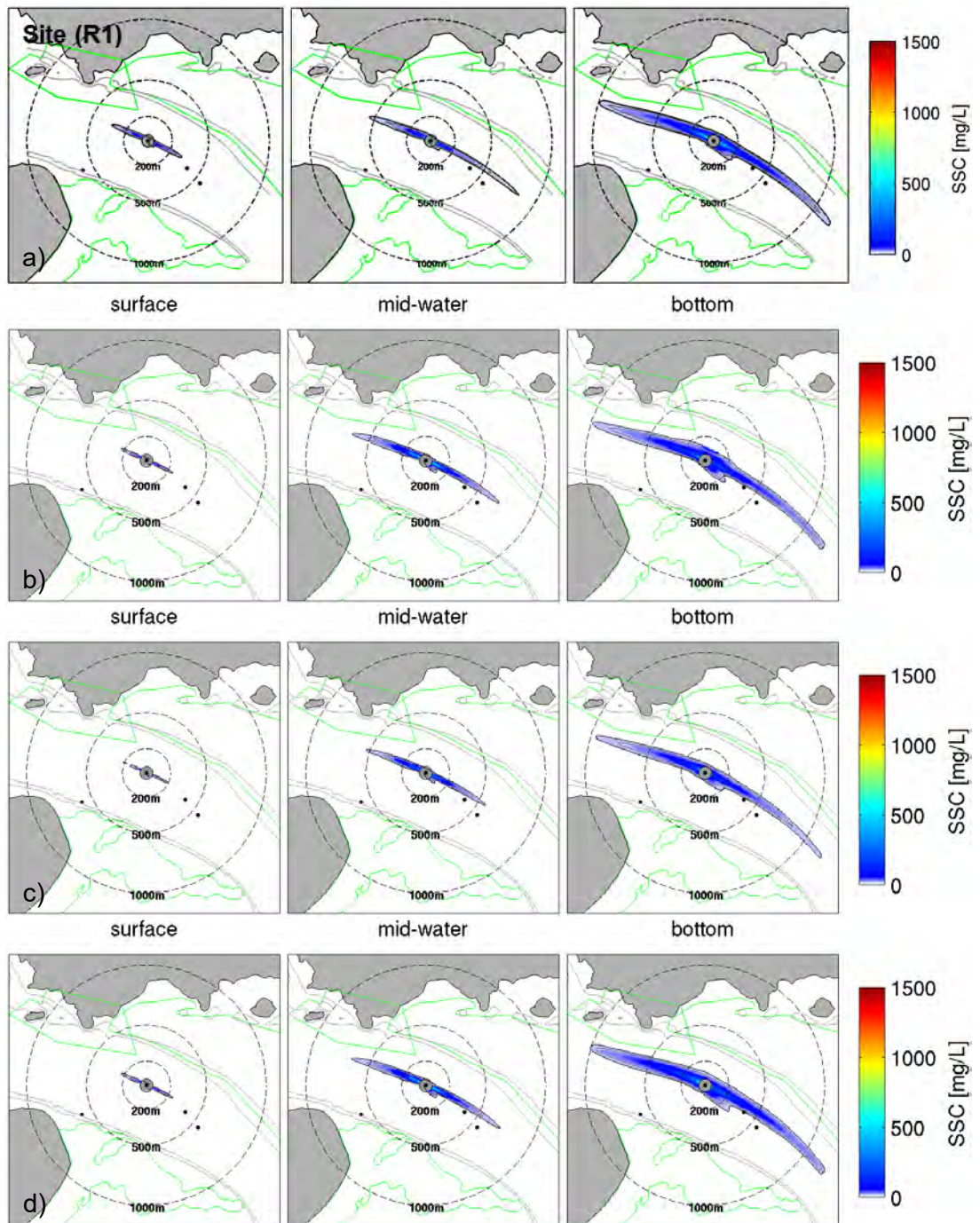
Parameters tested to simulate the plume dispersion during overflow phase (large trailing suction hopper dredger, TSHD) for a period of 79 min.

Cases	Overflow release	Silt fraction in release	Settling velocity (mm/s)
	Cylinder		
a)	2 m High, 60 m radius	5%	1
b)	2 m High, 100 m radius	5%	0.4
c)	4 m High, 60 m radius	5%	0.4
d)	4 m High, 60 m radius	10%	0.4

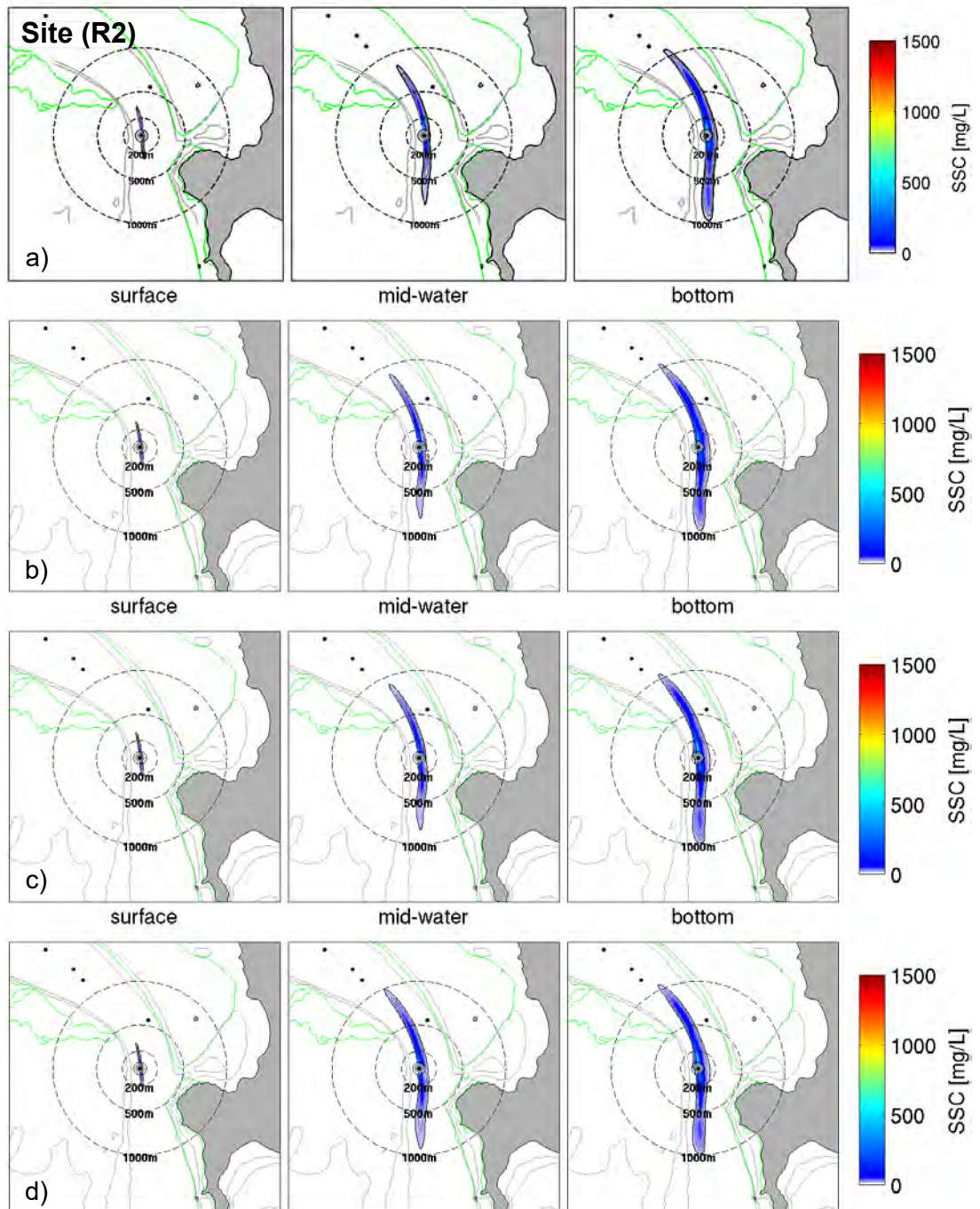
Probabilistic SSC plumes during overflow phase (large trailing suction hopper dredger, TSHD) at site R0 at three levels of the water column for a 79 min period for four model configurations (a, b, c, d) described in the previous table.



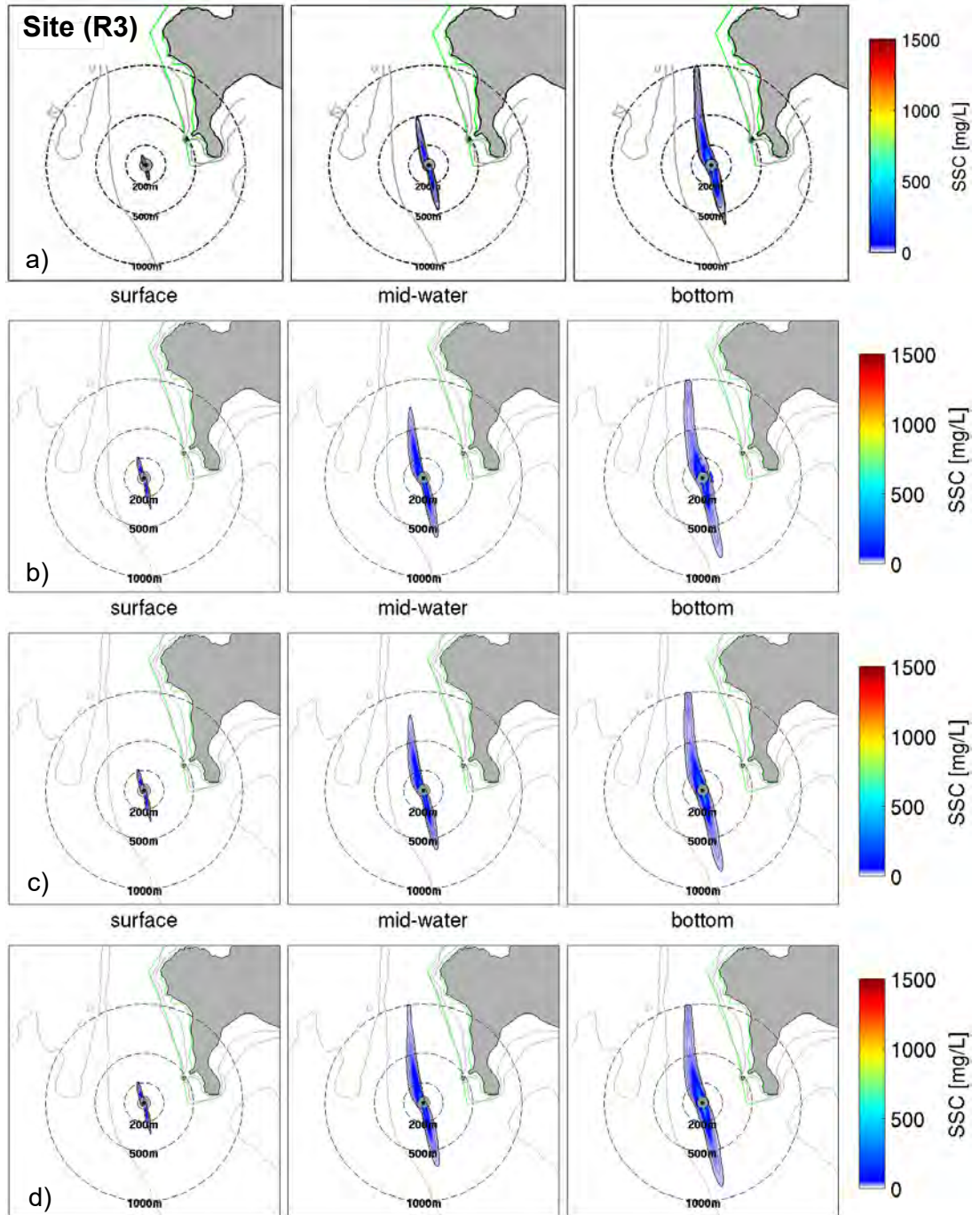
Probabilistic SSC plumes during overflow phase (large trailing suction hopper dredger, TSHD) at site R1 at three levels of the water column for a 79 min period for four model configurations (a, b, c, d) described in the previous table.



Probabilistic SSC plumes during overflow phase (large trailing suction hopper dredger, TSHD) at site R2 at three levels of the water column for a 79 min period for four model configurations (a, b, c, d) described in the previous table.



Probabilistic SSC plumes during overflow phase (large trailing suction hopper dredger, TSHD) at site R3 at three levels of the water column for a 79 min period for four model configurations (a, b, c, d) described in the previous table.





**CRUDE SHIPPING PROJECT**

**PROPOSED DEEPENING AND REALIGNING  
OF THE WHANGAREI HARBOUR ENTRANCE  
AND APPROACHES**

**VOLUME THREE:**

**ANNEXURE TWO (c) TO ANNEXURE TWO (d)**

---

Prepared for:

**ChanceryGreen on behalf of the New Zealand Refinery Company Limited**

**August 2017**

Prepared by:

**Ryder**

---

Crude Shipping Project

**Proposed Deepening and Realigning of the Whangarei Harbour Entrance and Approaches**

**Prepared for:** New Zealand Refining Company Limited

**Prepared by:** Gavin Kemble, *Managing Director and Environmental Planner*  
Cole Burmester, *Associate and Environmental Planner*  
Myaan Bengosi, *Environmental Planner*

**Date Finalised:** August 2017

## **Annexure Two: Technical Reports**

- c) Dredging and Disposal Options – Synthesis Report – Consultation Draft. T & T. Richard Reinen-Hamill. Dated July 2017**
- d) Crude Shipping Project – Coastal Processes Assessment. T & T. Richard Reinen-Hamill. Dated July 2017**



## **Annexure Two: Technical Reports**

**c) Dredging and Disposal Options – Synthesis Report – Consultation  
Draft. T & T. Richard Reinen-Hamill. Dated July 2017**





## Crude Shipping Project

Dredging and Disposal Options -  
Synthesis Report

Prepared for  
ChanceryGreen for Refining NZ

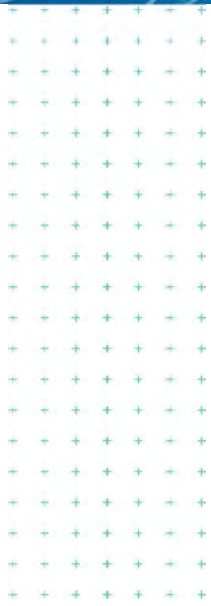
Prepared by  
Tonkin & Taylor Ltd

**Date**

July 2017

**Job Number**

30488.DDO.v9



*Exceptional thinking together*

[www.tonkintaylor.co.nz](http://www.tonkintaylor.co.nz)

Distribution:

ChanceryGreen for Refining NZ

Tonkin & Taylor Ltd (FILE)

PDF copy

1 copy

## Table of contents

1	Introduction	1
1.1	Background	1
1.2	Report layout	2
2	Project description	4
2.1	Channel alignment and dimensions	4
2.1.1	Capital dredging	5
2.1.2	Maintenance dredging	5
2.2	Marine disposal areas	7
3	Physical characteristics of the dredge and disposal area	9
3.1	Materials to be dredged in the entrance channel	9
3.2	Seabed characteristics at the disposal areas	9
3.2.1	Area 3-2	9
3.2.2	Area 1-2	11
4	Meteorological and sea-state conditions	13
5	Dredging equipment selection and dredging methods	14
5.1	Dredge equipment	14
5.2	Dredging cycle	14
5.2.1	TSHD discharging to marine disposal areas	14
5.2.2	BHD	15
5.2.3	CSD	16
5.2.4	Support vessels for the dredging operation	16
6	Environmental considerations	17
6.1	Turbidity	17
6.2	Spills and emissions	17
6.3	Noise	17
7	Applicability	18
8	References	19

Appendix A : Royal HaskoningDHV Technical memos

Appendix B : Shipping channel – concept design report prepared by Royal HaskoningDHV

Appendix C : Memo on side slope stability assessment (T+T)

## Executive summary

Refining NZ is proposing to dredge the entrance to Whangarei Harbour to enable Suezmax ships - which currently visit the Marsden Point Refinery partially loaded - to carry greater loads while safely transiting to and from the Refinery. They have assembled an expert team to characterise the existing environment, identify possible dredged channel configurations, dredge methodologies and disposal options and then to consider the potential effects of these various options.

This report summarises key aspects on the dredging and disposal methodologies for the material required be dredged from the entrance channel. This assessment supports the Assessment of Environmental Effects and is part of a suite of technical reports that assess the actual and potential effects of the applications.

### Setting

The refinery is situated on Marsden Point at the entrance to Whangarei Harbour which is located at the northern end of Bream Bay. The harbour is accessed through a natural tidal inlet which varies from 15 to 32 m at its deepest point.

The harbour is relatively shallow due to extensive intertidal flats. The harbour is accessed through a relatively narrow tidal inlet which is around 680 m wide and 32 m at its deepest point. The inlet is bounded by Tertiary volcanic rocks on the northern side and a Holocene prograded sandy barrier spit on the southern side, which forms Marsden Point. Several bays indent the northern shoreline of the lower harbour, the largest of which is Parua Bay. The inlet channel separates a large ebb tide delta that extends seaward to around the 20 m depth contour. Mair Bank is situated on the northern side of the channel, largely within the intertidal and subaerial portion of the southern ebb tide delta. Snake Bank and McDonald Bank are the two main flood-tidal deltas located within the harbour inlet embayment.

The existing channel can be divided into three areas, the inner (including the berthing jetty pocket to the eastern extent of Mair Bank), the middle (between the end of Mair Bank and the southern end of Home Point) and the outer channel.

### Proposed channel

The preferred channel alignment has evolved through the design process taking into account navigational safety, potential changes to the hydrodynamic system and environmental considerations and will provide for unrestricted design vessel access except in extreme wave climate or swell events (i.e. accessible for 98% of the time). The channel avoids rock substrates so dredging methods such as blasting are not required.

The proposed channel depths vary from 19.0 m below Chart Datum (CD) at the entrance to the channel, to 16.5 m below CD at the berth area with -17.9 m CD at the berth pocket. These depths include a sedimentation allowance of 0.5 m for the mid and outer parts of the channel, 0.3 m for the inner part of the channel and 0.37 m for the berthing pocket.

### Capital and maintenance dredging material and volumes

Dredging of the channel is within the predominantly fine to medium sand layer that overlies predominantly clay and silts and bedrock situated well below the base of the channel and are not affected by the proposal. The main areas for dredging are the outer channel and the berth pocket. In the remaining areas only targeted dredging is required. The estimated capital dredge volume is up to 3,700,000 m<sup>3</sup> for the preferred channel configuration and the area of the channel extent is 1.44 km<sup>2</sup>.

Relatively low rates of sedimentation is expected to occur within areas of the dredged channel with annual average sedimentation rates expected to be between 56,000 and 122,000 m<sup>3</sup>/yr.

Maintenance dredging may need to occur every 2 to 5 years in the berth pocket area to maintain navigable draft around the jetty dolphins as well as at localised areas along the channel such as adjacent to Busby Head and at sections of the right hand side of the channel in the mid-section. Assuming uniform distribution of sedimentation within the outer section, the 0.5 m sedimentation allowance could be reached in the order of 5 to 20 years of the completion of the capital dredging. Maintenance dredging will be placed in either of the marine disposal areas, or be used for beneficial land based disposal.

### Proposed marine disposal areas

Refining NZ seeks some operational flexibility in the volume of material to be disposed at specific locations. Two marine disposal areas are proposed. Area 3-2 is situated approximately 45 m below Chart Datum to the south east of the channel within Bream Bay and Area 1-2 is situated on the outer part of the ebb tide shoal. Area 1-2 is included to provide a means of maintaining a sediment transport pathway to the coast. Accordingly, it is anticipated that up to 97.5% of capital dredging is to be placed in Area 3-2, between 2.5% and 5% is placed in Area 1-2 with the option to dispose of some proportion of the dredged material to land (subject to separately obtaining any authorisations for that disposal, if required). Flexibility is also sought in respect of maintenance dredging, with the ability sought to place dredged material either within Area 3-2 or Area 1-2, or to land (again subject to separately obtaining any necessary authorisations).

Area 3-2 has been conservatively sized to enable all capital and maintenance dredging to be placed within the area for the duration of the maximum consent period allowed (35 years) without having adverse effects either on the surrounding ecology or the hydrodynamics (tides, waves and currents) operating in this area. Disposal Area 1-2 is sufficiently large to enable different locations to be targeted for the placement of maintenance dredging as required both to retain sand within the littoral system and to promote onshore sediment movement.

### Dredging method

While ultimately the final selection of the dredging methodology proposed will be made by the dredging companies tendering for the campaign, based on a combination of factors it is likely that a small to medium sized Trailing Suction Hopper Dredger (TSHD) will be used for the majority of the dredging campaign possibly augmented with a backhoe dredger (BHD) with an associated barge or a Cutter Suction Dredge (CSD) for the localised dredging work in the vicinity of the berth pocket and the upper channel dredging. The size of the TSHD vessel to complete this work based on hopper capacity is likely to be between 1,800 m<sup>3</sup> and 8,500 m<sup>3</sup>. These are characterised as small to medium dredge vessels.

The capital dredge campaign will depend on the vessel size and the location where dredged sediment will be placed. However, taking into account the range of likely possibilities, the capital dredge programme is likely to last up to 6 months. During the capital dredge campaign the main dredge vessels will be accompanied by smaller launches for completing survey work and transferring crew. A tug may also be utilised for towing small barges of sand from the BHD operation.

Maintenance dredging is likely to require similar dredging plant although the vessel size may well be smaller than that used for the capital dredging and have a shorter programme.

# 1 Introduction

Refining NZ (RNZ) refinery is situated on Marsden Point at the entrance to Whangarei Harbour which is located at the northern end of Bream Bay. The harbour is accessed through a natural tidal inlet which varies from 15 to 32 m at its deepest point.

RNZ is investigating options of dredging the entrance to their site at Marsden Point to allow existing vessels to have larger cargoes while safely transiting to and from the Marsden Point refinery. They have assembled an expert team to characterise the existing environment, identify possible dredged channel configurations, dredge methodologies and disposal options and then to consider the potential effects of these various options.

## 1.1 Background

Crude shipments are currently brought to site via smaller fully loaded Aframax ships and larger, partially loaded, Suezmax ships. Suezmax ships are partially loaded in order to clear the shallower parts of the tidal inlet. Refining NZ are looking to increase the amount loaded to reduce shipping costs and improve efficiency. This will help sustain Refining NZ's overall competitiveness with overseas refineries and long term sustainability of its business. Preliminary option studies that considered alternative approaches such as ship to ship transfer, a deep water Single Point Mooring system and deepening of the access channel have indicated the preferred option is to carry out targeted dredging of the channel to enable more fully laden existing Suezmax vessels to reach the terminal (Poten & Partners, 2016).

A comprehensive range of high level studies and investigations have been carried out by the team on dredge channel alternatives to better understand and characterise the existing environment and to identify possible dredge and disposal options. This was followed by more detailed studies, investigations and analysis to refine understanding of how these options would affect the environment and to develop more preferred options.

After consideration of tide and wave conditions, navigation safety and manoeuvrability for a range of possible channel configuration alternatives, three channel options that provided safe all tide and 98% of wave condition access were shortlisted for more detailed assessment. Following that detailed assessment, the preferred option both in terms of navigation safety and overall environmental effects is Option 4-2. This option limits the majority of dredging to the outer reaches seaward of Home Point, with targeted dredging at selected areas in the mid and upper parts of the channel and at the berth.

A similar exercise was used to evaluate potential areas to place the dredged sediments. A range of adjacent and distant deep-water (greater than 60 m water depth), intermediate water depth (30 to 60 m) and shallower water depth disposal areas were considered together with land based disposal options. Two disposal options are preferred, being a site at around 45 m water depth (Area 3-2), and the placement of sediment on the ebb delta (Area 1-2) in water depth of between 7 and 15 m below Chart Datum. It is anticipated that up to 97.5% of capital dredging is to be placed in Area 3-2, between 2.5% and 5% is placed in Area 1-2 with some dredging disposed of to land. Maintenance dredging may be placed in either Area 3-2, Area 1-2 or to land, depending on the requirements and results on monitoring.

A plan of the area dredged and the location of the marine disposal areas is included in Drawing 01. This drawing includes areas of significance in the vicinity of the work areas.

## 1.2 Report layout

As part of the technical studies being carried out, Chancery Green (on behalf of Refining NZ) commissioned Tonkin + Taylor Ltd (T+T) to report on the dredging and disposal methodologies for the material required to be dredged from the entrance channel (refer Drawing 30488-01). This report summarises key aspects from the various technical reports prepared by the expert team, and in particular the following which are included as appendices to this synthesis report:

- RHDHV (2016a) Dredging methodology assessment – technical memo. Ref. M&APA102N006D04; prepared by Royal HaskoningDHV for Chancery Green on behalf of Refining NZ, 10 August 2016 (included as Appendix A).
- RHDHV (2016c) Dredging control measures – technical memo. Ref. M&APA1028N008D03; prepared by Royal HaskoningDHV for Chancery Green on behalf of Refining NZ, 2 December 2016 (included as Appendix A).
- RHDHV (2016b) Shipping channel – concept design report. Ref. M&APA1-28R002D05; prepared by Royal HaskoningDHV for Chancery Green on behalf of Refining NZ, 5 June 2016 (included as Appendix B).
- T+T (2016) Memo on side slope stability assessment, 3 August 2016 (Appendix C).



## 2 Project description

### 2.1 Channel alignment and dimensions

The preferred channel alignment has evolved through the design process taking into account navigational safety, potential changes to the hydrodynamic system and environmental considerations and will provide for unrestricted design vessel access except in extreme wave climate or swell events. The process included avoiding potentially rocky outcrops at Home Point to exclude the requirement of blasting or clearing of rock outcrops. The technical assessments are summarised in RHDHV (2016a and 2016b).

The key characteristics of the channel are:

Alignment – refer Drawing 01 and Drawing PA1028/MA/1123 rev A in Appendix A.

Widths (excluding batter slopes) – base channel widths have been developed using PIANC guidelines (RHDHV, 2016b, Appendix B) and vary from 210 m to 280 m, with the channels widening at the bends in the channel.

Depths – the depths vary from 19.0 m below Chart Datum (CD) at the entrance to the channel to 16.5 m below CD at the berth area and 17.9 m below CD at the berth pocket (refer Figure 2-1 and Drawing PA1028/MA/1123 rev A in Appendix B). These depths include a sedimentation allowance of 0.5 m (for the mid and outer parts of the channel) and 0.3 m (for the inner part of the channel).

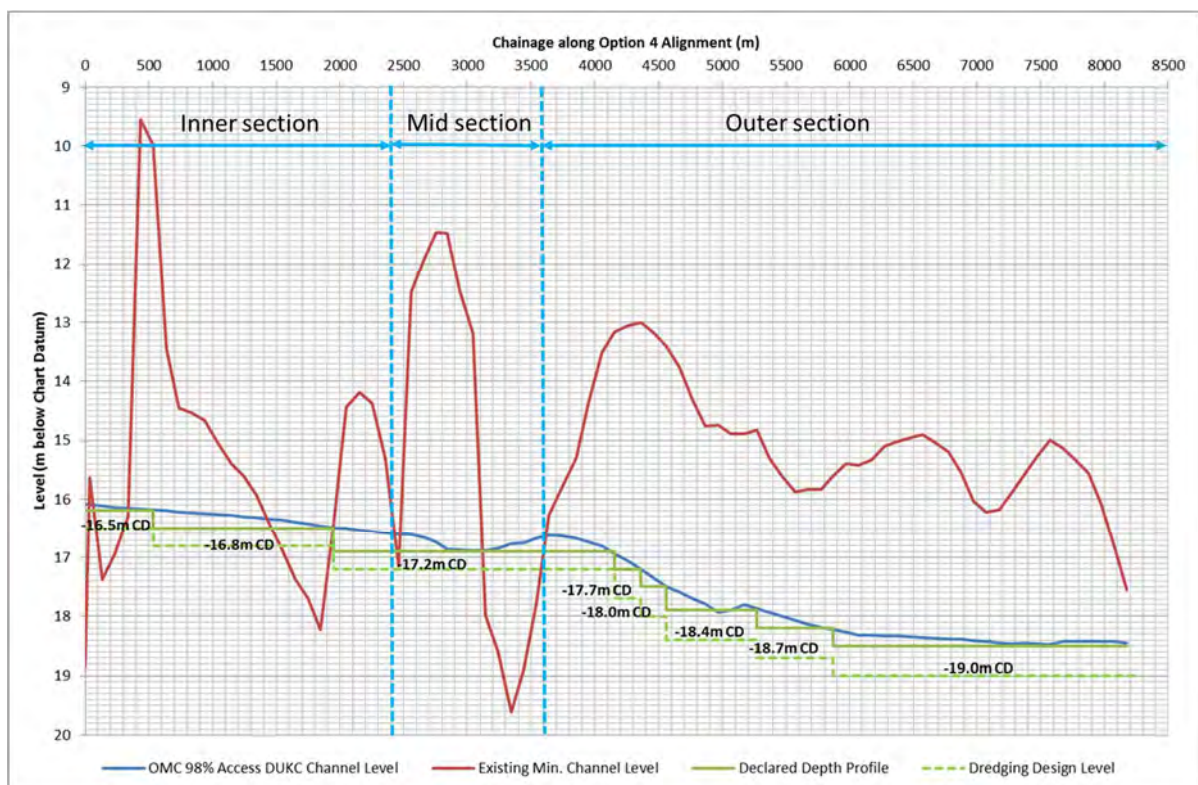


Figure 2-1 Channel design depths for Option 4-2 (Source: RHDHV, 2016b)

Side slopes – 1V:4H for all channel slopes and a stepped slope at the berth area with a bench at 4.2 m CD (refer T+T Technical Memo, Appendix C).

### 2.1.1 Capital dredging

The estimated capital dredge volume, inclusive of 0.3 m over-dredge allowance is 3,620,200 m<sup>3</sup> for the preferred channel configuration (refer Table 2-1). It is noted that these are maximum volumes for the maximum desired channel depth. The main areas for dredging are the outer channel and the berth pocket/dolphin mooring area. In the remaining areas only targeted dredging is required. The total footprint of proposed channel area is 3.9 km<sup>2</sup> and the area of the channel dredging is 1.44 km<sup>2</sup>. The majority of the dredging (more than 95%) occurs below the 15 CD depth contour.

Table 2-1 Capital dredge volumes with and without over dredge allowance (Source: RHK\_DHV Drawing PA1028/MA/1123 rev C)

Location	Dredge volume to design level (m <sup>3</sup> )	Dredge volume including over-dredge (m <sup>3</sup> )
Inner section - Beth pocket (Area A1)	132,000	153,000
Inner section - Dolphin (Area 2)		
Inner section - Turning circle (Area B)	294,400	397,500
Inner Section - Port Buoy 14 A (Area C)	34,900	43,400
Mid section - Starboard Buoy No. 11 (Area D)	49,900	57,200
Outer channel from Port Buoy No. 10 to No. 6 (Area E)	750,700	851,500
Outer channel from Port Buoy No. 6 to end of channel (Area F)	1,900,500	2,117,600
TOTAL	3,162,400	3,620,200

### 2.1.2 Maintenance dredging

Maintenance dredging is to be expected, particularly within the first few years following the capital dredging exercise as side slopes settle, with lower sedimentation rates occurring after this initial period. The main areas for maintenance dredging to occur is in the vicinity of the berth pocket due to sand transported from the ebb delta over Mair Bank and at the outer section of the channel where the majority of capital dredging has occurred. In the outer channel average annual sedimentation rates are predicted to be within the range of 42,000 to 95,000 m<sup>3</sup> per annum (rounded up to 50,000 to 100,000 m<sup>3</sup> per annum to take into account uncertainty, MSL (2016)). This sediment could be distributed reasonably evenly along the channel although slightly greater deposition was observed in the model along the northern edge of the channel. In the berth pocket the volume of sedimentation to manage is based on sand transported over Mair Bank from the southern part of the ebb tide delta (expected to be around 8,000 to 15,000 m<sup>3</sup> per annum along the entire bank and of this volume, between 3,000 to 6,000 m<sup>3</sup> per annum within the berth pocket and dolphin area). There will also be sediment deposition along the tidal channel due to slight reductions in tidal flows at certain locations (estimated to be between 6,000 and 12,000 m<sup>3</sup> per annum). Therefore, the average annual rate of sedimentation is assessed to be between 56,000 and 122,000 m<sup>3</sup> per annum (i.e. between 1.5 and 3.4% of the capital dredge volume) with the main areas of focus expected to be the berth pocket and the outer section of the channel.

A breakdown of the likely range of sedimentation for each of the areas is set out in Table 2-2 and described in the sections below.

Table 2-2 Estimate of range of possible annual sedimentation rates

Area	Location	Annual sedimentation rate (m <sup>3</sup> /year)	
		Lower bound	Upper bound
A	Berth Pocket (A1)	600	1,200
	Dolphin Area (A2)	2,400	4,800
B	Turning circle	3,000	6,000
C	Port Buoy 14 A – Calliope Bank	3,000	6,000
D	Starboard Buoy No. 11 – Ebb tide shoal	5,000	9,000
E	Outer Channel - Port Buoy 10 to 6	7,500	20,000
F	Outer Channel - Port Buoy 6 to end	34,500	75,000
	TOTAL	56,000	122,000

#### 2.1.2.1 Berth pocket and dolphin area (Area A)

This area is currently experiencing wave driven overwash of sand from the ebb tide delta. The proposed dredging is unlikely to change the overwash process or volume, but will change where the overwashed sand will settle out. We expect it will result in accretion occurring within the dredged area both due to lateral movement of sand moving over Mair Bank and down the cut slope as well as from sedimentation of the shelf around the dolphins at -4.3 m CD and the berth pocket due to a slight reduction in tidal currents. The recent dredging around the mooring dolphin will help refine ongoing maintenance dredging, but annual infill volumes of around 3,000 m<sup>3</sup> to 6,000 m<sup>3</sup> has been estimated based on the analysis of historic data and it is anticipated that as much as 80% of the annual sedimentation will be by overwash that will largely be within the shelf around the dolphins (Area A2) with the remaining volume by tidal current driven transport along the channel affecting the berth pocket (Area A1).

This area is likely to require ongoing maintenance dredging every two to five years. The dolphin area and the shallower parts of the channel slope could be done using a smaller barge mounted hydraulic excavator although the deeper parts of the channel will require different plant. However, if dredging within the dolphin area is effective there is possible that reduced accumulation will occur in the Berth Pocket, but still this area will experience sedimentation due to sediment transport along the channel. The dolphin area may be require dredging on a two yearly basis over the initial period (assumed to be 6 years), but the frequency of dredging may be reduced to three yearly over time. It is anticipated that the berth pocket will also require two yearly dredging over the first six years, but that maintenance dredging may reduce to five yearly thereafter.

#### 2.1.2.2 Turning circle shoal (Area B)

There is a relatively small area of the channel floor that appears to be formed from a lag deposit of coarser sediment and shell downstream of the narrowest part of the channel. Sedimentation of this area is therefore due to the reduction in tidal velocity causing larger particles to settle out. This is illustrated by modelling of a range of fair weather and combined storm and fair weather events and the relatively small difference in accretion between these two events. Figure 7.30 to 7.32 of MSL, 2017 show accretion rates in the order of 10 to 15 cm suggesting ongoing maintenance dredging of

this entire area every 2 years in the short term (assumed 6 years from the initial dredge) reducing to 5 yearly over the longer term. Due to the depth and location of the sedimentation, this is likely to require a TSHD or cutter suction dredge.

#### 2.1.2.3 Localised corners in Area C and D

The modelling carried out by MSL show the corner area adjacent to Starboard Buoy No. 11 (Area C) to have very minor levels of sedimentation and erosion. It is likely that this location may adjust over the first six years. However, it is anticipated the entire area will require some maintenance dredging with dredging frequencies of every two years, to frequencies in the order of 5 yearly after this initial adjustment period.

The edge of the channel in the vicinity of Port Buoy 14A and 12C (Area D) is more dynamic as a result of being part of the ebb tide shoal with overwash and along channel edge transport. Dredging of this entire area is likely to be ongoing every 2 years for the first six years and reduce to a 3 yearly frequency thereafter.

#### 2.1.2.4 Outer channel from Port Buoy No. 10 to No. 6 (Area E)

Modelling carried out by MSL (2017) show that sedimentation is more likely along the northern half of the channel and the a 100 m wide strip along the north-eastern edge of the channel and lower part of the side slope (i.e. 75 m of the channel floor and 25 m of the lower side slope) may need to be dredged 2 yearly. This means around 40% to 80% of the optimistic dredge volume (i.e. around 4,000 to 8,000 m<sup>3</sup>) could be required every 2 years for the first six years. After this initial period, the remaining channel floor may require dredging, but with larger volumes every five years.

#### 2.1.2.5 Outer channel from Port Buoy No. 6 to the end of the channel (Area F)

Modelling by MSL (2017) show this area to have more uniform sedimentation across the channel floor but still with slightly greater levels of sedimentation along the north-eastern edge. A similar 100 m wide strip as described in the previous section may require 2 yearly dredging over the first size year period (i.e. a smaller volume of around 8,000 m<sup>3</sup> to 16,000 m<sup>3</sup>), with the full channel area dredged every 5 to 10 years.

## 2.2 Marine disposal areas

Marine disposal areas are shown on Drawing 30488-01. Flexibility in the volume of material to be disposed at specific locations is sought in this application. It is anticipated that up to 97.5% of capital dredging is to be placed in Area 3-2, between 2.5% and 5% is placed in Area 1-2 with some dredging disposed of to land. These volumes are similar to the volume dredged above the 10 m depth contour. Maintenance dredging may be placed in either Area 3-2, Area 1-2 or to land, depending on the requirements and results on monitoring.

Area 3-2 has been conservatively sized to provide for 100% of all capital and maintenance dredging. The area of placement in Area 3-2, is 2.5 km<sup>2</sup>, although a maximum area of 5.75 km<sup>2</sup> which defines the outer boundary of where placed sediment may settle over time. Area 3-2 is situated 45 m below Chart Datum to the south east of the channel.

If the sediment is uniformly distributed, the average height of the placement mound after the capital dredging has occurred will be approximately 1.5 m. However, it is possible that targeted disposal could occur within the larger disposal area resulting in maximum placement heights for both capital and maintenance dredging of not more than 4 m. That equates to less than 9% of the water depth.

The maximum height is conservative and based on the following assumptions:

- the upper rate of predicted annual sedimentation;
- all maintenance dredging being placed in this area; and
- no settlement or loss of material from this area occurs over time.

Some sediment (2.5 to 5%) is proposed to be placed in the nearshore known as Area 1-2. Area 1-2 is a 2.5 km<sup>2</sup> area of seabed situated on the southern end of the ebb tidal delta in water depth of between 7 and 15 m Chart Datum. Area 1-2 is designed to enable placed sediment to be slowly transported landward during higher energy wave events to maintain sediment volumes on the ebb delta. It is also sufficiently large to enable different locations to be targeted for the placement of maintenance dredging. If the dredged sediment is placed uniformly in this area the average depth would be around 0.06 m. However, it is more likely that there would be a smaller area targeted within this larger area during each dredge campaign, with average placement depths of around 0.6 m (i.e. covering an area of around 250,000 m<sup>2</sup> or 10% of the total placement area).

Both marine disposal areas comprise sand of a similar composition to the channel area to be dredged. Land based locations may also be used to dispose of some of the capital dredging although this will only be undertaken where there is a demand by others, and they have the necessary environmental authorisations (including resource consents) in place to enable the use.

### 3 Physical characteristics of the dredge and disposal area

A series of investigations have been carried out as part of this study to augment historic investigations of the channel area and its environs (RHDHV, 2016a).

#### 3.1 Materials to be dredged in the entrance channel

Dredging of the channel is within the predominantly fine to medium sand layer that overlies predominantly clay and silts and bedrock situated well below the base of the channel. Based on an analysis of sediment chemistry the dredged sediment is clean with most potential contaminant levels either below detection or within the lower range of acceptable guidance criteria (Coffey, 2016). Table 3-1 shows the volumes of sediment to be dredged and Table 3-2 shows the proportion of silts and clays based on total volumes for each location based on the anticipated volumes to be dredged for the preferred access channel configuration.

Table 3-1 Volume of material (cubic metres, m<sup>3</sup>) to be dredged by average sediment classification

Location	Clays	Silt	Fine Sand	Medium Sand	Coarse Sand	Gravels (shells)	Total
Berth pocket	200	3,000	8,000	49,000	3,000	8,000	81,200
Inner channel	4,900	24,000	78,000	274,000	29,000	75,000	484,900
Mid channel	200	2,000	9,000	64,000	10,000	15,000	100,200
Outer channel (3.5 to 5.5 km)	3,100	17,000	36,000	643,000	185,000	144,000	1,028,100
Outer channel (5.5km to end)	1,900	56,000	327,000	1,227,000	104,000	227,000	1,942,900
<i>Total</i>	<i>10,300</i>	<i>102,000</i>	<i>468,000</i>	<i>2,257,000</i>	<i>331,000</i>	<i>469,000</i>	<i>3,637,300</i>

Table 3-2 Percentage of silt and clays for each dredged area based on total volume

Location	Percentage of silt and clays
Berth pocket	3.9%
Inner channel	6.0%
Mid channel	2.2%
Outer channel (3.5 to 5.5 km)	2.0%
Outer channel (5.5km to end)	3.0%

#### 3.2 Seabed characteristics at the disposal areas

##### 3.2.1 Area 3-2

Area 3-2 is situated in 45 m water depth to the south-east of the channel (refer Drawing 30488 01 and Figure 3-1). The seabed in this area comprises predominantly fine to medium sands with some areas of silt and shell deposits (refer). Figure 3-2 shows a comparison of the sediment gradings within the dredged channel and in the vicinity of Area 3-2 showing that the sediments dredged within the channel are very similar to the sediments on the seabed of Area 3-2.

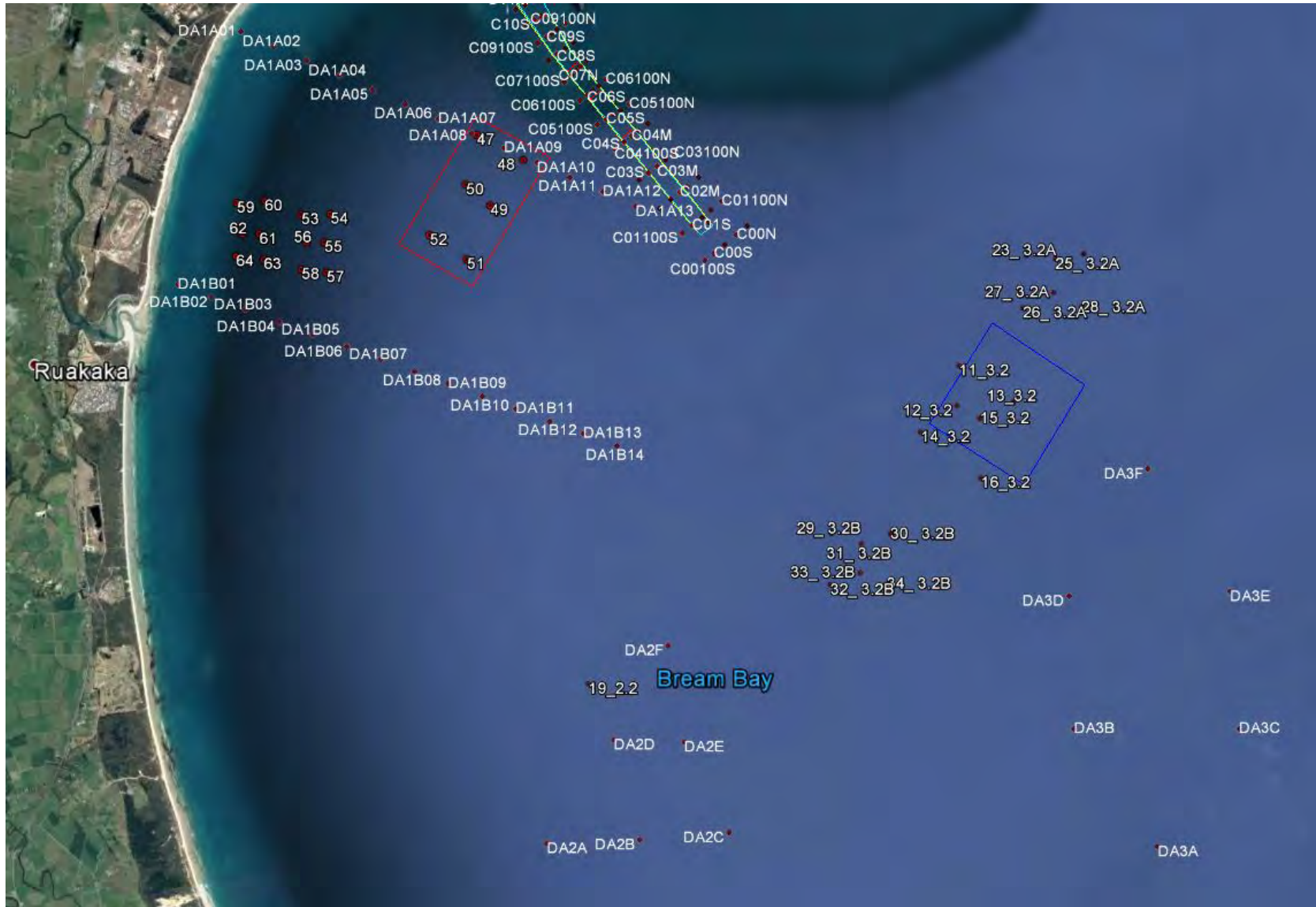


Figure 3-1 Sediment sampling within Bream Bay with the Site 1-2 (red box) and Site 3-2 (blue box) showing proposed disposal areas

Table 3-3 Sediment grading (percent passing) in the vicinity of Area 3-2

Site ID	Clays	Silt	Fine Sand	Medium Sand	Coarse Sand	Gravels (shells)
	<0.002 mm	0.063	.30 mm	.63 mm	2 mm	25 mm
11-3.2	3%	14%	72%	87.34%	91%	100%
12-3.2	6%	27%	62%	81%	93%	100%
13-3.2	6%	8%	13%	40%	78%	100%
14-3.2	0%	1%	10%	54%	97%	100%
15-3.2	0%	6%	22%	65%	95%	100%
16-3.2	0%	2%	12%	57%	89%	100%
Minimum	0	1%	10%	40	78	100%
Average	3	10%	32	64	91	100%
Maximum	6	27%	72	87	97	100%

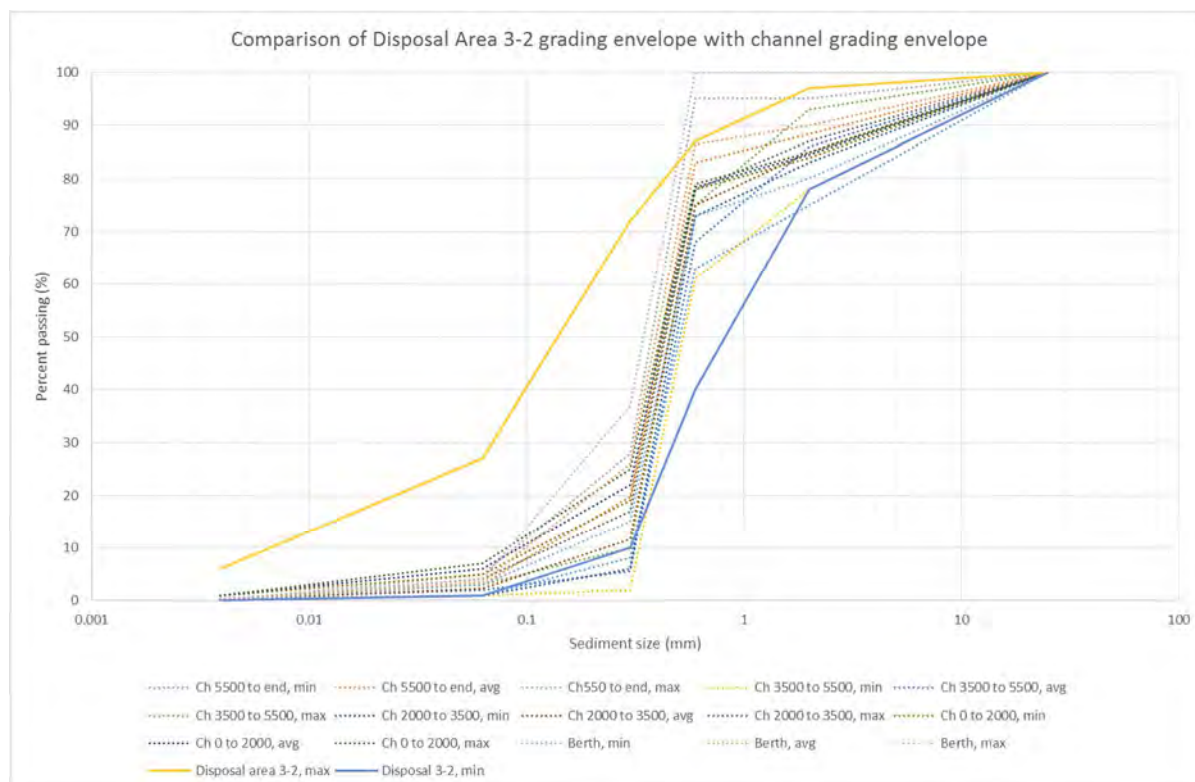


Figure 3-2 Comparison of Area 3-2 grading envelope with channel grading showing channel sediments similarly graded to the seabed sediment in Area 3-2

### 3.2.2 Area 1-2

Area 1-2 is situated on the south-eastern edge of the ebb delta (refer Drawing 30488 01 and Figure 3-1) comprises predominantly fine to medium sands with no significant portions of clays and silts (refer Table 3-4). This is to be expected due to the open coast wave climate that acts on this location. Figure 3-3 shows a comparison of the sediment gradings within the dredged channel and in the vicinity of disposal area 1-2. It shows that the dredged material is typically slightly coarser

with a higher proportion of shell than the Area 1-2 and less fine sands. This is optimal in terms of potential issues of turbidity during placement (i.e. less fines) and provides a good match for the beach sands along the coastal edge which tends to be coarser than the sands on the ebb tide delta.

Table 3-4 Sediment grading (percent passing) in the vicinity of Area 1-2

Site ID	Clays	Silt	Fine Sand	Medium Sand	Coarse Sand	Gravels (shells)
	<0.002 mm	0.063	.30 mm	.63 mm	2 mm	25 mm
DA1A04	0.0%	3.2%	57.7%	99.1%	100.0%	100%
DA1A05	0.0%	3.0%	56.7%	98.9%	100.0%	100%
DA1A06	0.0%	4.0%	59.8%	99.1%	100.0%	100%
DA1A07	0.0%	3.3%	56.1%	98.6%	100.0%	100%
DA1A08	0.0%	4.2%	60.1%	99.1%	100.0%	100%
DA1A09	0.0%	4.5%	52.7%	95.9%	100.0%	100%
Minimum	0.0%	3.0%	52.7%	95.9%	100.0%	100.0%
Average	0.0%	3.7%	57.2%	98.5%	100.0%	100.0%
Maximum	0.0%	4.5%	60.1%	99.1%	100.0%	100.0%

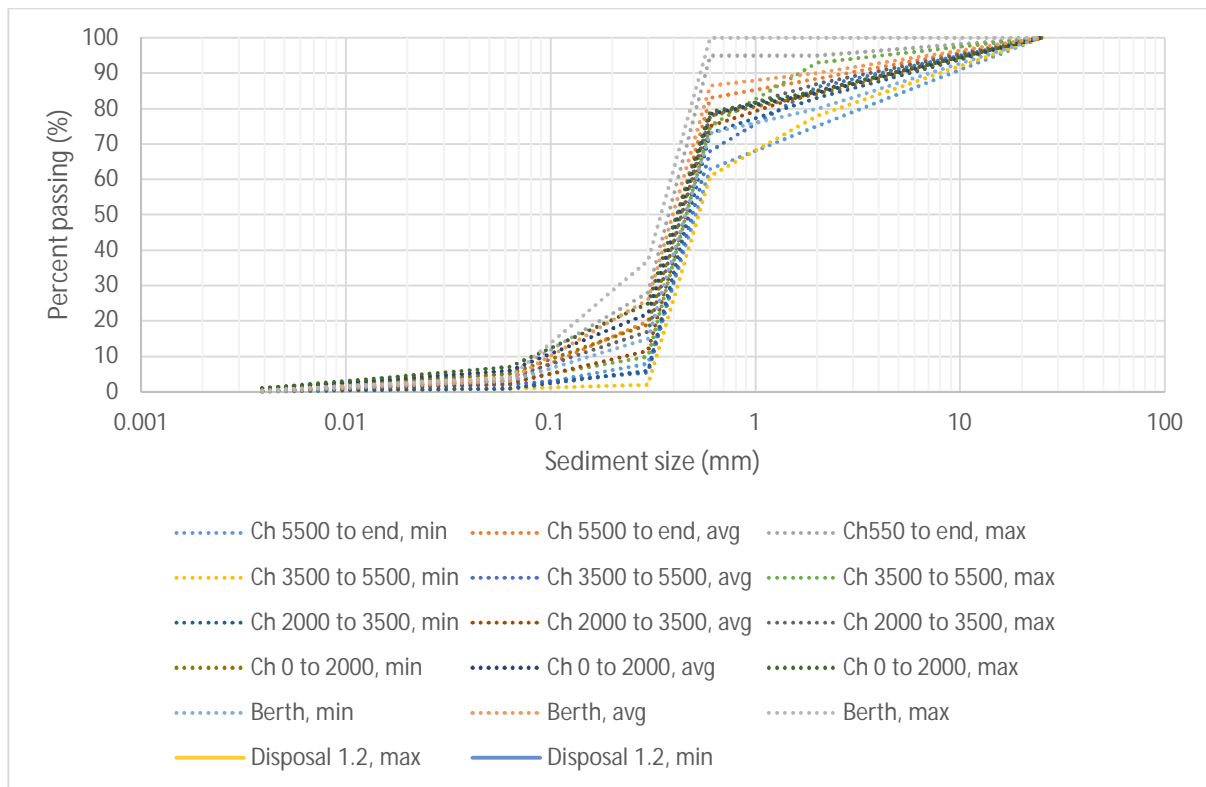


Figure 3-3 Comparison of sediment gradings within the dredge channel area and the sediments gradings in the vicinity of A 1 -2 showing the channel sediments to be slightly coarser and with more shell content

## 4 Meteorological and sea-state conditions

Meteorological conditions for this area have been assessed by MetOcean Solutions Ltd (2017) and summarised by RHDHV (refer technical memo, Appendix A). The local environment is characterised by relatively low wind speeds, low to moderate wave heights and moderate tidal currents within the confines of the channel.

Typically calm conditions exist (winds less than 2 m/s) more than 90% of the time and moderate to low wave climate (sea and swell wave heights less than 1 m) occur for more than 90% of the time at the entrance to the channel. Within the mid and upper parts of the channel wave heights are less than 0.6 m 99% of the time. Peak tidal velocities reach 2 to 2.5 knots over the length of the channel with localised areas receiving velocities of up to 3 knots.

## 5 Dredging equipment selection and dredging methods

### 5.1 Dredge equipment

Royal HaskoningDHV describe a range of possible dredging equipment and their characteristics and control measures (refer technical memos in Appendix A). While the final selection of the dredging methodology will be made by the dredging company commissioned for the campaign, it is expected that a Trailing Suction Hopper Dredger (TSHD) do the majority of the dredging campaign, particularly for the outer channel area, with possibly augmented with a backhoe dredger (BHD) or a Cutter Suction Dredge (CSD) for the localised dredging work in the vicinity of the berth pocket and the inner/mid channel dredging, with the BHD likely to be the preferred option for the jetty pocket due to the vicinity of marine structures and the greater control that can be applied with the BHD.

The size of the TSHD vessel to complete this work based on hopper capacity is likely to be between 1,800 m<sup>3</sup> and 8,500 m<sup>3</sup>. These are characterised as small to medium dredge vessels and they would be fitted with green valves to reduce air content in the overflow discharge pipe which reduces turbidity at the water surface and increases the speed of settlement to the seabed (RHDHV, 2016). A larger TSHD (i.e. around 11,000 m<sup>3</sup>) is possible if one was already undertaking dredging in New Zealand, but is unlikely to be mobilised specifically for this project due to high mobilization costs.

Based on the meteorological conditions set out in the previous section, it is likely that the medium TSHD would only be constrained from operation around 1% of the time due to large waves and could operate with all wind and tidal current conditions (RHDHV, 2016a). A small TSHD would have a slightly greater downtime (2%) due to some peak tide conditions. There would be less downtime due to meteorological or hydrodynamic conditions with any dredge type in the mid and inner channel area.

### 5.2 Dredging cycle

#### 5.2.1 TSHD discharging to marine disposal areas

A production cycle for a TSHD comprises four consecutive operations:

- Loading
- Sailing with full load
- Unloading
- Sailing empty after discharge.

The base operational condition for this area is for 24 hours per day seven days per week.

##### 5.2.1.1 Loading

The time required to fill the hopper and the resulting volume of sediment in the hopper depends on the sediment parameters and dredge depth. To optimise the dredging cycle it is preferable to work with controlled overflow. This means that the TSHD will continue dredging with excess water flowing out of the hopper back to the sea via an outlet at the bottom of the hull (the keel). A green valve will be used to reduce air bubbles within the discharge both to reduce the potential for turbidity and to increase the speed of settlement of the dynamic plume.

At this location the presence of predominantly medium and fine sands with low silt contents (less than 6%) both increases the operational efficiency of filling and significantly reduces the extent of turbid plumes during dredging and placement of sediment in the disposal areas.

#### 5.2.1.2 Sailing with full load

When the loading of the vessel is complete the vessel will proceed to the disposal area where its load will be deposited. During sailing the watertight bottom doors of the hopper remain closed. The distance from Busby Point to the centre of Area 3-2 is around 7 km and it is around 4.5 km to the berthing jetty. The distance to Area 1-2 is around 3 km (refer Drawing 30488-01).

#### 5.2.1.3 Unloading

When the TSHD reaches the marine disposal area it reduces speed and manoeuvres itself via GPS to the allocated area where the load can be discharged. When the vessel is at the correct location the dredge-master opens the bottom doors and the sediment drops out of the hopper.

If the TSHD it is to take material for land based disposal it would sail to a wharf area (say at North Port) and be unloaded by an onboard slurry pump or by hydraulic excavator.

#### 5.2.1.4 Sailing empty

When the hopper is empty the dredge-master closes the bottom doors. The vessel then sails back to the dredging areas and the cycle repeats until the channel is dredged to the required levels.

#### 5.2.1.5 Production rates

Production times and rates for the range of TSHD have been developed by RHDHV (Appendix B). The cycle time ranges from 110 to 180 minutes resulting in between 55 and 90 operations per week taking into account weather and operational allowance. The total duration for this activity is around 6 months.

### 5.2.2 BHD

The BHD is specifically required for dredging around the berthing area and would not be used for the main dredging activity. The dredged material would either be placed in a barge for marine disposal or taken ashore for land based disposal).

A production cycle for a BHD comprises four consecutive operations:

- Loading to an adjacent barge
- Sailing with full load
- Unloading
- Sailing empty after discharge.

The base operational condition for this area is for works to occur during daylight hours, seven days per week (i.e. around 70 hours per week excluding weather delays but taking into account 30% berth occupancy).

#### 5.2.2.1 Loading

The capacity of this form of dredging depends on the bucket capacity, the water depth and the size of the adjacent barge. Typical bucket capacity ranges from 4 to 11.0 m<sup>3</sup>.

#### 5.2.2.2 Sailing with full load

Due to typically smaller split hull barges being used in this operation (typical barge capacity in the order of 500 m<sup>3</sup> to 1,000 m<sup>3</sup>), sailing time will be slower and operational conditions more limited.

### 5.2.2.3 Remaining cycle

The remaining cycle is similar to that described for the TSHD.

### 5.2.2.4 Production rates

Production times and rates for the BHD have been developed by RHDHV (Appendix B). In general backhoe dredgers have efficiencies of between 60 and 65% without weather delays. This gives dredging rates of around 300 to 500 m<sup>3</sup>/hr and two barge sailings per day (i.e. up to 2,000 m<sup>3</sup>/day). Based on this production rate it would take 2 to 3 months to complete the dredging in the berth pocket area.

## 5.2.3 CSD

A CSD can discharge into a barge moored adjacent to the works or through a discharge pipeline that transports the sediment as a slurry to the proposed disposal area. It is less efficient than a TSHD in channel dredging as its position needs to be fixed. Therefore it is only likely to be considered for the dredging around the berthing pocket and in the inner and mid-channel areas, or for maintenance dredging. For the berth pocket dredging the use of the CSD would need to be carefully managed to avoid damage to the marine infrastructure.

### 5.2.3.1 Production cycle

A production cycle for a CSD is the same as the TSHD if a barge is to be used for disposal and the barge is fitted with a green valve. If it uses a discharge pipe it can run continuously, although some down time would be expected if the discharge location needs to be changed. If the CSD is used for the berth pocket area it is likely that a slurry pipeline would be used to discharge the sediment to land.

### 5.2.3.2 Production rates

Production rates for a CSD are less than a TSHD as the vessel has a fixed position while operating. However, it has a greater production rate than that of a BHD.

## 5.2.4 Support vessels for the dredging operation

There are a range of ancillary vessels to support a dredging operation. These include:

- Survey vessels to complete hydrographic survey of the dredged areas. These are typically small craft (around 9 to 11 m in length) and will be present within the vicinity of the project area (channel and disposal areas) for the duration of the project.
- Crew boat for the transfer of crew members and project staff between the dredger and shore. This typically is a small launch 8 to 15 m in length. This could average 4 trips per day.
- A tug for towing the bottom dump barge to the disposal location that could make 2 trips per day.

All support vessels will generally sail within the shipping channel, but due to the shallower draft of these vessels they can go outside the channel if shipping traffic is present.

## 6 Environmental considerations

Environmental impacts, safety concerns and management measures have been summarised in RHDHV's technical memos (Appendix A).

### 6.1 Turbidity

As identified in Table 3-1 the dredge area has a low proportion of silts and clays (on average around 3.1% and a maximum of 6%). This reduces the likelihood of turbidity due to the reasonable fall velocity of sand particles compared to clays and silts.

The technical memo in Appendix A on dredge control measures set out a set of dredging control measures for each type of dredging plant considered and the dredge programme will include appropriate responses should localised areas with higher silt be encountered.

For the TSHD the use of a green valve for the discharge and avoiding shallow areas is the most efficient way of further reducing the risk for turbidity with a TSHD. If these management techniques are insufficient to reduce the risk of turbidity affecting areas of significance, dredging during particular stages of the tide where currents are directed away from sensitive areas is another alternative. However, the results of the plume modelling showed that the plumes did not disperse to the adjacent beaches, sand banks or marine management areas (MetOcean, 2016), therefore all tide dredging is likely to be feasible in all areas.

For the CSD the use of a green valve for the discharge and avoiding shallow areas is the most efficient way of further reducing the risk for turbidity. Improvements can also be made at the cutter head and by limiting the speed of the operation.

For the backhoe operation around the jetty and wharf area the risk of turbidity can be limited by a closed grab or by reducing the speed of the bucket through the water and by careful operation to maintain a level bucket. The volume of solids within the bucket tend to be very high and this, combined with the high proportion of clean sands, limits the potential risk of plume discharge. However, if these management techniques are insufficient to reduce the risk of turbidity affecting areas of significance, dredging during favourable tidal conditions (e.g. on a slack tide; maximum high or low) or on an ebb tide may be an additional management technique where currents are directed away from sensitive areas.

### 6.2 Spills and emissions

Spills and emissions are typically managed through appropriate management plans that should also include emergency management procedures.

### 6.3 Noise

Noise can be created by the excavation process, vessel operation and during the depositing of dredged material. Terrestrial and underwater noise effects have been assessed and are reported separately (Styles Group, 2016a, b).

## 7 Applicability

This report has been prepared for the exclusive use of our client ChanceryGreen for Refining NZ, with respect to the particular brief given to us and it may not be relied upon in other contexts or for any other purpose, or by any person other than our client, without our prior written agreement. We understand and agree that Refining New Zealand will submit this report in support of an application for resource consent and that the consent authority and third parties (stakeholders, submitters and interested parties) will rely on this report for the purpose of assessing that application.

Tonkin & Taylor Ltd

Report prepared by:

Authorised for Tonkin & Taylor Ltd by:

  
.....

Richard Reinen-Hamill  
Coastal Engineer

  
.....

pp Tim Fisher  
Project Director

RRH  
p:\30488\issueddocuments\reporting\2. disposal assessment report\20170210.rrh.dredging summary report.r9.docx

## 8 References

MetOcean Solutions Ltd (2017) Predicted physical environmental effects from channel deepening and offshore disposal, Report ref P0297-02.

Poten & Partners (2016) Crude shipping alternatives, Marsden Point, NZ. Unpublished report prepared for Refining NZ, August 2016.

RHDHV (2016a) Dredging methodology assessment – technical memo. Ref. M&APA102N006D04; prepared by Royal HaskoningDHV for ChanceryGreen on behalf of Refining NZ, 25 May 2016.

RHDHV (2016b) Shipping channel – concept design report. Ref. M&APA1-28R002D05; prepared by Royal HaskoningDHV for ChanceryGreen on behalf of Refining NZ, 1 June 2016.

RHDHV (2016c) Dredging control measures – technical memo. Ref. M&APA1028N008D03; prepared by Royal HaskoningDHV for ChanceryGreen on behalf of Refining NZ, 2 December 2016.

Styles Group (2016a) Whangarei Harbour Entrance and Marsden Point Channel Realignment and Deepening: Underwater Acousting Modelling for the Marine Mammal Impact Assessment, October 2016

Styles Group (2016b) Whangarei Harbour Entrance and Marsden Point Channel Realignment and Deepening: Assessment of Environmental (Airborne) Noise Effects, October 2016

## Appendix A: Royal HaskoningDHV Technical memos

- Dredging methodology assessment
- Dredging control measures

## Technical Memo

**Haskoning Australia PTY Ltd.  
Maritime & Aviation**

To: Refining NZ, Attn: Dave Martin  
 From: Richard Mocke, Justin Cross  
 Date: 11 August 2016  
 Copy: Chancery Green, Attn: Chris Simmons  
 Ryder Consulting, Attn: Gavin Kemble  
 Our reference: M&APA1028N006D06  
 Classification: Open

**Subject: Dredging Methodology Assessment**

### 1 Introduction

Royal HaskoningDHV (RHDHV) is assisting RefiningNZ (RNZ) in regards to channel design, dredging and disposal aspects for the proposed deepening of the Marsden Point channel to facilitate deeper draft vessels to access its wharf facility. To support the environmental assessment process, RHDHV has been commissioned to undertake an assessment of possible dredging methodologies for the proposed capital dredging works and future maintenance dredging campaigns.

This technical note describes the pros and cons of various alternative dredging methodologies for consideration by key stakeholders and will be used as input into a multi-criteria analysis (MCA) which will be prepared by others.

Documents previously prepared for this project, and which have been used as input for this assessment, are presented in Table 1.

*Table 1: Referenced RHDHV reports*

Reference	Dated	Title
<b>RHDHV (2015);</b> 151026_PA1028_RevB	26 Oct 2015	Review of Geophysical Study and Recommended Additional Studies
<b>RHDHV (2016a);</b> PA1028_N_004_v13.01.16	13 Jan 2016	RefiningNZ Dredging – Concept Channel Options, Dredging Footprints and Indicative Cost Estimates
<b>RHDHV (2016b);</b> M&APA1028R002D04	05 Feb 2016	Shipping Channel – Concept Design Report
<b>RHDHV (2016c);</b> M&APA1028N005D01	06 Apr 2016	Dredge Input Parameters for Hydrodynamic Modelling of Plumes – RefiningNZ

*Note: A complete list of references is provided at the end of this report.*

## 2 Site Conditions

### 2.1 Subsurface Conditions

The following site investigations and reports have been used to develop an understanding of the subsurface conditions:

- Boreholes from 2009 Hawthorn Geddes report: *Geotechnical Investigation and Report on Future Dredging at the Entrance to Whangarei Harbour*;
- Boreholes from 1992 Beca Carter Hollings and Ferner report: *Geotechnical Investigation, Proposed Marsden Point Port Development*;
- Boreholes from 1984 Tonkin Taylor report: *New Zealand Refining Company Limited Jetty Dolphin Upgrading Soils Investigations*;
- MES 2015 report: *Marine Geophysical Investigations*; and
- Geotechnical factual report on vibrocore investigation from 2016 Tonkin Taylor report: *Marsden Point Refinery- Crude Freight project*.

Sub-bottom profiling undertaken as part of the marine geophysical investigation (MES, 2015) was used to identify three main subsurface geological layers, those being:

- **Unit 1** – Silty and sandy layer that extends from the seafloor to the top of Unit 2. This unit ranges from 0.0m to 23.3m thick and the base of this unit ranges from -8.3m to -38.9m Chart Datum (CD).
- **Unit 2** – Predominantly clayey and silty layer with complex depositional and erosional features such as infilled palaeochannels. This unit extends from the base of unit 1 to the top of unit 3.
- **Unit 3** – Interpreted as bedrock with the top of this unit being very irregular in level and outcrops in numerous locations. The top of this unit ranges from -4.5m to -61.5m CD.

A total of 26 vibrocores was undertaken in early 2016 (T+T, 2016). Samples were collected for geotechnical laboratory testing and environmental testing. An assessment of the suitability of disposing the dredged material offshore, based on the results of the environmental testing, is being undertaken by others. However, for the purpose of this dredge methodology assessment, it is assumed that the material will be suitable for offshore disposal.

The target depth for each vibrocore was based on the design dredge depth (refer Section 4) plus 0.5m allowance for over-dredge. In the majority of cases, the target depth was achieved (at 20 out of 26 test locations).

A general description of the materials encountered is provided in Table 2.

Table 2: General subsurface conditions (T+T, 2016)

Site area	Crude Jetty	Turning Basin	Inner Chanel	Outer Channel
Typical subsurface conditions	Fine to medium SAND, some shells (broken), dark grey, well graded	Fine SAND, some medium sand and shell, trace silt, grey, well graded	Shelly medium to coarse SAND, minor fine sand, light grey, well graded	Shelly fine to medium SAND, some coarse sand, grey to dark grey, well graded